4-2007

Global and Quantitative Gene Expression Analysis of the Effects of Drinking Water Exposure to Lead Acetate in Fisher 344 Male Rats Liver

Worlanyo Eric Gato
Western Michigan University

GLOBAL AND QUANTITATIVE GENE EXPRESSION ANALYSIS OF THE EFFECTS OF DRINKING WATER EXPOSURE TO LEAD ACETATE IN FISHER 344 MALE RATS LIVER

by

Worlanyo Eric Gato

A Dissertation
Submitted to the
Faculty of The Graduate College
in partial fulfillment of the
requirements for the
Degree of Doctor of Philosophy
Department of Chemistry
Dr. Jay Means, Advisor

Western Michigan University
Kalamazoo, Michigan
April 2007

GLOBAL AND QUANTITATIVE GENE EXPRESSION ANALYSIS OF THE EFFECTS OF DRINKING WATER EXPOSURE TO LEAD ACETATE IN FISHER 344 MALE RATS LIVER

Worlanyo Eric Gato, Ph.D.

Western Michigan University, 2007

The primary objective of this research is to analyze global gene expression patterns occuring in Fisher 344 rat livers exposed to varying levels of lead and times. The hypotheses were that: 1) effects associated with Pb exposure are both dose and time dependent and 2) several genes will be over-expressed or repressed including transcripts associated with calcium signaling. Initially, the effects of Pb exposures upon morphometric indices, liver and kidney tissue histology, Pb distribution, Pb interaction with other trace metals including Zn, Cu, Co, Fe, Ni and Ca were assessed. Results showed a significant accumulation of lead in blood, liver, kidney and bone marrow in lead exposed groups with the kidney demonstrating greater damage compared to the liver. Potential interactions of calcium, iron, cobalt, copper, zinc and nickel and lead examined showed positive and negative correlation for 30 and 90 days treatment period respectively. Differentially expressed genes included genes cited in the literature and several not previously reported to be affected by lead toxicity. Expression profiles were clustered and gene ontology (GO) revealed 15 GO categories affected by chronic (90d) exposure, while 3 GO categories were affected during (30d) exposures. Pathways emphasized the importance of Pb in modulating various cellular events in a manner similar to calcium regulation, including phosphorylation and dephosphorylation, calcium

signaling, histone acetylation and deacetylation. Conclusions include:

1. Pb controls mammalian protein synthesis via regulating phosphorylation or dephosphorylation events of eukaryotic elongation/initiation factors
2. Pb regulates gene expression through the regulation of histone acetylases
3. Pb regulates calcium dependent transcription factor myocyte enhance factor-2

Quantitative PCR was employed in validating the microarray result and showed that Microarrays and qRT-PCR yield comparable results.

INFORMATION TO USERS

The quality of this reproduction is dependent upon the quality of the copy submitted. Broken or indistinct print, colored or poor quality illustrations and photographs, print bleed-through, substandard margins, and improper alignment can adversely affect reproduction.

In the unlikely event that the author did not send a complete manuscript and there are missing pages, these will be noted. Also, if unauthorized copyright material had to be removed, a note will indicate the deletion.

ProQuest Information and Learning Company
300 North Zeeb Road
P.O. Box 1346
Ann Arbor, MI 48106-1346

ACKNOWLEDGEMENTS

I am indebted to my late grandmother Malwine Adzoa Boateng, my wife Vivian Mawuse Gato and children Worlanyo Eric Gato, Jr. and Elikem Winifred Gato, to whom I dedicate this dissertation.

I want to thank the Chemistry Department of Western Michigan University for giving me the opportunity to study for a doctoral degree in Chemistry. I also want to thank Dr. Jay C. Means for allowing me to work in his laboratory and supporting me financially. I am grateful to my committee members Drs. David Huffman and Robert Eversole for their thoughtful comments and support in various ways. Also, I want to express my deep appreciation to Dr. Michael Barcelona for the various ways in which he has helped me through this program.

This Chemistry program has given me the opportunity to meet and interact with people from diverse cultural, ethnic and intellectual backgrounds. I am glad to meet colleagues from Sri Lanka - Thushara Ghunasinghe, Kumar Tilak, Nayane Prasange, Piyardasha and Aruna Weerasinghe, China - Minghong Liu, Wen Guo, Luchin Lin, Wend, Kenya - Wilson Okumu, David Achila, Patrick Ochieng, Joshua Muia, Paul Oshule and Joy Mwalimu; U.S. - Jenny Powell, Elizabeth Sodt and Elizabeth Semkiw, Brian Zeider and William Lizik, India - Shankar Varangati, Swapna Katram, Pramod Thekkat, Suhitha Meka and Sandhya Nair. I appreciate the friendship of these guys and a host of others. I appreciate the friendship provided by Paul Knoll and Trisha Basford my

laboratory colleagues. Thank you, Trisha Basford for helping me to learn the techniques required for this project.

Drs. David Reinhold, Susan Stapleton and Sherine Obare have provided mentoring and references for me. Pam McCartney and Annie Dobbs have been helpful in many ways. For these, I say thank you and I appreciate your kindness very much.

Finally, I want to express my deep thanks to the members of Westwood Baptist Church for being a family to us.

Worlanyo Eric Gato

TABLE OF CONTENTS

Table of Contents – Continued

CHAPTER

CHAPTER

LIST OF TABLES

LIST OF FIGURES

CHAPTER I

INTRODUCTION

The most ancient and relevant environmental poison to be used by man is lead. According to Jernigan *et al* [1], hundreds of millions of people have been affected by the toxicity of lead during the last 4500 years either as mining slaves, or as consumers of adulterated wine and food or from breathing urban air. Written archeological evidence exists that lead was used widely in the ancient world. In recent times, lead has been used in gasoline which makes it widely distributed in the environment.

This dissertation is organized as follows; chapter 1: introduction, chapter 2: literature review, chapter 3: assessment of lead toxicity by inductively-coupled plasma mass spectrometry and histopathology, chapter 4: gene expression analysis by microarray DNA gene chips, chapter 5: validation of microarray gene expression data by real-time quantitative polymerase chain reaction (RT-qPCR) and chapter 6: conclusions. In chapter 1, a brief background to the study is provided with project objectives clearly laid out. Chapter 2 provides a review of background knowledge of lead to date. Topics discussed are history of lead production and use, sources of lead contamination and exposure, body absorption and distribution of lead, lead health effects, toxicity mechanisms, ways of remediating lead polluted soils and water and how to reduce lead body burden. Chapter 3 introduces the experiments that were conducted to address goals one through three whilst goals four through seven are addressed in chapters 4 and 5. Finally the study is concluded in chapter 6.

Heavy metals such as lead and its compounds are natural constituents of the environment moving between atmosphere, hydrosphere, lithosphere and biosphere through natural mobilization processes [3, 11]. De Treville [12] estimated the average lead content of the earth's crust to be 16 ppm with acid rocks containing more than basic rocks in the ratio of 20:8. Subsequent distribution of lead in the environment results from natural process and anthropogenic activities [13]. Florea and Büsselberg [13] classified the main anthropogenic sources of lead as fossil fuel combustion, industrial and agricultural processes. The major outdoor sources of lead emissions include aircraft fuel combustion, stationary point and area fuel combustion, autobody refinishing, secondary lead recycling, cogeneration plants, sawmills and paperboard mills, incineration, foundries and steel mills, paints and coatings, battery manufacturing and cement manufacturing [16].

Lead is used in manufacturing storage batteries and alloys of lead are employed in bearings, brass and bronze and some solders, sheets and pipe for nuclear and X-ray shielding, cable covering, noise control materials,, chemical resistant linings, ammunitions, ceramic glazes, plastic stabilizers, caulk and paints [5]. In 2003, primary and secondary lead production was 0.245 and 1.15 million metric tons in the United States respectively whilst world production in 2002 amounted to 2.91 million metric tons [5, 21].

Lead as a component of natural minerals is ubiquitous in the environment. It is present in all kinds of soil in a wide range of concentrations. The average lead content of the upper continental metamorphic rock combined with magma intrusions for an unpolluted earth crust is 17 ppm on a worldwide scale [2]. Lead background levels have

increased to thousands of ppm soils close to very busy roads or near smelters. Sauvé *et al* [27] notes that most urban soils in industrialized nations have total Pb levels above the geochemical "background levels" of 10-20 mg of Pb per kg as a result of anthropogenic Pb emissions [26]. Lead is sparingly soluble in water but it is capable of forming complexes with chloride, hydroxyl ion and it forms molecules with carbonates, sulfides, phosphates and organics ligands thus increasing the possibility of lead mobility through the soil profile [26-28]. Godelitsas [38] notes that, the chemical mobility of lead in the environment and its harmful effects are mediated via aquatic pathways which include surface and underground waters. They report that major water quality problems are associated with non-point sources of pollution including lead which are comprised agriculture, forestry, mining, construction, livestock feedlots, urban runoffs and roads. In 2004 the EPA [40] reports that a total of 121,760 pounds of lead or lead compounds were discharged to surface waters. Freshwater systems have a greater tendency to transport dissolved lead than marine systems. This is largely due to a higher inorganic and organic suspended material available in fresh aquatic systems. As a result, movement of lead in freshwater is closely linked with turbulent transport of particulate matter [32]. According to Meyer *et al* [44], air in industrial and metropolitan areas is more contaminated with heavy metals than air from rural areas. The presence of lead in the atmosphere is due to both anthropogenic and a variety of natural sources [4, 32, 45]. Lead among other heavy metals such as As, Cd, Co, Ni, Sb, V, Zn are characterized as road-specific metals. Because they are mostly derived from combustion residues and losses from fuels, engines and transmission oils, tire abrasions, brake linings, exhaust catalysts, road pavement and corrosion of galvanized protection barriers [46]. The half-life of lead in the atmosphere is

typically short. This can range from several hours to several days. Lead is removed from the atmosphere via wet, dry or cloud or fog deposition and this deposition is highest near the source as a result of large particle precipitation.

Routes of lead exposure are closely associated with environmental lead sources. Lead entry into the body may be by drinking water, ingestion of food, breathing lead particulates or by dermal contacts. Lead contaminated soil could provide a direct route of lead ingestion for infants or indirectly via contaminated food. According to Romieu *et al* [24], inhalation or ingestion of dust and soil contaminated with lead can play a crucial role in the total body burden of lead in children. In the US, leaded-gasoline contributes significant levels of lead to air and top-soil until it was banned in 1995. It has been estimated that for each $1\mu g/m^3$ rise in airborne lead levels, a child's average blood lead level increases by 5-6 μg/dl [5]. Other routes of lead exposure include dishware (i.e. pottery, crystal or commercial dishware), lead based solder cans, children's toys, household products like wicks, and vertical blinds and car keys.

Lead intake and absorption routes are determined by the routes of exposure. Castellino and Castellino [2] summarized the routes of Pb intake and absorption as being via respiratory tract, gastrointestinal tract, skin and placenta. Lead particles absorbed via the respiratory tract are eventually deposited in the lung where they are cleared through sequestration by alveolar cells or through the lymphatic vessels to the lymph nodes or it may dissolve in the tissue fluids and pass into the blood [3]. According to Ragan [69], the primary route of entry metal pollutants into the body is the gastrointestinal tract. Dietary intake of lead from recycled Pb in the form of contaminated meats and plants leads to direct intake of lead. Also, Pb traces may be present in drinking water, milk or beverages

as another direct Pb-consumption. In addition, lead can be ingested by infants in the form of contaminated soil, dust or chipped paint. Pregnancy and lactational periods are probably an important period of lead exposure for both the unborn infant and a child on breast milk [118-121]. Lead is mobilized during pregnancy because the maternal bone is resorbed in order to produce the fetal skeleton.

Although the precise mechanism of lead and other trace metal absorption is not entirely understood it is thought to involve both active and passive transport mechanisms [70-72]. Intestinal lead absorption is observed in all parts of the intestine with the most significant portion occurring in the small intestine [2, 77]. Important parameters influencing the absorption of Pb include ingested metal form, environmental matrix, gastrointestinal tract contents, diet, nutritional status, age and in some cases genotype [78, 79]. The concentration of lead in tissues accumulate in the decreasing order of bone > kidneys > liver > brain > muscle [88]. Lead levels in the body are speciated into two primary pools and these have varied rates of turnover. The slowest and largest pool is found in the skeleton with resident time of more than 20 years. The more labile pool of Pb is found in soft tissues and has a consequent half-life of about 20 days [89, 90]. The primary routes of lead excretion are through the urine or feces though bile and secretions by glands such as salivary, pancreatic, sweat and mammary play a much lesser role in clearing Pb from the body [80, 92-93].

The health effects associated with Pb exposure reported in the literature are numerous. These range from unobservable symptoms to extreme cases of death in exposed victims. Health effects may be manifested via neurobehavioral, cancer, genotoxic, reproductive, developmental and immunological changes [5].

Several molecular and cellular mechanisms of Pb actions have been documented to explain the processes through which lead exerts its negative cellular and molecular influences. Lidsky and Schneider [198] classified Pb neurotoxicity mechanisms as being both direct and indirect while Goyer [196] defined them as being morphological and pharmacological. The neuropharmacological interactions of Pb include substitution for calcium, iron and zinc, increased neurotransmitter release, protein kinase C activation, Na-Ca ATPase inhibition and alterations in energy metabolism. Morphological interactions of Pb on the other hand consist of interference with cellular adhesion molecules, impaired cell:cell programming connections and miswiring of the neurons in the central nervous system. Various studies have examined the role of Pb^{2+} on messenger RNA (mRNA) expression. These studies have been designed to either explore pathways that involve the production of reactive oxygen intermediates since the literature is emphatic concerning the increased cellular oxidative stress observed due to lead toxicity or the mitogen-activated protein kinase (MAPK) family because activation of some members of this protein family could lead to activation of transcription factors and to apoptosis. Several genes transcripts are reported in the literature to be regulated by Pb exposure either directly or through some other consequential metabolic pathway. In recent years, studies involving Pb have shifted focus to elucidating how Pb regulates mRNA transcription. The greatest challenge of this approach is that until very recently readily available methods allowed the examination of only a single gene at a time. Fortunately, the completion of the human genome project has lead to the emergence of DNA microarray technology. The emergence of DNA chip technology has dramatically increased the number genes that can be studied simultaneously. This technology has

afforded toxicologists the opportunity to study thousands of genes at the same time thereby facilitating the ability to examine pathways and to associate transcription factors with target genes [209]. The acceptance of DNA chip technology for examination of molecular and cellular processes is demonstrated by the increasing number of published literature that employed this technique. The primary objective of this dissertation project is to analyze global gene expression patterns that occur in Fisher 344 rat liver exposed to varying levels of lead for different periods of time, with the hypothesis that effects associated with Pb exposure are both exposure and time dependent and that several genes will be repressed with the most important being mRNA transcripts associated with calcium signaling. The specific experimental goals are;

1. Assess Pb^{2+} distribution in blood, liver, kidney and bone marrow
2. Assess Pb^{2+} interaction with trace metals such as Ca, Zn, Cu, Co and Ni in blood, liver, kidney and bone marrow
3. Assess lead effects on the cells of the liver and kidney
4. Assess large-scale gene expression profiles
5. Determine differential gene expression levels
6. Identify likely molecular targets of lead intoxication
7. Assess large-scale view of perturbations involving cellular and molecular pathways

Using DNA chip technology, we have been able to confirm the responses of genes already known to be regulated by Pb toxicity but also to identify new mRNA transcripts that are targets of lead poisoning. We have also been able to observe some pathways that

are important in lead toxicity giving us the opportunity to hypothesize new mechanisms by which the toxicity of lead occurs.

CHAPTER II

LITERATURE REVIEW

Lead Background Information

Historical Background

The most ancient and relevant environmental poison to be used by man from natural processes is lead. According to Jernigan *et al* [1], hundreds of millions of people have been affected by the toxicity of lead during the last 4500 years either as mining slaves, or as consumers of adulterated wine and food or as mere breathers of urban air. There is written and archeological evidence that lead was used widely in the ancient world. For instance in the tribute lists of Pharaoh Thutmosis III (1500 BC), there is a mention of captured lead, which his armies are known to have brought home from Mesopotamia. Jernigan *et al* surmised that it could be used to trace the anatomy and evolution of engineering technology of man since its use can be dated back as far as the beginning of civilization some 12,000 years ago.

Even before the beginning of the metal age around 3500 BC, human activities been associated with metals. This age marked the discovery of copper in its natural state and lead which can be extracted easily from mineral ores [2]. Lead is one of the seven principal metals of antiquity [3] and it has followed the Euro-Asian and American civilizations at least in part since their beginning. Copper and lead beads, rings and pendants were found in Catal Huyuk (Turkey) dating back to the seventh century BC. At about this time, lead minerals such as galena were employed in the extraction of silver

which often is found combined with lead. The oldest known metallurgic process called cupellation was typically used in separating lead from its noble partner silver [1].

It is probable the toxic effects of lead might have been known for almost as long as lead has been used [4, 7]. Waldron [7] quoting Pliny says 'For medicinal purposes lead is melted in earthen vessels ... whilst it is being melted the breathing passages should be protected ... otherwise the noxious and deadly vapor of the lead furnace is inhaled; it is harmful to dogs with special rapidity'. Pliny also said 'red lead is a deadly poison and should not be used medicinally'. Also, Vitruvius from the first century wrote 'water is much more wholesome from earthenware than from lead pipes. For it seems to be made injurious by lead because cerruse ($PbCO_3$) is produced by it; and this is said to be harmful to the human body. Thus if what is produced by anything is injurious, it is not doubtful but that the thing is unwholesome in itself. One symptom exhibited by the workers with lead who had complexions affected by pallor. For when, in casting, the lead receives the current air, the fumes from it occupy the members of the body and rob the limbs of the virtues of the blood. Therefore it seems that water should not be transported in lead pipes if we desire to have it wholesome (quoted by Waldron) [7]. In fact some authors believe the fall of the Roman Empire was due in part to lead poisoning. They report such adverse effects as blindness, insanity and sterility [8, 9].

As Smith [4] rightly wrote, 'the history of lead is that knowledge of lead toxicity and the effects of lead have been periodically ignored and then (on occasions) rediscovered'. McCord [10] describes it as an 'aping disease' because of the wide range of symptoms which it may produce and the number of other diseases which it may

imitate, and this may be the most important reason why the cause was often not recognized.

What is Lead?

Lead originally appears shiny silver luster although it quickly weathers taking on its usual dull grey-bluish color. It is naturally occurring element with a chemical symbol of Pb and an atomic weight of 207.2 amu deduced from its stable isotopes with atomic weights 204, 206, 207, 208 amu. Their respective abundances are 1.35 – 1.5 %, 23.5 – - 27 %, 20.5 - 23% and 51 – 53 %. These isotopes are decay products of radioactive elements. Lead 206 from uranium, 207 from actinium and 208 from thorium [4, 5].

Unlike gold, silver or copper, lead does not exist in its metallic form in nature so that all lead is obtained from ores. Galena (lead sulfide) found as a shiny black metallic-looking stone is the principal lead ore. Other weathering products of galena found nearer the surface are cerussite (lead carbonate), anglesite (lead sulfate) and less commonly crocoite (lead chromate) and wulfenite. Approximately 0.002 % of the earth's crust is lead. These are localized into deposits sufficient enough for mining. Lead ore deposits are widely distributed across all five continents [6]. These ores are extremely abundant in the US, Spain, South America and China [1].

All the many forms of lead can be simply divided into lead in metallic form and lead in chemical compounds. Metallic lead form may again be subdivided into unalloyed and alloyed lead. Unalloyed lead is lead with no intentional addition of other metals although there is no such thing as 'pure' lead. Alloys of lead are formed from controlled addition of other metals to lead for example to make tin. Lead compounds are either

inorganic or organic. A principal example of organic lead compounds are tetra-ethyl lead and tetramethyl lead previously used as anti-knock additives in gasoline [4].

All the various forms of lead may exhibit different physical and chemical properties. Lead can be found in Pb(0), Pb(II) and Pb(IV) states, with the Pb(II) state being the most common in the environment. Under extreme oxidizing conditions, Pb(IV) compounds are found whiles organolead chemistry is dominated by the tetravalent oxidation state. Among metals, it is unique in being very soft and malleable but has virtually no elasticity and little mechanical strength. The heavy dense nature of lead coupled with its lack of mechanical strength and softness gives lead a tendency to flow or creep under its own weight. Lead carbonate forms a film on the surface via reaction between lead and air thus making lead resistant to corrosion. This protective film gives lead its dull grey appearance [4, 5]. Metallic lead is solid, melts at 327.4 °C, boils at 1740 °C, at 20 °C has a density of 11.34 g/cm3, at 25 °C is insoluble in water and a vapor pressure of 1.77 mmHg at 1000 °C. lead is commercially valuable because it is easy to cast, density is high, melting point is low, low strength, fabrication is easy, resistant to acid, electrochemical reaction with sulfuric acid and chemically stable in air, water and soil [18-20].

Sources of Lead in the Environment

Heavy metals and compounds are natural constituents of the environment moving between atmosphere, hydrosphere, lithosphere and biosphere because the earth's crust provides natural mobilization source [3, 11]. De Treville [12] estimates the average lead content of the earth's crust to be 16 ppm with acid rocks containing more than basic rocks

in the ratio of 20:8. The subsequent distribution of lead in the environment is as a result of natural process and anthropogenic activities [13].

According to Patterson [14], six most significant natural lead sources in their increasing order of importance are; meteoric smoke, aerosolic sea salts, forest fire smokes, volcanic silicate smokes, volcanic halogen aerosols and silicate dust from natural soils. Some important natural process contributing to lead distribution within the ecosystem include volcanoes, erosion, spring water and bacterial activity.

Florea and Büsselberg [13] classed the main anthropogenic sources of lead as fossil fuel combustion, industrial and agricultural processes. Table 1 below shows the annual lead production in the United States from 1999 through 2003.

Table 1

U.S Lead Production (metric tons) from 1999 to 2003 [5].

	Production volumes in metric tons				
Production	1999	2000	2001	2002	2003
Mined (recovered: domestic ores) recoverable lead content	503,000	449,000	454,000	440,000	449,000
Primary (refined): domestic/foreign ores and base bullion	350,000	341,000	290,000	262,000	245,000
Secondary (refined): lead content	1,110,000	1,130,000	1,100,000	1,120,000	1,150,000

From this data, the main source of lead to the US market is recycled lead. Han *et al* [15] shows estimates of actual and cumulative global lead production.

These authors estimate that in 2000, the cumulative industrial age anthropogenic global production of lead was 235 million tons whiles lead burdens per capita in the same year was 38.6 kg [15].

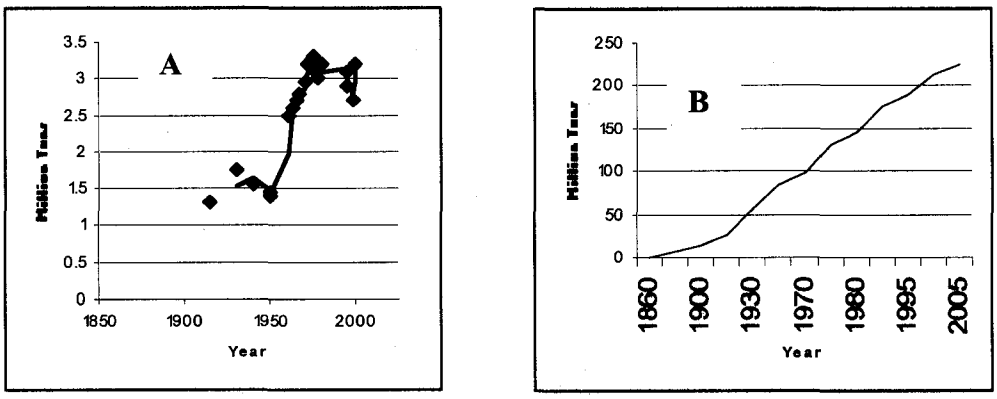

Figure 1: (A) Actual global annual industrial age lead production and (B) global cumulative industrial age lead production [15].

The major outdoor sources of lead emissions include aircraft fuel combustion, stationary point and area fuel combustion, autobody refinishing, secondary lead recycling, cogeneration plants, sawmills and paperboard mills, incineration, foundries and steel mills, paint and coatings, battery manufacturing and cement manufacturing [16].

Lead Use History

Lead use dates back to ancient times. All the various civilizations from the Egyptians, Phoenicians, Greeks and Romans have found lead useful in everyday life in one way or another [1-2, 4].

For example Lucas and Harris [17] reported that the Egyptians employed metallic lead for small human and animal figurines, sinkers of fishing nets, rings, beads and other small ornaments, model dishes and trays, vessels, tanks and plugs. During these times, the Babylonians used it in building hanging gardens. Lead carbonate or cerussite was used in enamel for glazed pottery and in cosmetics tot whiten the face [2]. Similarly, the Greeks collected water from lead roofs, transported water through lead metal gutters to lead-lined cisterns. They also used iron clamps embedded in lead metal in stabilizing stone building blocks, ships sheathed with lead metal to repel wood-worms and salves, ointments, paints and cosmetics were made from lead compounds. Also, grape sugars were boiled down in lead pots and added to wines to reduce souring and lead-tin alloys were widely being used to line the inside of bronze utensils to keep copper out of foods and liquids [1].

The levels of lead use previously are nothing compared to the Roman era. The Romans were reported to extract lead from several countries of the Empire, Gaul, Britain and Germany but their most important source was Spain. In the 1^{st} and 2^{nd} centuries, it is estimated the annual lead use in Italy was nearly 0.004 ton of lead/person/year [1, 3]. The Romans extensively used lead in lining their aquaducts and water reservoirs. Like the Greeks their lined their bronze cooking pots with lead. This eliminates the bitterness associated with unlined bronze pots as well producing sweeter tastes in food [3].

With the fall of the Roman Empire, interest in lead declined dramatically until the beginning of the modern era, possibly because no new knowledge with regards to lead applications was discovered. Lead was used in the same applications as in ancient times and also in new areas. Lead sheeting was used in construction to cover public buildings

and cathedrals in France, Italy and England. It was used in the art of glassmaking, printing, medicine, lead smelting, paints, varnishes, pigments and additive in gasoline. Lead is also used in the following areas; low-solubility lead glazes in the pottery industry, lead arsenate in the manufacture of insecticides, borate in the manufacture of certain plastics and pipes, cisterns, roof coverings and metallization of wires [2].

In summary, lead is also used in manufacturing storage batteries, alloys of lead employed in bearings, brass and bronze and some solders, sheets and pipe for nuclear and X-ray shielding, cable covering, noise control materials, chemical resistant linings, ammunitions, ceramic glazes, plastic stabilizers, caulk and paints [5].

Production, Disposal and Regulations

Galena (PbS) is the principal lead ore. Lead oxide is reducible at temperatures below 800 °C. This process simultaneously results in the reduction of galena to its oxide form with the subsequent reaction with unchanged galena to yield metallic lead. The reaction is shown below [3];

$$2PbO + PbS = 3Pb + SO_2$$

The bulk of lead produced currently is secondary lead. Primary lead is lead obtained directly from the mines. Secondary lead is obtained from recycling of manufactured products containing lead such as lead-acid batteries or lead-metal scrap. Table 2 below provides statistics on the current US and global lead production levels [21].

The increase in secondary lead production is a useful way of lead disposal. Larrabee [22] points out that no other metal has a recycling rate comparable to lead. For example in

2002, 81 % of refined lead produced in the United States was recovered from recycled scrap. The majority of the lead recycled comes from lead-acid batteries. About 6 % of recycled lead comes from such sources as building construction materials, cable covering, and solder [5].

Table 2

Lead Statistics with values in metric tons. Data for US apparent consumption are for refine lead and calculated using the formula: Apparent Consumption = Production + Imports – Exports ± Changes in Stock ± Government Shipments.

Year	Primary production	Secondary production	Imports	Exports	Apparent consumption	World production
1998	337,000	1,060,000	310,000	40,000	1,690,000	3,100,000
1999	350,000	1,060,000	323,000	37,000	1,760,000	3,020,000
2000	341,000	1,080,000	365,000	49,000	1,740,000	3,100,000
2001	290,000	1,040,000	284,000	35,000	1,640,000	3,150,000
2002	262,000	1,070,000	218,000	43,000	1,510,000	2,910,000

There are several federal and state regulations guiding the disposal of waste containing lead or lead compounds. Lead is listed as a toxic substance under Section 313 of the Emergency Planning and Community Right to Know Act (EPCRA) under Title III of the superfund Amendments and Reauthorization Act (SARA). Waste products made of lead comprise storage batteries, lead-based paint, ammunition waste, ordnance, sheet lead, solder, pipes, traps, solid waste and tailings from lead mining, solid waste created by mineral ore processing, iron and steel production, copper and zinc smelting, and production and use of other lead-containing products [5, 23].

Lead in Air

According to Meyer *et al* [44], air in industrial and metropolitan areas is more contaminated with heavy metals than air from rural areas. The presence of lead in the atmosphere is due to both anthropogenic and a variety of natural sources [4, 32, 45]. Lead among other heavy metals such as As, Cd, Co, Ni, Sb, V, Zn are characterized as road-specific metals. Because they are mostly derived from combustion residues and losses from fuels, engines and transmission oils, tire abrasion, brake linings, exhaust catalysts, road pavement and corrosion of galvanized protection barriers [46]. This is shown in the rapid decline in atmospheric Pb deposition to terrestrial and aquatic ecosystems since the ban on lead use in gasoline [49]. The half-life of lead in the atmosphere is typically short. This can range from several hours to several days. A residence time of lead is particle size dependent. Size also accounts for the length of transport of these lead particles and their ability to penetrate into the lungs. Lead is removed from the atmosphere via wet, dry or cloud deposition and this deposition is highest near the source as a result of large particle precipitation. Obviously wet deposition is relatively important during wet seasons as dry deposition accounts for most lead removal from the atmosphere in summer dry seasons. Lead eventually ends up on land or in aquatic systems with the possibility of polluting ground water [4, 32, 45]. Miller and Friedland [49] reporting from several sources showed that lead concentration due to precipitation in the north-eastern U.S. was greater than 30 μg/L in the 1960s and early 70s but reduced to 17 μg/L by 1982 and further declined to less than 2 μg/L.

In fact the residence time of 0.1-2 μm size aerosol was estimated between 3 to 7 days with the capacity for atmospheric transport over several thousand kilometers [46]. Miller and Friedland [49] agreed by saying significant amount of Pb is released as volatile compounds or sorbed on fine aerosols which can be circulated into the upper troposphere and transported thousand of kilometers due the relatively long residence time. This is confirmed by elevated Pb levels documented in Greenland and polar snow and accumulated concentrations in sediment, peats and organic horizons of forest soils since the introduction of leaded-gasoline. Lead is reported to fall within this category of heavy metals that closely associate with fine dust. Zereini *et al* [46] found in their study of airborne heavy metal concentration and distribution in Frankfurt am Main, Germany that As, Cd, Pb and V were part of the fine particles of diameter <2.1 μm. It should be noted that fine particles of diameter less than 10 microns are the main fraction of airborne aerosols. This constitutes about 80 % of aerosols [47]. The above observation was also reported by Samara and Voustsa [47] who studied the association between particulate matter and heavy metals. According to them, heavy metals showed three distinct behaviors with regards to size distribution. Lead and cadmium masses resided within the accumulation mode, Ni, Cu and Mn were distributed between fine, intermediate and coarse modes whilst Fe was reported to fall in a diameter larger than 2.7 μm. Apart from physical speciation by size, chemical speciation of lead in air include soluble and exchangeable metals, carbonates, oxides and reducible metals; oxidizable and sulfidic metals bound to organic matter and residual metals [48].

Lead in Soil

Kaste *et al* [26] reports that soils in the northeastern United State receive total atmospheric lead concentrations of 1 to 4 g Pb per square meter in remote environments. According to these authors, the forest canopy serves as an initial recipient of atmospherically delivered Pb or dissolved Pb in rain which is retained. Subsequent litter-fall and decomposition leads to enriched lead-organic layer overlying the mineral soil. Forest floor Pb contents have been documented to range from 75 to 300 $\mu g g^{-1}$ and this is typically one or two orders higher than parent material Pb concentration [33, 34].

Lead is sparingly soluble in water but it is capable of forming complexes with chloride, hydroxyl, carbonates, sulfides, phosphates and organics thus increasing the possibility of lead mobility through the soil profile [26-28]. Lead has been observed observed to be stable in soil. Experiment have been conducted to determine the stability constant for lead and a host of other metals in their association with anionic microbial surfactant, rhamnolipid, using ion-exchange resin technique. The Pb-complex was found to be more stable than Cd^{2+}, Zn^{2+}, Fe^{2+}, Hg^{2+} and Ca^{2+}. Only Cu^{2+} and Al^{3+} are stable in the list of metals tested [30]. There is evidence to suggest that some fraction of Pb has been moving into the mineral layer beneath and others have pointed out that lead is moving in association with soil organic matter [26, 33-35]. Thus mobilization of organic matter as dissolved or particulate will determine to a great the extent Pb mobility in soil. This was confirmed by Marsh and Siccama [34] who showed decreased lead levels with soil depth and reduced organic matter content. They reported decreasesin Pb concentrations from 350 mg cm $depth^{-1}$ m^{-2} at 0-2 cm depth to 102-108 mg cm $depth^{-1}$ m^{-2} between 10 and 20 cm depth. At all the sites tested, lead concentrations with depth were

correlated with decline in the amount of organic matter. Also they estimated that 35 % of presumably anthropogenically received lead was in the forest floor and the rest 65 % in the upper mineral layer.

Knowledge of the processes involved in trace metal speciation is essential in estimating metal bioavailability and risk assessment strategies. This is even more important when one realizes that total metal concentrations in soils are poor indicators of metal toxicity because metals exist in varied solid-phase forms [37]. Besides metal bioavailability, biological uptake and ecotoxicological effects on soil biota is better understood by understanding chemical speciation. For example, in contaminated soils, Pb is insoluble, precipitated or bound to soil colloids. Short-term plant available lead is the lead in the soil solution whiles long term bioavailable lead will depend on lead-bearing minerals like carbonates, phosphates or sulfides [27] in addition to the effect of principal soil chemical properties like organic matter and pH. Sauvé and McBride [27] observed that higher solution pH increased organic matter solubility which is likely to induce dissolution of lead phosphate by organic complex reactions. An optimum pH of 5.5 to 6.5 is required to reduce solubility, mobility and bioavailability after soil amendments and lime application [27].

Lead can be toxic to plants and soil microorganisms. Lead is known to cause harmful effects on the physiology and biochemistry of plants and as a result lowering yield [36]. Also laboratory experiments provide evidence that as low as 200 mg kg-1 of lead can disrupt organic matter decomposition and associated N and P mineralization in ecosystems [26]. Mishra and Choudhuri [36] reports that treating rice seeds with lead resulted in decreased germination percentage, germination index, shoot and root length,

tolerance index, vigor index and dry mass of shoot and root but increased percentage phytotoxicity.

Lead in Aquatic Systems

Godelitsas [38] notes that, the chemical mobility of lead in the environment and its harmful effects are mediated via aquatic pathways which include surface and underground waters. According to them, this is strongly correlated with interactions with different geomedia represented by rocks, soils and their mineral components. Chang and coworkers [39] agreed with this assessment. They reported that major water quality problems are associated with non-point sources of pollution including lead which comprises agriculture, forestry, mining, construction, livestock feedlots, urban runoffs and roads. In 2004 the EPA [40] reported that a total of 121,760 pounds of lead or lead compounds were discharged to surface waters. Surface water includes discharges to streams, rivers, lakes, oceans and other water bodies. The primary sources of lead in rivers are runoff and direct deposition from air (mostly anthropogenic) or erosion (natural). Similarly, most of the lead in oceans is from atmospheric deposition except in estuaries and some coastal waters where riverborne lead, direct dumping of sewage and industrial wastes become the major sources of lead [4, 32].

Freshwater systems have a greater tendency to adsorb dissolved lead than marine systems. This is largely due to a higher inorganic and organic suspended available material in fresh aquatic systems. As a result, movement of lead in freshwater is closely linked with turbulent transport of particulate matter [32]. Much of the lead deposited in seas and oceans end up at the bottom. In fact, this is one way by which past lead use is

determined from sediments. Because of high chloride concentration and lower concentration of particulate matter, much of the lead is in the dissolved form and thus may be bound by salts so that it ends up as marine deposits [4, 32]. In freshwaters, F^-, Cl^-, SO_4^{2-}, OH^- and HCO_3^- are the most important ions responsible for metal uptake. The tendency of these ligands to bind to lead and thus control its bioavailability depends on pH in open waters and electron donor/acceptor in sediments [41, 42, 43]. For instance in sediments, bacteria use oxidized forms of metals as electron acceptors to produce soluble metallic ions.

Lead Cycling in Soils and Surface Waters

Lead is considered a good indicator of pollution for the following reasons. It is easy to analyze, non-mobile in natural environmental archives like lake sediments, it is emitted from different kinds of sources such as mining and metal industry and by fossil fuel burning. Analyzing lead in sediment time-series can provide a broad picture of atmospheric pollution as well as chronology of lead pollution [57]. Lead is thought to enter the ecosystem via precipitation and dry deposition in particulate form [50]. As a result, Pb is deposited at places far from the principal source of contamination. There have been documented cases of forests in remote areas and higher elevations showing lead levels greater than expected background concentrations [51, 52]. Wet deposition is primarily in the form of rainfall at low elevations or cloudwater interception at high elevations or dry deposition contributing about 20 % of total Pb flux in some regions [50]. Increased lead levels were observed in the organic horizon at high elevations of forest soils because of greater precipitation and deposition at these elevations [50, 53].

The over 3000 years of metal use in one form or the other has resulted in accumulation of heavy metals in the environment. In the organic horizon overlying the forest mineral soils of podzol (soils that are acidic with characteristics of circumpolar boreal forest coniferous forests that cover large regions of Fennoscandia, Russia and North America. Podzols are stratified into a surficial organic horizon (O horizon), which is a humus layer, also called the mor layer, which covers the mineral soil like a blanket, a gray eluvial horizon (E horizon) where Al and Fe are leached, a dark illuvial horizon (Bs) where Al, Fe and organic complexes have accumulated below a gradation into unchanged parent mineral soil C horizon) [58], typical Pb concentration values fall between 50 mg kg^{-1} and 100 mg kg^{-1} which most authors consider to be about 1000 times greater than natural background Pb content. Lead inventories in Swedish boreal forest soils range from 0.5 to above 3 g Pb per square meter [54-57]. Natural background Pb concentrations in these soils are assumed to be in the range of 10-15 $\mu g\ g^{-1}$. Current levels range from 40-100 $\mu g\ g^{-1}$ [55].

Most researchers in the past thought lead was strongly retained in the organic horizons. Data over the last two decades show otherwise. Pb levels on the forest floors of a number of eastern North American sites have decreased by 20-40 % over the last 20 years [49, 59]. This rapid movement loss of Pb from the forest floor has lead to concerns that it might also move rapidly through the soil profile resulting in groundwater contamination. [49]. It has been estimated that the large quantity of Pb deposited in North America after the 1960s might begin to be released into upland streams sometime in the middle of the 21st century. Pb transport velocities in forested soils have been documented to range from 0.39 to 0.83 mm year-1 in over 40 sites across Europe, 5 mm year-1 in

Mediterranean soils and between 8.2 and 19.7 mm year-1 at Vermont, USA [49, 60-62]. In a study to assess the vertical distribution of lead in Swedish boreal forests, the authors reported that lead was distributed across the profile of an undisturbed forest soil whereas the agricultural revealed completely opposite pattern. Pb concentration was between 60-100 μg g-1 in the mor layer in southern Sweden and about 30 μg g-1 in northern Sweden as well as moving down to 20 and 60 cm. According to these authors, the largest pollution of Pb was observed at the Bs horizon. On the agricultural soil, all the lead was evenly distributed in the 20 cm thick topsoil [56].

The key determinant of metal biogeochemical cycling is their chemical form which in turn determines bioavailability and mobility in the various media. Common lead fractions employed in its fractionation include water soluble and exchangeable. Carbonate, Fe-Mn oxides, organic carbon and residual Pb [63, 64]. In site previously employed in discharging batteries, 42.5-44.5 % of the soil surface Pb was associated with the carbonate fraction. Lead in both the carbonate and water soluble and exchangeable fraction was more than 50 % indicating that a substantial portion of the Pb might be available for plant uptake [64].

In a similar study, Huang and Matzner [65] investigated the biogeochemistry of trimethyllead (TML) in a forested ecosystem in NE-Bavaria Germany. Tetraalkyllead compounds undergo the following sequence of decomposition in the environment: $R4Pb \leftrightarrow R3Pb^{+} \leftrightarrow R2Pb^{2+} \leftrightarrow Pb^{2+}$. They observed lead concentration of 11.56 mg ha^{-1} and 222 mg ha^{-1} for TML and total-Pb respectively. They estimated the annual total deposition (sum of throughfall and litterfall fluxes) from the atmosphere at 52 g ha^{-1} $year^{-1}$ for total-Pb and 3.7 mg ha^{-1} $year^{-1}$ for TML. More than 90 % of the soil storage of TML

was found in wetland soils representing 30 % of the area understudy and it seems to stable under anoxic conditions. TML was observed to degrade relatively rapidly in the forest floor. It had a half-life of 33.5 days in the O-horizon, 421 days in the E-horizon and 612 days in the mineral soil. Adsorption affinity for was highest in E-horizon followed by organic horizon and then the mineral layer. The adsorption capacity of TML and Pb^{2+} depended on the type of soil. In predominantly organic layers, Pb^{2+} was more adsorbed thereby increasing the tendency of TML to be mobile. On the contrary, in soils having high cation exchange capacity TML is more strongly adsorbed.

In another investigation in Canada to examine lead biogeochemistry in the littoral zones of south-central Ontario lakes using lead isotopes, the authors concluded that "the exchange of Pb between lakewater and sediment 'carbonate', and subsequently between 'carbonate', 'oxide' and other sediment fractions was the most likely water-sediment pathway of lead movement. pH controlled Pb fractionation within surficial sediments, with the 'organic' pool comprising 80-97 % of total Pb in most acidic lakes and 15-60 % in alkaline lakes. About 28 % of the Pb in Nymphea odorata shoots was accumulated directly from waters and sediments. Plant Pb isotopes strongly resemble the historical Canadian atmospheric (alkyl Pb) signature. A possible explanation is that, like essential trace metals, historically accumulated Pb was highly conserved during the annual growth cycle of this long-lived macrophyte, being stored over-winter in underground rhizomes and recycled into spring growth. Given the low rate of 'new' Pb uptake, historical alkyl Pb may continue to dominate plant tissues for some time, even though it was not detectable in littoral waters and sediment" [66].

Human Lead Exposure Routes

Routes of human lead exposure are closely associated with environmental lead sources. Lead entry into the body could be by drinking water, ingestion of food, breathing lead particulates or by dermal contacts.

Lead contaminated soil could provide a direct route of lead ingestion for infants or indirectly via contaminated food. According to Romieu *et al* [24], inhalation or ingestion of dust and soil contaminated with lead can play a crucial role in the total body burden of lead in children. In the US, leaded-gasoline used to contribute significant levels of lead to air and top-soil. It was estimated that for each 1$\mu g/m^3$ rise in airborne lead levels, a child's average blood lead level increases by 5-6 μg/dl [5]. Since the decrease in use of leaded-gasoline in the mid-1970s, there has been a decline blood lead levels [25] but food grown on contaminated soils might have high lead levels. In a study conducted in Mexico, high levels of lead were reported in vegetables. In another study, these authors correlated blood lead levels to canned chili consumption [24]. Lead-based paint provides a direct route of lead ingestion for infants and children. Lead-based paint that is naturally broken down to smaller particles by moisture damage, friction, temperature fluctuations, exposure to acid liquids such as acid rain or by renovation activities can result in contaminated dust, soil and food, or toys [24, 25].

Drinking water provides another exposure route of lead. Drinking water contamination is as a result of plumbing solder. In the US, contamination from lead pipes, lead connectors and lead service lines is rare except in Detroit, Chicago, New York, Philadelphia and most older cities. Potential lead contamination could come from the wire mesh of the faucet when it traps solder particles. Presence of lead due to

plumbing can be increased by whether the water is acidic or have mineral content. In Mexico City, lead levels in their drinking water are low due to the high alkaline pH of the water [24, 25].

Many lead-based products are banned in the U.S. but sometimes household items exhibit high lead levels because they were imported from Asia, Central or South America, Eastern European countries or Mexico. These routes provide direct ingestion by hand, dust or food.

Direct occupational exposures to lead can be common for those who work in lead smelting or fabrication into various products. They may also carry lead-contaminated dust on hair, clothing and shoes to their homes. Industries that work with and emit lead can cause lead contamination of air, soil and food produced from contaminated soil [25].

Lead Remediation

Remediation of heavy metal contaminated soil and water is vital to our survival. This is why the number of articles on this subject has exponentially grown over the last two decades. The approaches to remediation range from engineering through use of plants to chemical means. Adoption of which method to employ depends on extent of pollution, speciation effectiveness of method and cost. Some of these methods are electrokinetic, capping and dredging, phytoremediation or phytoextraction, bioremediation, liming, sorption onto calcium carbonates, iron oxides or humic substances, membrane separation, solvent exchange and recently the application of nanomaterials, among others [151-155].

Most of these methods, though they have been used for a long time, have one problem or another associated with them. The engineering techniques are simply very expensive and often not tenable on small scale. The other methods either turn to reduce their bioavailability for which long term implications and ever-changing weather pattern effects are still not entirely understood. The rest are not entirely efficient in removing these metals from contaminated media such as water or soil. As a result low cost, accessible and effective remediation alternatives are required. Interestingly, the area of nanotechnology seems to have opened a new chapter and possibilities of research into heavy metal remediation. It is showing a lot of promise with respect to cost, accessibility and efficiency in removing metal ions from polluted water and soil.

Lead Absorption, Distribution and Excretion

Lead intake and absorption routes are determined by the routes of exposure. As previously mentioned under 'exposure of routes' section; lead entry into the body could be by drinking water, ingestion of food, breathing lead particulates or by dermal contacts. Castellino and Castellino [2] summarize the routes of Pb intake and absorption as via respiratory tract, gastrointestinal tract, skin and placenta.

Lead uptake through the respiratory tract greatly varies from urban to rural areas and to industrial environment. Lead intake via the respiratory tract is a function of particle size distribution, particle shape, solubility and rates of inhalation [2, 3]. Other parameters important in the deposition of lead particulates in the lung include age-related factors for example nose-breathing against mouth breathing, airway geometry and air-stream velocity within the respiratory tract [67]. Deposition of particles in the respiratory

tract is determined by the size. In all nasal cavities, particles the size of 10 μ or greater are removed while particles about 1 μ in size are not removed that easily [3].

Particles can be deposited in respiratory tract by gravitational sedimentation, inertial impaction and diffusion or Brownian movements [2]. Gravitational deposition is important for large particles and mainly in the large bronchi. Inertial impaction occurs, when a particle undergoing laminar flow encounters and obstacle and suddenly changes direction. It is important for particles within the range of 2-5 μm. Particles involved in inertial impaction are deposited on bronchial surface. Brownian movement is important for particles less than 1-2 μm in diameter. These particles acquire a casual movement (Brownian movement) as a result of continual collision with other particles that cannot be compensated for and are thus transported to the alveoli by concentration gradient (from high to low). The compartments are first; nasopharynx or the upper respiratory tract; which begins with the anterior pharynx back and down through the posterior pharynx to the level of the larynx. Second is the tracheobronchial compartment that is "the trachea and bronchial tree down to and including the terminal bronchioles". These two constitute the entire of the epithelial area of the respiratory tract. The third is the pulmonary compartment which consists of respiratory bronchioles, alveolar ducts, atria, alveoli and alveolar sacs. These make up the functional areas of exchange space in the lung [2, 65].

Experiments to measure the half-life of submicron lead particle in the lung have reported values ranging from 6-11.5 hours. This lead to one author concluding that sub-micron lead is cleared from the lung within 24 hours of absorption. Lead particles from the lung are cleared via sequestration by alveolar cells or through the lymphatic vessels to the lymph nodes or it may dissolve in the tissue fluids and pass into the blood [3].

Similarly, Castellino and Castellino [2] categorized the Pb-particle clearance from the lung into two processes which are mucociliary and alveolar clearance. Clearance from the first two compartments nasopharyngeal and tracheobronchial is mainly by mucociliary process. The mucociliary process involves a type of transport in which particles are either shifted from the upper respiratory tract to the gastrointestinal tract or ejected as phlegm. It is a continuous shifting of a layer of mucus toward the esophagus at speeds ranging from mm/minutes or cm/minutes. Larger particles are deposited in the upper tract of the respiratory arbor for quick clearance whilst slower moving mucus particles are cleared slowly from the lower compartments. Alveolar clearing takes place in compartment three. The processes involved include; a) lead particles are transferred form alveolar compartment into mucociliary escalator vial the mechanisms of phagocytosis operated by alveolar macrophages, b) lead particles penetrate through the junctions of the alveolar pneumocytes to interstitial spaces and then into lymph and blood and c) particles pass into the pulmonary tissue where they might remain for a quite sometime [2].

According to Ragan [69], the primary route of entry metal pollutants into the body is the gastrointestinal tract. Dietary intake of lead from recycled Pb in the form of meat and plants leads to direct intake of lead. Also Pb traces may be available in drinking water, milk or beverage for another direct Pb-consumption. In addition, lead can be ingested by infants in the form of contaminated soil, dust and chipped paint. This is particularly important for infants within the ages of 6-24 months. Older infants also have a tendency to ingesting nonfood items which could be Pb-contaminated. Food groups that might be important in Pb transfer include vegetables, cereals, roots, tubers and fruits. Meat products and milk derivatives like cheese might equally be important.

Although the precise mechanism of lead and other trace metal absorption is not entirely understood it is thought to involve both active and passive transport mechanisms [70-72]. The calcium pump which employs active transport mechanism in channeling Ca^{2+} ions is reported to be replaced by other divalent cations including Pb and thus actively transported. In fact, Pb has been reported to be actively absorbed in the rat duodenum and also actively transported out of red blood cells [73, 74]. In a study to examine the evidence of Pb-active transport by calcium pumps using efflux from resealed human red cell ghosts, Simons [70] reports that there was an ATP-dependent net lead transfer from the cell interior to the outside. This author also observed that lead efflux was antagonized by internal calcium and is inhibited by vanadate with the same inhibition constant with which vanadate inhibits calcium pumping. These findings seem to be supported by Deane and Bradbury [72] who found evidence for efflux of Pb^{2+} from brain capillary cells via the Ca^{2+}-ATPase. On the contrary, a study by Deane and Bradbury [72] using in vivo perfusion of Pb in rats revealed evidence for passive transport of Pb that is pH dependent and unaltered by the present of calcium ions. According to these authors, the transport species is $PbOH^{+}$. Other possible mechanisms of Pb transfer reported of in the literature include Pb entry through voltage-gated Ca^{2+} channels in bovine adrenal medullary cells [75], lead uptake by red blood cells via anion transport probably as $PbCO_3$ [76] or store-operated cation channels due to intracellular depletion of calcium stores [71].

Intestinal lead absorption is observed in all parts of the intestine with the most significant in the small intestine [2, 77]. Several factors are responsible for the extent of Pb absorption in the small intestine, perhaps the most important control level is the

intestinal mucosal cells. Primary absorption of Pb is the duodenum from where it enters the epithelial mucosal cells [69, 80]. Important parameters influencing the absorption of Pb include the ingested metal form, the environmental matrix, the gastrointestinal tract contents, diet, nutritional status, age and in some cases genotype [78, 79]. Increasing intraluminal doses causes a relative block of the mucosa cells and substances that increase the solubility of lead enhance its absorption. Iron, zinc and calcium reduce the absorption of lead without affecting its solubility most probably through the competition for shared absorptive receptors in the intestinal mucosa [77, 80-83]. According to Conrad and Barton [80] Pb does not seem to have a feedback mechanism because its total burden does not affect Pb absorption. Researchers have observed that during periods of rapid growth and in iron-deficient animal, lead absorption is greatly enhanced. Contrarily, the cumulative effect of iron-overload and starvation significant reduces lead absorption. A report by several authors showed that intestinal lead absorption in newborn animals and babies are greater compared to young and adults [83-87]. These authors found that lead absorption was inversely correlated with age by a factor of six- to eight-fold from more than 50 % to approximately 10 % or less between the ages of two weeks to eight years in humans.

The concentration of lead in tissues accumulate in the decreasing order of bone > kidneys > liver > brain > muscle [88]. Lead levels in the body are speciated into two pools and these have varied rates of turnover. The slowest and largest pool is found in the skeleton with resident time of more than 20 years. The more labile pool is found in soft tissues and has a consequent half-life of about 20 days [89, 90]. In a survey of lead levels of 60 corpses (four had occupational Pb exposure history) in 1970 by Barry and

Mossman [91], the authors observed distribution of Pb in soft, bone and blood as follows for the non-occupationally exposed group: adult men – soft tissues 9.5 mg (range 5.3-21.1), bone 152 mg (range 21.0-340.9), blood 162.2 mg (range 26.6-352.3), adult females – soft tissues 5.6 mg (range 2.6-8.4), bone 106.8 (range 12-236.6), blood 112.5 mg (range 18.8-243.7) and children – soft tissues 0.55 mg (range 0.12-1.58), bone 0.99 mg (range 0.21-2.4), blood 1.53 mg (range 0.46-3.1). Blood Pb contributions from bone from three groups were 94.1 %, 94.9 % and 64 % respectively. Clearly the important of continuous availability of Pb due to ageing cannot be overestimated.

The most essential routes of lead excretion are through the urine or feces though bile and secretions by glands such as salivary, pancreatic, sweat and mammary play a much less role of clearing Pb from the body [80, 92-93]. Gulson *et al* [94] explains that renal excretion of lead is typically with glomerular filtrate with some renal absorption. Elevated blood levels will lead to augmentation by transtubular transport. Lead may also be excreted with body fluids like milk and for pregnant women; lead crosses the placenta and is transferred to the infant via cord blood. Conrad and Barton [80] employed radio-labeled lead in examining Pb excretion and observed that erythrocytes were important in transporting Pb with excretion occurring in the urine and stool and bile playing an important role in excreting Pb in the gut. Another study by Arai *et al* [92] investigating the excretion of organic lead after injection found that 4 % of administered Pb was excreted in via urine after 7 days post-injection while 68 % was excreted through the feces. According to these authors, approximately 85 % of urinary excretion was diethyllead and 92 % was inorganic lead in the feces.

Lead Toxicokinetics

Toxicokinetic behaviors of lead govern its systemic exposure and associated toxic effects. Understanding the toxicokinetic behavior of Pb requires an interdisciplinary effort in biochemistry, mathematics, physiology and toxicology disciplines [95]. According to Mushak [95], toxicokinetics can be defined in of physico-chemical and mathematical terms or from the perspective of toxicology and epidemiology. The first definition is "the quantification of the rate and extent of lead uptake, distribution/redistribution among transport and deposition tissues, body and tissue retention and finally excretion through various routes". The second is "the biological and toxicological basis for the biological monitoring of lead exposure and the various dose-effect and dose-population response relationships that have been reported".

Lead toxicokinetics is important in quantifying Pb body burden and toxicity. Toxicokinetic models of Pb-uptake are useful in estimating Pb body burden and understanding lead movement between soft and bone tissues. Three models have been most used among toxicokinetic researchers and these include the Leggett model, EPA's integrated exposure uptake biokinetic model (IEUBK) and the O'Flaherty model [95-98]. Both Leggett and O'Flaherty models are physiologically based whilst the EPA's IEUBK is a descriptive model intended to reproduce blood lead concentrations in children up to sevens years of age using urban exposure patterns. A brief description of each of the models is provided below:

The Leggett model is physiologically based model that describes the time-dependent distribution and excretion of lead that has been injected or absorbed into blood [98]. This model is implemented as a central plasma diffusible compartment which is

linked to other tissues and organs within the body. This diffusible plasma Pb is the key central compartment through which Pb is transferred between other compartments of the body including fetus or breast milk. Some organs can be represented by more than one compartment. These compartments consist of bone (n = 6), soft tissues (n = 3), liver (n = 2), brain, kidney, urine, plasma protein, erythrocytes, extracellular fluid [99]. Pb transport between compartments is assumed to follow linear first-order kinetics as long as concentration in red blood cell (RBC) stays below a nonlinear threshold levels. If the RBC concentration of Pb exceeds the threshold value, the transfer rate from diffusible plasma to RBC is assumed to decline linearly with plasma concentration. However deposition fractions in other compartments will increase as a result of reduced competition from RBC but first-order transport between all other compartments are assumed to be maintained at all levels of exposure. Although this model provides a framework to address calcium-like elements, it is considered a starting point for Pb biokinetics in children or adults at high concentrations of exposure but it does not account for sex-related transfers [98, 99].

The US EPA IEUBK model adopts high adult Pb exposure values and applies it to children seven years and lower [100]. This pharmacokinetic model was developed to predict a) risk of elevated blood lead levels in children (under seven years of age) that are exposed to environmental lead, b) the probability that a child exposed to lead via some specified media will have a blood Pb concentration equal to or greater than the threshold value of 10 μg/dL and c) preliminary remediation objectives for a contaminated media [97]. Thus this model is structured to relate environmental Pb concentration with potential blood levels in children via exposure, uptake, biokinetic and blood lead

distribution or variability modules [101-103]. Total or net exposure is quantified amount of lead inhaled or ingested from environmental media such as soil, house dust, drinking water, air or food in μg/g, μg/l or $\mu g/m^3$ typically multiplied by a term to account of amount of contact represented as g/day, m^3/day or liters/day and a term for length of exposure usually days. Uptake refers to the amount of Pb absorbed per unit time from the gut or lung into the systemic blood circulation. Bioavailability or absorption fraction which is the fraction of lead entering the body via respiratory or GI tract is accounted for in the parameterization process. Uptake is measured in μg/day. The biokinetic module employs mathematical expressions to convert total lead uptake rate from the uptake component as an input for the central plasma-extracellular fluid compartment. Then transfer coefficients are used to model transfers between internal components and excretion pathways, thus changing concentration of Pb can be recalculated by combining all the input parameters. Variability in blood Pb distribution is addressed through the log-normal probability distribution [101-103]. Since this model was developed specifically for lead absorption in children, it cannot be used in predicting the impact of Pb exposure on adults Pb kinetics and extrapolations outside of the physiological age will be inaccurate because parameter values used to calibrate the model were strictly kinetic but not physiological [104].

The O'Flaherty model has an age-dependent volume, composition and metabolic activity of liver, kidney, well-perfused, poorly-perfused tissues and bone as compartments [105, 106]. This model uses fractional absorption values; 0.5 at birth to 0.08-0.11 by age 10 in the GI tract. In the lung typical values are 0.5 and these values are independent of exposure level. Pb clearance is set at 30 % from the liver and 70 % from

the kidney. Body clearances, cardiac output, organ and tissue volumes are dependent on body weight and degree of growth. The model takes into account age, body weight by using five-parameter expression that takes into consideration rapid growth at early childhood and accelerated growth at puberty. These values are different for males and females. Lead concentrations in the plasma determine the rate of transfer out blood and this relationship is controlled by capacity-limited Pb binding to erythrocytes. Pb movement between blood and tissues follow flow-limited exchange behavior with deposition in bone or return to plasma via bone resorption or slow exchange throughout bulk bone. Diffusion-limited process describes the slow exchange between plasma and bone. The exposure component of the O'Flaherty is similar to the IEUBK model except the background exposures are date dependent to reflect the marked reduction in Pb levels in air and food since the 1970s. A significant limitation of the model is that it is deterministic and its output does not include estimates of population distribution [96, 104-106].

Lead metabolism in the body is controlled by physiologic and metabolic processes and understanding these processes are crucial for predicting Pb partitioning and toxicity for an organism. Lead is partitioned between blood plasma and the red blood cell (erythrocytes) with this association determining the transport of Pb throughout the body [106, 107]. This relationship can be described as capacity-limited binding of lead by the constituents of erythrocytes. It is reported that Pb binds to constituents of erythrocytes such as hemoglobin, low-molecular weight proteins and to sites on the red cell membrane which are capacity-limited thus leading to changes in blood concentrations [108-109]. In a similar study which is more recent, inductively-coupled plasma mass spectrometry

showed a close association between plasma and red blood cell (RBC) lead with plasma became saturated under high exposure conditions. This situation was attributed to slow gradual saturation of binding sites on the RBC. They also reported that RBC Pb binds to delta-aminolevulinate dehydratase (ALAD), albumin and α-globulin [106, 110-111].

Liver and kidney are important excretion pathways of lead as well as exhibiting higher concentration of this toxicant than other soft tissues. Lead rapidly accumulates in the liver between 10-15 % of systemic Pb although much of it is lost within a few weeks. Adults who have been exposed for long periods have 2-3 % of total-body lead in the liver and the ratio between blood to liver is 0.2 [98, 112-113]. Pb is lost from liver by biliary secretion into the gastrointestinal tract and a possible Pb recycled to blood. Rodents and dogs intravenously injected with radio-labelled Pb accumulate about 15-20 % in the kidney within the first 1-2 hours with a substantial portion of the early accumulation is reabsorbed or lost via urine. In the case of rats, the kidneys accumulated approximately 10 % of intravenously injected Pb after day and less than 2 % post-injection. Similarly, baboon kidneys contained 4 % after day 1, 0.6 % after 30 days and 0.1 % after 60 days post-injection of radio-Pb [98, 114-115]. Comparing the rate of Pb clearance from the kidney, it was estimated that the half-life of intravenously injected Pb in baboon kidneys will be one-half that in the liver for the first two months.

Lead is reported in the literature to follow the movement of calcium to a greater degree and that it is physiologically controlled in a manner similar to that of calcium. This is particularly true for its behavior in bone. Pb is found to compete with calcium for bone deposition and similarly distributes among different bones, between trabecular and cortical bone structures [98, 116-117]. Data inferred from healthy adult male humans,

baboons and beagles show that the adult skeleton may accumulate 10-15 % of radio-Pb intravenously injected within the first hours of injection. Over the first day or two, there was a decline bone radio-Pb content and then a gradual increase over a period of weeks as Pb is returned from soft tissues through plasma and erythrocytes for deposition in the bone. After 3-4 weeks post-injection, the bone accumulated about 25 % of administered Pb. Also, Pb was reported to initially concentrate in trabecular bone than cortical bone and this is supported by a study in dogs that found five times radioactive Pb in trabecular bone compared to cortical bone [98].

One theme that has been repeated throughout the previous paragraphs of lead toxicokinetics is that age and physiological status significantly influence Pb bioavailability and metabolism. In the following sections these factors are discussed.

Pregnancy and lactational periods are probably an important period of lead exposure for both the unborn infant and a child on breast milk [118-121]. Lead mobilized during pregnancy because the bone is resorbed in order to produce the fetal skeleton. For example when lactating and nonlactating mice were intravenously administered 0.05 mg of Pb, lactating mice had twice the Pb volume in plasma compared to nonlactating. Pb clearance in plasma was 4.25 liter/hr/kg in lactating mice and 1.07 kg/hr/kg in nonlactating mice whilst one-third of injected Pb was excreted via milk [120]. In a similar study in Australia, female migrants who were of child bearing age were monitored during gestation and for up to six or more months after pregnancy to examine the effect of lactation on Pb mobilization from the skeleton. Results revealed that breast milk could contribute between 36-80 % infant blood Pb levels and a significant correlation between Pb concentrations and breast milk, blood, urine and diet for infants

and mothers [121]. Pb was reported to be transported to milk by binding to specific and nonspecific carrier proteins [123]. The simple reason for increased blood Pb levels in breast milk is physiology. According to Goyer *et al* [122], bone turnover is affected by pregnancy, lactation, osteoporosis and certain disease states which are likely to produce a rise in lead mobilization from skeleton, thus increasing blood Pb levels. This statement is supported by Franklin *et al* [118] from a study involving monkeys using stable Pb isotopes. They observed a 29-56 % reduction in bone lead mobilization in the first trimester followed by an increase in the second and third trimesters up to 44 %. Also, maternal and fetal bone, brain, liver and kidneys showed substantial transplacental transfer of endogenous Pb. About 7-39 % of fetal skeletal Pb originated from maternal skeleton due to bone resorption to meet the required calcium levels for the developing fetus. Zeigler *et al* [124] investigated the metabolic activity of 12 infants ranging from 14 to 746 days in 1978. The authors report a daily intake of Pb was more than 5 μg/kg with an average absorption of 41 % and net retention of 31.7 %. For infants whose daily intake was less than 5 μg/kg had greater fecal Pb excretion than intake with means absorption approximately 5 %.

O'Flaherty [126] stated that bone loss is a natural ageing process. Ageing is accompanied by numerous degenerative processes most of which increase vulnerability to exogenous and endogenous toxicants, an example being lead [125-126]. Bone mass plateaus at ages 25 to 30 years and gradually reduces thereafter for both men and women. Researchers have observed higher blood Pb levels in post-menopausal women which they attribute to bone resorption with age followed by mobilization of lead previously sequestered in bone. Follow up studies by others also reported similar results. They found

Pb in both midfemur and pelvic bone declined steadily with age in the human population from 50 years and above with the most pronounced effects in females [125]. As previously pointed out, lead both competes with and mimics calcium the main constituent of bone. Lead has been shown to be incorporated into the crystalline structure of bone replacing calcium at some sites. It is buried beneath the surface in areas of bone formation and is eventually distributed throughout the bone volume. Bone cell metabolizes Pb similar to calcium. Most of the Pb in bone is rapidly exchangeable and is controlled by the same ions and hormones that modulate bone calcium metabolism, nevertheless, high Pb content will damage bone cells and interfere with bone remodeling [98]. Once in the bone, Pb is slowly diffused by exchange from the bone via canaliculi to blood or by structural remodeling involving resorption of bone by osteoclast cells and then new mineral apposition follows [105].

Health Effects Associated with Pb^{2+} Exposure

The health effects associated with Pb exposure reported in the literature are numerous. These range from unobservable symptoms to extreme cases of death in exposed victims. This section is organized into health effects manifested via neurobehavioral, cancer, genotoxic, reproductive, developmental and immunological [5].

Neurobehavioral Effects

The early symptoms of lead neurotoxicity in both adults and children include diffuse muscle weakness, general fatigue, joint pain or arthritis, loss of appetite, headache, insomnia, irritability, diminished libido, decreased attention span and

personality changes [195]. Chronic lead exposure could produce abdominal pain or cramping, nausea or vomiting, depression, short-term memory loss and depression with severe blood Pb over 30 μg/dL in victims showing signs of frank paralysis, severe lethargy and abdominal colic. The most reported and severe lead neurotoxic symptom in adults is peripheral neuropathy and encephalopathy (general term to describe disturbance of brain function [195, 197]. Children with blood Pb levels ranging from 10-35 μg/dL are at risk of lowered IQ and poor attentiveness. Goyer [196] reported that typically children with blood Pb content below 25 μg/dL were found to have reduced IQ scores. In the assessment of children at 4 years of age, the apparent IQ value had reduced between 1 and 5 IQ points for every 10 μg/dL increase in blood lead. Järup [197] also made similar conclusions after meta-analysis of four prospective studies in Boston, Cincinnati, Port Pirie and Sydney. The combined evidence from these four studies, show a mean reduction of in IQ of 2 points for 10 μg/dL rise in blood lead level at the 95 % confidence interval.

It is quite obvious from the previous paragraph that the neurotoxic effects on children are more severe than on adults. This is likely due to because gastrointestinal absorption of Pb by children is much higher than adults, systemically circulating bioavailable Pb is able to gain a greater access to the brain of children than adults and the vulnerability associated with the developing nervous system [198].

Several neurotoxic mechanisms of Pb actions have been documented to explain the processes through which lead exerts its negative cellular influence. Lidsky and Schneider [198] classed Pb neurotoxic mechanisms as direct and indirect whilst Goyer [196] defined it as being morphological and pharmacological. The neuropharmacological

interactions include substitution for calcium, neurotransmitter release, protein kinase C, Na-Ca ATPase and energy metabolism. Morphological interactions on the other hand consist of interference with adhesion molecules, impaired cell:cell programming connections and miswiring of the central nervous system. Lead is thought to cross the brain barrier rapidly by disrupting the brains' main structural components as a result of injury to astrocytes and endothelial microvasculature. Once in the brain, lead is found to affect two key proteins involved in learning and cognitive function, protein kinase C and N-methyl-D-aspartate subtype glutamate receptor. Other studies have attributed Pb's neurotoxicity to its ability to influence several biological activities at various levels of regulation due interference on regulatory action of calcium function in cells. So, lead can interfere with homeostatic cellular processes thereby acting as a chemical stressor [199, 200]. Detailed mechanisms of lead toxicity are also discussed under the section on "lead toxicity mechanisms".

The implication of the above observation is that there is apparently no threshold below which lead is without effect on the central nervous system. The only problem associated with this statement is the inability to quantify effects at very low lead exposure. However recent findings have suggested toxicological effects at low dose lead exposure [197, 200].

Developmental Effects

This section examines the effect of Pb on growth parameters that are neither neurological nor behavioral. A number of epidemiological studies have investigated the relationship between Pb exposure and growth parameters such as body weight, stature

and head circumference. For example, a study of 223 mother-infant pairs in Mexico found that increasing tibia and patella bone Pb results in decreasing birth length, birth weight and head circumference of newborns respectively, with an estimated increased risk of 1.02 μg/g [201, 202]. A similar study was conducted on 329 mother-infant pairs to examine the association between breast milk Pb and anthropometric feature, weight gain. The authors reported that infant Pb content was negatively related to weight gain. They also found that exclusively breast-fed babies had significantly higher weight gains, nevertheless this weight gain declined significantly with rising patella Pb [203]. Other studies carried out in Spain, Russia, Norway and the U.S. have not been consistent. Women from Camden, New Jersey with blood Pb of 1.5 μg/dL did not produce any significant association between low birth weight and preterm delivery while the study involving Russian and Norwegian women with maternal and cord blood of 1.2 μg/dL negatively impacted birth weight and body mass index. Similar results were reported for Spanish women who had much higher placental blood levels. Birth weight, head, abdominal circumference or shorter length at birth were not affected [5].

One part of the body likely to experience inhibition of growth is the skeleton. According to Ronis *et al* [204], the growth of the skeleton is the primary stimulator of somatic development. It is reported in the literature that Pb can accumulate in the bone throughout the developmental period, localize in regions of bone mineralization and growth, delay growth plate chondrocyte maturation and inhibit bone formation and mineralization [205, 206]. Specifically, male and female rats exposed to lead showed reduced somatic growth, longitudinal bone growth and bone strength during the period of puberty [204].

It has been reported recently that lead exposure might delay growth and pubertal development in girls. A study of 600 non-Hispanic white, 805 non-Hispanic African-American and 781 Mexican-American girls with blood lead concentration of 3 μg/dL or less, showed significant delays in breast and pubic-hair development in African-American and Mexican-American girls with no effects at this concentration in white girls. African-American girls were the most affected. Using Tanner staging (as described in the Physician Examiners Training Manual), African-American girls experienced delays in reaching Tanner stages 2, 3, 4 and 5 due to lead exposure of 3 μg/dL compared with 1 μg/dL at 3.8, 5.3, 5.8 and 2.1 months correspondingly for breast development and 4.0, 5.5, 6.0 and 2.2 months respectively for pubic-hair development. Menarch delay was at 3.6 months [207]. A similar study of 1,706 girls ages 8-16 with blood Pb ranging from 0.7-21.7 μg/dL found higher blood Pb to be significantly associated with delayed attainment of menarche and pubic hair but not with breast development [208]. Both study accounted for race/ethnicity, age, family size, residence in metropolitan area, poverty income ratio, body mass index and any other confounding factors that might be important.

Lead Carcinogenecity

Lead is considered a probable carcinogen by the EPA [176] whilst the Department of Health and Human Services consider lead and its compounds as posing reasonably anticipated human cancer risk [177]. The International Agency forRresearch on Cancer (IARC) also said inorganic lead is probably carcinogenic to humans though organic Pb could not be classified as to its carcinogenicity to humans [178]. The classification by

these agencies reflects the limited evidence of cancer in humans due to lead exposure. Several studies in Britain, Sweden, Italy and Finland among occupationally exposed individuals found limited evidence of brain, spleen, stomach, lung, kidney, bladder and overall cancer risk [179-182].

So far, the most evidence demonstrating the possibility of lead as a carcinogen has come from animal models. The experiments have focused on transplacental or translactational, oral, subcutaneous, intratracheal, intramuscular and intraperitoneal administration of inorganic Pb to rats, mice and hamsters [183]. Most of the tumors that develop from these routes of exposure are renal tumors. The process involves alterations in glomerular function as seen in proteinuria then acute morphological changes that might slowly progress to chronic irreversible nephropathy finally to adenocarcinoma. Initial transformations include the formation of lead-protein inclusion bodies (nuclear inclusion bodies) and ultrastructural damage in cellular organelles particularly the mitochondria.

Although cancinogenic effects of Pb are not obvious, it is thought to play a facilitative or permissive role in cancer induction. In his recent review, Silbergeld [183], stated "epidemiological and mechanistic data are consistent with a facilitative role for lead in carcinogenesis, that is lead by itself may not be both necessary and sufficient for the induction of cancer but at a cellular and molecular level lead may permit or enhance carcinogenic events involved in DNA damage, DNA repair and regulation of tumor suppressor and promoter genes".

Immunological Effects

Most of the studies examining the influence of lead on immunological parameters have been inconclusive. While some reported negative effects, others did not find any association between blood Pb levels and IgA, IgG, IgM and peripheral blood lymphocyte phenotypes including T cells, B cells, NK cells and CD4/CD8 subsets [5]. A study by Kimber *et al* [170] among workers whose blood Pb levels range from 25 to 53 μg/dL found no significant IgA, IgA and IgM concentrations from unexposed group. This finding is supported by Alomran and Shleamon [171] and Basaran and Ündeger [172]. These authors report that mean blood Pb concentrations of 64 and 74.5 μg/dL produced no significant alterations in IgA and IgM compared to non-exposed control group however IgG was significantly reduced. On the contrary, Ewers *et al* [173] showed a significant decline in serum IgM which they associated with increases in colds and influenza with age. In this study, neither serum IgA or IgG were significantly different. Salivary IgA, a major factor in defense against respiratory and GIT infections, was significantly reduced compared to control group.

Experimental observations involving *in vitro* and *in vivo* models and children reported in the literature appear similar to above results seen in adult human beings. For example, Bauer *et al* [174] employed dynamic light scattering to study the effect of Pb and other heavy metals on aggregation behavior of rat IgG1 and antibody-antigen complexation with monoclonal mouse IgG1 and found Pb to interact with antibodies and immune complexes thereby inducing large soluble aggregates. The authors also found no effect on antibody-antigen binding activity even at very high concentrations of Pb treatment. Similar results were reported for female pregnant rats exposed to Pb during

breeding and pregnancy. No alterations were observed in immune function. However, the offspring showed altered cytokine production and a rise in serum IgE [175].

Reproductive Effects

There is evidence in the literature supporting an association between occupational and environmental Pb exposure to reproductive anomalies such as abortion and pre-term delivery in women and changes in sperm and a decline in fertility in men [5]. In the past, occupational high Pb exposure in pregnant women in certain parts of Europe showed increases in spontaneous abortions, stillbirths, premature births and neonatal deaths [184]. Fairly recent epidemiological studies in Mexico City, Mexico and Port Pirie, Australia revealed the possibility of moderate blood Pb levels causing spontaneous abortion (loss of pregnancy by gestation week 20) and still birth. Mean blood-Pb content of cases and control were 12.0 and 10.1 μg/dL respectively while that of the Port Pirie were 10.6 and 7.6 μg/dL [5, 185] correspondingly. The Mexico study found correlation between increasing blood levels and spontaneous abortion at 1.13-fold. On the contrary, the Port Pirie study did not find any association between blood-Pb levels between exposed and control residents but reported 22 of 23 miscarriages and 10 of 11 stillbirths at Port Pirie compared to 1 miscarriage and 1 stillbirth outside of Port Pirie. Experimental evidence of Pb effects in women from animal models include reduced concentration of progesterone which might be due to impaired luteal function, longer and greater variability in menstrual cycles, shorter menstrual flow, suppressed levels of luteinizing hormone and follicle-stimulating hormone [5, 188].

Men are likely to contribute to spontaneous abortions via passage of Pb through the semen to the mother, lead in work clothes, equipment, hands and changes in sperm [185]. Men exposed to relatively high Pb levels are at risk of male-infertility due to the quantity and quality of sperm production. This has been observed in experimental samples as reductions in sperm concentration which are indications of alterations in sperm chromatin, asthenospermia, hypospermia, teratospermia, reduced seminal plasma constituents, reduced motility, low semen volumes, reduced functional maturity of sperm and most importantly below normal and total sperm count relative to control groups. Most of the studies documenting Pb reproductive effects in men report at least mean blood-Pb levels of 35 μg/dL. Pb minimizes sperm quality and quantity by alterations in chromatin, act directly on the testes causing depression of sperm count and peritubular testicular fibrosis, reduced testosterone, disruption of regulation of luteinizing hormone and DNA-protamine packing [5, 186. Lead is likely to compete with or replace Zn atoms normally bound to nuclear protamines as a result of its binding to free thiols, which might affect disulfide bond formation and thus alter DNA-protamine biding or impair chromatin decondensation during fertilization [187].

Genotoxic Effects

Experiments testing the genotoxicity of Pb *in vitro* and *in vivo* models have produced inconsistent results, which seems to be the case in humans as well. For example an epidemiological study of battery plant workers in Poland using micronucleus (MN), in situ fluorescence (FISH), analysis of sister chromatid exchange (SCE) and the comet assay found increased incidence of MN in peripheral lymphocytes due to either clastogenic and aneugenic effects. Also, there was a significant rise in the frequency of

SCEs and leukocytes with DNA fragmentation relative to controls. Blood Pb concentrations ranged from 282-655 μg/dL for the exposed group and 17-180 μg/dL for the control population [189]. Contrarily, 78 individuals exposed to mixtures of cadmium, cobalt and lead found no correlation between Pb-exposure and DNA single strand break [190].

The mechanism of lead genotoxicity is considered to be indirect. In the literature, only one article reported that G. C base pairs might be the primary target for lead mutagenesis [191]. Other processes reported include inhibition of nucleotide excision repair [192], production of reactive oxygen species by rapid induction of hydrogen peroxide or stimulation of activities of copper-zinc superoxide dismutase and xanthine oxidase [193]. Although lead is considered by most researchers as a weak mutagen, it could be a potent comutagen and this has been demonstrated *in vitro* by de Restrepo *et al* [194]. According to these authors, lead sensitizes cells to damage in order to induce genotoxicity.

Lead Mechanisms of Action

Lead Toxicity Mechanisms

Lead is known to either replace or interact with polyvalent cations such as calcium, and zinc ions in the molecular machinery of cells so that lead can affect diverse biological processes in living organisms. Examples of these processes include metal transport, energy metabolism, apoptosis, ionic conduction, cell adhesion, inter- and intracellular signaling, various enzymatic processes, protein maturation and genetic regulation [127, 128]. Essential metal ions in biological systems have functions including

charge carriers, intermediates in catalyzed reactions and structural components or elements for stabilization of proteins. These essential metal ions have binding sites that facilitate selectivity and functionality. For instance the binding-sites of calcium are wide, regular charge distribution to facilitate quick ion exchange, oxygen atom conformation and coordination numbers of 6 and 7. Zinc binding-sites on the other hand involve sulfur and nitrogen atoms that have high zinc affinity slowing exchange of zinc and have low coordination numbers [129, 130].

Selectivity of metal-binding sites is limited to essential metal ions in the cell, thus environmental contaminants like Pb^{2+} which can mimic physiologically important metal ions become a major problem for the cell because there is a lack of specific mechanism to deal with them. In the case of calcium, it does not have a strong enough affinity to bind to zinc-binding sites while zinc cannot be dehydrated by calcium coordinating groups for it to bind to calcium sites. Other ion-specific features like electronegativity, coordination geometry, preference for ligand atom, electric charge and ionic radius ensure that metal interaction with protein targets are specific [129, 130]. The electronegativity of zinc is 1.65 while that of Pb is 2.33.

According to Godwin [131], lead is ubiquitous in its ability to bind several protein targets because it can interact in a flexible coordination number with oxygen and sulfur. In fact zinc binding sites made up of thiols have the most affinity for Pb due to the strong bonds that lead forms with sulfur. Magyar *et al* [132] examined the interaction of Pb(II) with thiol-rich structural zinc-binding proteins using X-ray absorption spectroscopy. The authors found that whilst zinc binds in a four-coordinate mode, Pb(II) binds in a three-coordinate Pb(II)-S_3 mode, which is consistent with trigonal pyramidal Pb(II)-S_3 model.

But this is at odds with the small molecule complexation literature that suggested Pb(II)-S_4 as the preferred mode of binding. These authors reexamined the above literature and found that the coordination number of Pb(II)-S4 is 5, 6 or 8 which means Pb avoids the four coordination in sulfur rich environments and instead adapts trigonal pyramidal in Pb(II)-S_3 or Pb(II)-S_{5-8}.

Perhaps the most important metal ion in the body is calcium. It has an ionic radius of 0.99 Å and is required for bone building, blood clotting, may act as a second messenger in signal transduction, muscle contraction triggering and transmission of nerve impulses [129]. Maintaining a stable level of calcium in the extracellular space and cytosol requires use of calcium pumps which create concentration gradients and selective binding of calcium-binding proteins like calmodulin. Calcium has an electronegativity of 1.0 with a charge distribution that is spherical. Calcium binding motifs are made up of 6 or 7 metal-bound oxygen atoms, though sometimes they can be eight. For instance in the mannose-binding protein complexed with oligosaccharide, calcium motifs within the protein have coordination number of 7 or eight if the substrate is included [129, 133]. Similarly, the calmodulin binding site has seven oxygen atoms at the vertices of pentagonal bipyramid coordinated to the central Ca ion at approximately 2.4 Å [134]. There is evidence supporting the binding of lead to predominantly calmodulin [135]. This Calmodulin protein is intracellular calcium binding receptor protein that is enriched in neurons and therefore regulates neuronal processes like neurotransmission, axoplasmic transport, cellular cytoskeleton, cAMP metabolism, protein phosphorylation and memory [135]. Calmodulin has an "EF-hand" domain and C2 motifs that have a high affinity for Pb [127, 136-137]. The EF-hand is made up of about 29 amino acid residues and has a

helix-loop-helix arrangement. Binding of calcium and other metals to this site is due to conformational changes that exposes hydrophobic regions of the protein. The C2 domain has approximately 130 residues with its main mechanism of binding to metal ions considered to be an 'electrostatic switch' because domain modifications are electrical rather than conformational and thus C2 motifs interact directly with biological membranes 127, 138-139].

In the bone, a non-collagenous protein osteocalcin has been reported to have a higher affinity for Pb than calcium at similar concentrations. This protein is exclusively synthesized by osteoblasts and odontoblasts and is made up three calcium binding residues γ-carboxyglutamic acid. The protein is documented to be involved in bone resorption, osteoclast differentiation, crystal formation and growth and may also play a role in the regulation of bone formation and remodeling [140].

Lead is reported to interact either directly or indirectly with molecules (calcium channels, calcium binding proteins and calcium dependent kinases) involved in signal transduction and gene expression regulation [141-145]. Signal transduction by lead is reported in the literature to be primarily protein kinase C (PKC) or calmodulin II (CaMKII) mediated although some other kinase-dependent mechanisms have been documented [142, 146-147]. PKC belongs to a family of phospholipid-dependent serine-threonine protein kinases crucial to many signal transduction pathways. The interaction of lead with PKC is not straightforward. Low lead levels were observed to replace calcium in PKC whilst high Pb-concentrations inhibited the activity of PKC. At the molecular level, Pb is found to regulate the mRNA expression of PKC via c-fos induction. Similarly, the activity of CaMKII is directly modulated by Pb or indirectly via

the stimulation of adenylyl cyclase and phosphodiesterase. Recently, studies have shown the possibility of lead effecting signaling pathways via not directly linked to PKC and CaMKII pathways. Leal *et al* [143] employed adrenal chromaffin cells and human SH SY5Y cells to investigate the effect of Pb^{2+} on protein phosphorylation. The authors found a significant rise in the number of proteins phosphorylated and they concluded that lead can modulate the phosphorylation of heat shock protein (Hsp27) through the activation of $p38^{MAPK}$ pathway.

A few studies have examined the role of Pb^{2+} on mRNA expression. These studies were designed to either exploit pathways that involve the production of reactive oxygen intermediates since the literature is emphatic on the increased cellular oxidative stress due to lead toxicity or the Mitogen-activated protein kinase (MAPK) family because activation of some members of this family could lead to activation of transcription factors and apoptosis. MAP kinases are grouped into four distinct groups which include extracellular signal-regulated kinases (ERK)-1/2, Jun NH_2-terminal kinases (JNKs) $p38^{MAPK}$ and ERK5. Ramesh *et al* [142] studied the effect of lead on oxidative stress proteins nuclear factor kappa B ($NF\text{-}_KB$) and activator protein (AP-1) and mitogen activated protein kinase (MEK) and JNK in murine pheochromocytoma cells (PC-12). Their results showed an up-regulation of MEK and JNK. Also, $NF\text{-}_KB$ and AP-1 were activated by Pb whilst the inhibitory subunit of $NF\text{-}_KB$, $I_KB\alpha$ was degraded. Another study was carried out by Hanas *et al* [141] to elucidate the mechanisms by which Pb might alter the DNA-binding of cysteine-rich zinc finger protein. These zinc finger proteins are thought to play roles in regulating gene expression, signal transduction, cell growth and differentiation and chromosome structure. In this experiment, the effect on Pb

on Cys_2His_2 zinc finger protein transcription factor IIIA (TFIIIA), transcription factor Sp1 and another Cys_2His_2 finger protein that binds GC-rich regions in RNA polymerase II were assessed. Results revealed inhibition of DNA-binding by TFIIA, Sp1 and another Cys_2His_2 finger protein with indications that inhibition mechanism minimally involves N-terminal fingers of TFIIIA. A similar study was conducted by Ghering *et al* [169] using spectroscopy to evaluate the binding of Pb^{2+} to GATA proteins. GATA proteins are considered transcription factors that have affinity for GATA DNA elements via Cys_4 structural zinc binding motifs. These proteins are important in regulating neurological and urogenital development and the onset of cardiac disease. The affinity of Pb for C-terminal domain from chicken GATA-1 (CF) and double-finger motif from human GATA-1 (DF) were assessed spectroscopically. Pb^{2+} coordination with CF and DF were observed in the near-UV (250-380 nm) spectrum as the appearance of intense bands as lead forms tight complexes with cysteine residues in the zinc-binding sites as well as displacing Zn from CF and DF. The presence of lead also reduced the ability of GATA to bind DNA and subsequently induce transcription.

Lead is known to effect the regulation of the synthesis of heme. Pb is reported to reduce the bioavailability of heme via induction of hepatic expression of heme oxygenase thereby degrading heme and also the inhibition of the enzyme, delta aminolevulinate synthase through heme synthesis pathway [144]. This eventual decline in heme production levels was observed to decrease the function of P450. The cytochrome P450 family of heme containing proteins that are essential for the oxidative metabolism of both and endogenous and exogenous compounds. This family of proteins is responsible for transforming xenobiotics to non-toxic or carcinogenic metabolites [145, 148]. In the liver,

P450 is a major hemoprotein so that the inhibition of heme will interfere with the biogenesis of functional P450. Two ways this is considered to take place include incomplete saturation of P450 apoprotein due to insufficient heme supply or the reduction in the synthesis of P450. Jover *et al* [145] concluded from their study of the role of heme in cytochrome P450 transcription and function in mice treated with lead acetate that, the mechanism involved is two-fold. The first is independent of heme, in that lead reduces the transcription of P450, whilst the second is heme-dependent, in which synthesis of heme is inhibited and consequently decreases the heme saturation of P450 and/or apo-P450 level. Another study by Korashy and El-Kadi [148] revealed the mechanism of heavy metals including Pb regulating the transcription of P450 specifically Cyp1a1 to be aryl hydrocarbon receptor (AhR) dependent. The authors found that the inhibition of AhR degradation enhanced the induction of Cyp1a1 mRNA transcript. Also, Pb and other heavy metals reduced the degradation rate of Cyp1a1 protein, a rise in heme oxygenase-1 (HO-1) with a consequent decrease in cellular heme levels.

Another documented mechanism by which lead toxicity is observed is the interaction with ion channels particularly calcium and potassium channels. This mechanism of action is considered the primary mode by which Pb is a neurotoxin [149, 150]. These authors report that lead acts as a depressant of voltage-operated calcium channels, N-methyl-D-aspartate receptors, adenylate-cyclase and delayed-rectifier potassium currents in neurons. Pb^{2+} acts as a competitive antagonist to Ca^{2+} in blocking Ca^{2+} channels identified in electrophysiological experiments as Pb^{2+} induced blocking of end plate potential (EPP) because of reduced amplitude of the EPP and this effect is reversible [150]. Similarly, micromolar concentrations of Pb^{2+} were reported to be a

reversible blocker of delayed-rectifier potassium currents in hippocampal neurons and this effect is voltage-dependent [149].

Reducing the Toxicity Effect of Pb^{2+} Exposure

In this section, a brief description of current strategies that are employed in reducing the toxic effects of lead is provided. Most of the strategies outlined here are reported in the literature, for which some are actual clinical practice, others are experimental evidence which is not proven and therefore should not be considered as a guide for treatment of lead exposure.

As is always the case, prevention is better than cure. Creating conditions that reduce environmental lead levels will continue to be the most effective way of minimizing exposure to lead and its consequent health effects. As pointed out in other parts of this write-up, deficient levels of calcium, iron and zinc enhances the absorption and metabolism of Pb^{2+} because calcium, iron and zinc have been observed to inhibit the absorption of Pb^{2+} from the gut. In fact a number of studies involving children, pregnant women and nursing mothers examining the role of dietary supplements of these essential metals and found them to significantly reduce Pb absorption and metabolism [5, 94, 195, 156-158]. Thoroughly washing of skin with soap and water or flushing of eyes with water or saline following acute exposure to lead is recommended. Ingestion of lead compounds is removed by gastric lavage or whole gut lavage using osmotic neutral polyethyelene glycol electrolyte solution (GO-Lytely®) or employing surgical excision to remove lead bullets or shrapnel [5].

To reduce the body burden of lead, chelation agents are typically used. These agents are able to bind inorganic Pb to facilitate its transfer from soft tissues to the circulation system so that excretion is enhanced via the kidney. Obviously extra precaution is need for patients with renal problems. Chelating agents in use currently include dimercaprol (British Anti-Lewiste, or BAL), $CaNa_2$-EDTA (EDTA), penicillamine and 2,3-dimercaptosuccinic acid (DMSA; Succimer®) [5, 195, 159-161]. Guilarte *et al* [162] proposed environmental enrichment as an alternative to chelation therapy for childhood lead intoxication. The authors defined environmental enrichment as the "combination of complex inanimate objects and social stimulation" which was found to enhance the recovery of deficits in N-methyl-D-aspartate receptor subunit 1 mRNA and induction of brain-derived neurotrophic factor (BDNF) mRNA in the hippocampus. Long-term potentiation, a cellular model for learning and memory and spatial learning are controlled by N-methyl-D-aspartate type of glutamate receptors (NMDAR) that is also inhibited by Pb. Exposed Pb^{2+} animals that were provided enriched environments had learning impairments reversed.

Lead Regulation of Gene Expression

Several genes transcripts are reported in the literature to be regulated by Pb either directly or via some other consequential means. In the last several years, studies involving Pb have shifted focused on elucidating how Pb regulates mRNA transcription. This section will look at some of the studies designed to understand the role of lead in the expression of genes.

Cabell *et al* [163] stated that one possible means by which lead might induce the synthesis of heme oxygenase-1 (HO-1) is oxidative stress. HO is plays a crucial role in heme catabolism. It oxidatively cleaves the porphyrin to form biliverdin. Heme oxygenases include HO-1, HO-2 and HO-3 isoforms. HO-3 has low heme oxygenase catalytic activity whilst HO-2 though expressed in many cell types is less induced by most stress types. The expression of HO-1 gene is controlled by heat shock element, metal-responsive element, antioxidant response element, AP-1, NFκB and Sp1. Lead is reported to cause increases in hydroxyl radicals, lipid peroxidation, enhanced production of reactive oxygen species, increased levels of reduced glutathione (GSH) which is will consequentially induce the synthesis of a number of stress proteins. According to these authors, HO-1 synthesis is induced in astrocytes but not hippocampal neurons, and this induction was reduced by the presence of radical scavengers dimethylthiourea (DMTU) and mannitol but not by inhibitors of calmodulin, calmodulin-dependent protein kinase C or extracellular signal-regulated kinases (ERK), leading them to suggest the importance of oxidative stress as a mediating event in the induction of HO-1 by Pb^{2+} in astrocytes.

Lead is also cited to effect the expression of inducible nitric oxide synthase (iNOS). NO from iNOS mediates immune defence as well modulating gene transcription, translation and protein function. In this study by Eckhardt *et al* [164], $PbCl_2$ increased NO production and iNOS activity in a dose-dependent manner in pancreatic β cells. They also found an increase in iNOS mRNA expression and iNOS protein content as determined by semi-quantitative reverse transcriptase-PCR and Western blotting respectively, leading them to conclude that Pb^{2+} up-regulates iNOS gene expression at the level of transcription.

Other studies have employed cloning techniques to understand the role of heavy in inducing transcription. Cheung *et al* [165] isolated gene sequences of tilapia metallothioneins (tiMT) and characterized them *in vitro* using cultured cell lines PLHC-1. Administration of Pb^{2+} and other heavy metals showed the induction of tiMT transcription. A similar cloning experiment in which zebrafish metallothionein (zMT) was isolated, characterized in HepG2 cell line and exposed to Pb2+ and other heavy metals revealed the inability of lead to induce zMT transcription *in vitro* [166]. Metallothioneins are low molecular weight cysteine-rich that intracellularly binds proteins for the control of essential and detoxification of non-essential metals. MTs are important metal homeostasis, acts as chelating metal ions via the formation of metal-thiolate bonds or provide Cu^{2+} and Zn^{2+} reservoirs required in the biosynthesis of metalloenzymes and metalloproteins.

Another investigation to determine the role of the binding activity of AP-1 in PC12 cells revealed this binding to be dependent on protein kinase C (PKC) [167]. Activator protein-1 complex (AP-1) is a homodimeric complex that has members of jun family or a heterodimer with family members jun and fos. Jun family members are c-Jun, JunB and JunD whilst fos members are c-Fos, FosB, fos-related antigen-1 (Fra-1) and fos-related antigen-2 (Fra-2). AP-1 complex has a high affinity and binds specifically to DNA consensus sequence –TGACTCA- close to the promoter region of the early response gene. Results from this experiment show a rise in AP-1 derived transcription with an increase in AP-1 DNA binding activity that requires PKC. Inhibition and depletion of PKC reduced increase in AP-1 DNA binding in the presence of Pb^{2+} while

the use of specific antibodies in supershift assay implicated Fra-2 and JunD as the main components responsible for increased activity due to Pb^{2+}.

Korashy and El-Kadi [168] examined the differential effects of heavy metals mercury, lead and copper on the constitutive and inducible expression of aryl hydrocarbon receptor (AhR)-regulated genes; Cyp1a1, NAD(P)H: quinone oxidoreductase (QOR) and glutathione S-transferase Ya (GST Ya) in cultured hepatoma Hepa 1c1c7 cells. AhR is basic helix-loop-helix transcriptional factor that is ligand-activated found in the cytoplasm and bound to 90-kDa heat-shock proteins (HSP90) and AhR interacting protein (AIP). When bound to a ligand, AhR is activated, thus HSP90 and AIP are dissociated subsequently leading to a translocation of ligand-receptor complex to the nucleus where it forms a heterodimer with transcriptional factor protein, aryl hydrocarbon receptor nuclear translocator (ARNT). To initiate mRNA transcription, AhR/ARNT binds to a specific DNA sequence called the xenobiotic-responsive element (XRE) found in the promoter region of Cyp1a1 [148]. Lead alone did not change significantly the Cyp1a1 activity and protein content but mRNA expression was significantly increased, however in the presence of a ligand, no Pb^{2+} effect on Cyp1a1 was observed. Both the activity and mRNA expression were increased by lead in absence and presence of AhR-ligand. Again Pb increased the activity and mRNA of GST Ya.

CHAPTER III

ASSESSING LEAD EFFECTS USING ICP-MS AND HISTOPATHOLOGY

Introduction to Study

The importance of lead as an environmental chemical species exhibiting various form of toxicity in humans has been well documented. [227-230]. As a result of its past uses history, lead is widely distributed in water, soil and air. This is particularly of great importance considering lead use in gasoline and paint was curtailed more than two decades ago. As a result, the potential exposure to significant lead levels, especially infants in the population, is high [5].

Pb exposure targets organ systems such as the skeletal, hematopoeitic, renal, endocrine and nervous systems [231], thereby partitioning between soft and hard tissues in the body with approximately 95 % and 70 % being found in the bones and teeth of adults and children, respectively. Bone then serves as a pool to replenish excreted lead from blood. Some adverse conditions associated with lead poisoning include DNA damage, neurological impairment, abnormal heart function, osteoporosis among others [232-233]. In addition, a weakened immune defense system, sterility in male and females, abnormal fetal development, and glycosuria are also associated with chronic lead poisoning.

Lead perturbs the functions of enzymes and proteins of varied classes. Studies have shown that, lead exerts its influence physiologically and biochemically as a mimetic agent substituting for essential elements participating in metabolism such as calcium, iron and zinc. For instance, it directly interferes with zinc and iron in the biosynthesis of

heme, in the function sulfhydryl group rich protein enzymes and in protein synthesis in general either directly or indirectly [232-233]. Lead binds to different kinds of transport proteins including metallothionein, transferin, calmodulin and calcium-ATPase. By associating with these proteins, it is transported to specific tissues where it causes its damage. Lead transport and assimilation are optimum when there is the dietary deficiency of iron or calcium, zinc because lead is able to displace these metals in transport proteins and during specific protein-mediated physiologic processes [234].

Liver and kidney damage have been linked to lead toxicity although the exact toxicity mechanism is not entirely understood. Other than the use of histopathology to assess the effects of lead poison in hepatocytes, the use of other methods has been inconclusive. The objective of this study is to assess the interaction of lead with calcium, iron, copper, zinc, cobalt and nickel in blood, liver, kidney and bone marrow using rat model. Histopathology of the liver and kidney will also be examined. ICP-MS is a useful analytical tool for quantifying multi-elements from such matrices as geological, environmental and biological samples at sub parts per billion. That is, it has a detection limit of 1-100 parts per trillion and a linear dynamic range of about eight orders of magnitude. The range of analytes that can be employed in ICP-MS has recently been extended to both metals and nonmetals including radionuclides, rare earths, and some halogens like Br and I. ICP-MS works by generating ions in the plasma which are directed into the ion focusing region using turbomoelcular pumps backed by rotary pumps. Then electrostatic ion and extraction lenses sort the negative and positive ions so that positive ions are directed towards the quadrupole. Ions then enter the separation hardware, the quadrupole mass spectrometer where the electric field forces them into

wavelike motion. Ions with stable trajectories are filtered according to their mass to charge ration (m/z) in the quadrupole. Finally, individual ions are detected by ion counting electron multiplier [298].

The Fisher 344 rat inbred strain was developed in 1920 to address the lack of reproducible animal model for cancer research. In 1970, the National Cancer Institute selected Fisher 344 rat as a replacement for the Osborne-Mendel rat model in cancer bioassay program because tumor latency due to chemical exposure is relatively short whilst maintaining good survivability. Fairly recent literature has indication that F344 rats are prone to exhibit inflammatory effects and mononuclear cell leukemia due to exposure of a range of chemicals and pharmaceuticals. Nevertheless, this animal model has been employed in as many cancer, toxicological, aging, neurological, organ transplant, heart disease etc studies in the literature [243-246].

This experiment is part of a larger project investigating the overall effects of Pb^{2+} on gene expression in the rat. Results from this investigation will enable us to determine what specific tissue levels of Pb in rat lead to alterations in gene regulation.

Materials and Methods

Experimental Design

Forty-eight six weeks post-weaning male Fisher 344 (F344) rats were exposed to 0 ppm, 50 ppm or 500 ppm of Pb^{2+}, respectively, in the form of lead acetate through drinking water *ad libitum* for 30 and 90 days, respectively. Control drinking water was distilled water. Prior to commencing treatment, rat diet, control and treated water were

analyzed by inductively-coupled plasma mass spectrometry (ICP-MS) (model # 4202387, serial # A0126) for lead contamination and to verify accurate exposure levels. Rats were housed at the Western Michigan University Animal Facility. The animals were treated according to the principles outlined in the NIH Guide for the Care and Use of Laboratory Animals. There were eight rats assigned randomly to each treatment group. After each exposure period, rats were euthanized with CO_2 and blood was collected by cardiac puncture for serum analysis using ICP-MS. Also, some of the liver, kidney and bone marrow were preserved for multi-elemental analysis. A portion of each of the livers and kidneys were also fixed in 10% neutral buffered saline for subsequent histology analysis.

Multi-Elemental Analysis

Determinations of lead and other metal ion levels in blood, liver, kidney and marrow, an elemental analysis were carried out by ICP-MS. Approximately 1 g each of blood, liver, kidney and marrow was weighed into Teflon carousels containing 10 ml of 50 % nitric acid (ultra trace purity) and digested at high pressure in a microwave oven. After digestion, the samples were transferred to 50 mL conical tubes and diluted with 3 % nitric acid to the 50 mL mark. They were further diluted in a ratio of 1:10, 3 % nitric acid for final analysis. A 10 μL Yttrium internal standard (10 ug/mL) was added to each sample just prior to inductively-coupled plasma mass spectrometry analysis. There were three replicates for each treatment and each sample was analyzed in triplicate.

Histopathology

Liver and kidney samples were fixed in 10 % neutral buffered formalin. Fresh fixative was added to the samples and stored at 4 °C until ready for analysis. Briefly, the samples were passed through graded alcohol solutions for dehydration, xylene washed and then embedded in paraffin block cassettes. Then, tissues were sectioned in transverse and deparaffinated and stained with hematoxylin and eosin (H & E). Stained sections were examined under light microscopy to detect structural changes in the cells of the liver and kidney.

Data Analysis

Significant differences in lead, zinc, nickel, cupper, cobalt as well as morphometric parameters such as body weight and organ weights were analyzed by student t-test and ANOVA. Regression analysis was also conducted to follow distributions of lead and the other metal ions in blood, liver and kidney as function of time and dose level. Data was presented as means ± standard deviation (SD) or means ± standard error (SE), and differences were considered significant at $P < 0.05$ or $P < 0.01$. ANOVA and t-test were applied specifically to the data set shown in Tables 3, 4, 5 and 6. Figures 2, 3 and 4 were analyzed by ANOVA and Figures 5, 6 and 7 by regression analysis. H & E stained slides were observed under low- and high-power optical microscopes at the Biological Imaging Center, Western Michigan University.

Results

Lead Effects on Selected Animal Morphometric Parameters

Selected measurements of animal health at time of sacrifice are reported in Table 3. Body weight gains as well as absolute liver and kidney weights were not significantly altered in both the 30-day and 90-day treatment groups relative to controls. The amount food consumed (gram) per gram of body weight gain was also not found to be significant. However, some significant differences were observed for the hepatosomatic and renal somatic indexes (organ wt./body wt.) in both the 30 and 90 days exposure period groups . In the 30-day treated rats, liver and kidney weights and the renal somatic index were decreased. In contrast, in the 90-day treated rats, liver weights, hepatosomatic and renal somatic indices respectively increased 8 %, 11 % and 5 % relative to controls.

Metal Distribution in Blood, Liver, Kidney and Marrow

In Table 4, lead accumulation in blood, liver, kidney and bone marrow were all increased significantly in lead exposed groups relative to the control groups. With the exception of kidney, the 90-day treatment groups also showed markedly higher levels of lead in blood, liver and marrow than the 30-day treatment groups. The amount of lead accumulated in blood was between 6-15-fold greater in the 90-day treated than the 30-day exposed group. This trend is similar to what was observed in the liver and bone marrow. In the kidney, it is a ratio of one-to-one.

Table 3

Selected organ weights (g) and their indexes (organ wt. X 10^3/Body Wt.) *P<0.05

30 Days Pb^{2+} Exposure

Dose	**Liver** (grams)	**Liver/Body** (10^3)	**Kidney** (grams)	**Kidney/Body** (10^3)	**Food/B. W. Gain** (gram/gram)
0 PPM	11.29 ± 1.32	118.18 ± 18.03	2.67 ± 0.28	27.90 ± 3.80	5.74 ± 0.80
50 PPM	11.15 ± 0.93	108.79 ± 19.24	2.56 ± 0.29*	24.99 ± 5.14*	5.35 ± 0.93
500 PPM	10.79 ± 0.90*	114.72 ± 14.24	2.59 ± 0.35*	27.63 ± 4.71	5.47 ± 0.67

90 Days Pb^{2+} Exposure

Dose	**Liver** (grams)	**Liver/Body** (10^3)	**Kidney** (grams)	**Kidney/Body** (10^3)	**Food/B. W. Gain** (gram/gram
0 PPM	11.86 ± 0.43	67.54 ± 5.83	2.98 ± 0.23	16.92 ± 5.83	9.02 ± 0.75
50 PPM	12.04 ± 0.98	67.68 ± 5.13	3.06 ± 0.27	17.18 ± 5.13	8.86 ± 0.40
500 PPM	12.85 ± 1.58*	74.64 ± 8.53*	3.05 ± 0.23	17.76 ± 1.43*	9.02 ± 0.44

Table 4

Lead distribution in selected tissues. **P<0.01

30 Days Pb^{2+} Exposure				
	Blood	**Liver**	**Kidney**	**Marrow**
Dose	(ppb)	(ppb)	(ppb)	(ppb)
0 PPM	1.385 ±0.28	0.616±0.41	1.520±0.81	0.977±0.47
50 PPM	5.08±1.88	4.557±2.37	127.8±29.3	2.436±1.26
500 PPM	15.6±3.33	42.59 ±15.7	838 ± 96.6	14.76 ±6.91
	(n = 8)**	(n = 8)**	(n = 8)**	(n = 8)**
90 Days Pb^{2+} Exposure				
	Blood	**Liver**	**Kidney**	**Marrow**
Dose	(ppb)	(ppb)	(ppb)	(ppb)
0 PPM	7.755 ±1.756	5.529 ±1.537	7.000 ±1.389	4.306 ±1.342
50 PPM	78.51 ±11.45	69.05 ±15.89	83.32 ±19.40	39.98 ±13.65
500 PPM	95.17 ±38.90	81.25 ±28.29	666.32 ±155.1	54.67 ±19.33
	(n = 8)**	(n = 8)**	(n = 8)**	(n = 8)**

Effect of Lead Poisoning on Some Essential Trace Metals

As mentioned to in the introduction, lead exerts its toxic effects through mimicking the behavior of some other essential trace metals. We evaluated the responses of calcium, iron, cobalt, nickel, copper and zinc to varying levels of lead intoxication in some rat tissues. In Figure 1, the levels of zinc are shown in selected tissues as a function of lead exposure and time. The 30-day treatment group showed significant losses of zinc ($P<0.05$) in the liver at both the 50 ppm and 500 ppm Pb doses, with kidney and marrow levels remaining statistically unaltered. For the 90-day exposure period group, zinc concentrations reduced significantly in liver, marrow ($P<0.05$) and kidney ($P<0.01$).

Not many significant alterations in calcium and iron levels in blood, liver, kidney or marrow were observed at either time point or in either treatment regime, except

calcium was depressed in the blood of 90 day high dose animals ($P<0.01$) and iron ($P<0.05$) in marrow in the 90 day high exposure group.

Table 5

Total calcium levels in selected tissues. **P<0.01

30 Days Pb^{2+} Exposure				
	Blood	**Liver**	**Kidney**	**Marrow**
Dose	(ppb)	(ppb)	(ppb)	(ppb)
0 PPM	136 ± 20.5	54.9 ± 11.1	471 ± 332	115 ± 127
50 PPM	167 ± 51.8	61.2 ± 17.0	374 ± 167	47.6 ± 65.5
500 PPM	159 ± 25.3	88.8 ± 55.1	343 ± 114	18.8 ± 21.2
	(n = 8)	(n = 8)	(n = 8)	(n = 8)
90 Days Pb^{2+} Exposure				
	Blood	**Liver**	**Kidney**	**Marrow**
Dose	(ppb)	(ppb)	(ppb)	(ppb)
0 PPM	155 ± 26.6	488 ± 45.9	850 ± 227	3545 ± 3643
50 PPM	146 ± 25.6	497 ± 128	818 ± 216	774 ± 650
500 PPM	114 ± 19.3	476 ± 105	894 ± 323	638 ± 16.5
	(n = 8)**	(n = 8)	(n = 8)	(n = 8)

Table 6

Iron content in selected tissues. *P<0.05

30 Days Pb^{2+} Exposure				
	Blood	**Liver**	**Kidney**	**Marrow**
Dose	(ppb)	(ppb)	(ppb)	(ppb)
0 PPM	1097 ± 474.3	81.32 ± 17.59	80.11 ± 37.60	5.684 ± 2.606
50 PPM	843 ± 164	81.2 ± 16.3	75.9 ± 28.4	2.878 ± 0.926
500 PPM	966 ± 196	79.4 ± 29.6	76.4 ± 28.5	3.143 ± 1.500
	(n = 8)	(n = 8)	(n = 8)	(n = 8)
90 Days Pb^{2+} Exposure				
	Blood	**Liver**	**Kidney**	**Marrow**
Dose	(ppb)	(ppb)	(ppb)	(ppb)
0 PPM	680 ± 307	145 ± 44.2	99.5 ± 23.67	12.6 ± 5.49
50 PPM	787 ± 237	172 ± 46.4	91.8 ± 22.9	6.04 ± 2.38
500 PPM	796 ± 292	170 ± 43.3	84.7 ± 24.9	5.25 ± 1.68
	(n = 8)	(n = 8)	(n = 8)	(n = 8)*

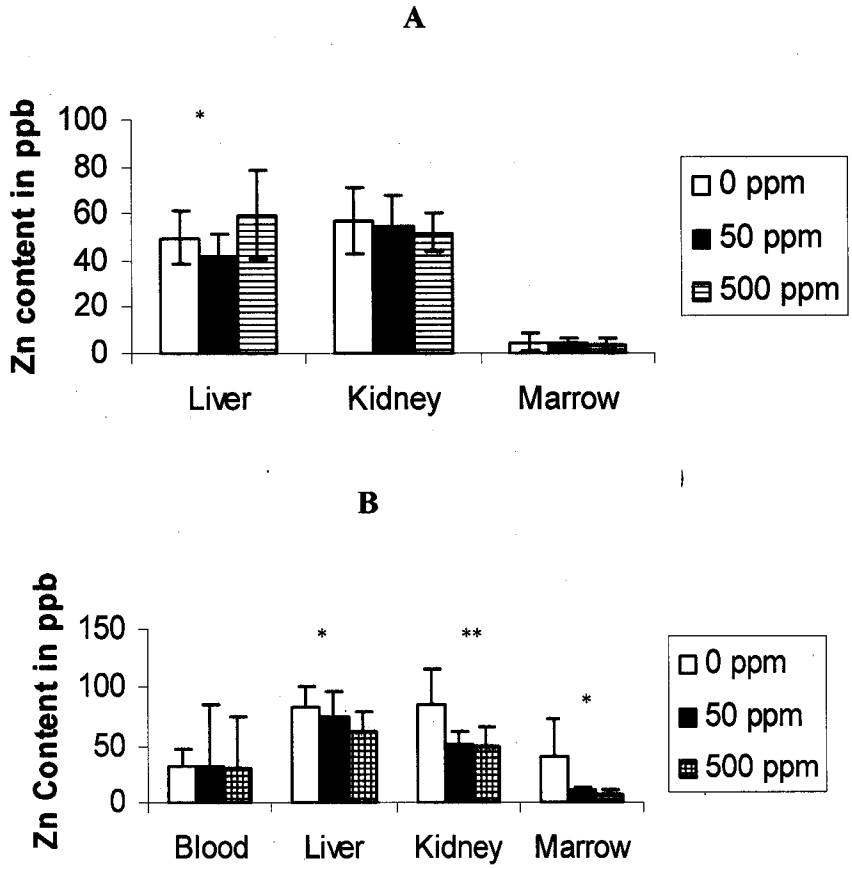

Figure 2: Distributions of zinc (ppb) due to lead exposure for (A) thirty days and (B) ninety days. Significant decreases in zinc concentration due to lead intoxication were observed at both time points in the various tissues assayed. *P<0.05, **P<0.01

The concentrations of nickel (ppb) in the selected tissues analyzed are presented in Figure 3. While long-term chronic (D) lead exposure resulted in significant nickel reduction in liver at 50 the ppm dose group only and marrow in the 500 ppm dose group only (P<0.05), short -term acute (C) exposure to lead did not yield any significant changes in nickel levels in liver, kidney or marrow tissues at any dose.

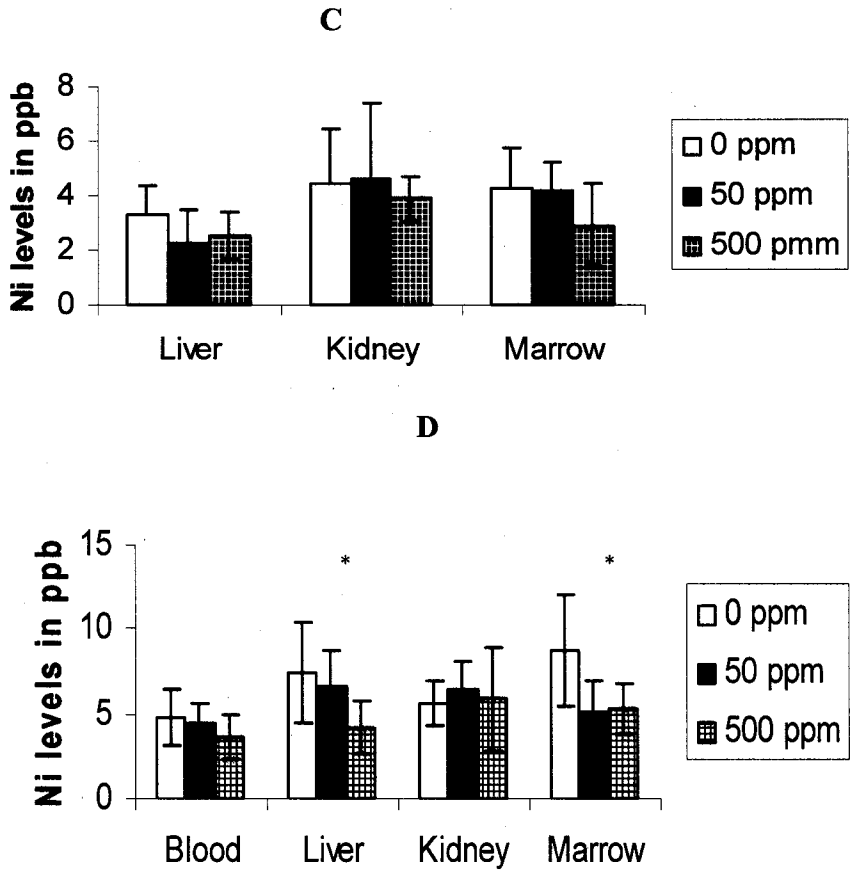

Figure 3: Levels of nickel in blood, liver, kidney and marrow (ppb) as a result of exposure to lead for 30 and 90 days. No significant differences were observed for the shorter (C) time period. On the contrary, significant differences were observed in the liver and marrow for the longer treatment period (D). *P<0.05.

Similarly, cobalt levels (ppb) were not significant changed for the thirty days treatment group. Though, cobalt in the liver was significantly altered in the groups treated with lead for ninety days. For the 30-day treatment group, cobalt decreased 34 % in liver, and increased 12.5 % and 2.5-fold in kidney and marrow respectively. Blood, liver and marrow level cobalt decreased by 84 %, 85 % and 83 % respectively whereas that of the kidney increased by 7 % in the 90-day treatment group (data not shown).

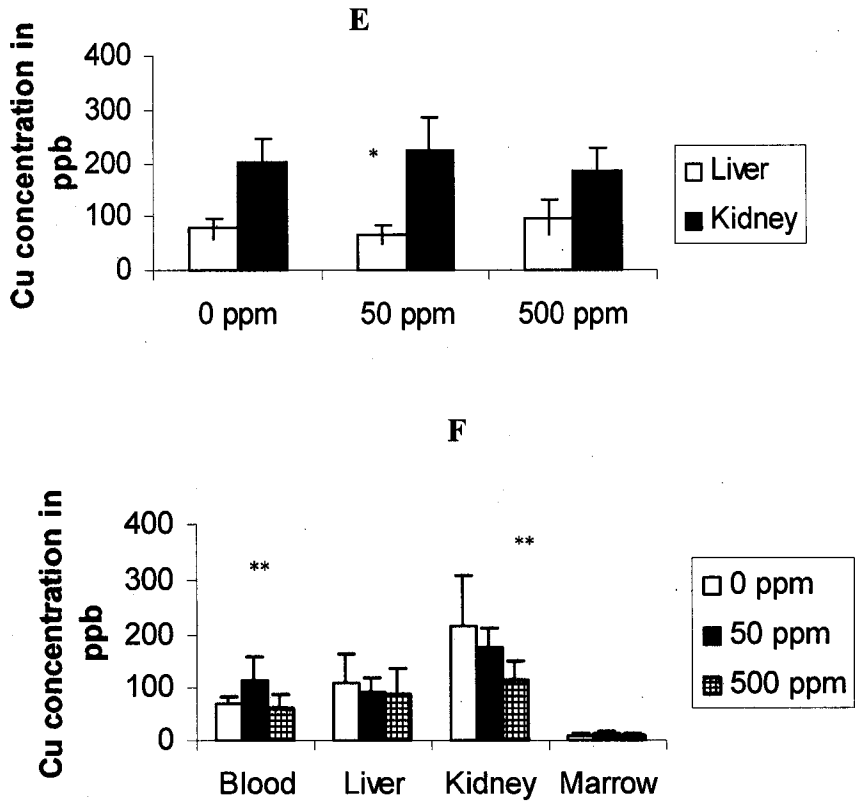

Figure 4: Copper concentration in blood, liver, kidney and marrow (ppb) due to lead poison for 30 and 90 days. Copper levels in the short term treatment group were statistically changed only in the liver (E) whereas the other group was changed both in the blood and kidney. *P<0.05, **P<0.05.

Figure 4 shows Cu (ppb) distribution in selected tissues at (e) 30 days and (f) 90 days. The 30-day exposure group showed a significant Cu reduction in the liver (P<0.05). Also, rats treated for 90 days showed marked changes in blood, liver and kidney, only in blood and kidney were copper reduced significantly.

The next several figures illustrate the relationship between various lead concentrations and essential trace metals in specific tissues. Though these relationships are too simplistic with respect to the direct influence of lead levels on the levels of these

other metals or for explaining mechanisms involved in lead action, they nevertheless provide useful information as to the metal-targets of lead. Figures 5 and 6 shows scatter plots of liver concentrations of lead on the horizontal axis against zinc, nickel and copper concentrations on the vertical axes for 30 day and 90 day exposures, respectively. Both figures were fitted to both linear and polynomial functions and the best fuction selected. The short-term (30d) exposure groups have R^2 values ranging from 0.093 to 0.6109. Similarly, the 90d experimental groups had R^2 values in the range of 0.0245 to 0.2311. The Pb-Ca and Pb-Fe relationships were curvilinear in nature. Although two of the long - term treatment groups reveal a weak negative correlation, the majority of the treatment groups showed a quadratic relationship indicative of dose-response, thus, reflecting the most accurate response of the cell to lead toxicity. These results confirm that the response of living organisms to the toxic effects of lead, like many other contanminants, is not likely to be a linear relationship. Whereas some of the treatment groups show positive associations, the others demonstrate negative interactions. Interactions of metals in blood and marrow were all negative. In contrast, some liver associations were positive, in the cases of Ca and Fe (Figure 7) at 90d of exposure Pb-Ca. in the kidney.

In Table 7 above, lead excretion through the feces increased 10 orders of magnitude from the 0 ppm to 50 ppm to 500 ppm treated groups. Clearly, this observation agrees with what we would expect that the more Pb exposure there is in a population to a particular chemical, the greater excretion amounts of that particular chemical.

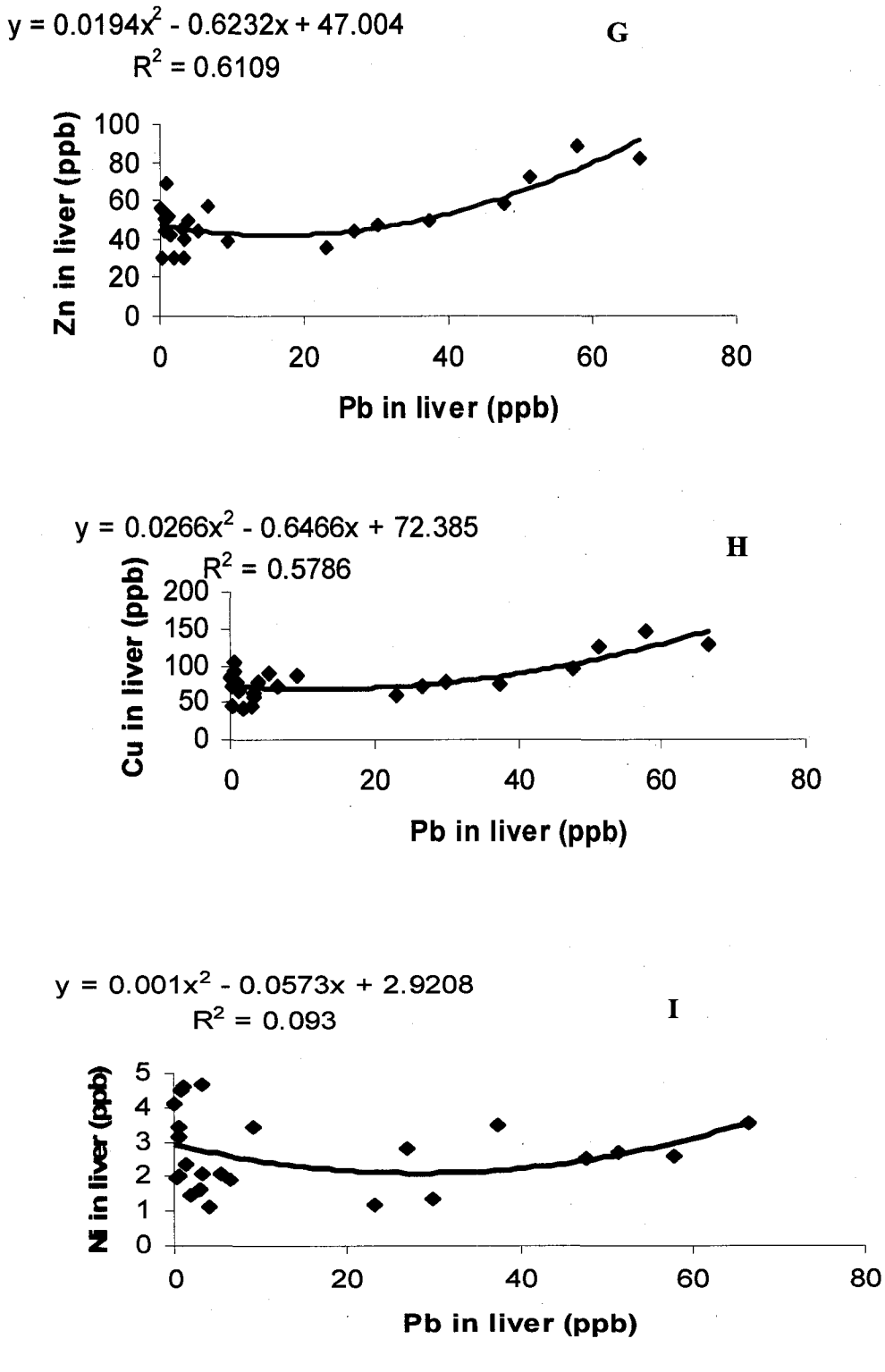

Figure 5: Plots of Pb (ppb) versus (G) Zn, (H) Cu and (I) Ni (ppb) in liver for 30 days. Data fit to a polynomial function.

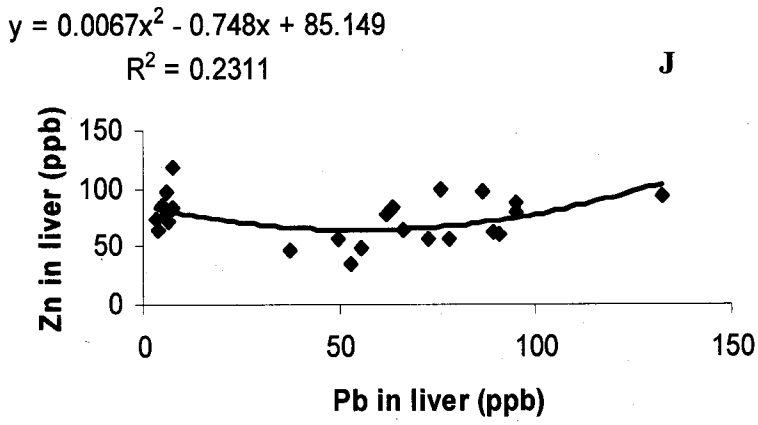

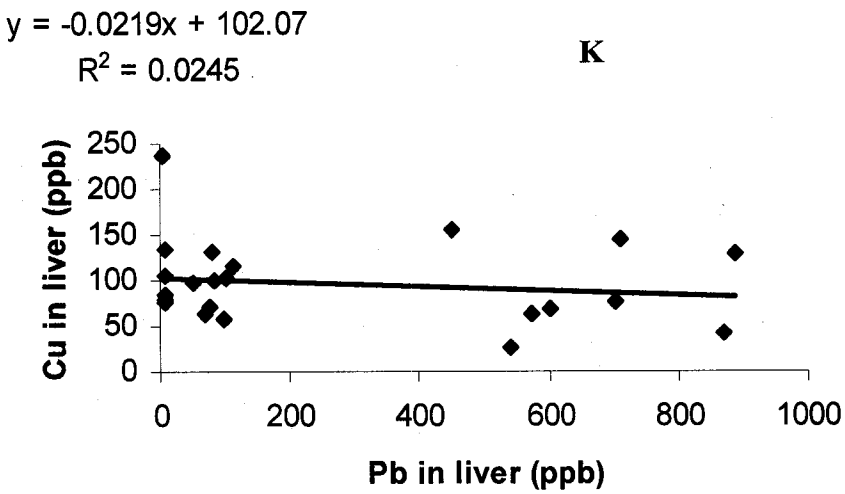

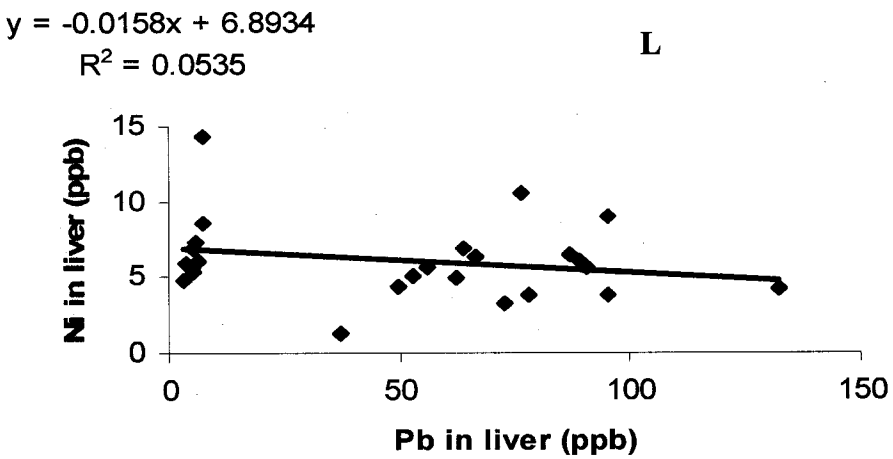

Figure 6: Plots of Pb (ppb) versus (J) Zn, (K) Cu and (L) Ni (ppb) in liver for 90 days. Data fit to both linear and polynomial function.

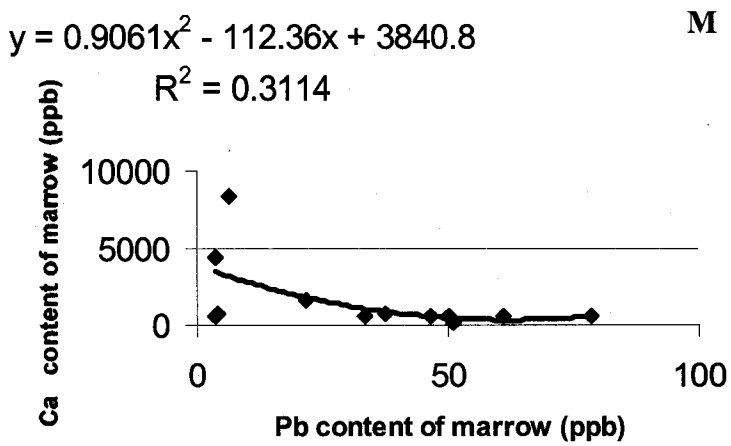

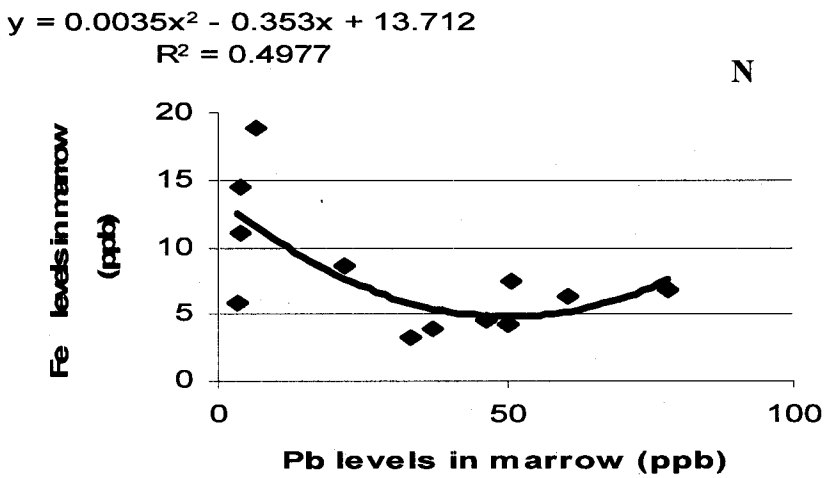

Figure 7: Plots of Pb (ppb) versus (M) Ca and (N) Fe (ppb) in the marrow for 90 days. Data fit to a polynomial function.

Table 7
Lead, copper, nickel and cobalt levels in feces. *P<0.05, **P < 0.01

Dose	**Lead** (ppb)	**Zinc** (ppb)	**Copper** (ppb)	**Nickel** (ppb)	**Cobalt** (ppb)
0 PPM	2135.83±56.0	2047.85±38.92	2067.61 ± 69.23	443.73 ± 25.71*	52.48 ± 1.85
50 PPM	22113.54±415.0	1503.86±14.90**	1728.07 ± 33.37	273.50 ± 2.93	37.92 ± 0.81*
500 PPM	286495.60±9335**	1571.40±10.47	1950.45 ± 31.13	294.47 ± 11.55	42.14 ± 0.54

The fecal amounts of zinc, copper, nickel and cobalt extreted were all greater in the control groups than in the the treated groups. All three metals were minimally excreted in the 50 ppm exposure group relative to the controls.

Compared to the controls, zinc, copper, nickel and cobalt excretion were 27 %, 16 %, 38 % and 27 % less, respectively, in the low dose treatment group. Similarly, excretion of these metals was reduced by 23 %, 5 %, 34 % and 19 %, respectively, in the high dose group relative to controls

Histopathology

Images of H and E stained cells of the liver and kidney are shown in Figure 8. Necrotic tissue which is evidenced by nuclear shrinkage and fragmentation patterns were observed mostly in the long term treated group. The kidney tissues appeared to suffer more damage than the liver even at the same treatment. This is shown by H&E as hydropic degeneration and increase basophilia in renal epithelium.

Discussion

Generally, the degree and duration of lead intoxication does not appear to be reflected in the body weight gain of the test species, although morphometric indices of tissue weights and their relative contribution to the total body weight gain might prove to be useful measures of frank toxicity to lead. In this study, no alterations were observed in total body weight gain, but rather, kidney and liver weights and their ratios of weights to total body weights at higher lead concentrations were affected. A change in body weight due to lead exposure is not clearly shown in the literature.

A: 30d, 90d Liver Control

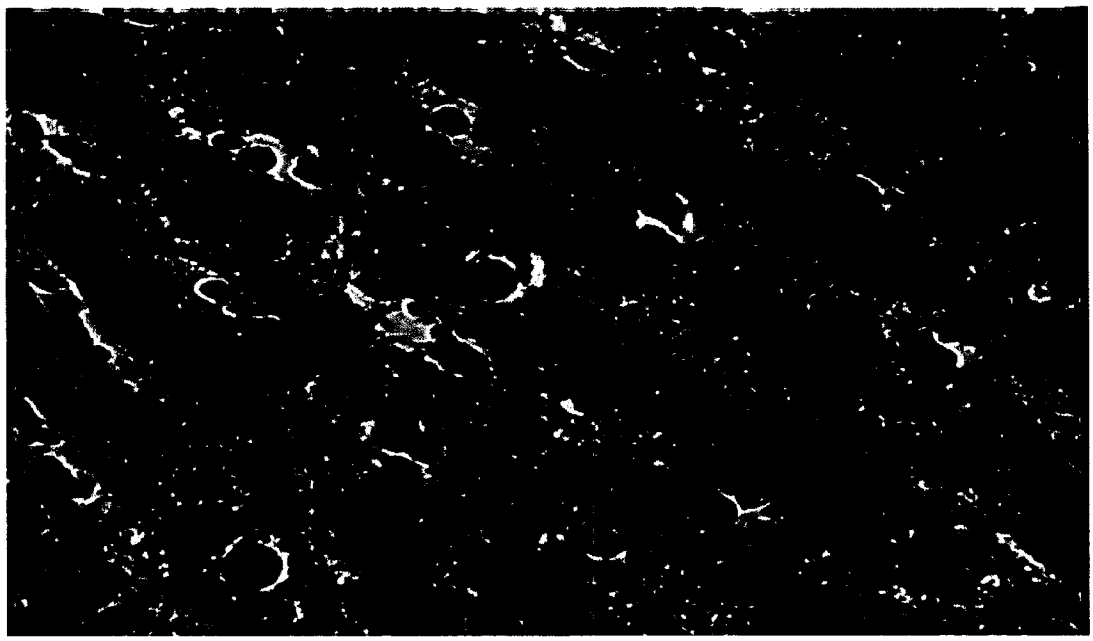

B: 30d, 90d Kidney Control

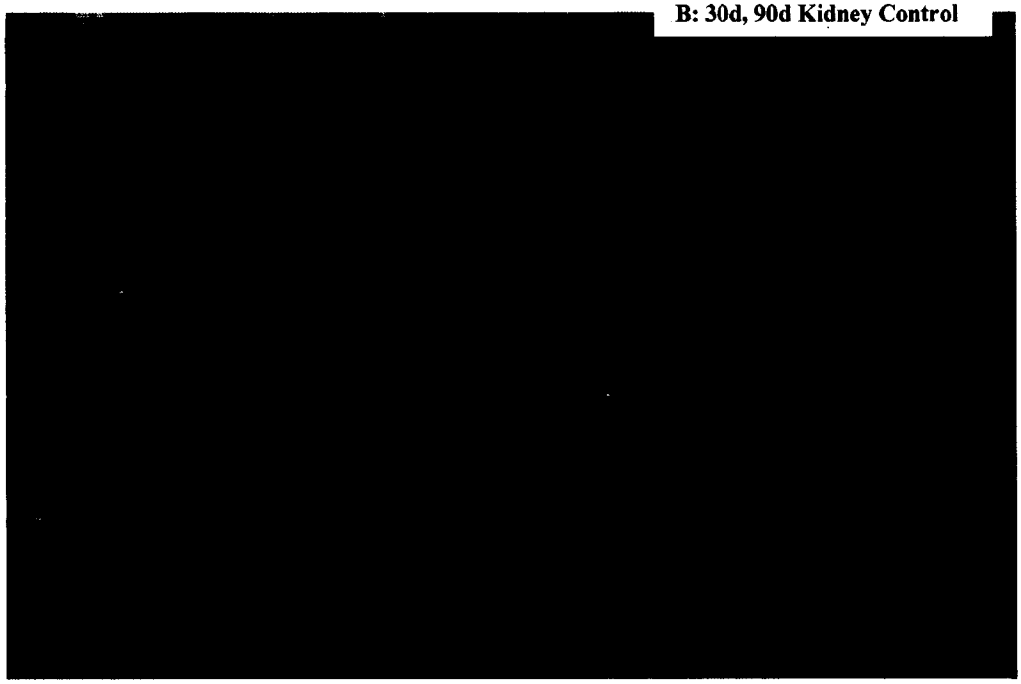

Figure 8: H&E staining X 80 (C) necrotic liver showing both pyknosis and karyorrhexis (D) necrosis of the kidney characterized hydropic degeneration and basophilia of the renal tubule epithelia. Both were exposed to 500 ppm Pb^{2+} for 90 days. The 50 ppm treated in liver and kidney respectively (E and F) also shows signs of pyknosis and karyorrhexis, though not as pronounced.

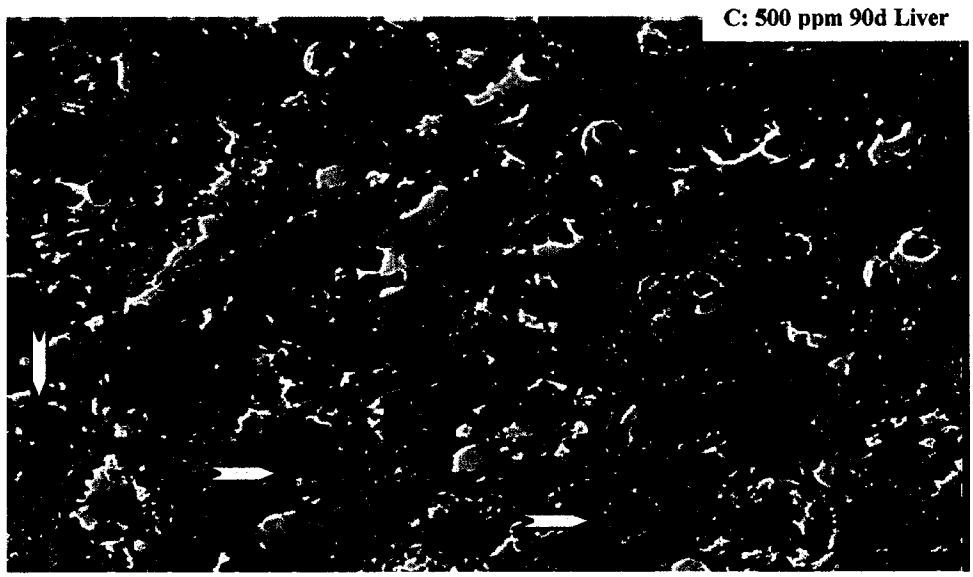

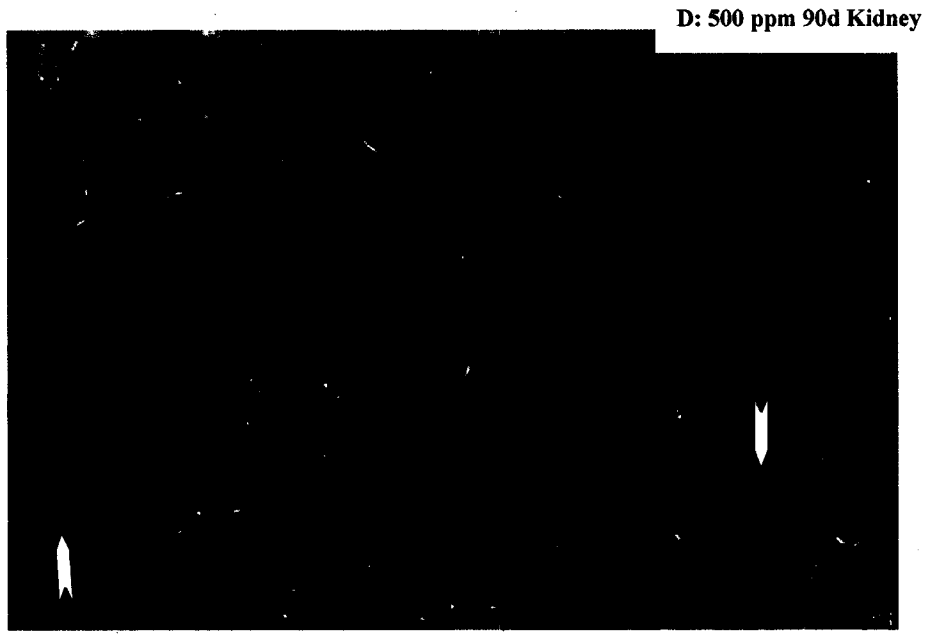

Figure 8 - Continued

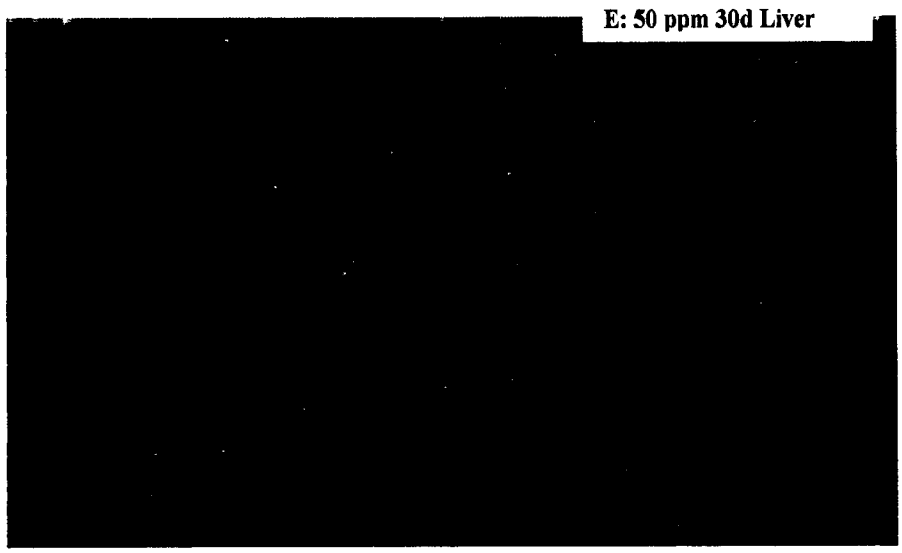

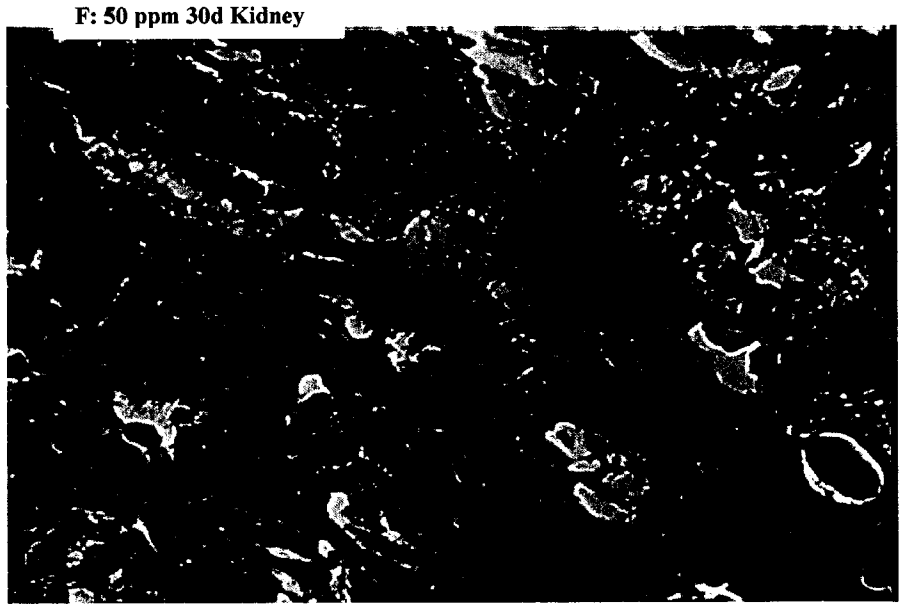

Figure 8 – Continued

For instance, whereas Miller *et al* [235], Corpas *et al* [232] and others did not find reduction in body weight as a result of increasing lead concentration, Adonaylo and Oteiza [236] observed lower body weights of rats intoxicated with lead. According to Corpas and coworkers, lack of evidence with respect to body weight gain does not necessarily mean lead has no effects. Instead the effects are rather intrinsic and continuously affecting the animal during its entire life at the tissue and cellular function level.

Tissue distributions of lead were consistent with applied doses and duration of exposure. In both time points, the 500 ppm exposed group accumulated greater lead levels than either the control or 50 ppm treatment groups in all tissues analyzed. Surprisingly, accumulated lead levels in kidney were almost the same irrespective of treatment time (30d vs. 90d). Lead accumulated in these tissues is a result of conjugation in the liver with metallothionein or other metal chelating proteins which are passed on to the kidney and other tissues, with the balance of the Pb being excreted either in feces or urine [230]. It is generally reported in the literature that a greater proportion of lead is excreted through the feces than urine [5]. The very high fecal content in our experimental animals is consistent with this obervation. Lead either bound to plasma proteins or the free salt form is introduced to the kidney through the apical membrane and in these forms it is cannot readily leave the blood stream through the basolateral membrane [237]. Another reason for the relatively high levels of lead accumulation in the kidney might be the indirect activities of metallothioneins and glutathione. These proteins have cysteine in their configuration which has an affinity for heavy metals [238]. Other workers have found that lead bioavailability in kidney and brain relates to binding to a low molecular

weight protein that is rich in aspartic and glutamic dicarboxyl amino acids [242] other than metallothionein. According to Zalups [238], heavy metals such as lead can induce the synthesis of metallothionein and glutathione within the liver which then traps the metal ions within the cell by forming peptide conjugates. During the process of liver cell renewal, the heavy metal-metallothionein or metal-glutathione complexes are released into the systemic circulation and then delivered to the kidney [239]. This type of cycle is likely to result in higher levels of metal ions in the kidney than in most other organ systems.

The importance of trace metals to the normal function of the cell cannot be over emphasized. Essential trace metals exhibit a narrow range of concentrations within which they must function. Deficiencies result when their levels are below that level and when it is greater than that range of concentrations, the metals are toxic. As a result, trace metals are tightly controlled in the body to maintain homeostasis and normal cell metabolism. Levels of cobalt, copper, nickel and zinc were altered in the various tissues analyzed as the result of lead exposure in the corrent expeiments. It appears the metals most affected by lead intoxication are copper and zinc particularly during the long-term exposures. This is supported by the authors Goyer [241] and Peraza *et al* [234].

The interaction of lead with cobalt, cupper, nickel and zinc were all observed in these experiments. Cell homeostasis is maintained by adequate levels of cations such as Zn(II), Cu(II) and others. These metals are involved in various regulatory and physiological activities. Garza *et al* [240] notes that lead is able to substitute for other polyvalent cations that are involved in important molecular processes. According to them, lead has a higher binding affinity for chemical functional groups that would

coordinate divalent cations in proteins. The ionic interaction of lead with these negatively charged acidic amino acid residues making it possible for lead to bind a wide variety of proteins results in a change in the structure and electric charge balance of proteins. The results presented here suggest that the interactions of lead with Zn Cu, Ni and Co are time dependent. The entire 30 day treatment group showed that increasing lead concentration results in no increases of these essential divalent metals in rat tissues. The opposite was however true for the 90 day exposure group. In these animals the levels of Zn, Cu and Co were lowered. These trends are quite different from what was seen in other studies. For example, Goyer [241] reported that lead increases the excretion of zinc and reports a negative correlation between blood lead levels and the activity of zinc-containing heme enzymes. They suggest that lead replaces zinc on the enzyme. Again, he reported that lead exposed rats showed significant reductions in copper levels in the liver.

Examination of hepatic histopathology produced no evidence of necrosis or changes in cellular structure of hepatocytes in the 0 ppm and 50 ppm for the short-term exposure period. In contrast, both necrosis and alterations in cellular structure and cell distribution were observed in the liver and the kidney in both the 50 ppm and 500 ppm Pb^{2+} 90-day treatment groups. Analysis of liver and kidney of long-term exposed lead groups showed varying degrees of necrosis. The 90 day 500 ppm Pb^{2+} treated group showed signs of pyknosis and karyorrhexis of the liver. In the kidney, hydropic degeneration and basophilia of the renal tubule epithelia were observed. The 50 ppm treated in liver and kidney also revealed signs of pyknosis and karyorrhexis though these effects were not as pronounced as in the high dose groups. Literature reports suggest that the kidney is the most susceptible organ to lead toxicity. The work by Corpas *et al* [232],

found no abnormalities in the liver structure or liver deposition of lead in young neonates intoxicated with lead. On the other hand, Jarrar and Mahmoud [230] found lead to have caused tubular and glomerular alterations in kidney. They observed anisokaryosis, nuclear pyknosis, and vacuolization among other histopathological effects in the kidney.

In summary, effects associated with lead exposure were observed to be both dose and time dependent in our study. Short-term exposures did not produce as serious damage, as did long-term, high dose intoxication levels. Histopathology changes in tissue morphology were consistent with the lead concentration in liver and kidney. For instance, high lead concentration of lead in kidney cells results in pronounced cell necrosis in varied forms. There was a positive correlation between lead levels in tissues and the levels of other trace metals in the short-treatment period. However, a negative correlation between lead levels and other trace element levels in tissues was observed for chronic exposure levels in rat.

CHAPTER IV

GENE EXPRESSION ANALYSIS BY AFFYMETRIX MICROARRAY GENE CHIPS

Microarray Background Information

Recently toxicologists have employed molecular tools in the assessment of risk to humans using different animal models. These molecular tools involve the measurement of so-called expression biomarkers. Biomarker levels in an organism can provide indications of contaminant bioavailability (if organism is still in the natural environment), exposure levels and a whole host of possible effects at the molecular level. Biomarkers could be protein levels or activity or enzyme activity and very recently, the expression or suppression of relevant and specific genes. About a decade ago, gene expression analysis was accomplished on a one gene at a time basis. The emergence of DNA chip technology has dramatically increased the number genes that can be studied simultaneously. It has afforded toxicologists the opportunity to study thousands of genes at the same time thereby enabling them to examine entire pathways and associate transcription factors using a suite of selected target genes [209]. The acceptance of DNA chip technology for examination of molecular and cellular processes is demonstrated by the increasing number of published papers in the literature that employed this technique.

The term 'gene expression' refers to the transcription of DNA sequence-encoded information into mRNA that is subsequently translated into proteins that regulate cell function. In brief, gene expression involves transcription which also requires translation [210, 211]. DNA templates are transcribed by RNA polymerases into mRNA molecules while translation is carried out by enzymes associated with the ribosomes. Genes that

code for mRNAs and other RNAs are regulated in order that they are expressed adequately and appropriately to meet the needs of the cell such as growth, proliferation or at maintenance and this process is dynamic. This highly dynamic gene expression process is controlled by changes within the cell, environment or disease states.

There are currently four main microarray types available in the market. These include expression profiling, single nucleotide polymorphisms (SNP), comparative genomic hybridization (CGH) and resequencing array instruments. Expression profiles are employed to examine gene expression alterations (up or down) due to different disease, intoxication or normal states or to compare gene expression variations in cells over time (growth and differentiation) and these latter measurement have applications in tumor classification, development of predictive or prognostic markers of disease or intoxication or in development of drugs. SNPs are used identify mutations or polymorphisms in a gene sequence that cause genetic variation and they have applications in the investigation of predisposition to genetic disease, disease progression monitoring and selection of DNA-based drugs. Similarly, CGH is used to detect genetic amplifications or deletions of genes or examination of the copy number changes in a specific gene. It can be applied in tumor classification, assessment of risk, prognostic and predictive markers development. Finally, re-sequencing arrays are employed in sequencing portions of the genome. This is used for the assessment of germline mutations or to identify somatic mutations in cancer [211].

Gene chip DNA microarray provides a rapid means of quantifying the level of messenger RNA (mRNA) abundance in a tissue sample. Quantified mRNA content is an indication of gene expression levels because mRNA is directly transcribed from the DNA

[212]. DNA microarray or "chip" consists of an orderly arrangement of equidistant microscopic DNA spots that are attached to a solid surface like glass or plastic or silicon chip. This chip is made up of thousand of distinct sequences referred to as "probes" found in defined locations on a grid. Complementary DNAs (cDNAs), oligonucleotides of varying length or genomic sequences that are fluorescently or radioactively labeled is hybridized to corresponding probes that recognize and attach to the solid support [211, 212]. Subsequently, an array consisting of thousands of immobilized spots at predetermined grid locations is generated via pins or inkjet technology or *in situ* photolithographic synthesis of oligonucleotides [211-215]. The basic premise is that, nucleic acids molecules show a highly selective binding to their complementary sequences. As a result, the addition of the "target" (pool of mRNAs in the sample-derived nucleic acid sample) to the chip surface leads to a highly parallel searching and sorting of molecular partners, that is, probes linking with their respective complementary targets and this selection process is made quantitative through the presence of millions of identical probes at each single location on the array. A fluorescent-based detection scheme is then employed to quantify mRNA transcript level. This typically involves the excitation of fluorescent-labeled mRNA molecules with a laser. The fluorescence emission is digitized with a fluorescence scanner and the intensity data is subsequently transferred to a computer-linked database [211, 212, 216].

The amount of data generated from microarray experiments is usually large and this has resulted in a parallel growth in the field of bioinformatics. Over the last few years, the mathematical and statistical approaches and corresponding software packages for analyzing microarray data have been increasing rapidly. Irrespective of the software

or analysis approach adopted, almost all gene expression studies utilizing microarrays can be grouped into the categories of class comparison, class prediction, class discovery and pathway analysis [216, 217]. Class comparison involves identifying genes that are differentially expressed. It is intended to determine whether gene expression profiles are different among samples selected from predefined classes. Class comparison is similar to class prediction except the latter is focused on developing a statistical model to predict classes to which new samples might belong using expression profiles. Class prediction is useful in medical problems of diagnostic classification, prognostic prediction and disease treatment selection. The purpose of class discovery tools is to identify novel sub-types within a population based on the theory that similar clinical and morphological specimens that vary biologically may be discernible at the molecular level. This tool allows for identifying groups of co-expressed genes and detecting patterns in expression profiles using clusters analysis or classification into sub-groupings. Finally, pathway analysis provides the opportunity for identifying genes that are co-regulated or which are located along the same biochemical pathway [216].

A number of microarray platforms are currently in use. These include Affymetrix, conventional spotted arrays, Agilent and CodeLink™ Bioarray platforms. The Affymetrix GeneChips have extensive genetic content and a high level of reproducibility. The GeneChip contains short single-strand DNA segments, oligonucleotides or "oligos" that are chemically synthesized on the chip itself. High-density arrays are made using light-directed DNA synthesis which employs a combination of photolithography and solid-phase DNA synthesis methods. GeneChips have an advantage over traditional microarrays in that they are synthesized *in silico* so that synthetic management of clone

libraries is insured and this minimizes or eliminates the risk of tube, clone, cDNA or spot misidentification. In addition, they exhibit good signal-to-noise ratios, a wide dynamic range and reduced cross-hybridization because multiple independent oligonucleotides are designed on to the chip surface to hybridize to varied regions of the same mRNA.

Although microarray technology has been demonstrated to be a powerful technology, for studying biological processes in the cell, there are still challenges and limitations that the user should be aware of. For example, understanding the complexity of biological systems with gene expression profiling requires a good understanding of bioinformatics, molecular biology and other fields of study. Also, the huge amount of data generated from typical microarray experiment presents a greater opportunity for user errors or misinterpretation. Thus, the accuracy, reliability and reproducibility of the resulting data depend heavily upon tightly managed good laboratory practices and quality controlled of experiments. Due to their sophistication, microarray experiments are currently expensive [211, 218]. Other sources of error encountered in microarray experiments include the quality and quantity of starting biological tissue samples, chip production, probe hybridization, image quantification, normalization and data interpretation. Currently there are no research community accepted, standardized processes to address inter-experimental variability in microarray studies.

Introduction to Study

The importance of lead as an environmental chemical species exhibiting various toxicity symptoms has been well documented. [227-230]. Lead targets diverse organ systems such as the skeletal, hematopoeitic, renal, endocrine and nervous systems [5],

thereby partitioning between soft and hard tissues with approximately 95 % and 70 %, respectively, found in the bones and teeth of adults and children. Bone then serves as a pool to replenish excreted lead from the blood. Some adverse conditions associated with lead poisoning include DNA damage, neurological impairment, abnormal heart function, osteoporosis among others [232-233]. In addition, weakened immune defense system, sterility in male and females, abnormal fetal development, and glycosuria are also associated with chronic lead poison.

Lead perturbs the functions of enzymes and proteins of varying types. Studies have shown that, lead exerts its influence physiologically and biochemically as a mimetic agent for essential elements such as calcium, iron and zinc. For instance, it directly interferes with zinc and iron in the biosynthesis of heme, Pb binds to sulfhydryl group protein enzymes and thus interferes with protein synthesis either directly or indirectly [232-233]. Lead binds to different classes of transport proteins including metallothionein, transferin, calmodulin and calcium-ATPase. By associating with these proteins, it is transported to specific target tissues where it causes its damage. Lead transport and assimilation is optimum when there is the deficiency of iron, calcium, or zinc because lead is able to displace these metals during specific physiologic processes [234]. The interaction of lead and calcium alters the proper functioning of calcium channels and ionic pumps. This leads to inadequate energy generation because of mitochondrial damage. Lead also causes defects in protein folding because of its binding to sulfhyryl groups and it can alter the structure of DNA binding motifs by disrupting their conformation [240].

Recently toxicologists have employed molecular tools such as microarrays in the assessment of risk to humans using different animal models. These molecular tools involve the measurement of so-called expression biomarkers. Biomarker levels in an organism can provide evidence of contaminant bioavailability (if organism is still in the natural environment), exposure and also a variety of possible effects. Biomarkers can include such parameters as protein levels or activity in cells or enzyme activity in a specific tissue and more recently, the expression of relevant and specific genes.

Until recently, gene expression analysis was limited to the analysis of one gene at a time. The emergence of DNA chip technology has dramatically increased the number of genes that can now be studied simultaneously. Gene chips have afforded toxicologists the opportunity to study thousands of genes at the same time thus enabling them to examine entire metabolic or signaling pathways and associated transcription factors with target genes [209]. The primary objective of this project is to analyze and profile global gene expression patterns in Fisher 344 rat liver exposed to lead (Pb^{2+}) at different doses and over different time periods of exposure using Affymetrix Microarray Analysis.

Lead can alter the function or activity of genes. For instance Korashy and El-Kadi [148] reported the induction of Cyp1a1 gene expression as a response Pb^{2+} and other metals. This process they attributed to an AhR-dependent process via transcriptional and post-translational mechanisms. Other workers attribute the dysregulation of genes by lead to feedback mechanisms involving interference of Pb with calcium-binding proteins or perturbation of the activity of protein kinase C (PKC) which in turn alters the transcriptional regulation of mRNA transcripts regulated by PKC [252, 253].

Gene expression analysis of a specific gene provides an estimate of the number of mRNA molecules obtained from DNA transcription of that particular gene in response to a stimulous. The assay process involves mRNA isolation from an organism's tissues, and the mRNA transcripts are then converted to labeled polynucleotides which are placed on microarraysand hybridized with the complimentary sequence tags on the chip. Affymetrix Microarray employs a high-density oligonucleotide arrays that are fabricated using *in-silico* synthesis of short oligonucleotide sequences on small glass chip by light-directed synthesis. Represented on the chip are known genes or potentially expressed sequences of 11-20 unique oligomeric probes which are 25 bases in length for each gene at different loci on the chip. The target sequence is a group of probes that correspond to a given gene or small group of highly similar genes. Targets are usually labeled enabling them to bind by hybridization to the probes on arrays with which they share sufficient complementary sequence [216].

Materials and Methods

Experimental Design

Forty-eight six weeks post-weaning male Fisher 344 rats were exposed to 0 ppm, 50 ppm or 500 ppm of Pb^{2+} in the form of lead acetate through drinking water *ad libitum* for 30 or 90 days, respectively. The control drinking water was distilled water. Prior to commencing treatments, the rat diet, control and treatment drinking water were analyzed by ICP-MS for lead contamination and for verification of accurate dose levels. Rats were housed at the Western Michigan University Animal Facility. The animals were treated according to the principles outlined in the NIH Guide for the Care and Use of Laboratory

Animals. There were eight rats which were randomly assigned to one of the three treatment groups. At the end of each exposure period (30d or 90d), rats were euthanized with CO_2 and blood was collected by cardiac puncture for serum analysis using ICP-MS. Livers were excised and snap frozen in liquid Nitrogen. Total RNA was isolated from rat livers using a Qiagen RNA Isolation kits for subsequent cDNA syntheses.

Total RNA Extraction

Total RNA was isolated from rat livers using a Qiagen RNA Isolation kit [247]. Between 0.05 – 1g liver samples were homogenized in RLT buffer. RLT buffer denatures and inactivates RNases. The RNA is then allowed to bind to a silica-gel membrane and finally eluted with RNase-free water. Total RNA was quantified using the UV-vis spectrophotometer at 260 and 280 nm absorbance and control eletrophoretic gels were run for RNA quality assurance purposes.

Microarray Experiment

Double stranded cDNA was synthesized from total RNA samples using reverse transcriptase and oligo dT primer. Then, this synthesized cDNA served as a template for T7 polymerase in an *in vitro* transcription (IVT) reaction in which amplified and biotin labeled antisense cRNA molecules were produced. These cRNA molecules were purified, fragmented and hybridized to GeneChip® Rat Expression Array Set 230 (RAE 230A) and subsequently scanned as described in Affymetrix GeneChip™ one-cycle eukaryotic target labeling assay [248]. The RAE 230A chip contains over 30,000 transcripts and variants representing more than 28,000 rat genes which were sensed by the instrument

and incorporated into the data. It consists of 31,042 probe sets with probe pairs of 11 and 25-mer oligonucleotide probe length.

Data Analysis

The Affymetrix microarray suite (MAS) software was used analyze the image data (.dat files) for computation of single intensity values for every probe locus on the arrays, and saved as .cel files. The fluorescence intensity due to proper hybridization of each target was estimated by examining the difference in fluorescence intensities in perfect match and mismatch probe pairs present at each locus on the chip. Then, intensities were scaled for all valid probes using a default target signal threshold of 500 units resulting in CHP data. These were saved as EXCEL files and imported into Biometric Research Branch – Array Tools (BRB-ArrayTools) software [249] for data collation, filtering, normalization and gene sub-setting. Genes which passed through the above quality assurance process were then analyzed for differential expression by scatter-plot analysis. Data collation involved importing data and aligning genes. BRB-ArrayTools converts either EXCEL or CHP files into a tab-delimited format. Individual arrays were filtered using spot filters. Spots on arrays which had signal intensities less than 10 were considered below a threshold and not analyzed further. A log base 2 transformation was applied to all data and each array was normalized to a reference array such that log-intensity differences between any experimental array and the reference array equaled zero over all the genes on the array. The reference was chosen to be the median array. Minimum gene fold-change filter was used to exclude probe sets from all arrays which did not meet the following criteria: the minimum fold change less than 20 %

of expression data values at least a 1.5-fold change in either direction from the gene's median value. Over 2300 genes met these criteria and thus were used in our subsequent analysis of differential gene expression and gene expression profiling.

Results

Differential Gene Expression Analysis

Figure 9 shows all of the greater than 2-fold differentially expressed genes of rats exposed to lead through drinking water. Figure 9A, E and B, F present the data for rat livers treated with 50 and 500 ppm Pb^{2+}, respectively for 30 days, whereas 9C, G and D, H represent data for rat livers that were exposed to 50 and 500 ppm Pb^{2+}, respectively for 90 days. Differentially expressed genes are those falling outside (above or below) of the pair of marker lines. These genes indicate expression ratios greater than 2- and 10-fold difference.

The differential gene expression in Fisher 344 rat liver exposed to varied concentrations of lead for both 30 and 90 days are shown in Table 8. At 2-fold expression difference, the number of genes either up/down-regulated appear to be similar for both treatments during the 30-day exposure period. Surprisingly, the 90-day, 50ppm treatment showed less than half the number of differentially expressed genes as compared to the 30-day treatment.

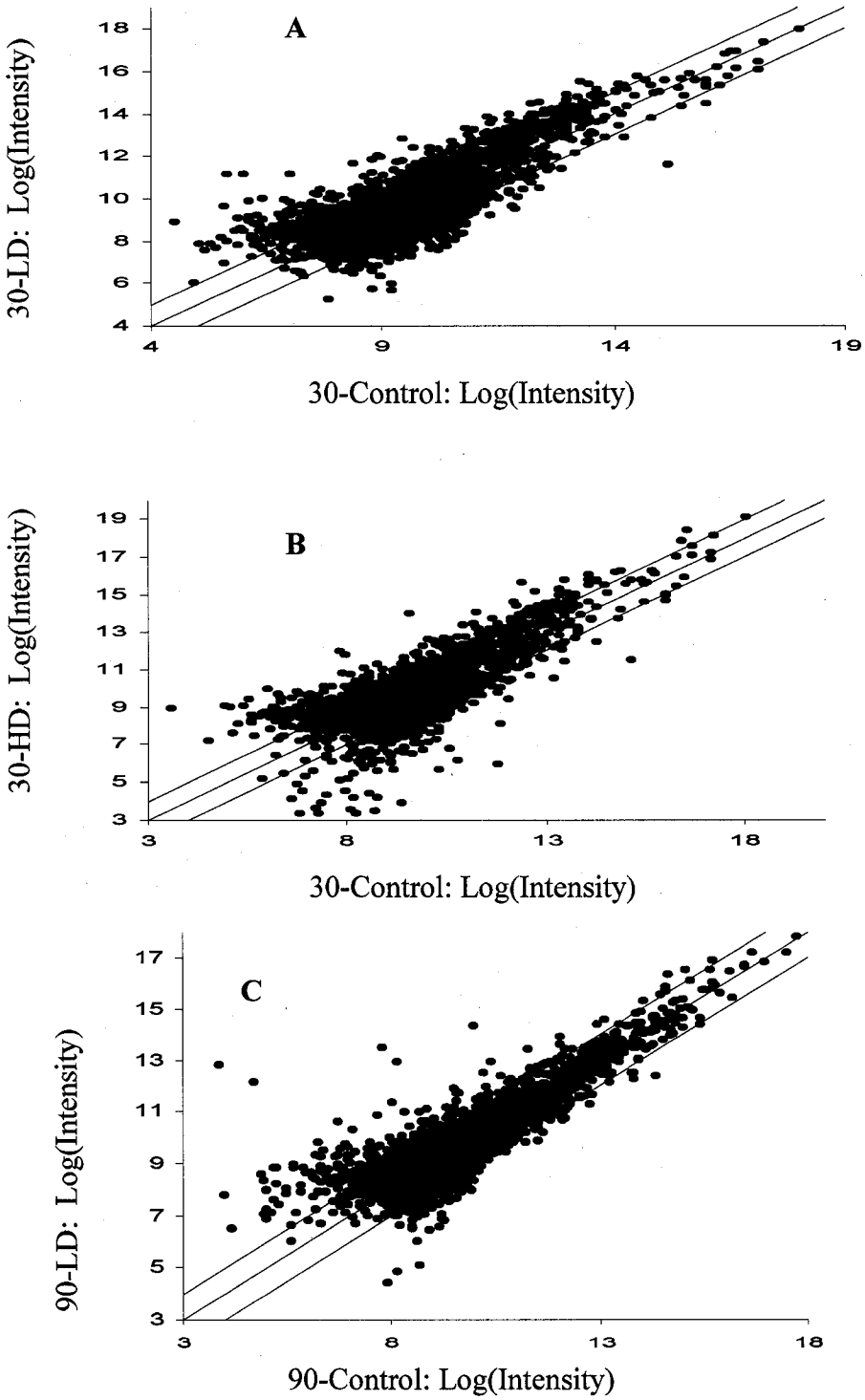

Figure 9: Genes expressed in the liver of Fisher 344 rats exposed to lead through drinking water for 30 days (A) 50 ppm Pb^{2+}, (B) 500 ppm Pb^{2+} or for 90 days (C) 50 ppm Pb^{2+}, (D) 500 ppm Pb^{2+} at two-fold change and (E) 50 ppm Pb^{2+}, (F) 500 ppm Pb^{2+} or for 90 days (G) 50 ppm Pb^{2+}, (H) 500 ppm Pb^{2+} at ten-fold change.

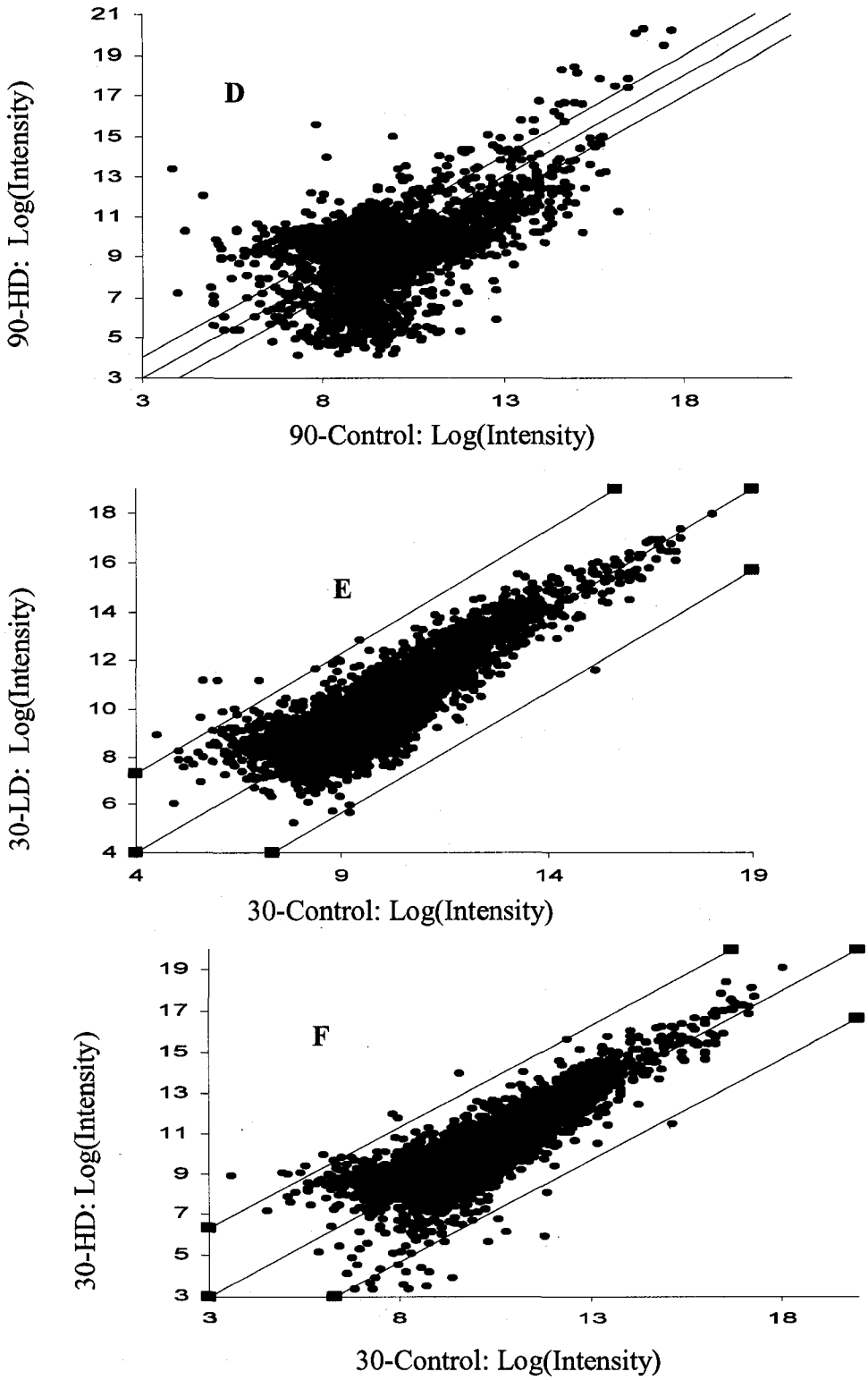

Figure 9 - Continued

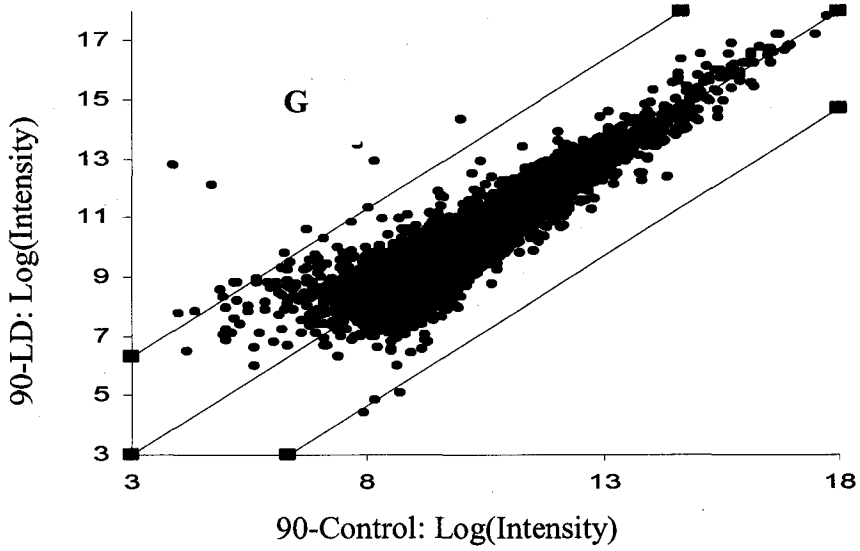

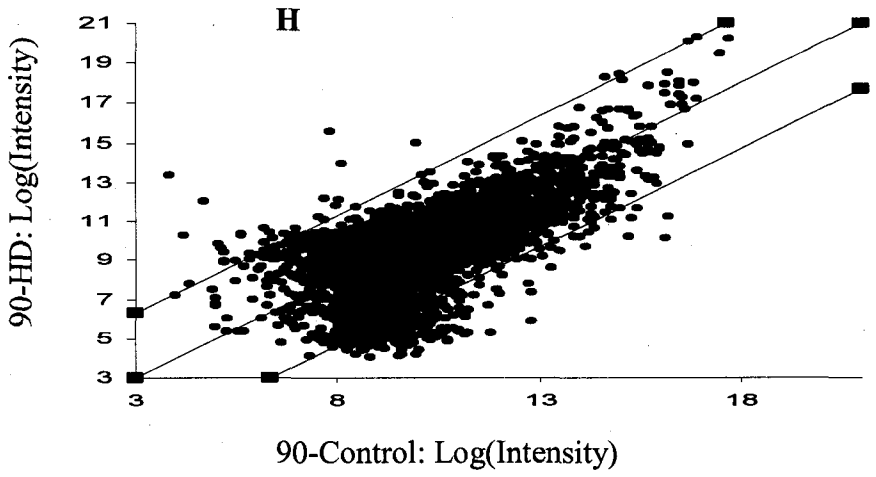

Figure 9 – Continued

In contrast, the 90-day 500ppm group exhibited over one thousand genes that were differentially expressed at 2-fold threshold level and more than twice the number of genes as the other treatment groups at the 3-, 5-, or 10-fold threshold levels. About 8 % of total transcripts after filtering and gene sub-setting were changed by ten-fold either by up or down regulation (Table 9).

Table 8

Transcripts whose expression levels were either suppressed or enhanced as a result of lead exposure.

		Regulation Type	**2-fold**	**3-fold**	**5-fold**	**10-fold**
30 Days Pb^{2+} Exposure	**50 ppm**	Up-regulation	585	179	43	9
		Down-regulation	488	134	24	2
	500 ppm	Up-regulation	543	181	48	10
		Down-regulation	436	147	49	19
90 Days Pb^{2+} Exposure	**50 ppm**	Up-regulation	181	54	20	13
		Down-regulation	224	29	4	2
	500 ppm	Up-regulation	498	234	76	32
		Down-regulation	1320	864	495	238

Transcriptional Profiling

Unsupervised Cluster Analysis

Clustering involves merging or grouping of samples or genes into subgroups that exhibit similar patterns of responses than the other experimental groups. In this study, hierarchical unsupervised clustering algorithm was adapted for comparing the gene expression profiles across all of the set of samples. By defining a measure of pair-wise similarity or distance between expression profiles, hierarchical clustering procedure produces sequentially nested merging of genes that are represented by a "dendogram". A "heat map" image of the log-ratio values with samples sorted according to dendogram order was generated [216, 249]. The results are shown in Figure 10A, B.

Table 9

Selected genes whose expression levels were either decreased or increased ten-fold.

Probe Set	Description	Gene Symbol	Regulation	Exposure
1388629_at	Inosine 5-monophosphate dehydrogenase 2	Impdh2	+ 4.031	30d 50ppm,
1367985_at	Aminolevulinic acid synthase 2	Alas2	- 4.704	30d 500ppm
1370993_at	Laminin, gamma 1	Lamc1	- 4.894	30d 500ppm
1370769_a_at	Inducible T-cell stimulator	Icos	+ 6.093	90d 500ppm
1372182_at	Phosphofructokinase, platelet	Pfkp	+ 3.422	90d 500ppm
AFFX-BioB-3_at	FBJ murine osteosarcoma viral oncogene homolog	Fos	+ 4.035	90d 500ppm
1367653_a_at	Malate dehydrogenase 1, NAD (soluble)	Mdh1	- 3.366	90d 500ppm
1367671_at	Proliferating cell nuclear antigen	Pcna	- 3.921	90d 500ppm
1368067_at	Zinc finger protein 148	Znf148	- 4.343	90d 500ppm
1368079_at	Pyruvate dehydrogenase kinase 1	Pdk1	- 5.208	90d 500ppm
1368403_at	Retinoblastoma-like 2	Rbl2	- 4.979	90d 500ppm
1369654_at	Protein kinase, AMP-activated, alpha 2 catalytic subunit	Prkaa2	- 5.096	90d 500ppm
1370274_at	Polyubiquitin	Ubb	- 3.830	90d 500ppm
1386894_at	Heat shock protein 1 (chaperonin)	Hspd1	- 4.065	90d 500ppm
1386950_at	Protein phosphatase 1, catalytic subunit, beta isoform	Ppp1cb	- 5.516	90d 500ppm

In Figure 10, snapshots of selected genes obtained via un-centered hierarchical clustering reveal log-ratio values that range from +4 to –9 for the long-term exposed rat group while the short-term treatment group had log-ratio values ranging from +6 to -7. The image plot matches log-intensity values with different colors. Most of the positive log-intensity values are coded red while the negative values are coded blue. In between the extremes of either +4 to -9 or +6 to -7 are yellow, green and light blue. Some of the genes captured by the snapshot are listed in the figure. Correlation coefficients on

the dendograms range from +1 to -0.2 and this relates to node width and distance from origin of the gene tree. Increases in correlation among genes leads to declining node width and a reduction in distance from the origin of the gene tree.

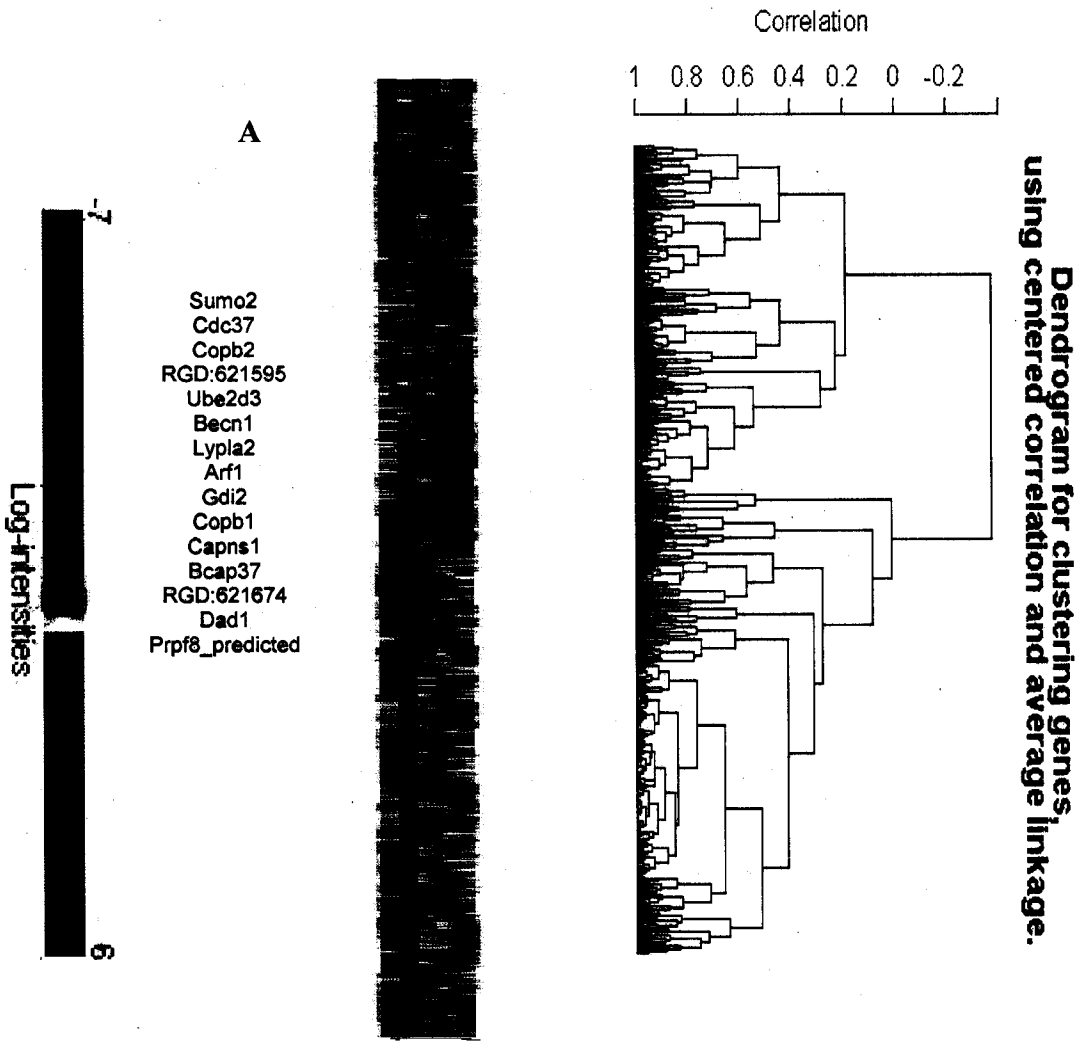

Figure 10: Hierarchical clustering using uncentered correlation and average linkage of genes across a set of lead treated hepatic samples. Figure showing dendograms and snapshots of heat map image for (A) 30 days treatment period and (B) 90 days exposure time.

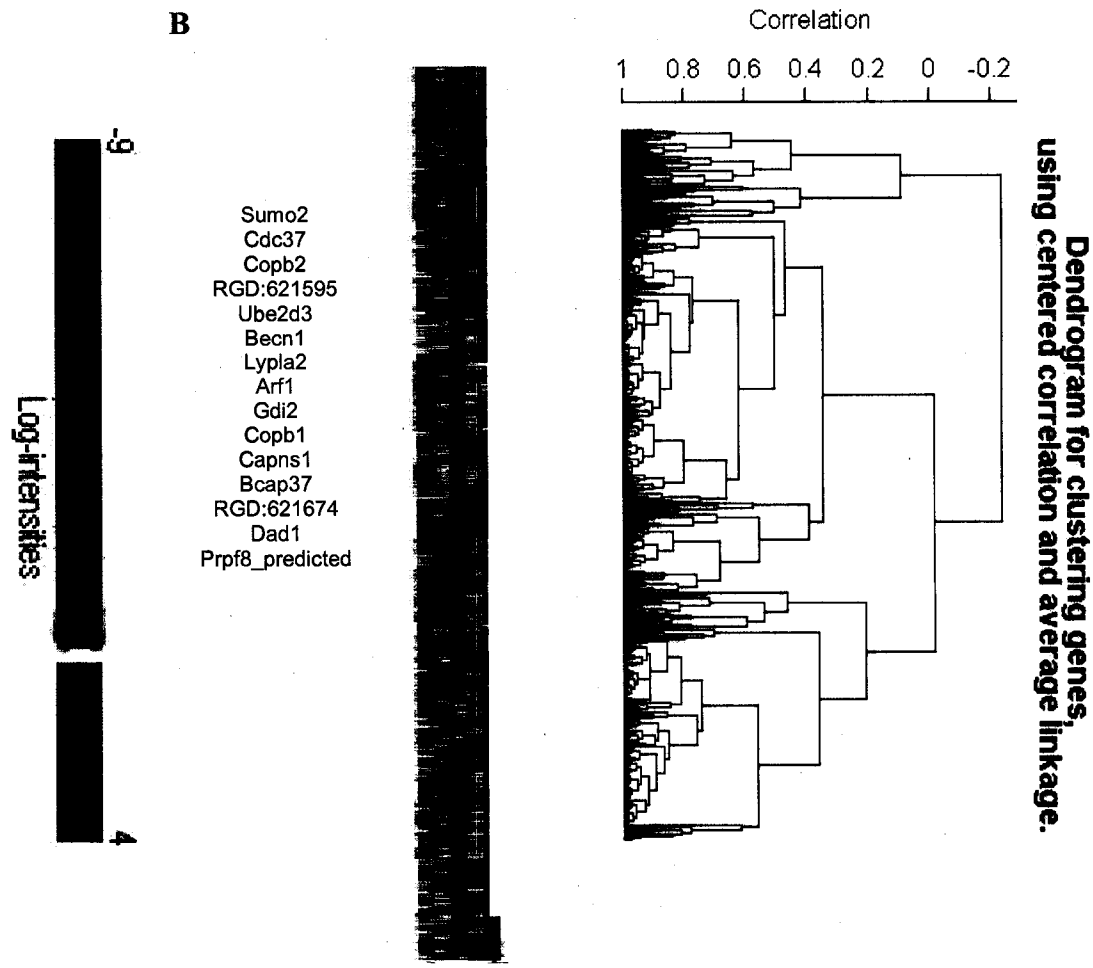

Figure 10 – Continued

Multi-dimensional scaling was used to compare pair-wise similarities between tissue samples. This analysis is similar to clustering analysis because the objective is to determine the relationships between samples without forcing them into specific clusters. The outcome is an un-centered correlation samples shown as a three dimensional rotating

cloud of spheres. Samples that have similar expression profiles are close together. Figure 11 is a graphical representation of multi-dimensional scaling of samples.

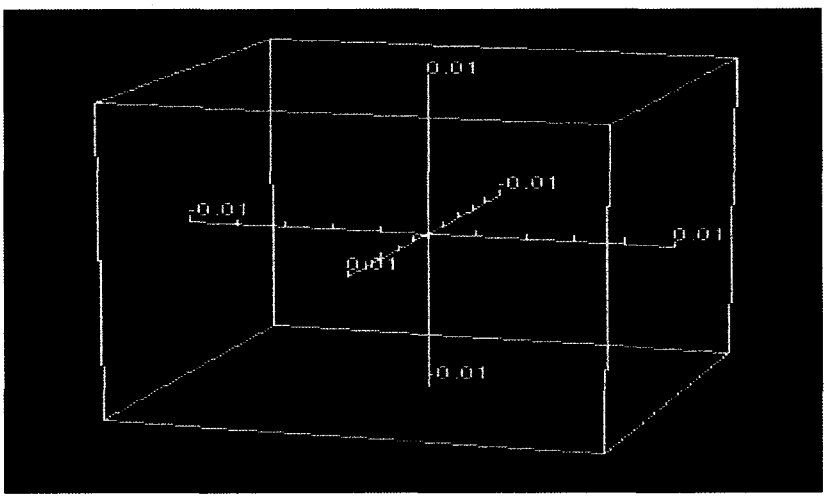

Figure 11: A graphical representation of multi-dimensional scaling of hepatic gene expression profiles of lead treated rats showing 30-day exposed rats (red spheres) and 90-day treatment groups (purple spheres).

Gene Ontology Analysis

In order to identify genes that were significantly correlated to such quantitative experimental parameters as dose levels and length of exposure, a Spearman Correlation Univariate Test was conducted. In the test a measure of correlation and parametric p-values were calculated by employing Spearman correlation coefficients [249]. These results are presented in Table 10.

In the Spearman Correlation Univariate Test at least ten genes were shown to correlate with either length of exposure period or with dose levels with p-values less than 0.01.

Table 10

Transcripts that were significantly correlated with either Pb dose-levels or with duration of exposure.

Trait: Dose

Probe Set	Description	Gene Symbol	Correlation Coefficient	Parametric p-value
1367683_at	Karyopherin (importin) alpha 2	Kpna2	-0.934	< 1e-07
1386868_at	Ribosomal protein S10	Rps10	+0.895	0.0014
1368288_at	Group specific component	Gc	+0.856	0.0035
1371548_at	Mitochondrial ribosomal protein S25 (predicted)	Mrps25predicted	-0.856	0.0035
1374465_at	Similar to ubiquitously-expressed transcript isoform 1	MGC105797	+0.856	0.0035
1398973_at	Adaptor-related protein complex 2 sigma 1 subunit	Ap2s1	+0.856	0.0035

Trait: Duration of Exposure

Probe Set	Description	Gene Symbol	Correlation Coefficient	Parametric p-value
1367802_at	Serum/glucocorticoid regulated kinase	Sgk	-0.87	0.0026
1367873_at	ATPase, H+ transporting, lysosomal (vacuolar proton pump) subunit 1	Atp6ap1	+0.87	0.0026
1367873_at	Forkhead box A2	Foxa2	+0.87	0.0026
1369312_a_at	Casein kinase 1 alpha 1	Csnk1a1	-0.87	0.0026
1370714_a_at	Sialyltransferase	Siat1	-0.87	0.0026
1371936_at	Eukaryotic translation initiation Factor 4A, isoform 1	RGD:735141	-0.87	0.0026
1399116_at	LUC7-like 2 (S. cerevisiae) (predicted)	Luc712_predicted	+0.87	0.0026

Some of these genes include Sgk, Atp6ap1, Foxa2, Kpna2, Rps10, Gc and Ap2s1 and these genes are involved in such gene ontology processes as sodium ion transport, apoptosis, protein amino acid phosphorylation, regulation of transcription, protein binding, protein transporter activity and vitamin D metabolism. For those gene transcripts that correlated with treatment duration, correlation coefficients were either +0.87 or -0.87. The dose level correlated group of genes had correlation coefficients of -0.934, -0.856, +0.895 and +0.856.

The Gene Ontology (GO) comparison tool was used to show the relationship between and the association of genes with respect to each other in function and biochemical pathways. This analytical tool provides GO categories of differentially expressed genes among samples than would be expected by chance. The procedure uses a functional class scoring approach. For each gene in the GO category, a p-value was calculated followed by using so-called LS and KS statistics to summarize the set of p-values of a GO category. LS is the average negative natural logarithm of p-values in a class while KS (Kolmogorov-Smirnov) statistic is employed in testing for uniform distribution of p-values. To determine the statistical significance of a GO category containing n number of genes, the empirical distribution of these summary statistics in random samples of n genes is computed. A 0.005 default p-value was used in this computation [249]. The results of the GO analysis of the data from the Lead exposed rat tissues are plotted as pie charts for the 30- and 90-day treatments.

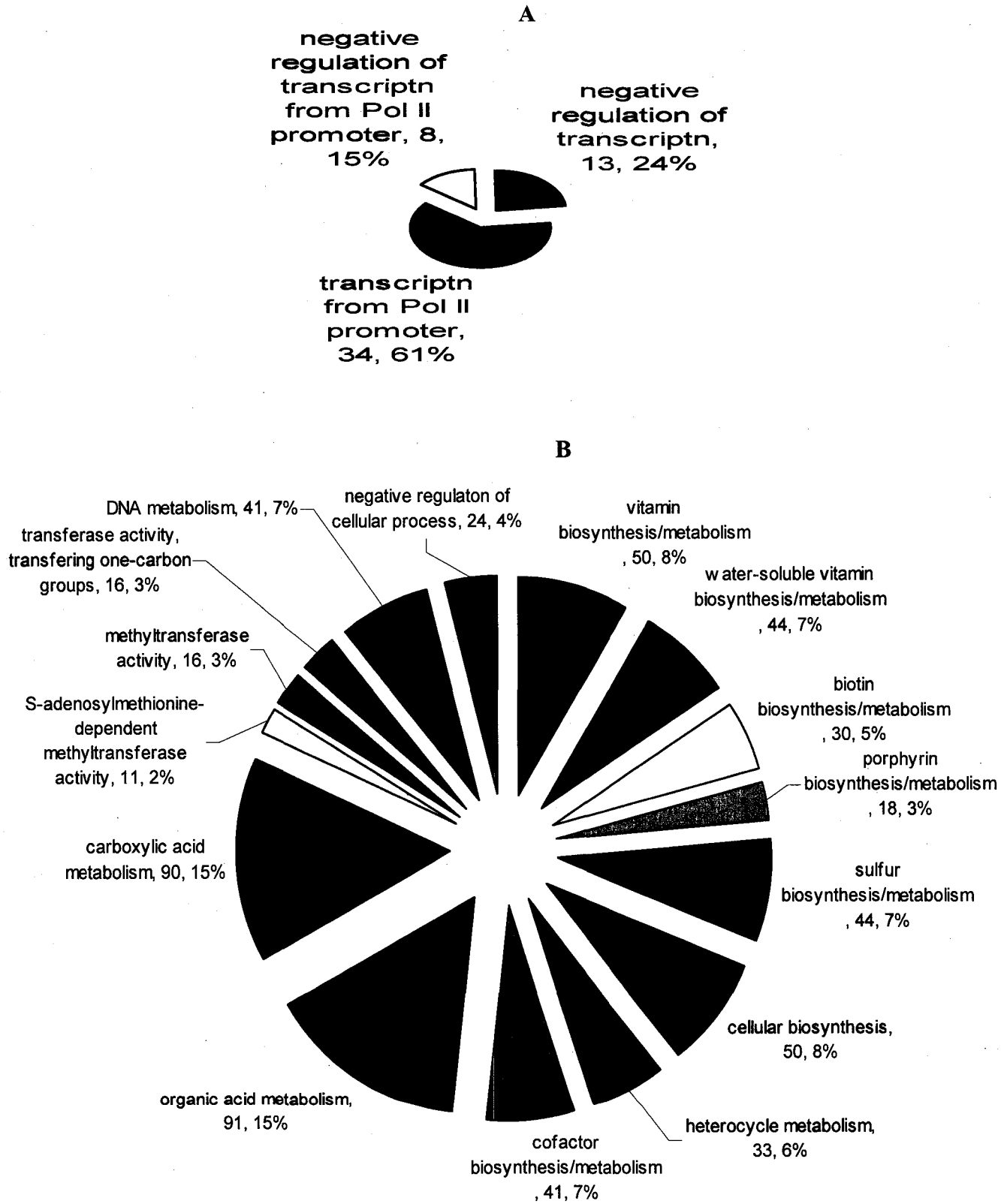

Figure 12: Gene ontology category difference of (A) 30-day treatment group and (B) 90 day treatment group.

Figure 12 presents the gene ontology categories for the two treatment groups. The short-term treatment group showed only three GO categories whereas the long-term exposure group showed 15 categories. The short-term exposure GO categories found were negative regulation of transcription, transcription from Pol II promoter and negative regulation of transcription from Pol II promoter in which each category was represented by 13, 34 and 8 genes, respectively. Some of the categories for the 90 days treatment groups are vitamin biosynthesis and metabolism, porphyrin biosynthesis and metabolism, DNA metabolism, carboxylic acid metabolism and biotin biosynthesis and metabolism. The number of genes in each category ranged from 2 % (11 genes) to 15 % (91 genes). The carboxylic/organic acid metabolism category had the highest number genes affected, whereas S-adenosylmethionine-dependent methyltransferase activity had the lowest percentage of genes affected by lead treatment in its category.

The gene ontology comparison tool provides for the option of grouping genes by metabolic or signaling pathways which are likely to be significantly effected instead of by GO categories. In this case, the affected genes are group by BioCarta pathways. "BioCarta" is a trademark of BioCarta Incoporated. Pathways found to be significantly impacted by lead intoxication include: regulation of eIF4e and p70 S6 Kinase, control of skeletal myogenesis by HDAC and calcium/calmodulin-dependent kinase (CAMK), role of MEF2D in T-cell Apoptosis and regulation of PGC-1a (Table 11). The regulation of Eif4e and p70 S6 kinase pathway was observed to have the following genes: Mapk14, Pdk2, Pdk1, Akt1, Ghr, Pten, Eif4a1, Eif4ebp1, Ebp, Mapk1 and Eif4e. Those genes found to control skeletal myogenesis are: Ywhah, Mapk14, Ppp3ca, Akt1, Calm1, Igf1, Cabin1, and Pik3r1.

Table 11

Pathways significant at nominal 0.005 levels of LS Permutation test or KS Permutation test.

Pathway ID	Pathway Description	Number of Genes	LS Permutation p-value	KS Permutation p-value
Biocarta: m_eif4Pathway	Regulation of eif4e and p70 S6 Kinase	12	0.00014	0.01327
Biocarta: m_hdacPathway	Control of skeletal myogenesis by HDAC & calcium/calmodulin-dependent kinase (CAMK)	11	0.00802	0.00299
Biocarta: m_mef2dPathway	Role of MEF2D in T-cell Apoptosis	6	0.01487	0.00353
Biocarta: M_pgc1aPathway	Regulation of PGC-1a	6	0.02253	0.00353

The pathway "Role of MEF2D in T-cell Apoptosis" has: Ppp3ca, Calm1 (1369936_at, 1369937_at, 1370368_at, 1387772_at) and cabin1. Finally, the regulation of the PGC-1a pathway has gene components: Ywhah, Ppp3ca (1373479_at and 1368277_at), Calm1 (1369936_at, 1369937_at and 1387772_at).

Pathway Descriptions

Regulation of eif4e and p70 S6 Kinase

Synthesis of proteins in mammalian systems is controlled by changes in the phosphorylation states of eukaryotic initiation and elongation factors (eIFs and eEFs, respectively) as well as other regulatory proteins. The p70 S6 kinase plays a crucial role in regulation of cell-cycle progression, cell survival and control of mRNA translation through phosphorylation of the 40 S ribosomal S6 protein [256-257]. In other words, the phosphorylation/inactivation of p70 S6 kinase and phosphorylation/inactivation of 4E-BP1 is essential for protein translation initiation.

Regulation of eIF4E complex, p70 S6 kinase and eEF2 is linked to the mammalian target of rapamycin (mTOR). mTOR which is composed of several regulatory signaling pathways is a multi-domain protein of 290 kDa with regions that are similar to lipid kinases of the phosphoinositide kinase family [257]. For example, a major mTOR signaling pathway involves the 70 kDa ribosomal protein S6 kinase that is reported to regulate the translation of a set of mRNAs. These have 5' terminal tracts of pyrimidines and encode for ribosomal proteins and elongation factors. A second example involves eIF4E-binding proteins (4E-BPs), which interacts with eIF4E and prevents it from interacting with a scaffolding protein eIF4G that is required for assembly of the

translation-factor complex eIF4F. The presence of insulin activates translation leading to the phosphorylation of 4E-BP1 through a pathway inhibited by rapamycin and as such involves mTOR, thereby leading to dissociation of eIF4E so that it becomes available to bind to eIF4G [257-258].

Control of Skeletal Myogenesis by HDAC & Calcium/Calmodulin-Dependent Kinase (CAMK)

Differentiation of myoblasts depends on myocyte enhancer factor-2 (MEF2) family of transcription factors association with positive and negative partners. The members of MEF2 family of transcription factors play a central role in skeletal muscle differentiation as well as serving as the end point for diverse intracellular signaling pathway that regulate myogenesis and muscle hypertrophy. MEF2 has four protein types namely; MEF2A, -B, -C, and –D. These proteins share homology in amino-terminal MCM1 agamus deficiens serum response factor (MADS) domain, which mediates DNA-binding, dimerization and cofactor interactions [263].

Histone acetylation/deacetylation is an important process in gene expression regulation. Histones are acetylated by histone acetyltransferases (HATs) leading to nucleosome relaxation so that transcription is stimulated. In contrast, the activity of HATs are inhibited by histone deacetylases (HDAC) resulting in transcription repression. HDACs are classed as I or II depending on size, sequence homology and formation of distinct complexes. In class I are HDACs-1, -2 and -3. These are ubiquitously expressed. Class II HDACs include HDAC-4, -5, -6 and -7 that are most abundant in heart, brain and skeletal muscle. Class II histone deacetylases HDAC4 and HDAC5 are known to repress transcription. Skeletal myogenesis is activated as a result of MEF2 associating with basic

helix-loop-helix transcription factors like MyoD. When these MEF2 proteins interact with HDAC4 and HDAC5 deacetylases, transcription of MEF2-dependent genes are repressed. In contrast, calcium/calmodulin dependent kinase (CAMK) signaling stimulates myogenesis through dissociating MEF2-HDAC complexes [262-265].

A model published by McKinsey *et al* [262] explains the how HDAC, MEF2 and CAMK interact to allow for myogenesis. This model illustrates the control of signal-dependency of myogenesis. Muscle differentiation is blocked by HDAC through repressing the transcriptional activity of MEF2. CaMK phosphorylates HDAC5 and stimulates its nuclear export thereby freeing MEF2 to cooperate with MyoD to activate genes required for skeletal myogenesis.

Role of MEF2D in T-cell Apoptosis

Although apoptosis of the T lymphocytes can be induced by multiple signaling pathways, Youn and coworkers [259] report a calcium-dependent expression of steroid receptors Nur77 and Nor1 that mediate T cell receptor (TCR)-induced apoptosis of thymocytes. The expression of orphan steroid receptor Nur77 requires an increase in intracellular calcium levels. Besides, two calcium regulated DNA elements in the Nur77 promoter were found to be consensus binding sites for MEF2, thus implicating MEF2 as a calcium-dependent transcription factor for Nur77 expression.

Calcineurin, an essential cytosolic calcium transmitting signal is activated by calcium and calmodulin. Cabin1 (calcineurin binding protein) binds to activated calcineurin and also interacts with myocyte enhancer factor 2 (MEF2) and calmodulin in a mutually exclusive way. Interaction of Cabin1 with MEF2 suppresses MEF2 transcriptional activity via the recruitment of the mSin3 corepressor complex using the

NH_2-terminal region of Cabin1. Nevertheless, high calcium levels, allows for calmodulin to bind cabin1 so that MEF2 is free to recruit coactivator p300 for transcriptional activation of MEF2 targets [259-261]. Similarly, Youn and Liu [260] also reports noted at least two mechanisms by which Cabin1 represses the activity of MEF2. First, cabin1 recruits mSin3 along with HDAC1 and HDAC2. This inhibition can be reversed by histone deacetylases. Secondly, Cabin1 binds to MEF2 at the N-terminal MADS/MEF2 domain leading to competition for against coactivator p300 for MEF2 binding in the absence of calcium.

Youn and Liu stated that TCR-induced expression of Nur77 family of proteins results in thymocytes apoptosis. The absence of TCR signal leads to cause Cabin1 silencing Nur77 promoter silent. But this inhibition is relieved by a second messenger calcium in response to TCR signaling. MEF2 is bound to Nur77 at all times and in an unactivated T cells, MEF2 is found bound to transcriptional repression complex made up of Cabin1, mSin3, HDAC1 and HDAC2. TCR signaling and calcium influx then results in activated calmodulin binding to Cabin1, thus relasing it from MEF2, vacating the MADS/MEF2 domain for association with the coactivator p300. Therefore, calcium-dependent association and dissociation of two opposing classes of enzymes tightly control Nur77 gene expression so that thymocytes only commit to apoptosis upon TCR signaling [259-260].

Regulation of PGC-1a

Peroxisome proliferators-activated receptor (PPARγ)-co-activator 1 (PGC-1) is a transcriptional cofactor involved mitochondrial gene regulation. PGC-1 is highly

expressed in tissues that have high energy demands and mitochondrial content. For example heart, kidney, brain, and brown fat. It was originally identified as important for regulating PPAR gene expression. PGC-1 is now known to also regulate nuclear respiratory factors (NRF-1, -2), uncoupling protein UCP2, hormone receptors; mineralocorticoid and estrogen receptors and MADS-protein MEF2C [266-267]

The coordinated interaction of PGC-1 with NRF-1 and PPAR factors controls program mitochondrial biogenesis and adaptive thermogenesis in brown adipose tissue and skeletal muscle [266-267]. Levels of PGC-1 were up-regulated in brown fat during exposure to cold. Scarpulla [268] reports that PGC-1 is involved in the control of blood glucose levels via the regulation of enzymes involved in gluconeogenesis. This was demonstrated in fasting mice in which PGC-1 was strongly up-regulated in liver. Also, an artificial over-expression of PGC-1 in cultivated hepatocytes and in vivo induced a series of gluconeogenetic enzymes [266, 268]. Scarpulla [268] explains that PGC-1 family members (PGC-1, PGC-1β or PRC) have a tendency to be induced by thermogenic, proliferative or gluconeogenic signaling pathways which can act on the appropriate target tissues. According to him, these coactivators can interact with DNA binding transcription factors leading to the expression of nuclear genes necessary for mitochondrial function and biogenesis. Activator-coactivator interactions can be direct or mediated by other proteins such as HCF and NRF-2 (GABP), so that the complexes formed may facilitate the recruitment of histone-modifying and RNA processing factors that contribute to the proper expression of gene targets.

The pathways outlined above show the importance of Pb in modulating phosphorylation and dephosphorylation events, calcium signaling, histone acetylation and

deacetylation in gene transcription regulation. Phosphorylation is reported to be particularly important in the case of MAP kinases which are believed to be phosphorylated at the Thr-Glu-Tyr motif. The description of the first pathway affected in our study suggests that this dephosphorylation event might occur via Serine residues. Histone acetylation and deacetylation processes in gene transcription regulation are the main focus of the second pathway outlined in this study. This process is likely to take place in manner dependent on calcium signaling, because CaMK activates mRNA transcription by dissociating myocyte enhancer factor-2 transcription factors from histone deacetylases (HDAC) complexes. Also, the third pathway 'role of MEF2D in T-cell apoptosis' is dependent on the activity of calcineurin (Cabin1), a cytosolic calcium transmitting signal that is activated by calcium and calmodulin. For instance, high calcium content will result in the binding of cabin1 to calmodulin so that MEF2 activates transcription. The last pathway identified in this study to be important in the study of Pb toxicity is important in the mitochondria and tissues that require high energy and this pathway was demonstrated to be important modulating gluconeogenesis enzymes. Since this pathway is important in the control of enzymes involved in gluconeogenesis, we might be seeing for the first time why gluconeogenesis is reported to be inhibited in rats exposed to Pb [232].

We can conclude from the above explanations that, the importance of calcium signaling in mediating Pb toxicity cannot be overestimated. This observation is consistent with our study hypothesis that the mRNA transcripts likely to be repressed or enhanced due to Pb exposure are essentially related to calcium signaling. Also, we can hypothesize the following for future study:

1. Pb controls mammalian protein synthesis via regulating phosphorylation or dephosphorylation events of eukaryotic elongation/initiation factors
2. Pb regulates gene expression through the regulation of histone acetylases
3. Pb regulates calcium dependent transcription factor myocyte enhance factor-2 (MEF-2)

Discussion

The advent of microarray technology has offered molecular biologists and geneticists, toxicologists among others, the opportunity assess several thousands of genes simultaneously. This technology has been employed in studying molecular phenotyping, functional genomics, pharmacogenomics, developmental biology and DNA sequencing and mutational analyses [212]. Since lead is known to cause a broad range of adverse effects upon exposure, this method was adopted in assessing the differential gene expression profiles of Fisher 344 male rat liver due to lead intoxication at different dose levels and over different exposure periods. In the process, it has been possible to outline some pathways that are likely to be affected and thus are important in the continuing study of lead toxicity.

The data scatter-plots of gene expression values with reference to controls and the subsequent follow-up tables reveal that, about 42 % of all genes were up-regulated at 2-fold change. Approximately 8 % of these genes were either up- or down-regulated at 10-fold. For the short-term treatment period, both low- and high-dose groups showed a gene expression in approximately 1:1 ratio for 2-, 3-, 5-, and 10-fold changes, except the 5-

and 10-fold down-regulation values. In contrast, the long-term exposed group revealed a more pronounced pattern gene expression alteration in the high-dose group than in the low-dose group. The ratio of high- to low-dose for 2-, 3-, 5- and 10-fold up-regulation were 2.75:1, 4.33:1, 3.8:1 and 2.46:1, respectively. Those for down-regulation were 5.89:1, 29.8:1, 123.75:1 and 119:1 correspondingly.

Comparing the 90-day treatment period to the 30-day period for the 50 ppm Pb^{2+} group, between one-half and one-third more transcripts were either 2-, 3-, and 5-fold up-regulated at 30 days than at 90 days exposure period. Similar trends were observed for down-regulated gene expression values. Interestingly, the 500 ppm Pb^{2+} group showed a different result between the time points. Chronically exposed rat groups exhibited 47 %, 56 %, 61 % and 71 % of transcripts up-regulated either 2-, 3-, 5-, and 10-fold, respectively. Similarly, 75 %, 85 %, 90 % and 93 % of genes between 30- and 90-day treatment period were either 2-, 3-, 5- and 10-fold down-regulated as a result of chronic lead intoxication. These results are quite different from those reported by Bouton *et al* [251] in their study of gene expression of lead exposed in rat astrocytes in which Clontech microarrays were employed. Of the 418 genes detected in their array, 94 passed the set criteria (ratio expression value $\geq$ 1.8 and t-test value of $p<0.05$). Eighty (85 %) were up-regulated and 14 (15 %) down-regulated.

Genes already known to be strong targets for lead exposure were observed to be differentially expressed in this study. Some of these are aminolevulinic acid synthase (Alas1, 2), FBJ murine osteosarcoma viral oncogene homolog (fos), heat shock protein 1 (hspd1), zinc finger protein 148 (Znf148) and protein kinase, AMP-activated, alpha 2 catalytic subunit (prkaa2), vascular endothelial growth factor A (Vegf), zinc finger

protein 189 (predicted) (Znf189_predicted) and mitogen activated protein kinase 14 (Mapk14) [145, 167, 251, 254]. According to the literature [145, 167, 251, 254], these effects are achieved through the perturbation of PKC activity by lead, the binding of lead to zinc-finger nucleotide binding proteins or inhibition of ALA dehydratase. This study also revealed other equally important genes that are likely to be affected by lead. Examples of these genes are: proliferating cell nuclear antigen (PCNA), Caspase (Casp 3), solute carrier family 25, member 30 (Slc25a30), ATPase inhibitor (Atpi), polyubiquitin (Ubb) and protein phosphatase 1, catalytic subunit, beta isoform (Ppp1cb), GATA binding protein 4 (Gata4), insulin-like growth factor 1 (Igf1), Forkhead box A2 (Foxa2), Karyopherin (importin) alpha 2 (Kpna2), Adaptor-related protein complex 2 sigma 1 subunit (Ap2s1), eukaryotic translation initiation factor 4E (Eif4e), tyrosine 3-monooxygenase/tryptophan 5-monooxygenase activation protein, eta polypeptide (Ywhah), protein phosphatase 3, catalytic subunit alpha isoform (Ppp3ca) and calcineurin binding protein 1 (cabin1).

According to Bouton *et al* [251], the altered regulation of numerous specific genes might produce distinct or diagnostic patterns of gene expression profiles, which can be grouped into clusters based upon similar shared properties. However, the clusters produced from dendograms or heat maps are not necessarily unique to a single toxicant. Patterns of clustering observed in our data across the time points of 30 days and 90 days appear similar though the 30 days exposure group have a ±2-fold lesser or greater number of affected genes than in the chronic treatment group. This observation seems to be confirmed by the multi-dimensional scaling plot. Eight out of the ten arrays aggregate

around the origin except two of the short-term treatment group arrays that are located either far to the right on the x-axis or far down below the origin on the y-axis.

Gene Ontology is useful in organizing differential gene expression information into biological processes, molecular function and cellular components. Results are implemented as GO categories in the form of tables and pathways (KEGG) which correlated to groups of genes [255]. GO analysis using quantitative test parameters dose levels and duration of exposure produced different results. Using dose as a reference parameter yielded such genes as karyopherin (importin) alpha 2, ribosomal protein S10, group specific component and adaptor-related protein complex 2 sigma 1 subunit. Similarly, length of exposure as a reference parameter produced gene markers such as serum/glucorticoid regulated kinase, ATPase, H^+ transporting, lysosomal (vacuolar proton pump) subunit 1, forkhead box A2, casein kinase 1 alpha 1 and sialyltransferase. Both experimental parameters produced both positive and negative correlations to specific gene expression values due to lead exposure.

GO category analysis revealed a significant shift in lead effects from a small group of molecular effects to a broad spectrum of biological and cellular level effects of lead intoxication between 30- and 90-days of exposure. Short-term effects on GO categories involve transcription regulation while chronic lead exposure effects were observed in the biosynthesis and metabolism of carboxylic acid, vitamins, biotin, porphyrin and cofactor. Some of the key gene transcripts involved in the GO category for the 30-day exposure group include Stat3, Taf9, Nab1, Bzw1, Nrbf2, Gata4, Thrsp and Zfp189_predicted. For the long-term group, some of these key genes are Pgd, Pcca, Alas1, Alas2, Gsta5, Gstt1, Pnpo, Mapk14, Srr, Cyp2c23, Igf1, Egfr, Vegf and Casp3.

The results of this series of experiments indicate that exposure time is importance in the assessment of dose-response relationships of lead toxicity. Dose levels are not crucial when the exposure period is short when considered based upon the number of genes affected. If exposure to lead becomes chronic, then dose was observed to become a more relevant factor. Responses to lead intoxication were observed to be similar for the short-term treatment period irrespective of lead dose. However, when the dose levels were low over long periods of time, toxic effects seemed to be minimized possibly due to an adaptive response over time. Williams and Iatropoulos [250] explain that the hepatic adaptive response could be beneficial if it leads to the enhancing the capacity of all cellular units to respond to chemical induced stress in order to preserve viability. The process involves modulation of the various cellular and extracellular functions of the cell leading towards homeostasis. Adverse effects often result, when the conditions necessary for homeostasis cannot be maintained. This was seen in the chronic treatment groups in this experiment, particularly at the high dose level.

Garza *et al* [240] pointed out that lead distribution within the cell is typically even and as a result, Pb reaches the endoplasmic reticulum, mitochondria and cell nucleus. This is manifested in the wide range of gene ontology categories and pathways that were identified as being affected by lead from our study. At least forty discrete pathways have been identified as being altered by lead intoxication. These categories ranges from biosynthetic and energy metabolism such as nucleotide synthesis and glycolysis through cell cycle regulation, apoptosis and DNA repair to calcium signaling and protein degradation by ubiquitin.

In summary, effects associated with lead exposure are dose and time dependent. Response to lead poisoning was observed to be almost similar for the short term treatment period irrespective of lead dose levels. However, when the dose levels were low over long periods of time, toxic effects are minimized due to adaptive response over time. On the contrary, lead exposure for long periods of time results in adverse effects in the form of increase incidence of lead-induced gene expression. Several of the differentially expressed genes are associated with essential pathways such as transcriptional, signaling and metabolism. Clustering patterns appear to be similar for all time points and dose levels. However, the short term exposure group have a ±2-fold less or greater than the sub-chronic treatment group. This was confirmed by multidimensional scaling plot which shows majority of arrays congregate around the origin. Gene ontology analysis revealed 15 GO categories affected by chronic lead exposure whiles three GO categories were observed to be significantly affected for short exposure periods. The following pathways; Regulation of eIF4e and p70 S6 Kinase, Control of skeletal myogenesis by HDAC and calcium/calmodulin-dependent kinase (CAMK), Role of MEF2D in T-cell Apoptosis are significantly perturbed by lead poison in vivo.

CHAPTER V

MICROARRAY DATA VALIDATION BY QUANTITATIVE REAL-TIME REVERSE TRANSCRIPTION POLYMERASE CHAIN REACTION (qRT-PCR)

qRT-PCR Background Information

Since its invention in the 1990s, real-time PCR has been increasingly employed to quantify nucleic acids for mutation, genotyping and chimerism analysis, consequently, the number of publications in which real-time PCR has been used in one way or another has also increased exponentially [219]. It has been described by Bustin [220] as the enabling technology of the genomic era and it is now considered the scientific standard for detection and quantification of RNA targets [221, 222]. Real-time PCR is unique in that amplified PCR products are monitored in real time so that information obtained from amplification curves can be used to determine the initial amounts of template molecules with high precision over a wide concentration range [219, 223]. The principle adapted in PCR is one in which target DNA gene sequence is amplified during denaturation-annealing-extension over a number of cycles. With conventional PCR, only the final concentration of the amplicon is monitored via a DNA-binding fluorescent dye while in qRT-PCR the amplicon concentration is monitored throughout 30-40 amplification cycles, also using fluorescent dyes. The fluorescent reagents bind to the amplified products without causing damage at the end of each amplification cycle so that amplification can continue. During the process, emitted fluorescence intensity is an indication of amplicon being produced in real time.

Several detection schemes are currently in use. The notable ones can be divided into three categories namely double-stranded binding dyes (dsDNA), DNA-sequence specific probes and DNA sequence-specific primers [223]. Examples of DNA-sequence specific probes include the Taqman®, molecular beacon and dual hybridization probe. DNA sequence-specific primers have the examples Amplifuor® primer, scorpion primer, Light Upon eXtension (LUX) and universal template systems [223]. The most widely used of these are SYBR Green I, Taqman® and molecular beacon. SYBR Green is the most frequently used dye in monitoring dsDNA amplification by qRT-PCR. Synthesis of dsDNA from single-stranded denatured DNA occurs during the extension phase of PCR cycle and the binding of this to SYBR green dye makes it possible to track the amount of amplified DNA using the fluorescence intensity of SYBR Green I. Taqman® probes are 5' terminally labeled oligonucleotides with a reporter fluorophor and 3'-sequence terminally labelled with a quencher. Quenching occurs on intact probes so that they do not fluoresce. During the extension phase of the primers, the probe is bound to the single-stranded PCR product. The probe is complementary to the amplicon sequence. TaqDNA polymerase sheers and cuts the probe with an endonuclease to release the quencher from the fluorophor, thus it can be excited and fluoresces. Increasing fluorescence is proportional to the amount of amplicons. Like the Taqman® probe, the molecular beacon is labeled on both ends but the middle end of the probe is complementary to the amplicon sequence while the terminal 10-15 nucleotides are self-complementary. This probe has a "hairpin" (stem-loop) structure in which the reporter is kept close to the quencher. At the annealing stage of the PCR cycle, fluorescence intensity of the reporter increases with distance from the quencher and this indicates the target DNA concentration. The rise in

temperature due to subsequent extension results in the detachment of the DNA segment though the hairpin structure is retained and this can rebind to the target DNA segment in the next cycle. Design and detection of molecular beacon probes are very demanding and are very sensitive to hybridization conditions thus they are difficult to optimize. Nevertheless, they have a high specificity and thermally stable because of the hairpin structure and they can discriminate between DNA sequences that differ by a single nucleotide substitution. These probes are therefore employed in mutation analysis or single nucleotide polymorphism analyses [219, 223].

The difference between RT-PCR and PCR is the preliminary step added to account for the conversion of mRNA into a cDNA template by RNA-independent DNA polymerase (reverse transcriptase). Also, in real-time PCR, the amplified PCR product is measured at each cycle throughout the PCR reaction rather than at the end of the amplification process. Thus, real-time PCR makes it possible to follow the amplification of PCR product over time during the exponential phase of the PCR process so that the precise amount of starting material can be determined. Unlike end-point PCR methods, the result obtained from real-time PCR is independent of the plateau that corresponds to the saturation of the reaction, which causes inaccurate quantification of the products [221, 224].

Compared with conventional PCR, qRT-PCR is provides a rapid, sensitive and specific means of detecting nucleic acid sequence targets. In addition, it is quantitative rather than qualitative [219, 221, 222, 224, 225]. RT-PCR is rapid and provides reliable data mainly as a result of the progress made during the last few years in detection instrumentation, such that some machines can accommodate 384 well plates containing

individual reactions as well as the ability que processes over 24h without stopping. This might become important in running high through-put assays. Data from RT-PCR has a wide dynamic range detection (>10^7-fold) and is reliable because the entire amplification profile is known so that individual reactions that deviate in their amplification efficiency due to the presence of polymerase inhibitors or other inhibitors can be identified. In summary, the combination of DNA sequence amplification and simultaneous detection steps into one continuous assay system reduces the need for post-PCR processing thereby increasing sensitivity. The wide dynamic range means that very low to very high concentrations of gene products can be determined in the same tissue extracts. That means that analysis of target gene abundances in samples that differ by orders of magnitude can be done. Although qRT-PCR has become the benchmark method for analyzing mRNA targets and its use is increasing popular with researchers, there are still a few technical challenges the user should take into consideration. These include issues of template quality, operator variability, reverse transcription step reproducibility, and the potential subjectivity of data analysis and reporting. Furthermore, there are currently no standardized qRT-PCR protocols [226].

Description of Genes Selected for Validation from Microarray Data

Calmodulin

Calmodulin (CaM) is considered a small ubiquitous eukaryotic calcium-binding protein that is a principal mediator of calcium signalling via the regulation of CaM-binding proteins [269-271]. Calmodulin which is a heat-stable acidic protein that is involved in such critical cell functions as regulation of cell division and differentiation,

control of gene expression, initiation of programmed cell death or apoptosis, DNA replication and repairing and exocytosis of hormone/neurotransmitter [272]. This protein is encoded in mammals by three different genes namely Calm1, Calm2 and Calm3 [270-273]. Knaup and Roemer [271] report that the three genes are located on different chromosomes with 20 % divergence in their coding regions. The structure of CaM is characterized by four calcium-binding motifs called helix-loop-helix EF-hands [272]. Ca^{2+}-ATPase which is responsible for calcium transport is regulated by calcium concentrations that are mediated by the activation or auto-inhibition of calmodulin (CaM) [275-276]. CaM may exist in both the active and inactive form in cells depending upon cell free-calcium levels. At high calcium levels, Ca^{2+} binds to calmodulin to form a calcium-calmodulin complex which is activated, and subsequently this complex binds to the domain of Ca^{2+}-ATPase so that calcium-ATPase is activated [275]. According to Lee and East [274], Ca^{2+}-ATPase crystal structure exhibits ten trans-membrane α-helices attached to three clear globular domains on the cytoplasmic end of the membrane whereas the lumenal end of the protein is made up of small loops. The transport of calcium is thought to occur according to the following scheme: first, E complexes with calcium and ATP to form a "high energy" intermediate E~P.2Ca^{2+}; second, there is the relaxation of this intermediate to its "low-energy" conformation E-P resulting in the release of calcium outside of the cell. Third, phosphate is hydrolyzed yielding E and finally making it possible for calcium binding-capacity recovery for another cycle of the reaction [275].

Aminolevulinate Synthase

Heme and heme proteins are important for the metabolism and transport of oxygen in vertebrates [277]. Aminolevulinate synthase, a protein located in the mitochondria, catalyzes the first and rate-limiting reaction in the biosynthesis of heme as well as playing a key role in heme biosynthesis pathway [277-279]. The reaction involves condensation of glycine and succinyl-CoA to form aminolevulinate. This enzyme is encoded by two genes ALAS1, which is ubiquitously expressed in tissues and ALAS2 that is expressed only in erythroid cells. ALAS1 is the drug-responsive, housekeeping gene that provides hemes for CYPs and other hemoproteins. On the other hand, ALAS2 is responsible for the generation of functional hemoglobin in erythrocytes [279]. Though the catalytic regions of these two proteins are similar and highly conserved in various genomes, their amino-terminal ends are different. The cellular expression and localization of both genes are regulated by heme itself. Regulation of ALAS2 is uncomplicated as compared to the regulation of ALAS1. ALA2 is typically controlled by the availability of iron that regulates the interaction with iron-binding proteins and the iron-responsive element in ALAS2-mRNA in order to control gene translation. ALAS1 is believed to be controlled by a feedback mechanism by heme itself however, the exact process by which this takes place is not fully understood.

ATP Synthase, H^+ Transporting, Mitochondrial F1 Complex, O Subunit

The F1Fo ATP synthase complex plays a vital role in cellular energy metabolism. This type of protein complex is found in bacteria, plant chloroplasts and mitochondria [280-284] and it acts to synthesize ATP from ADP and inorganic phosphate employing a

proton motive force that is generated across the mitochondrial membrane by electron flow [282-283]. Tucker *et al* [284] report that the general structure of this multi-subunit enzyme is highly conserved and composed of a globular F1 domain protruding out of the inner side of the membrane, Fo, a membrane-spanning proton channel and a stalk linking F1 to Fo [281-284]. Substrates, inorganic phosphates and ADP, are located in the catalytic binding site, F1 domain. Chen and coworkers [283] note that, energy is transferred to the catalytic site most probably via a proton flux through Fo as a result of conformational changes through the stalk.

Protein Phosphatase-3, Catalytic Subunit Alpha Isoform

Protein phosphatase is a calmodulin-regulated protein that plays a vital role in signal transduction. Phosphatases are important in controlling protein function via reversible phosphorylation-dephosphorylation cycles, especially those cellular processes that are in response to extracellular stimuli. Grove *et al* [287] estimates that nearly one-third of intracellular proteins phosphorylate. Protein phosphatase is one of the major cellular serine/threonine phosphatase proteins. Phosphatases are classified as 1, 2A, 2B, and 2C based upon preferences for different phosphoprotein substrates, their sensitivity to selective inhibitors and their specific Ca^{2+} or Mg^{2+} requirements. They are reported to be involved in such regulation processes as energy metabolism, receptor and ion channel functioning, transcription, RNA splicing, and cell growth and transformation [285-287]. According to Wang *et al* [285], these enzymes are heterodimers with molecular weights of 58-59 kDa and comprised of a calmodulin binding catalytic subunit and a small Ca^{2+}-binding regulatory subunit. The B form of the enzyme is conserved in all tissues except

the testes and is encoded by a single gene. The A form of the protein on the other hand has three isoforms (alpha, beta and gamma) which are encoded by genes on three different chromosomes.

Cytochrome P450, Family 3, Ssubfamily A, Polypeptide 13

Cytochromes P450 (CYPs) enzyme system plays a vital role in the oxidation of structurally diversified compounds, for example pharmaceutical agents, chemical carcinogens, lipophilic xenobiotic chemical and endogenous steroids, fatty acids, prostaglandins and vitamin D_3 [288-291]. Though the CYPs comprise a very large family of heme thiolate proteins, CYP3As are the most abundantly expressed sub-family in humans and account for ~50 % of clinically active drugs metabolized via this enzyme system. In the liver, about 30 % of P450s expressed are CYP3As and they are particularly important in the metabolism of pharmacologically, physiologically and toxicologically important agents. Although the CYPs are expressed in very limited amounts in the brain, they are reported to show evidence of involvement in brain development and its basic functions. The CYPs show gender-, tissue-, and age-dependence in their expression. Isoforms present in different species that are classified as part of the CYP3A subfamily are four human, five rat, six mouse gene isoforms and many more in other species [288-289].

Mitogen Activated Protein Kinase 1

Mitogen-activated protein kinases (MAPK) are proline-directed Ser/Thr protein kinases that are controlled via external signals such as growth factors, mitogens and

cellular stress. In other words, they are activated by dual phosphorylation on Tyr and Thr residues within the motifs of Thr-Glu-Tyr (ERK), Thr-Pro-Tyr (JNK) or Thr-Gly-Tyr (p38). The three most well characterized MAPKs are grouped as extracellular signal-regulated kinases (ERKs), c-Jun amino-terminal kinases (JNKs) that are critical regulators of transcription and the p38 MAPKs that are activated by inflammatory cytokines and environmental stress [292-294]. The cascade of these three modules is successively activated by phosphorylation events. Therefore, MAP kinase is phosphorylated and activated and in turn activates other kinases. For example, JNK is known to activate mapk4 and mapk7, while p38 is activated by mapk3, mapk6 and mapk4, and ERK is activated by mapk1 and mapk2 [294].

Materials and Methods

Total RNA Extraction

Total RNA was isolated from rat livers using a Qiagen RNA Isolation kit [247]. Between 0.05–1g liver samples were homogenized in RLT buffer. RLT buffer is responsible for denaturing and inactivating RNases. The RNA is then allowed to bind to a silica-gel membrane and finally eluted with RNase-free water. Total RNA was quantified using the spectrophotometer at 260 and 280 nm absorbance and gel electrophoresis was also run for quality assurance purposes.

Quantitative Real-Time Polymerase Chain Reaction (qRT-PCR)

To validate gene expression data from microarray experiments, quantitative real-time polymerase chain reaction (qRT-PCR) was employed to quantify the mRNA

expression of seven selected genes and a control gene β-Actin. Using the National Center for Biotechnology Information (NCBI) database, the FASTA mRNA sequence of β-Actin, calm1, calm2, Alas1, Atp5o, Ppp3ca, Cyp3a13 and Mapk1 were obtained for *Rattus norvegicus* and employed in the Taqman® Assay-on-Demand™ system provided by Applied Biosystems [295], thus offering us optimized probe and primer in a single tube. Synthesized cDNA from total RNA as described in Taqman® Gold RT-PCR kit [295] was diluted to different three concentrations each with three replicates per concentration assayed and loaded together with Taqman® Universal PCR Master Mix and the optimized probe and primer in the form of Taqman® Gene Expression Assay Mix in a 25 μL volume and run on ABI Prism® 7700. PCR temperature cycling conditions were 95 °C for 10 minutes DNA polymerase activation, followed by 40 cycles of 15s at 95 °C and 1 minute at 60 °C for denaturation and annealing, respectively.

Raw fluorescence intensity data were exported for normalized gene expression (NGE) analysis using data analysis for real-time PCR (DART-PCR) and relative expression software tool (REST©) which are both implemented in Excel [296-297]. Reaction efficiency was calculated by DART-PCR. Peirson *et al* [296] suggested that DART-PCR is a simple tool and reliable tool for analyzing PCR data from raw fluorescence data. Theoretical values of R_o are calculated from raw data on the basis the fluorescence is proportional to DNA concentration. The normalized theoretical value is the ratio of the target gene theoretical value to reference gene theoretical value. Efficiency is determined according to the following equation:

$$Efficiency = 10^{\left(1/slope\right)} - 1 \quad (1).$$

Expressions of genes relative to β-Actin were conducted by REST. Pfaffl and co-workers [297] report that such relative expression is increasingly employed in analyzing the expression of target genes after standardizing to a non-regulated reference gene(s). This statistical model employs a pair-wise fixed reallocation randomization test. Normalized gene expression values were calculated according to the equation as implemented in REST©.

$$NGE = \frac{\left(E_{target}\right)^{\Delta CP_{target(control-sample)}}}{\left(E_{ref}\right)^{\Delta CP_{ref(control-sample)}}} \quad (2)$$

Where E is PCR efficiencies, CP is threshold cycle and Δ is the difference of unknown sample verses a control.

Results

In order to validate gene expression data obtained by the Affymetrix Microarray assays, we used Taqman RT-qPCR to quantify the expression of nine selected genes that are crucial in studying potential lead toxicological effects. The selected genes were: calmodulin, aminolevulinate synthase, ATP synthase, H^+-transporting, mitochondrial F1 complex-O subunit, Protein phosphatase-3 (catalytic subunit alpha isoform), Cytochrome P4503A13, Mitogen activated protein kinase-1, Insulin-like growth factor-1 and Pyruvate dehydrogenase kinase-1. The gene expression levels of these genes as determined from Affymetrix Microarray are re-shown in Table 12.

Table 12

The expression of selected transcripts determined from Gene Chip Affymetrix Microarray.

Duration of treatment	30 Days		90 Days	
Treatment	50 ppm	500 ppm	50 ppm	500 ppm
Calm1	NC	-1.363	-1.73123	-1.169
Calm2	1.537	1.145	-1.77	-1.098
Alas1	1.083	2.039	-2.533	-2.571
Atp5o	1.892	1.103	-1.611	1.272
Ppp3ca	1.576	-1.804	-2.295	-1.0982
Cyp3a13	1.486	1.506	-1.102	-2.1
Mapk1	1.268	1.08	NC	-1.092

Most of the transcripts in the 30d exposure group were up-regulated whilst most in the 90d treatment were down-regulated. Calm1, Calm2, Atp5o, Ppp3ca and Mapk1 were all up-regulated in the short treatment regime.

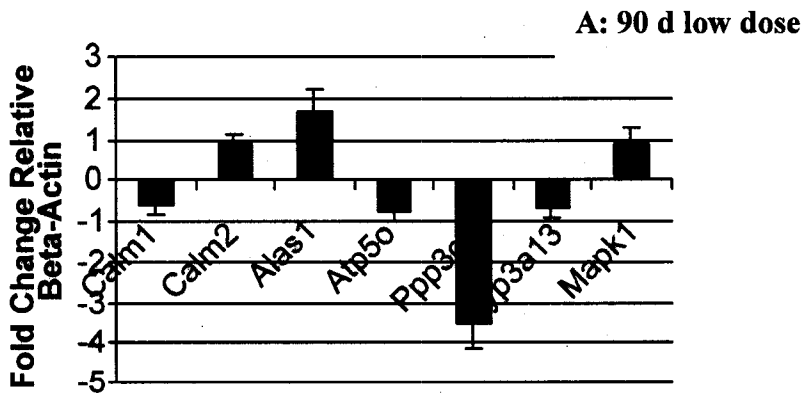

Figure 13: Expression of genes determined by QRT-PCR exposed to (A) 90d 50 ppm, (B) 90d 500 ppm, (C) 30d 50 ppm and (D) 30d 500 ppm.

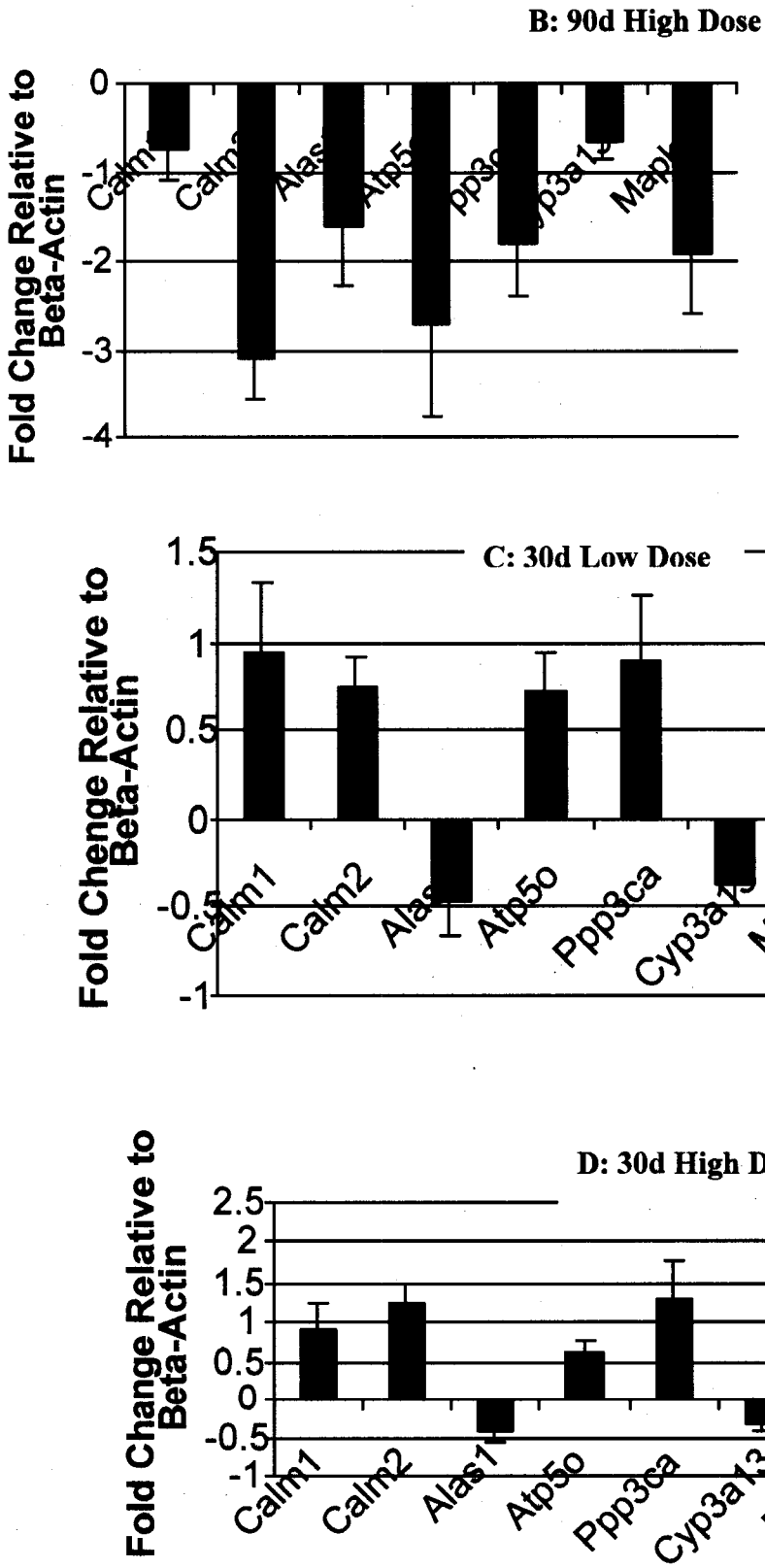

Figure 13 - Continued

For the chronic exposure group, Calm1, Calm2, Atp5o, Ppp3ca, Mapk1 were all down-regulated except Calm2 in the 50 ppm treatment group. Similarly, Alas1 was negatively regulated in all treatment groups except the 90d 50 ppm group. Cyp3a13 was negatively regulated in all treatment groups during all time points.

The relative comparison of gene transcripts analyzed by microarray gene chips and qPCR are shown in Table 13. Most of the mRNA transcripts favorably compare between the two analytical methods although the magnitude of expression varies.

Table 13

Comparison of transcripts determined by both Microarray Gene Chips and quantitative PCR. The first column indicates gene expression by microarray while the second shows the relative expression of genes evaluated by QPCR.

Genes	30 Days		90 Days	
	50 ppm	500 ppm	50 ppm	500 ppm
Calm1	0/+	-/+	-/-	-/-
Calm2	++/+	+/++	-/+	-/- - - -
Alas1	+/-	+/-	-/++	- -/- -
Atp5o	++/+	+/+	- -/-	-/- - -
Ppp3ca	++/+	-/++	- -/- - - -	-/- -
Cyp3a13	+/-	+/-	-/-	- -/-
Mapk1	+/+	+/++	0/+	-/- -

Discussion

Quantitative PCR was employed in validating the microarray results. This approach has been used in practically every microarray experiment for such purposes. Transcripts chosen for validation are involved in processes such as regulation of cell division and differentiation, metabolism and transport of oxygen in vertebrates, cellular energy metabolism, signal transduction, metabolism of pharmacologically, physiologically and toxicologically important agents, transcription regulation, activation of signal transduction pathways involved in the expression of transcriptional regulators of tumorigenesis and glucose metabolism.

From our study, gene expression as determined by microarray gene chips and qRT-PCR are comparable although the relative expression values are somewhat different. For example, in the higher dose chronically-exposed group, almost all mRNA transcripts evaluated by qPCR had greater fold-change values relative to the ones determined by Gene Chips. Apart from Calm1 and Mapk1 transcripts measured by gene chips in the 30d/50ppm and 90d/50ppm, respectively, all the mRNA transcripts showed expression levels. Most of the selected gene transcripts in the chronically exposed (90d) rats were down-regulated in the high dose group. The effects were less pronounced for the Calm1 and Cyp3a13 genes than for the others assayed. Chronic low dose exposures to lead yielded a mixture of gene regulation responses. Calm2, Alas1 and Mapk1 were up-regulated in this group while all other genes were slightly down-regulated except for Ppp3ca which was strongly down-regulated. Ppp3ca was actually more strongly down-regulated at the 50 ppm dose than at the 500 ppm dose.

In this study, we employed β-actin as an internal control because studies by Jover *et al* [145] found that the expression of β-actin is independent of dose or time of treatment lead acetate although dependent on RNA level in liver tissues of mice. In their experiment, they found that the injection of lead acetate results in about 45 % decrease Cyp3a11 mRNA levels after 12 hours. Instead of mRNA expression, other studies have examined the activities and protein levels associated with $p38^{MAPK}$ and calcium-calmodulin-dependent protein kinase II (CAMKII) in the brains of rats or zebra fish due to Pb exposure. The results indicate the phosphorylation of $p38^{MAPK}$ and a decrease in CaMKII levels in exposed rats. Also observed were a 40 % decrease of CaMKII β expression in hippocampal cytosolic fractions with no alterations in CaMKII α protein content [143, 299].

CHAPTER VI

CONCLUSIONS

The most ancient and relevant environmental poison to be used by man is lead and as such; it is ubiquitous in the environment. It is present in all kinds of soil and aquatic media in a wide range of concentrations, as a result lead can enter into the body by drinking water, ingestion of food, breathing lead particulates or by dermal contacts. Lead contaminated soil could provide a direct route of lead ingestion for infants or indirectly via contaminated food.

Lead is reported to be absorbed by both active and passive means with the most absorption occurring in the small intestine. The absorption of lead is influenced by several factors including ingested metal form, environmental matrix, gastrointestinal tract contents, diet, nutritional status, age and in some cases genotype. Lead is distributed in both soft and hard tissue. Its concentration increases in the order of muscle < brain < liver < kidney < bone. Lead can reside in the bone for as long as 20 years. Lead is essentially excreted via the urine or feces.

The health effects associated with Pb exposure reported in the literature are numerous. These range from unobservable symptoms to extreme cases of death in exposed victims. Health effects may be manifested via neurobehavioral, cancer, genotoxic, reproductive, developmental and immunological.

Several molecular and cellular mechanisms of Pb actions have been documented to explain the processes through which lead exerts its negative cellular and molecular influence. Lidsky and Schneider [198] classed Pb neurotoxic mechanisms as direct and

indirect whilst Goyer [196] defined it as being morphological and pharmacological. The neuropharmacological interactions include substitution for calcium, iron and zinc, neurotransmitter release, protein kinase C, Na-Ca ATPase and energy metabolism. Morphological interactions on the other hand consist of interference with adhesion molecules, impaired cell:cell programming connections and miswiring of the central nervous system. At the molecular level, lead is reported to regulate mRNA transcription. Several genes transcripts are reported in the literature to be regulated by Pb either directly or via some other consequential means. In the last several years, studies involving Pb have shifted focused on elucidating how Pb regulates mRNA transcription.

Experimental results from our study show that the effects associated with lead exposure and dose and time dependent. Short time span exposures do not produce serious damage, as long high dose intoxication levels. Histopathology results are consistent with lead concentration in liver and kidney as well other trace metals measured. For instance, high lead concentration of lead in kidney results in pronounced cell necrosis in varied forms. There was a positive correlation between lead and other trace metals for the short treatment period and a negative correlation for chronic exposure levels. ICP-MS results showed a significant accumulation of lead in blood, liver, kidney and bone marrow in lead exposed groups. With the exception of kidney, the 90-days treatment groups showed markedly high levels of lead in blood, liver and marrow than the 30-days exposed groups. Potential interactions of calcium, iron, cobalt, copper, zinc and nickel and lead examined showed positive and negative correlation for 30 and 90 days treatment period respectively. Hepatic histopathology produced no evidence of necrosis nor changes in architecture of hepatocytes in the 0 ppm and 50 ppm for the 30-day duration of exposure

in the case of the liver. In contrast, necrosis and alterations in the structure and disposition of the liver and kidney tissues were observed for the 500 ppm treatment group.

A total of over 2300 genes were then used in differential gene expression analysis by scatterplot with regards to the microarray experiment. The scatterplot data suggest a greater number of genes were differentially expressed in the 90 days 500 ppm Pb^{2+} treatment than the other dose groups. Using a 2-fold expression difference threshold, genes either up/down-regulated appear to be the same for both treatments during the 30 days exposure period. Interestingly, 90 days 50 ppm treatment showed less than half the number of genes expressed compared to the 30 days treatment. In contrast, the 90 days 500 ppm group had over one thousand genes differentially expressed at 2-fold and more than twice the number of genes of the other treatment groups at 3-, 5-, and 10-fold levels. Gene precursors for proteins such as FBJ murine osteosarcoma viral oncogene homolog, heat shock protein, protein kinase and proliferating cell nuclear antigen were ten fold up/down-regulated. Our study showed genes such as aminolevulinic acid synthase (Alas1, 2), calmodulin (Calm 1 and 2), mitogen activated protein kinase 14 (Mapk14) that are reported in the literature to be lead targets and Caspase (Casp 3), solute carrier family 25, member 30 (Slc25a30), ATPase inhibitor (Atpi), polyubiquitin (Ubb) and protein phosphatase 1, catalytic subunit, beta isoform (Ppp1cb), GATA binding protein 4 (Gata4), insulin-like growth factor 1 (Igf1) identified from this study to be potential targets of lead. Expression profiles were analyzed by clustering and gene ontology (GO). Clustering patterns appear to be similar for both time points and dose levels. However, the short term exposure group (30d) showed far fewer genes being affected by ±2-fold

than in the sub-chronic treatment group (90d). This was confirmed by multidimensional scaling plot which shows majority of arrays congregate around the origin. Gene ontology analysis revealed 15 GO categories affected by chronic (90d) lead exposure, whiles three GO categories were observed to be significantly affected for short exposure (30d) periods. The following pathways; Regulation of eIF4e and p70 S6 Kinase, Control of skeletal myogenesis by HDAC and calcium/calmodulin-dependent kinase (CAMK), Role of MEF2D in T-cell Apoptosis are significantly perturbed by lead poison in vivo.

To validate gene expression data acquired by Affymetrix Microarray, Taqman RT-qPCR was used to quantify the relative expression levels of selected genes already known to play important roles in mediating Pb^{2+} toxicity and others identified in our study that might be equally important in this process. Using Taqman RT reagents and Assay-On-Demand offered by Applied Biosystems, the expression of calm1, calm2, Alas1, Atp5o, Ppp3ca, Cyp3a13 and Mapk1 were measured relative to β-Actin. Most of the transcripts in the 30d exposure group were up-regulated while most transcripts in the 90d treatment were down-regulated, relative to controls. Calm1, Calm2, Atp5o, Ppp3ca and Mapk1 were all up-regulated in the short treatment regime. For the chronic exposure group, Calm1, Calm2, Atp5o, Ppp3ca, Mapk1 were all down-regulated except Calm2 in the 50 ppm treatment group, relative to controls. Similarly, Alas1 was negatively regulated in all treatment groups except the 90d 50 ppm group. Cyp3a13 was negatively regulated in all treatment groups during all time points. Confirming microarray results are the down-regulation of Calm2: -3.886, Alas1: -1.616, Atp5o: -2.706 and Cyp3a13: -1.79 genes in the long term exposure group.

Our results indicate the importance of time in the assessment of dose-response relationships of lead toxicity. Dose levels are not crucial when the exposure period is short. If exposure to lead becomes chronic, then dose becomes a relevant factor. Response to lead poisoning was observed to be almost similar for the short term treatment period irrespective of lead concentration. However, when the dose levels are low over long periods of time, toxic effects are minimized due to adaptive response over time. Williams and Iatropoulos [250] explains that, hepatic adaptive response could be beneficial if it leads to the enhancing the capacity of all units to respond to chemical induce stress in order to preserve viability. The process involves modulation of the various cellular and extracellular functions of the cell towards homeostasis. Adverse effects often result, when the conditions necessary for homeostasis cannot be achieved. This is seen in the sub-chronic treatment group.

Garza *et al* [240] pointed out that lead distribution in the cell is even and as a result, it reaches the endoplasmic reticulum, mitochondria and cell nucleus. This is manifested in the wide range of gene ontology categories and pathways that have noted to be affected by lead from our study. At least forty pathways have been outlined. The categories range from metabolism such as nucleotide synthesis and glycolysis through cell cycle regulation, apoptosis and DNA repair to calcium signaling and protein degradation by ubiquitin.

Summarily, effects associated with lead exposure are both dose and time dependent. Response to lead poisoning was observed to be almost similar for the short term treatment period irrespective of lead dose levels. However, when the dose levels are low over long periods of time, toxic effects are minimized due to adaptive response over

time. On the contrary, lead exposure for long periods of time results in adverse effects in the form of increase incidence of lead-induced gene expression. Several of the differentially expressed genes are associated with essential pathways such as transcriptional, signaling and metabolism.

REFERENCES

1. Jernigan EL, Bové JL, Langford JC, Morse RS, Magno PJ, Blanchard RL, Joshi LU, Patterson CC, Oliver RG, Hunt VR, Stanley RE, Potter GD, Kostial L, Scott KM, Murphy T, Hernberg S, Jovičić B, den Tonkelaar WAM, Omang SH, Groffman DM, Levine H, Prakash NJ and Sayre JW (1973) Lead poisoning in man an the environment MSS Information Corporation New York
2. Inorganic Lead Exposure: Metabolism and Intoxication Edited by Castellino N, Castellino P and Sannolo N (1995) Lewis Publishers Ann Arbor, Michigan
3. Waldron HA and Stöfen D (1974) Sub-clinical lead poisoning Academic Press New York
4. Lead Toxicity: history and environmental impact edited by Lansdown R and Yule W (1986) The John Hopkins University Press Baltimore, USA
5. Agency for Toxic Substances and Disease Registry (2005) Draft Toxicological Profile for Lead US Department of Health and Human Services Public Health Service
6. Lead Development Association (1974) Technical Notes on Lead: Production Properties and Uses. Lead Development Association, London
7. Waldron HA (1973) Lead poisoning in the ancient world MEDIEVAL HISTORY 17, 391-9
8. Nriagu JO (1965) Lead and lead poison in antiquity John Wiley and Sons New York
9. Nriagu JO (1983) Saturnine gout among Roman Aristocrats. Did lead poisoning contribute to the fall of the Empire? NEW ENGLAND J. MED. 308: 660-663

10. McCord CP (1953) Lead poisoning in early America. Benjamin Franklin and lead poisoning IND. MED. SURG. 22, 393-9

11. Bargagli R (2000) Trace metals in Antarctica related to climate change and increasing human impact REV. ENVIRON. CONTAM. TOXICOL. 166: 129-173

12. de Treville R (1964) ARCHIVES OF ENVIRONMENTAL HEALTH 8, 212 (Reported in Reference 7).

13. Florea A-M and Büsselberg D (2006) Occurrence, use and potential toxic effects of metals and metal compounds BIOMETALS 19:419-427

14. Patterson CC (1965) Contaminated and natural lead environments of man ARCHIVES OF ENVIRONMENTAL HEALTH 11:212

15. Xan FX, Banin A, Su Y, Monts DL, Plodinec MJ, Kingery WL and Triplett GE (2002) Industrial age anthropogenic inputs of heavy metals into the pedosphere NATURWISSENSCHAFTEN 89:497-504

16. Lankey RL, Davidson CI, and McMichael FC (1998) Mass balance for lead in the California South Coast Air Basin: an update ENVIRONMENTAL RESEARCH 78:86-93

17. Lucas A and Harris JR (1962) Ancient Egyptian materials and industries, 4th edition, Arnold, London

18. King M and Ramachandran V (1995) Lead. In: Kirk-Othmer encyclopedia of chemical technology 4th edition. John Wiley & Sons New York

19. Shea EE (1996) Lead regulation handbook. Rockville, MD: Government Institutes

20. Sutherland CA and Milner EF (1990) Lead. In Elvers B, Hawkins S, Schulz G eds. Ullmann's encyclopedia of industrial chemistry. 5th edition VCH Publishers, New York

21. DiFrancesco CA and Smith GR (2003) Lead Statistics United States Geological Survey (USGS)

22. Larrabee D (1998) Comments on chapter 4 of the draft toxicological profile for lead/metals division. U.S. Department of Commerce, February 11, 1998.

23. EPA 1982. U.S Environmental Protection Agency. Code of Federal Regulations. 40 CFR 60; EPA 1988 U.S Environmental Protection Agency. Code of Federal Regulations 40 CFR 372.65; U.S. Environmental Protection Agency. Code of Federal Regulations. 40 CFR 261, Appendix VIII

24. Romieu I, Palazuelos E, Avila MH, Rios C, Munos I, Jimenez C and Cahero G (1994) Sources of lead exposure in Mexico City ENVIRONMENTAL HEALTH PERSPECTIVES 102:384-389

25. Sources and toxicology of Lead Exposure of the Wisconsin Childhood lead poisoning prevention and control handbook

26. Kaste JM, Friedland AJ and Miller EK (2005) Potentially mobile lead fractions in montane organic-rich soil horizons WATER, AIR and SOIL POLLUTION 167:139-154

27. Sauvé S, McBride M and Hendershot W (1998) Lead phosphate solubility in water and soil suspensions ENVIRONMENTAL SCIENCE AND TECHNOLOGY 32:388-393

28. Sadiq M and Alam I (1996) Lead contamination of groundwater in an industrial complex WATER, AIR and SOIL POLLUTION 98:167-177

29. Nolan AL, Zhang H and McLaughlin MJ (2005) Prediction of zinc, cadmium, lead and copper availability to wheat in contaminated soils using chemical speciation, diffusive gradients in thin films, extraction and isotopic dilution techniques JOURNAL OF ENVIRONMENTAL QUALITY 34:496-507

30. Ochoa-Loza FJ, Artiola JF and Maier RM (2001) Stability constants for the complexation of various metals with a rhamnolipid biosurfactant JOURNAL OF ENVIRONMENTAL QUALITY 30:479-485

31. Su H-Y and Zhu Y-G (2005) influence of lead on atrazine uptake by rice (Oryza sativa L.) seedlings from nutrient solution ENVIRON. SCI and POLLUT RES 12:21-27

32. Lead, mercury, cadmium and arsenic in the environment edited by Hutchinson TC and Meema KM (1987) John Wiley and Sons New York

33. Mellor A and Bevan JR (1999) Lead in soils and stream sediments of an urban catchment in tyneside, UK, WATER, AIR and SOIL POLLUT 112:327-348

34. Marsh AS and Siccama TG (1997) Use of formerly plowed land in New England to monitor the vertical distribution of lead, zinc and copper in mineral soils WATER, AIR and SOIL POLLUT 95: 75-85

35. Kaste JM, Friedland AJ and Sturup S (2003) Using stable and radioactive isotopes to race atmospherically-deposited Pb in montane forest soils ENVIRON. SCI. TECHNOL. 37:3560-3567

36. Mishra A and Choudhuri MA (1998) Monitoring of phytotoxicity of lead and mercury from germination and early seedling growth indices in two rice cultivars WATER, AIR and SOIL POLLUTION 114: 339-346

37. Nolan AL, McLaughlin MJ and Mason SD (2003) Chemical speciation of Zn, Cd, Cu and Pb in Pore Waters of Agricultural and Contaminated soils using Donnan dialysis ENVIRON SCI TECHNOL 37: 90-98

38. Godelitsas A, Astilleros JM, Hallam K, Harissopoulos S and Putnis A (2003) Interaction of calcium carbonates with lead in aqueous solutions ENVIRON. SCI. TECHNOL. 37:3351-3360

39. Chang M, McBroom W and Beasley RS (2004) Roofing as a source of nonpoint water pollution JOURNAL OF ENVIRONMENTAL MANAGEMENT 73:307-315

40. TRI04. TRI explorer; providing access to EPA's toxic release inventory data. Washington, DC: Office of Information Analysis Access. Office of Environmental Information. U.S. Environmental Protection Agency. Toxics Release Inventory. http://www.epa.gov/triexplorer. June 9, 2006

41. Tao S, Li H, Liu C and Lam KC (2000) Fish uptake of inorganic and mucus complexes of lead ECOTOXICOLOGY AND ENVIRONMENTAL SAFETY 46: 174-180

42. Kang CL, Guo J, Guo P and Zhao YX, Dong (2005) Adsorption behavior of Pb^{2+} by organic components of natural biofilms in natural water and the influencing factors CHEMICAL JOURNAL OF CHINESE UNIVERSITIES-CHINESE 26: 2043-2045

43. Billon G, Ouddane B, Laureyns J and Boughriet A (2001) Chemistry of metal sulfides in anoxic sediments PHYSICAL CHEMISTRY CHEMICAL PHYSICS 3: 3586-3592

44. Meyer I, Heinrich J and Lippold U (1999) Factors affecting lead and cadmium levels in house dust in industrial areas of eastern Germany. SCI. TOTAL ENVIRON. 234:25-36

45. Jaradat QM, Momani KA, Jiries AG, El-Mufeed A, Batarseh MI, Sabri TG and Al-Momani IF (1999) Chemical composition of urban wet deposition in Amman, Jordan WATER, AIR and SOIL POLLUTION 112:55-65

46. Zereini F, Alt F, Messerschmidt J, Wiseman C, Feldmann I, Bohlen AV, Müllen J, Liebl K and Püttmann (2005) Concentration and distribution of heavy metals in urban airborne particulate matter in Frankfurt am Main, Germany ENVIRON. SCI. TECHNOL 39:2983-2989

47. Samara C and Voutsa D (2005) Size distribution of airborne particulate matter and associated heavy metals in the roadside environment CHEMOSPHERE 59:1197-1206

48. Fernandez-Espinosa AJ and Ternero Rodríguez M (2004) Study of traffic pollution by metals in Seville (Spain) by physical and chemical speciation methods ANAL BIOANNAL CHEM 379:684-699

49. Miller EK and Friedland AJ (1994) Lead migration in forest soils: response to changing atmospheric inputs. ENVIRON. SCI. TECHNOL. 28:662-669

50. Michopoulos P, Baloutsos G, Economou A, Nikolis EB and Thomaidis NS (2005) Biogeochemistry of lead in an urban forest in Athens, Greece BIOGEOCHEMISTRY 73: 345-357

51. Schlesinger WH, Reiners WA and Knopman DS (1974) Heavy metal concentrations and deposition in bulk precipitation in Montane ecosystems of New Hampshire, USA. ENVIRON. POLL. 6:39-47

52. Schlesinger WH and Reiners WA (1974) Depostion of water and cations on artificial foliar collectors in Fir Krummholz of New England Mountains. ECOLOGY 55:378-386

53. Friedland AJ, Johnson AH and Siccama TG (1984). Trace metal content of the forest floor in the green mountains of Vermont: Spatial and temporal patterns 21: 161-170

54. Klaminder J, Bindler R, Omteryd O, Appleby P and Grip H (2006) Estimating the mean residence rime of lead in the organic horizon of boreal forest soils using 210-lead, stable lead and a soil chronosequence BIOGECHEMISTRY 78:31-49

55. Bindler R, Brännvall M-L, Renberg I, Emteryd O, and Grip H (1999) Natural Lead Concentrations in Pristine Boreal Forest Soils and Past Pollution Trends: A Reference for Critical Load Models ENVIRON. SCI. TECHNOL 33: 3362 – 3367

56. Brännvall M.-L, Bindler R, Emteryd O and Renberg I (2001) Vertical distribution of atmospheric pollution lead in Swedish boreal forest soils WATER AIR SOIL POLLUTION. Focus 1: 357-376

57. Brännvall M.-L, Bindler R, Emteryd O and Renberg I (2001) Four thousand years of atmospheric lead pollution in northern Europe: a summary from Swedish lake sediments JOURNAL OF PALEOLIMNOLOGY 25: 421-435

58. FAO/UNESCO (1992) World Resources Report 60 FAO

59. Watmough SA, Hutchinson TC and Dillon PJ (2004) Lead dynamics in the forest floor and mineral soil in south-central Ontario BIOGEOCHEMISTRY 71:43-68

60. Dorr H and Munnich KO (1991) Lead and cesium transport in European forest soils. WATER AIR SOIL POLLUTION 57-58: 809-818

61. Erel Y (1998) Mechanisms and velocities of anthropogenic Pb migration in Mediterranean soils ENVIRON. RES. 78: 112-117

62. Erel Y, Veron A and Halicz L (1997) Tracing the transport of anthropogenic lead in the atmosphere and in soils using isotopic ratios Geochim. Cosmochim. Acta 61: 4495-4505

63. Nedwed T and Clifford DA (1998) A survey of lead battery recycling sites and soil remediation processes WASTE MANAGEMENT 17: 257-269

64. Cao X, Ma LQ, Chen M, Sing SP and Harris WG (2002) Impacts of phosphate amendments on lead biogeochemistry at a contaminated site ENVIRONMENTAL SCIENCE TECHNOLOGY 36: 52965304

65. Huang J-H and Matzner E (2004) Biogeochemistry of trimethyllead and lead in a forested ecosystem in Germany 71: 125-139

66. Outridge PM (1999) Lead biogeochemistry in the littoral zones of south-central Ontario lakes, Canada, after the elimination of gasoline lead additives WATER AIR and SOIL POLLUTION 118: 179-201

67. James AC, Stahlhofen W, Rudolf G, Köbrich R, Briant JK, Egan MJ, Nixon W and Birchal A (1994) Annexe D. Deposition of inhaled particles. ANNALS OF THE ICRP 24: 231-299

68. Task Group on Lung Dynamics (1966) Deposition and Retention Models for Internal Dosimetry of the Human Respiratory Tract. HEALTH PHYSICS 12: 173-207

69. Ragan HA (1983). The bioavailability of iron, lead and cadmium via gastroinstestinal absorption: a review

70. Simons TJB (1988) Active transport of lead by the calcium pump in hum red cell ghosts JOURNAL OF PHYSIOLOGY 405: 105-113

71. Kerper LE and Hinkle PM (1997) Lead uptake in brain capillary endothelial cells: activation by calcium store depletion TOXICOLOGY AND APPLIED PHARMACOLOGY 146: 127-133

72. Deane R AND Bradbury MWB (1990) Transport of lead-203 at the blood-brain barrier during short cerebrovascular perfusion with saline in the rat J. NEUROCHEM. 54: 905-914

73. Barton JC (1984) Active transport of lead-210 by everted segments of rat duodenum. AMERICAN JOURNAL OF PHYSIOLOGY 247: G193-98

74. Simons TJB (1984) Active transport of lead by human red blood cells FEBS LETTERS 172: 250-254

75. Tomsig JL and Suszkiw (1991) Permeation of Pb2+ through calcium channels: Fura-2 measurements of voltage- and dihydropyridine-sensitive Pb^{2+} entry in isolated bovine chromaffin cells. BIOCHIM. BIOPHYS. ACTA 1069: 197-200

76. Simons TJB (1986) The role of anion transport in the passive movement of lead across the human red cell membrane J. PHYSIOL (Lond.) 378: 287-312

77. Liubchenko PN (1984) Effect of several factors on lead absorption in the intestine VOPR PITAN 1: 55-7

78. Diamond GL, Goodrum PE, Felter SP and Ruoff WL (1997) Gastrointestinal absorption of metals DRUG CHEM TOXICOL 20: 345-368

79. Taggart MA, Figuerola J, Green AJ, Mateo R, Deacon C, Osborn D and Meharg AA (2006) After the Aznalcollar mine spill: arsenic, zinc, selenium, lead and copper levels in the livers and bones of five waterfowl species ENVIRON RES 100: 349-361

80. Conrad ME and Barton JC (1978) Factors affecting the absorption and excretion of lead in the rat GASTROENTEROLOGY 74:731-740

81. Luhovs'kyi SP (2001) The effect of iron and zinc on lead absorption in the tunica mucosa of various parts of rat small intestine FIZIO ZH 47: 41-45

82. Sullivan MF and Ruemmler PS (1987) Effect of excess Fe on Cd or Pb absorption by rats J TOXICOL ENVIRON HEALTH 22: 131-139

83. Forbes GB and Reina JC (1972) Effect of age on gastrointestinal absorption (Fe, Sr, Pb) in the rat J NUTR 102: 647-652

84. Kehoe RA (1964) Normal metabolism of lead ARCH. ENVIRON HEALTH 8: 232-235

85. Kostial K, Simonovic I and Pisonic M (1971) Lead absorption from the intestine in new born rats. NATURE 233: 564-564

86. Kostial K and Moncilovic B (1972) The effect of lactation on the absorption of Pb 203 and Ca 47 in rats HEALTH PHYS. 23: 383-384

87. Rabinowitz M, Leviton A and Needleman H (1973) Lead metabolism in the normal humans: stable isotope study SCIENCE 182: 725-727

88. Barry PSI (1975) A comparison of concentrations of lead in human tissues BR. J. IND. MED. 32: 119-139

89. Teodorova S, Metcheva R and Topashka-Ancheva M (2003) Bioaccumulation and damaging action of polymetal industrial dust on laboratory mice *Mus musculus alba*

I. Analysis of Zn, Cu, Pb, and Cd disposition and mathematical model for Zn and Cd bioaccumulations

90. Goyer RA (1996) Toxic effects of metals. In: Casarret and Doull's Toxicology. The basic science of poisons 5th Ed. Health Professions Division, New York

91. Barry PSI and Mossman DB (1970) Lead concentrations in human tissues BR. J. IND. MED. 27: 339-351

92. Arai F, Yamauchi H, Chiba K and Yoshida K (1998) Excretion of trimethyllead, diethyllead and inorganic lead in rabbits after injection of triethyl neopentoxy lead IND. HEALTH 36: 331-336

93. Gulson BL, Mizon KJ, Palmer JM, Korsch MJ and Donnelly JB (2000) Urinary excretion of lead during pregnancy and postpartum 262: 49-55

94. Gulson BL Mahaffey KR, Jameson CW, Mizon KJ, Korsch MJ, Cameron MA and Eisman JA (1998) Mobilization of lead from the skeleton during the postnatal period is larger than during pregnancy J. LAB. CLIN. MED 131: 324-9

95. Mushak P (1993) New directions in the toxicokinetics of human lead exposure NEUROTOXICOLOGY 14: 29-42

96. O'Flaherty EJ (1998) A physiologically based kinetic model for lead in children and adults ENVIRONMENTAL HEALTH PERSPECTIVES 106: 1495-1503

97. U.S. EPA Technical Review Workgroup (2005) The development and application of EPA lead models: the integrated exposure uptake biokinetic model (IEUBK) and the adult lead methodology (ALM) Washington DC

98. Leggett RW (1993) An age-specific kinetic model of lead metabolism in humans ENVIRONMENTAL HEALTH PERSPECTIVES 101: 598-616

99. Mason HJ (2000) A biokinetic model for lead metabolism with a view to its extension to pregnancy and lactation; (1) further validation of the original model for non-pregnancy adults THE SCIENCE OF THE TOTAL ENVIRONMENT 246: 69-78

100. Gulson BL, Mahaffey KR, Jameson CW, Vidal M, Law AJ, Mizon KJ, Smith AJM and Korsch MJ (1997) Dietary lead intakes for mother/child pairs and relevance to pharmacokinetic models ENVIRONMENTAL HEALTH PERSPECTIVES 105: 1334-1342

101. Zaragoza L and Hogan K (1998) The integrated exposure uptake biokinetic model for lead in children: independent validation and verification ENVIRONMENTAL HEALTH PERSPECTIVES 106: 1551-1556

102. Hogan K, Marcus A, Smith R and White P (1998) Integrated exposure uptake biokinetic model for lead in children. Empirical comparisons with epidemiological data ENVIRONMENTAL HEALTH PERSPECTIVES 106: 1557-1567

103. White PD, Leeuwen PV, Davis BD, Maddaloni M, Hogan KA, Marcus AH and Elias RW (1998) The conceptual structure of the integrated exposure uptake biokinetic model for lead in children ENVIRONMENTAL HEALTH PERSPECTIVES 106: 1513-1530

104. O'Flaherty EJ (1995) Physiologically based models for bone-seeking elements V. lead absorption and disposition in childhood TOXICOLOGY AND APPLIED PHARMACOLOGY 131: 297-308

105. O'Flaherty EJ (1993) Physiologically based models for bone-seeking elements IV. Kinetics of lead disposition in humans TOXICOLOGY and APPLIED PHARMACOLOGY 118: 16-29

106. Fleming DEB, Chettle DR, Webber CE and O'Flaherty EJ (1999) The O'Flaherty model of kinetics: an evaluation using data from a lead smelter population TOXICOLOGY and APPLIED PHARMACOLOGY 161: 100-109

107. O'Flaherty EJ, Inskip JM, Yagminas AP and Franklin CA (1996) Plasma and blood lead concentrations, lead absorption and lead excretion in nonhuman primates TOXICOLOGY and APPLIED PHARMACOLOGY 138: 121-130

108. Bruenger FW, Stevens W and Stover BJ (1973) The association of 210P with constituents of erythrocytes HEALTH PHYS 25: 37-42

109. Raghavan SRV and Gonick HC (1977) Isolation of low-molecular-weight lead-binding protein from human erythrocytes PROC. SOC. EXP. BIOL. MED. 155: 164-167

110. Bergdahl IA, Schütz A, Gerhardsson L, Jensen A and Skerfving S (1997) Lead concentrations in human plasma, urine and whole blood SCAND. J. WORK. ENVIRON. HEALTH 23: 359-363

111. Bergdahl IA, Schütz A and Grubb A (1996) Application of liquid chromatography-inductively coupled plasma mass spectrometry to the study of protein-bound lead in human erythrocytes J. ANAL. ATOM. SPECTROM. 11: 735-738

112. Blanchard RL and Moore JB (1970) Pb-210 and Po-210 in tissues of some Alaskan residents as related to consumption of caribou or reindeer meat HEALTH PHYS. 18: 127-134

113. Hamilton EI, Minski MJ and Cleary JJ (1972) The concentration and distribution of some stable elements in healthy human tissues form the United Kingdom. SCI. TOTAL ENVIRON. 1: 341-374

114. Victery W, Vander AJ, Mouw DR (1979) Effect of acid-base status on renal excretion and accumulated in dogs and rats AM. J. PHYSIOL 237: F398-F407

115. Keller CA and Doherty RA (1980) Distribution and excretion of lead in young and adult female mice. ENVIRON. RES. 21: 217-228

116. Pounds JG, Morrison D, Wright R, Casciano DA and Shaddock JG (1982) Effect of led on calcium-mediated cell function in the isolated rat hepatocyte. TOXICOL. APPL. PHARMACOL. 63: 402-408

117. Simmons RJB (1988) Lead-calcium interactions and lead toxicity. In: Handbook of Experimental Pharmacology. 83: 509-525 Springer-Verlag, Berlin

118. Franklin CA, Inskip MJ, Baccanale CL, Edwards CM, Manton WI, Edwards E and O'Flaherty EJ (1997) Use of sequentially administered stable lead isotopes to investigate changes in blood lead during pregnancy in a nonhuman primate (Macaca fascicularis) FUNDAMENTAL AND APPLIED TOXICOLOGY 39: 109-119

119. Gulson BL, Mizon KJ, Palmer JM, Patison N, Law AJ, Korsch MJ, Mahaffey KR and Donnelly JB (2001) Longitudinal study of daily intake and excretion of lead in newly born infants ENVIRONMENTAL RESEARCH SECTION A. 85: 232-245

120. Hallén IP, Jönsson S, Karlsson MO and Oskarsson A (1996) Toxicokinetics of lead in lactating and nonlactating mice TOXICOLOGY and APPLIED PHARMACOLOGY 136: 342-347

121. Gulson BL, Jameson CW, Mahaffey KR, Mizon KJ, Patison N, Law AJ, Korsch MJ and Salter MA (1998) Relationships of lead in breast milk to lead in blood , urine and diet of the infant and mother ENVIRONMENTAL HEALTH PERSPECTIVES 106: 667-674

122. Goyer RA, Epstein S, Bhattacharyya MH, Korach K and Pound J (1994) Environmental risk factors for osteoporosis. ENVIRONMENTAL HEALTH PERSPECTIVES 102: 390-394

123. Walsh CT and Neville MC (1994) Effects of xenobiotics on milk secretion and composition J. NUTR. BIOCHEM. 5: 418-441

124. Ziegler EE, Edwards BB, Jensen RL, Mahaffey KR and Fomon SI (1978) Absorption and retention of lead by infants. PEDIATR. RES. 12: 29-34

125. Cory-Slechta DA (1990) Lead exposure during advanced age: alterations in kinetics and biochemical effects TOXICOLOGY and APPLIED PHARMACOLOGY 104: 67-78

126. O'Flaherty EJ (2000) Modeling normal aging bone loss, with consideration of bone loss in osteoporosis TOXICOLOGICAL SCIENCES 55: 171-188

127. Garza A, Vega R and Soto E (2006) Cellular mechanisms of lead neurotoxicity. MED SCI MONIT 12: RA57-65

128. Kerper LE and Hinkle PM (1997) Cellular uptake of lead is activated by depletion of intracellular calcium stores. JOURNAL OF BIOLOGICAL CHEMISTRY 272: 8346-8352

129. Katz AK, Glusker JP, Beebe SA and Bock CW (1996) Calcium ion coordination: a comparison with beryllium, magnesium and zinc J AM CHEM SOC 118: 5752-5763

130. Fraústo da Silva JRR and Williams RJP (2001) The biological chemistry of the elements: the inorganic chemistry of life. 2nd edition, New York

131. Godwin HA (2001) The biological chemistry of lead. CURRENT OPINION IN CHEMICAL BIOLOGY 5: 223-227

132. Magyar JS, Weng T-C, Stern CM, Dye DF, Rous BW, Payne JC, Bridgewater BM, Mijovilovich A, Parkin G, Zaleski JM, Penner-Hahn JE and Godwin HA (2005) Reexamination of lead(II) coordination preferences in sulfur-rich sites: implications for a critical mechanism of lead poisoning. JOURNAL OF AMERICAN CHEMICAL SOCIETY 127: 9495-9505

133. Weis WI, Drickamer K and Hendrickson WA (1992) Structure of a C-type mannose-binding protein complexed with an oligosaccharide NATURE 360: 127-134

134. Kretsinger RH (1976) Calcium-binding proteins ANNUAL REVIEW BIOCHEMISTRY 45: 239-266

135. Sandhir R and Gill KD (1994) Effect of lead on the biological activity of calmodulin in rat brain. EXPERIMENTAL and MOLECULAR PATHOLOGY 61:69-75

136. Habermann E, Crowell K and Janicki P (1983) Lead and other metals can substitute for Ca^{2+} in calmodulin ARCHIVES OF TOXICOLOGY 54: 61-70

137. Bouton CMLS, Frelin LP, Forde CE, Godwin HA and Pevsner J (2001) Synaptotagmin I is a molecular target for lead. JOURNAL OF NEUROCHEMISTRY 76: 1724-1735

138. Rizo J and Sudhof TC (1998) C2-domains, structure and function of a universal Ca^{2+}-binding domain JOURNAL OF BIOLOGICAL CHEMISTRY 273: 15879-15882

139. Shao X, Fernandez I, Sudhof TC and Rizo J (1998) Solution structures of the Ca^{2+}-free and Ca^{2+}-bound C2A domain of Synaptotagmin I: does Ca^{2+} induce a conformational change? BIOCHEMISTRY 37: 16106-16115

140. Dowd TL, Rosen JF, Mints L and Gundberg CM (2001) The effect of Pb^{2+} on the structure and hydroxyapatite binding properties of osteocalcin BIOCHIMICA et BIOPHYSICA ACTA 1535: 153-163

141. Hanas JS, Rodgers JS, Bantle JA and Cheng Y-G (1999) Lead inhibition of DNA-binding mechanism of Cys2His2 zinc finger protein MOLECULAR PHARMACOLOGY 56: 982-988

142. Ramesh GT, Manna SK, Aggarwal BB and Jadhav AL (1999) Lead activates nuclear factor-$_K$B, activator protein-1 and amino terminal c-Jun kinase in pheochromocytoma cells TOXICOLOGY AND APPLIED PHARMACOLOGY 155: 280-286

143. Leal RB, Cordova FM, Herd L, Bobrovskaya L and Dunkley PR (2002) Lead-stimulated $p38^{MAPK}$ –dependent Hsp27 phosphorylation 178: 44-51

144. Satarug S, Nishijo M, Ujjin P, Vanavanitkun Y, Baker JR and Moore MR (2004) Evidence for concurrent effects of exposure to environmental cadmium and lead on hepatic CYP2A6 phenotype and renal function biomarkers in nonsmokers ENVIRONMENTAL HEALTH PERSPECTIVES 112: 1512-1518

145. Jover R, Lindberg LP and Meyer UA (1996) Role of heme in cytochrome P450 transcription and function in mice treated with lead acetate MOLECULAR PHARMACOLOGY 50: 474-481

146. Kim K-A, Chakraborti T, Goldstein GW and Bressler JP (2000) Immediate early gene expression in PC12 cells exposed to lead: requirement for protein kinase C. JOURNAL OF NEUROCHEMISTRY 74: 1140-1146

147. Kern M and Audersirk G (1995) Inorganic lead may inhibit neurite development in cultured hipppocampal neurons through hyperphosphorylation. TOXICOLOGY and APPLIED PHARMACOLOGY 134: 111-123

148. Korashy HM and El-Kadi AOS (2004) Regulatory mechanisms modulating the expression of cytochrome P450 1A1 gene by heavy metals. TOXICOLOGICAL SCIENCES 88: 39-51

149. Madeja M, Musshoff U, Binding N, Witting U and Speckmann E-J (1997) Effects of Pb^{2+} on delayed-rectifier potassium channels in acutely isolated hippocampal neurons J. NEUROPHYSIOL. 78: 2649-2654

150. Atchison WD (2003) Effects of toxic environmental contaminants on voltage-gated calcium channel function: from past to present. JOURNAL OF BIOENERGETICS AND BIOMEMBRANES 35: 507-532

151. Wang Q, Kim D, Dionysiou DD, Sorial GA and Timberlake D (2004) Sources and remediation for mercury contamination in aquatic systems-a literature review. ENVIRON. POLLUT. 131, 323-336

152. Virkutyte J, Sillanpaa M and Latostenma P (2002) Electrokinetic soil remediation-critical overview. THE SCIENCE OF THE TOTAL ENVIRONMENT 289, 97-121

153. Phanikumar MS, Hyndman DW, Zhao XD, Dybas MJ (2005) A three-dimensional model of microbial transport and biodegradation at the Schoolcraft, Michigan, site. WATER RESOURCES RESEARCH 41:W05011

154. Zhou P, Yan H, Gu BH (2005) Competitive complexation of metal ions with humic substances. CHEMOSPHERE 58, 1327-1337

155. Sanyal A, Rautaray D, Bansal V, Ahmad A and Sastry M (2005) Heavy metal remediation by a fungus as a means of production of lead and cadmium carbonate crystals LANGMUIR 21, 7220-7224

156. Gulson BL, Mizon KJ, Palmer JM, Korsch MJ, Taylor AJ, and Mahaffey KR (2004) Blood lead changes during pregnancy and postpartum with calcium supplementation. ENVIRONMENTAL HEALTH PERPECTIVES 112: 1499-1507

157. Zimmermann M, Muthayya S, Moretti D, Kurpad and Hurrell RF (2006) Iron fortification reduces lead levels in children in Bangalore, India. PEDIATRICS 117: 2014-2021

158. Sullivan MF and Ruemmler PS (1987) Effect of excess Fe on Cd or Pb absorption by rats. J TOXICOL ENVIRON HEALTH 22: 131-139

159. Schwartz BS, Lee B-K, Lee G-S, Stewart WF, Simon D, Kelsey K and Todd AC (2000) Associations of blood lead, dimercaptosuccinic acid-chelatable lead, and tibia lead with polymorphysms in the vitamin D receptor and delta-aminolevulinic acid dehydratase genes. ENVIRONMENTAL HEALTH PERSPECTIVES 108: 949-954

160. Cline HT, Witte S and Keith WJ (1996) Low lead levels stunt neuronal growth in a reversible manner PROC. NATL. ACAD. SCI. 93: 9915-9920

161. Cremin JD, Luck ML, Laughlin NK and Smith DR (2001) Oral succimer decreases the gastrointestinal absorption of lead in juvenile monkeys ENVIRONMENTAL HEALTH PERSPECTIVES 109: 613-619

162. Guilarte T, Toscano CD, McGlothan JL and Weaver SA (2003) Environmental enrichment reverses cognitive and molecular deficits induced by developmental lead exposure ANN NEUROL 53: 50-56

163. Cabell L, Ferguson C. Luginbill D, Kern M, Weingart A and Audesirk G (2004) Differential induction of heme oxygenase and neurons by inorganic lead. TOXICOLOGY and APPLIED PHARMACOLOGY 198: 49-60

164. Eckhardt W, Bellmann K and Kolb H (1999) Regulation of inducible nitric oxide synthase expression in β cells by environmental factors: heavy metals. BIOCHEM J 338: 695-700

165. Cheung, Lap AP, Lam VKL and Chan KM (2005) Tilapia metallothionein genes: PCR-cloning and gene expression studies BIOCHIMICA et BIOPHYSICA ACTA 1731: 191-201

166. Yan CHM and Chan KM (2004) Cloning of zebrafish metallothionein gene and characterization of its gene promoter region in HepG2 cell line BIOCHIMICA et BIOPHYSICA ACTA 1679: 47-58

167. Chakraborti T, Kim K-A, Goldstein GG and Bressler JP (1999) Increased AP-1 DNA binding activity in PC12 cells treated with lead JOURNAL OF NEUROCHEMISTRY 73: 187-194

168. Korashy HM and El-Kadi AOS (2004) Differential effects of mercury, lead and copper on the constitutive and inducible expression of aryl hydrocarbon receptor (AHR)-regulated genes in cultured hepatoma Hepa 1c1c7 cells TOXICOLOGY 201: 153-172

169. Ghering AB, Jenkins LMM, Schenk BL, Deo S, Mayer RA, Pikaart MJ, Omichinski JG and Godwin HA (2004) Spectroscopic and functional determination of the interaction of Pb2+ with GATA proteins J. AM. CHEM. SOC. 12&: 3751-3759

170. Kimber I, Stonard MD and Gidlow DA (1986) influence of chronic low-level exposure to lead on plasma immunoglobin concentration and cellular immune function in man. INT ARCH OCCUP ENVIRON HEALTH 57: 117-125

171. Alomran AH and Shleamoon MN (1988) The influence of chronic lead exposure on lymphocyte proliferative response and immunoglobulin levels in storage battery workers. J BIOL SCI RES 19: 575-585

172. Basaran N and Undeger U (2000) Effects of lead on immune parameters in occupationally exposed workers AM J IND MED 38: 349-354

173. Ewers U, Stiller R and Idel H (1982) Serum immunoglobulin, complement C3, and salivary IgA level in lead workers. ENVIRON RES. 29: 351-357

174. Bauer R, Müller A, Richter M, Schneider K, Frey J and Engelhardt W (1997) Influence of heavy metals ions on antibodies and immune complexes investigated by dynamic light scattering and enzyme-linked immunosorbent assay BIOCHIMICA et BIOPHYSICA ACTA 1334: 98-108

175. Miller TE, Golemboski KA, Ha RS, Bunn T, Sanders FS and Dietert RR (1998) Developmental exposure to lead causes persistent immunotoxicity in Fisher 344 rats

176. IRIS (2005) Lead. U.S. Environmental Protection Agency Washington, DC: Integrated Risk Information System (http://www.epa.gov/iris).

177. NTP (2005) Report on carcinogens. 11th edition. Research Triangle Park, NC: U.S. Department of Health and Human Services, National Toxicology Program (http://ntp-server.niehs.nih.gov/ntp/roc/toc11.html).

178. IARC (2004) Overall evaluations of carcinogenicity to humans: As evaluated in IARC monographs volumes 1-82 (at total of 900 agents, mixtures and exposures).

Lyon, France: World Health Organization, International Agency for Research on Cancer, (http://www-cie.iarc.fr/monoeval/crthall.html).

179. Malcolm D and Barnett HAR (1982) A mortality study of lead workers 1925-76 BRITISH JOURNAL OF INDUSTRIAL MEDICINE 39: 404-410

180. Gerhardsson L, Lundstrom NG and Nordberg G (1986) Mortality and lead exposure: A retrospective cohort study of Swedish smelter workers. BRITISH JOURNAL OF INDUSTRIAL MEDICINE

181. Anttila A, Heikkila P and Pukkala E (1995) Excess lung cancer among workers exposed to lead SCAND J WORK ENVIRON HEALTH 21: 460-469

182. Cocco P, Hua F and Boffetta P (1997) Mortality of Italian lead smelter workers. SCAND J WORK ENVIRON HEALTH 23: 15-23

183. Silbergeld EK (2003) Facilitative mechanisms of lead as a carcinogen MUTATION RESEARCH 533: 121-133

184. Rom WN (1976) Effects of lead on the female and reproduction: a review. MT SINAI J MED 43:544-552

185. Borja-Aburto VH, Hertz-Picciotto I, Lopez MR, Farias P, Rios C and Blanco J (1999) Blood lead levels measured prospectively and risk of spontaneous abortion AMERICAN JOURNAL OF EPIDEMIOLOGY 150: 590-597

186. Alexander HE, Checkoway H, van Netten C, Muller CH, Ewers TG, Kaufman JD, Mueller BA, Vaughan TL and Faustman EM (1996) Semen quality of men employed at a lead smelter OCCUP ENVIRON MED 53: 411-416

187. Quintanilla-Vega B, Hoover D, Bal W, Silbergeld EK, Waalkes MP and Anderson LD (2000) Lead effects on protamine-DNA binding AMERICAN JOURNAL OF INDUSTRIAL MEDICINE 38: 324-329

188. Foster WG (1992) Reproductive toxicity of chronic lead exposure in the female Cynomolgus monkey. REPROD TOXICOL. 6: 123-131

189. Palus J, Rydzynski K. Dziubaltowska E, Wyszynska K, Natarajan AT and Nilsson R (2003) Genotoxic effects of occupational exposure to lead and cadmium MUTATION RESEARCH 540: 19-28

190. Hengstler JG, Bolm-Audorff U, Faldum A, Janssen K, Reifenrath M, Götte W, Jung D, Mayer-Popken O, Fuchs J, Gebhard S, Bienfait HG, Schlink K, Dietrich C, Faust D, Epe B and Oesch F (2003) Occupational exposure to heavy metals: DNA damage induction and DNA repair inhibition prove co-exposures to cadmium, cobalt and lead as more dangerous than hitherto expected CARCINOGENESIS 24: 63-73

191. Yang JL, Yeh SC and Chang CY (1996) Lead acetate mutagenicity and mutational spectrum in the hypoxanthine guanine phosphoribosyltransferase gene of Chinese hamster ovary K1 cells MOL CARCINOG 17: 181-191

192. Calsou P, Frit P, Bozzato C and Salles B (1996) Negative interference of metal (II) ions with nucleotide excision repair in human cell-free extracts CARCINOGENESIS 17: 2779-2782

193. Ariza ME, Bijur GN and Williams MV (1998) Lead and mercury mutagenesis: Role of H_2O_2, superoxide dismutase and xanthine oxidase ENVIRONMENTAL and MOLECULAR MUTAGENESIS 31: 352-361

194. de Restrepo HG, Sicard D and Torres MM (2000) DNA damage and repair in cells of lead exposed people AMERICAN JOURNAL OF INDUSTRIAL MEDICINE 38: 330-334

195. Patrick L (2006) Lead toxicity, a review of the literature. Part I: exposure, evaluation and treatment ALTERNATIVE MEDICINE REVIEW 11: 2-22

196. Goyer RA (1996) Results of lead research: prenatal exposure and neurological consequences ENVIRONMENTAL HEALTH PERSPECTIVES 104: 1050-1054

197. Järup L (2003) Hazards of heavy metal contamination BRITISH MEDICAL BULLETIN 68: 167-182

198. Lidsky TI and Schneider JS (2003) Lead neurotoxicity in children: basic mechanisms and clinical correlates BRAIN 126: 5-19

199. Marchetti C (2003) Molecular targets of lead in brain neurotoxicity NEUROTOX RES. 5: 221-236

200. Finkelstein Y, Markowitz ME and Rosen JF (1998) Low-level lead-induced neurotoxicity in children: an update on central nervous system effects BRAIN RESEARCH EFFECT 27: 168-176

201. Hernandez-Avila M, Peterson KE, Gonzalez-Cossio T, Sanin LH, Aro A, Schnaas L and Hu H (2002) Effect of maternal bone lead on length and head circumference of newborns and 1 month old infants ARCH ENVIRON HEALTH 57: 482-488

202. Gonzalez-Cossio T, Peterson KE, Sanin LH, Fishbein E, Parazuelos E, Aro A, Hernandez-Avila M, and Hu H (1997). Decrease in birth weight in relation to maternal bone-lead burden. PEDIATRICS100: 856-862

203. Sanin LH, Gonzalez-Cossio T, Romieu I, Peterson KE, Ruiz S, Parazuelos E, Hernandez-Avila M and Hu H (2001) Effect of maternal lead burden on infant weight and weight gain at one month of age among breastfed infants. PEDIATRICS 107: 1010-1023

204. Ronis MJJ, Aronson J, Gao GG, Hogue W, Skinner RA, Badger TM and Lumpkin CK (2001) Skeletal effects of developmental lead exposure in rats. TOXICOLOGICAL SCIENCES 62: 321-329

205. Hicks DG, O'Keefe RJ, Reynolds KJ, Cory-Slechta DA, Puzas JE, Judkins A and Rosier RN (1996) Effects of lead on growth plate chrondrocyte phenotype. TOXICOLOGICAL and APPLIED PHARMACOLOGY 140: 164-172

206. Hamilton JD and O'Flaherty EJ (1995) Influence of lead in mineralization during bone growth. FUNDAM. APPL. TOXICOL. 26: 265-271

207. Selevan SG, Rice DC, Hogan KA, Euling SY, Pfahles-Hutchens A and Bethel J (2003) Blood lead concentration and delayed puberty in girls. NEW ENGLAND JOURNAL OF MEDICINE 348: 1527-1536

208. Wu T, Buck GM and Mendola P (2003) Blood lead levels and sexual maturation in U.S. girls: the third national health and nutrition examination survey, 1988-1994. ENVIRONMENTAL HEALTH PERSPECTIVES 111: 737-741

209. Hardiman G (2004) Microarray platforms – comparisons and contrasts. PHARMACOGENOMICS 5, 487-502

210. Stanfield WD, Colome JS and Cano RJ (1996) Schaum's outlines Molecular and Cell Biology. McGraw-Hill, New York

211. Abdullah-Sayani A, Bueno-de-Mesquita JM and van de Vijver MJ (2006) Technology insight: tuning into the genetic orchestra using microarrays-limitations of DNA microarrays in clinical practice NATURE CLINICAL PRACTICE ONCOLOGY 3: 501-516

212. Greenberg SA (2001) DNA microarray gene expression analysis technology and its application to neurological disorders NEUROLOGY 57: 755-761

213. Schena M, Shalon D, Davis RW and Brown PO (1995) Quantitative monitoring of gene expression patterns with a complementary DNA microarray. SCIENCE 270: 467-470

214. Hughes TR, , Mao M, Jones AR, Burchard J, Marton MJ, Shannon KW, Lefkowitz SM, Ziman M, Schelter JM, Meyer MR, Kobayashi S, Davis C, Dai H, He Y, Stephaniants SB, Cavet G, Walker WL, West A, Coffey E, Shoemaker DD, Stoughton R, Blanchard AP, Friend SH and Linsley PS (2001) Expression profiling using microarrays fabricated by an ink-jet oligonucleotides synthesizer. NATURE BIOTECHNOLOGY 19: 342-347

215. Lipshutz RJ, Fodor SPA, Thomas R. Gingeras TR and Lockhart DJ (1999) High density synthetic oligonucleotides arrays NATURE GENETICS 21: 20-24

216. Simon RM, Korn EL, McShane LM, Radmacher MD, Wright GW and Zhao Y (2003) Design and Analysis of DNA Microarray Investigations, Springer, New York

217. Slonim DK (2002) From patterns to pathways: gene expression data analysis comes of age NATURE GENETICS SUPPLEMENT 32: 502-508

218. Segal E, Friedman N, Kaminski N, Regev A and Koller D (2005) From signatures to models: understanding cancer using microarrays. NATURE GENETICS SUPPLEMENT 37: S38-S45

219. Wilhelm J and Pingoud A (2003) Real-time polymerase chain reaction CHEMBIOCHEM 4: 1120-1128

220. Bustin SA (2000) Quantification of mRNA using real-time reverse transcription PCR (RT-PCR): trends and problems JOURNAL OF MOLECULAR ENDOCRINOLOGY 25: 169-193

221. Bustin SA and Reinhold M (2005) Real-time reverse transcription PCR (qRT-PCR) and its potential use in clinical diagnosis CLINICAL SCIENCE 109: 365-379

222. Bustin SA, Benes V, Nolan T and Pfaffl MW (2005) Quantitative real-time RT-PCR – a perspective JOURNAL OF MOLECULAR ENDOCRINOLOGY 34: 597-601

223. Zhang T and Fang HHP (2006) Applications of real-time polymerase chain reaction for quantification of microorganisms in environmental samples APPL MICROBIOL BIOTECHNOL 70: 281-289

224. Gachon C, Mingam A and Charrier B (2004) Real-time PCR: what a relevance to plant studies? JOURNAL OF EXPERIMENTAL BOTANY 55: 1445-1454

225. Ding C and Cantor CR (2004) Quantitative analysis of nucleic acids – the last few years of progress JOURNAL OF BIOCHEMISTRY AND MOLECULAR BIOLOGY 37: 1-10

226. Bustin SA and Nolan T (2004) Pitfalls of quantitative real-time reverse transcription polymerase chain reaction JOURNAL OF BIOMOLECULAR TECHNIQUES 15: 155-166

227. Costa LG, Aschner M, Vitalone A, Syversen T and Soldin OP (2004) Developmental Neuropathology of environmental agents. ANNU. REV. PHARMACOL. TOXICOL. **44**, 87-110

228. Krocova Z, Macela A, Kroca MM and Hernychova L (2000) The immunomodulatory effect(s) of lead and cadmium on the cells of the immune system in vitro. Toxicology In Vitro **14**, 33-40

229. Chen L, Yang X, Jiao H and Zhao B (2004) Effect of tea catechins on the change of glutathione levels caused by Pb^{++} in PC12 cells. CHEM. RES. TOXICOL. **17**, 922-928

230. Jarrar BM and Mahmoud ZN (2002) Histochemical demonstration of the alterations in the renal dehydrogenase activities induced by lead in wistar albino rats (Rattus norvegicus). Journal of Health Science 48, 106-117

231. Szynaka B, Andrzejewska A, Tomasiak M and Augustynowicz A (1999) Exocrine cell mitochondria of the rat pancreas after lead intoxication. EXP. TOXIC. PATHOL 51, 559-564

232. Corpas I, Benito MJ, Marquina D, Castillo M, Lopez N and Antonio MT (2002) Gestational and Lactational lead intoxication produces alterations in the hepatic system of rat pups. ECOTOXICOLOGY AND ENVIRONMENTAL SAFETY **51**, 35-43

233. Johnson FM (1998) The genetic effects of environmental lead. Mutation Research 410, 123-140

234. Peraza MA, Ayala-Fierro F, Barber DS, Casarez E and Rael LT (1998) Effects of micronutrients on metal toxicity. ENVIRONMENTAL HEALTH PERSPECTIVES 106, 203-216

235. Miller GD, Massaro TF, Granlund, RW, Massaro EJ (1983) Tissue distribution of lead in the neonatal rat exposed to multiple doses of lead acetate. JOURNAL OF TOXICOLOGY AND ENVIRONMENTAL HEALTH 11, 121-128

236. Adonaylo VN and Oteiza PI (1999) Lead Intoxication: antioxidant defenses and oxidative damage in rat brain. TOXICOLOGY 135, 77-85

237. Barbier O, Jacquillet G, Tauc M, Cougnon M and Poujeol P (2005) Effect of heavy metals on, and handling by the kidney. NEPHRON PHYSIOLOGY 99, 105-110

238. Zalups RK (2000) Molecular interactions with mercury in the kidney. PHARMACOLOGICAL REVIEW 52, 113-143

239. Thevenod F (2003) Nephrotoxicity and the proximal tubule. Insights from cadmium. NEPHRON PHYSIOLOGY 93, 87-93

240. Garza A, Chavez H, Vega R and Soto E (2005) Cellular and molecular mechanism of lead neurotoxicity. SALUD MENTAL 28, 48-58

241. Goyer RA (1997) Toxic and essential metal interactions. ANNUAL REVIEW NUTRITION 17, 37-50

242. Fowler BA (1998) Roles of lead-binding proteins in mediating lead bioavailability. ENVIRONMENTAL HEALTH PERSPECTIVES 106, 1585-1587

243. Cameron TP, Hickman RL, Kornreich MR and Tarone RE (1985) History, survival and growth patterns of B6C3F1 mice and F344 rats in the National Cancer Institute Carcinogenesis testing program FUNDAN APPL TOXICOL 5: 526-538

244. Caldwell DJ (1999) Review of mononuclear cell leukemia in F-344 rat bioassays and its significance to human cancer risk: a case study using alkyl phthalates REGULATORY TOXICOLOGY AND PHARMACOLOGY 30: 45-53

245. Miller MJ, Lonardo EC, Greer RD, Bevan C, Edwards DA, Smith JH and Freeman JJ (1996) Variable responses of species and strains to white mineral oils and paraffin waxes REGULATORY TOXICOLOGY AND PHARMACOLOGY 23: 55-68

246. Gemma S, Testai E, Chieco P and Vittozzi L (2004) Bioactivation, toxicokinetics and acute effects of chloroform in Fisher 344 rats and Osborne Mendel male rats JOURNAL OF APPLIED TOXICOLOGY 24: 203-210

247. Qiagen 2001, RNeasy Mini Handbook

248. Affymetrix (2005), Affymetrix GeneChip® Expression Analysis Technical Manual

249. Simon R and Lam P (2005) BRB-Array Tools User's Guide version 3.3 (http://linus.nci.nih.gov/~brb/download.htm)

250. William GM and Iatropoulos (2002) Alteration of liver cell function and proliferation: differentiation between adaptation and toxicity TOXICOLOGIC PATHOLOGY 30, 41-53

251. Bouton CMLS, Hossain MA, Frelin PL, Laterra J and Pevsner J (2001) Microarray analysis of differential gene expression in lead-exposed astrocytes TOXICOLOGY AND APPLIED PHARMACOLOGY 176, 34-53

252. Jadhav AL, Ramesh GT and Gunasekar PG (2000) Contribution of protein kinase C and glutamate in Pb^{2+}-induced cytotoxicity TOXICOLOGICAL LETTERS 115, 89-98

253. Hossain MA, Bouton CM, Pevsner J and Laterra J (200) Induction of vascular endothelial growth facto in human astrocytes by lead J. BIOL. CHEM. 275, 27874-27882

254. Payne JC, Horst MA and Godwin HA (1999) Lead fingers: Pb2+ binding to structural zinc-binding domains determined directly by monitoring lead-thiolate charge-transfer bands J. AM. CHEM. SOC 121, 6850-6855

255. Herrero J, Vaquerizas JM, Al-Shahrour F, Conde L, Mateos A, Diaz-Uriarte JSR and Dopazo J (2004) NUCLEIC ACIDS RESEARCH 32, W485-W491

256. Proud CG, Wang X, Patel JV, Campbell LE, Kleijn M , Li W and Browne GJ (2001) Interplay between insulin and nutrients in the regulation of translation factors BIOCHEMICAL SOCIETY TRANSACTIONS 29: 541-547

257. Lekmine F, Uddin S, Sassano A, Parmar S, Brachmann SM, Majchrzak B, Sonenberg N, Hay N, Fish EN and Platanias LC (2003) Activation of the p70 S6 kinase and phosphorylation of the 4E-BP1 repressor of mRNA translation by type I interferons THE JOURNAL OF BIOLOGICAL CHEMISTRY 278: 27772-27780

258. Campbell LE, Wang X, Proud CG (1999) Nutrients differentially regulate multiple translation factors and their control by insulin BIOCHEM J. 344:433-441

259. Youn H-D, Sun L, Prywes R and Liu JO (1999) Apoptosis of T cells mediated by Ca^{2+}-induced release of the transcription factor MEF2 SCIENCE 286:790-793

260. Youn HD, and Liu HO (2000) Cabin1 represses MEF2-dependent Nur77 expression and T cell apoptosis by controlling association of histone deacetylases and acetylases with MEF2. IMMUNITY 13: 85-94

261. Woronicz JD, Lina A, Calnan BJ, Szychowski S, Cheng L and Winoto A (1995) Regulation of the Nur77 orphan steroid receptor in activation-induced apoptosis. MOL. CELL. BIOL. 15:6364-6376

262. McKinsey TA, Zhang C-L, Lu J and Olson EN (2000) Signal-dependent nuclear export of a histone deacetylase regulates muscle differentiation LETTERS TO NATURE 408:106-111

263. McKinsey TA, Zhang CL and Olson EN (2000) Activaton of the myocyte enhancer factor-2 transcription factor by calcium/calmodulin-dependent protein kinase-stimulated binding of 14-3-3 to histone deacetylase 5 PNAS 97:14400-14405

264. Zhang CL, McKinsey TA and Olson EN (2001) The transcriptional corepressor MITR is a signal-responsive inhibitor of myogenesis PNAS 98:7354-7359

265. Zhang CL, McKinsey TA and Olson EN (2002) Association of class II histone deacetylases with heterochromatin protein 1: potential role for histone methylation in control of muscle differentiation MOLECULAR AND CELLULAR BIOLOGY 22:7302-7312

266. Goffart S and Wiesner RJ (2003) Regulation and co-ordination of nuclear gene expression during mitochondrial biogenesis EXPERIMENTAL PHYSIOLOGY 88:33-40

267. Gleyzer N, Vercauteren K, and Scarpulla RC (2005) Control of mitochondrial transcription specificity factors (TFB1M and TFB2M) by nuclear respiratory factors (NRF-1 and NRF-2) and PGC-1 family coactivators MOL CELL BIOL 25: 1354-1366

268. Scarpulla RC (2002) Nuclear activators and coactivators in mammalian mitochondrial biogenesis BIOCHIMICA ET BIOPHYSICA ACTA 1576:1-14

269. Moon BC, Choi MS, Kang YH, Kim MC, Cheong MS, Park CY, Yoo JH, Koo SC, Lee SM, Lim CO, Cho MJ and Chung WS (2005) Arabidopsis ubiquitin-specific protease 6 (AtUBP6) interacts with calmodulin FEBS LETTERS 579: 3885-3890

270. Toutenhoofd SL and Strehler EE (2002) Regulation of calmodulin mRNAs in differentiating human IMR-32 neuroblastoma cells BIOCHIMICA ET BIOPHYSICA ACTA 1600: 95-104

271. Knaup KX and Roemer K (2004) Cell type-specific regulation of calmodulin 2 expression by mutant p53 FEBS LETTERS 569: 70-74

272. Huo L, Lee EK, Leung PC and Wong AOL (2004) Goldfish Calmodulin; Molecular cloning, tissue distribution and regulation of transcript expression in goldfish pituitary cells ENDOCRINOLOGY 145:5056-5067

273. Colomer J, Agell N, Engel P and Bachs O (1994) Expression of calmodulin and calmodulin binding proteins in lymphoblastoid cells

274. Lee AG and East M (2001) What structure of a calcium pump tells us about its mechanism. BIOCHEM J. **356**, 665-683

275. Voet D and Voet JG (1995) Biochemistry 2nd Edition, John Wiley and Sons Inc, New York

276. Kern M, Wisniewski M, Cabell L and Audesirk G (2000) Inorganic lead and calcium interact positively in activation of calmodulin. NEUROTOXICOLOGY **21**, 353-363

277. Roberts AG, and Elder GH (2001) Alternative splicing and tissue-specific transcription of human and rodent ubiquitous 5-aminolevulinate synthase (ALAS1) genes BIOCHIMICA ET BIOPHYSICA ACTA 1518: 95-105

278. Munakata H, Sun J-Y, Yoshida K, Nakatani T, Honda E, Hayakawa S, Furuyama K and Hayashi N (2004) Role of heme regulatory motif in the heme-mediated inhibition of mitochondrial import of 5-aminolevulinate synthase J. BIOCHEM 136:233-238

279. Fraser DJ, Podvince M, Kaufmann MR and Meyer UA (2002) Drugs mediate the transcriptional activation of the 5-aminolevulinic acid synthase (ALAS1) gene via the chicken xenobiotic-sensing nuclear receptor (CXR) THE JOURNAL OF BIOLOGICAL CHEMISTRY 277: 34717-347

280. Perdersen PL (2005) Transport ATPases: Structure, Motors, Mechanism and Medicine: A brief overview JOURNAL OF BIOENERGETICS AND BIOMEMBRANES 37:349-357

281. Gabalo A, Zanotti F and Papa S (2002) Structures and Interactions of Proteins involved in the coupling function of the proton motive FoF1-ATP Synthase CURR PROTEIN PEPT SCI. 3: 451-460

282. Repke KR and Schon R (1994) Synthesis of a self-contained concept of the molecular mechanism of energy interconversion by H(+)-transporting ATP synthase BIOL REV CAMB PHILOS SOC.69:119-145

283. Chen H, Morris MA, Rossier C, Blouin J-L and Antonarakis SE (1995) Cloning of the cDNA for he human ATP synthase OSCP subunit (ATP5O) by exon trapping and mapping to chromosome 21q22.1-q22.2 GENOMICS 28: 470-476

284. Tucker WC, Du Z, Hein R, Gromet-Elhanan Z and Richter ML (2001) Role of the ATP synthase α-subunit in conferring sensitivity to tentoxin BIOCHEMISTRY 40: 7542-7548

285. Wang MG, Yi H, Guerin D, Klee CB and McBride OW (1996) Calcineurin A alpha (PPP3CA), calcineurin A beta (PPP3CB) and calcineurin B (PPP3R1) are located on human chromosomes 4, 10q21→q22 and 2p16→p15 respectively CYTOGENET. CELL GENET 72:236-241

286. Zolnierowicz S, Csortos C, Bondor J, Verin A, Mumby MC and DePaoli-Roach AA (1994) Diversity in the regulatory B-subunits of Protein phosphatase 2A: identification of a novel isoform highly expressed in brain BIOCHEMISTRY 33:11858-11867

287. Groves MR, Hanlon N, Turowski P, Hemmings BA and Barford D (1999) The structure of the protein phosphatase 2A PR65/A Subunit Reveals the conformation of its 15 tandemly repeated HEAT motifs CELL 96:99-110

288. Anakk S, Kalsotra A, Shen Q, Vu MT, Staudinger JL, Davies PJA and Strobel HW (2003) Genomic characterization and regulation of CYP3A13: role of xenobiotics and nuclear receptors THE FASEB JOURNAL 17: 1736-8

289. Sakuma T, Takai M, Endo Y, Kuroiwa M, Ohara A, Jarukamjorn K, Honma R and Nemoto N (2000) A novel female-specific member of the CYP3A gene subfamily in the mouse liver ARCHIVES OF BIOCHEMISTRY AND BIOPHYSICS 377:153-162

290. Richardson TA and Morgan ET (2005) Hepatic cytochrome P450 gene regulation during endotoxin-induced inflammation in nuclear receptor knockout mice THE

JOURNAL OF PHARMACOLOGY AND EXPERIMENTAL THERAPEUTICS 314:703-709

291. Yanagimoto T, Itoh S, Sawada M and Kamataki T (1997) Mouse cytochrome P450 (Cyp3a11): Predominant expression in liver and capacity to activate aflatoxin B_1 ARCHIVES OF BIOCHEMISTRY AND BIOPHYSICS 340:215-218

292. Whitmarsh AJ, Yang S-H, Su MS-S, Sharrocks AD and Davis RJ (1997) Role of p38 and JNK Mitogen-activated protein kinases in the activation of ternary complex factors MOLECULAR AND CELLULAR BIOLOGY 17: 2360-2371

293. Johnson GL and Lapadat R (2002) Mitogen activated protein kinase pathways mediated by ERK, JNK and p38 protein kinases SCIENCE 298:1911-2

294. Chuang S-M, Wang I-C and Yang J-L (2000) Roles of JNK, p38 and ERK Mitogen-activated protein kinases in the growth inhibition and apoptosis induced by cadmium CARCINOGENESIS 21:1423-1432

295. Applied Biosystems Inc (2002) Taqman® Gold RT-PCR Kit (http://www.appliedbiosystems.com/)

296. Peirson SN, Butler JN and Foster RG (2003) Experimental validation of novel and conventional approaches to quantitative real-time PCR data analysis. NUCLEIC ACIDS RESEARCH 31, e73: 1-7

297. Pfaffl MW, Horgan GW and Dempfle L (2002) Relative expression software tool (REST©) for group-wise comparison and statistical analysis of relative NUCLEIC ACID RES. 30: e36

298. Grohse PM (1999) Elemental analysis of airborne particles edited by Sheldon Landsberger and Marsh Creatchman, Gordon and Breach Science Publishers Amsterdam, The Netherlands

299. Toscano CD, O'Callaghan JP and Guilarte TR (2005) Calciumcalmodulin-dependent protein kinase II activity and expression are altered in the hippocampus of Pb^{2+}-exposed rats. BRAIN RESEARCH 1044:51-58

APPENDIX A

Institutional Animal Care and Use Committee Approval Form

WESTERN MICHIGAN UNIVERSITY

Institutional Animal Care and Use Committee

ANNUAL REVIEW OF VERTEBRATE ANIMAL USE

PROJECT OR COURSE TITLE: Investigation of Markers of Cell Death and Immune Function in Rats Exposed to Selected Chemicals

RECEIVED
MAY 19 2004
I.A.C.U.C.

IACUC Protocol Number: 03-04-02
Date of Review Request: 06/10/03 Date of Last Approval: 6/10/03
Purpose of project (select one): ☐Teaching ☒Research ☐Other (specify):

PRINCIPAL INVESTIGATOR OR ADVISOR
Name: JayC. Means Title: Professor
Department: CHEM Electronic Mail Address: means@wmich.edu

CO-PRINCIPAL OR STUDENT INVESTIGATOR
Name: Lisa Baker Title: Assoc./Assist. Professor
Department: PSHC Electronic Mail Address: lisa.baker@wmich.edu

1. The research, as approved by the IACUC, is completed:
   ☐Yes (Continue with items 4-5 below.) ☒No (Continue with items 2-5 below.)

If the answer to any of the following questions (items 2-4) is "Yes," please provide a detailed explanation on an attached sheet of paper. Include details of any modifications made to the protocol based on new findings or publications, adverse events or mortalities.

2. Have there been any changes in Principal or Co-Principal Investigators? ☒Yes ☐No
3. Have there been any new findings or publications relative to this research? ☒Yes ☐No
   Describe the sources used to determine the availability of new findings or publications:
   - ☐No search conducted (Please provide a justification on an attached sheet.)
   - ☐Animal Welfare Information Center (AWIC)
   - ☒Search of literature databases (select all applicable)
     - ☐AGRICOLA ☐Current Research Information Service (CRIS)
     - ☒Biological Abstracts ☒Medline
     - ☒Other (please specify): CAS

   Date of search: 05/10/04 Years covered by the search: 1980-present
   Key words: gene expression, benzo[a]pyrene, PCBs, lead, immune system effects, DNA adducts, rat (Fisher 344), tumors, cancer, behavior, learning, maze
   - ☐Additional search strategy narrative:
4. Are there any adverse events, in terms of animal well being, or mortalities to report as a result of this research? ☐Yes ☒No
   Cumulative number of mortalities: 0 prior to euthanasia
5. Animal usage: Number of animals used during this quarter (3 months): 4 Cumulative number of animals used to date: 88

⇨ Jay C. Means 5/17/04
Principal Investigator/Faculty Advisor Signature Date

⇨ Lisa E. Baker 5/18/04
Co-Principal or Student Investigator Signature Date

IACUC REVIEW AND APPROVAL
Upon review of the relevant information regarding this protocol, the IACUC approval for this project has been extended for one year from the date of this signature.

⇨ [signature] 05/26/04
IACUC Chair Signature Date

Revised 10/01 WMU IACUC
All other copies obsolete.

APPENDIX B

Gene Annotation List

Probe set	Symbol	Probe set	Symbol	Probe set	Symbol
1367452_at	Sumo2	1367550_a_at	Bbp_predicted	1367603_at	Tpi1
1367453_at	Cdc37	1367551_a_at	RGD1306410_predicted	1367604_at	RGD:1302959
1367454_at	Copb2	1367553_x_at	Hbb	1367605_at	Pfn1
1367455_at	RGD:621595	1367554_at	Scgb2a1 /// Scgb2a2	1367606_at	Rps3a
1367456_at	Ube2d3	1367555_at	Alb	1367607_at	Cox4i1
1367457_at	Becn1	1367556_s_at	Alb	1367608_at	Cryba4
1367458_at	Lypla2	1367557_s_at	Gapd	1367609_at	Mif
1367459_at	Arf1	1367558_x_at	Andpro	1367610_at	Rpl19
1367460_at	Gdi2	1367559_at	Ftl1	1367611_at	Tkt
1367461_at	Copb1	1367560_at	Arbp	1367612_at	Mgst1
1367462_at	Capns1	1367561_at	Rpl27	1367613_at	Prdx1
1367463_at	Bcap37	1367562_at	Sparc	1367614_at	Anxa1
1367464_at	RGD:621674	1367563_at	Sparc	1367615_at	Svs5
1367465_at	Dad1	1367564_at	Nppa	1367616_at	Nppb
1367466_at	Prpf8_predicted	1367565_a_at	Fth1	1367617_at	Aldoa
1367469_at	Eif4g2	1367566_at	Scgb1a1	1367618_a_at	Gnb2l1
1367470_at	Sara1	1367567_at	Rpl6	1367619_at	Pgrmc1
1367472_at	LOC314432	1367568_a_at	Mgp	1367620_at	Atp5g3
1367476_at	Srp14_predicted	1367569_at	Lamr1	1367621_at	Dapk3
1367477_at	Mrpl53_predicted	1367570_at	Tagln	1367622_at	Atp5h
1367481_at	Vps28_predicted	1367571_a_at	Igf2	1367623_at	Rpl18
1367483_at	RGD1309148_predicted	1367572_at	Myl3	1367624_at	Atf4
1367484_at	Ube2e2_predicted	1367573_at	Rps6	1367625_at	Rpl10
1367487_at	MGC72586	1367574_at	Vim	1367626_at	Ckm
1367492_at	Dnajc8_predicted	1367575_at	Eno1	1367627_at	Gatm
1367494_at	RGD1310899_predicted	1367576_at	Gpx1	1367628_at	Lgals1
1367496_at	Tm9sf2	1367577_at	Hspb1	1367629_at	Cox7a3
1367497_at	Ptdss1_predicted	1367578_at	Prdx2	1367630_at	Rps11
1367502_at	Mrpl21_predicted	1367579_a_at	Tuba1 /// Tuba6_predicted	1367631_at	Ctgf
1367503_at	RGD:1302944	1367580_at	Rpl10a	1367632_at	Glul
1367506_at	mrpl11	1367581_a_at	Spp1	1367633_at	Glul
1367507_at	RGD:735224	1367582_at	Rpl29	1367634_at	Rpl31
1367510_at	RGD1304696_predicted	1367583_at	Tpt1	1367635_at	P4hb
1367512_at	RGD1305968_predicted	1367584_at	Anxa2	1367636_at	Igf2r
1367513_at	Tm9sf4_predicted	1367585_a_at	Atp1a1	1367637_a_at	Ppp1cc /// LOC360258
1367514_at	LOC361635	1367586_at	Ldha	1367639_a_at	Rps2

1367515_at	Cnot7_predicted	1367587_at	Csh1v	1367640_at	Rps12
1367518_at	RGD1305121_predicted	1367588_a_at	Rpl13a	1367641_at	Sod1
1367520_at	Apoa1bp_predicted	1367589_at	Aco2	1367642_at	Suclg1
1367523_at	RGD1304906_predicted	1367590_at	Ran	1367643_at	Bsg
1367524_at	Zfp592_predicted	1367591_at	Prdx3	1367645_at	Rps17
1367525_at	Thrap3_predicted	1367592_at	Tnnt2	1367647_at	Serpina1
1367529_at	RGD1311835_predicted	1367593_at	Sepw1	1367649_at	Palm
1367531_at	Wbscr1	1367594_at	Bgn	1367650_at	Lcn7
1367532_at	Dazap2_predicted	1367595_s_at	B2m	1367651_at	Ctsd
1367533_at	Statip1_predicted	1367596_at	Rps26	1367652_at	Igfbp3
1367535_at	Irf2bp1_predicted	1367597_at	Rps8	1367653_a_at	Mdh1
1367536_at	LOC295961	1367598_at	Ttr	1367654_at	Fath
1367546_at	Mrpl43_predicted	1367599_at	Atp5g1	1367655_at	Tmsb10
1367547_at	LOC305913	1367600_at	Des	1367656_at	Psmb7
1367549_a_at	Ap3d_predicted	1367601_at	Cited2	1367657_at	Btg1
1367659_s_at	Dci	1367602_at	Cited2	1367658_at	Shank3
1367660_at	Fabp3	1367712_at	Timp1	1367764_at	Ccng1
1367661_at	S100a6	1367713_at	Eif2s1	1367765_at	Tcn2
1367662_at	Hsd17b10	1367714_at	Eif2b2	1367766_at	Nme2
1367663_at	Psme1	1367715_at	Tnfrsf1a	1367767_at	Hmgcl
1367664_at	Ankrd1	1367716_at	Cda08	1367768_at	Lxn
1367665_at	Ankrd1	1367717_at	Rps27	1367769_at	Polr2g
1367666_at	Hnrph1	1367718_at	Chkb	1367770_at	Degs
1367667_at	Fdps	1367719_at	Dd5	1367771_at	Dsipi
1367668_a_at	Scd2	1367720_at	Alad	1367772_at	
1367669_a_at	Map1lc3b	1367721_at	Sdc4	1367773_at	Slc25a1
1367670_at	Fh1	1367722_at	Dpp7	1367774_at	Gsta5
1367671_at	Pcna	1367723_a_at	Lnk	1367775_at	Amacr
1367672_at	Hsd17b4	1367724_a_at	Atp6v0e	1367776_at	Cdc2a
1367673_at	Selenbp1	1367725_at	Pim3	1367777_at	Decr1
1367674_at	Pitpnb	1367726_at	Thra	1367778_at	Pcsk3
1367675_at	Cib1	1367727_at	Pscd2	1367779_at	Bin1
1367676_at	Hmgb2	1367728_at	Tsn	1367780_at	Pttg1
1367677_at	Prdx5	1367729_at	Oat	1367781_at	Pip
1367678_at	Sdha	1367730_at	Vdp	1367782_at	Cox6a2
1367679_at	Cd74	1367731_at	Gnb1	1367783_at	Gabarapl2
1367680_at	Acox1	1367732_at	Gnb1	1367784_a_at	Clu
1367681_at	Cd151	1367733_at	Ca2	1367785_at	Cnn1
1367682_at	Mdk	1367734_at	Aldr1	1367786_at	Psmb8

1367683_at	Kpna2	1367735_at	Acadl	1367787_at	Ica1
1367684_at	Crybb2	1367736_at	Rraga	1367788_at	Phkg2
1367685_at	Rps27a	1367737_at	Fuca	1367789_at	Slc27a1
1367686_at	RAMP4	1367738_at	Unc119	1367790_at	RGD:631340
1367687_a_at	Pam	1367739_at	Cox8h	1367791_at	Ramp1
1367688_at	Scamp4	1367740_at	Ckb	1367792_at	Psp
1367689_a_at	Cd36	1367741_at	Herpud1	1367793_at	Ddt
1367690_at	Ssr4	1367742_at	Cpt1b	1367794_at	A2m
1367691_at	Prkcdbp	1367743_at	Pfkl	1367795_at	Ifrd1
1367692_at	Sbp	1367744_at	Maged2	1367796_at	Mgat1
1367693_at	Ywhah	1367745_at	Dgkz	1367797_at	Men1
1367694_at	Hadhb	1367746_a_at	Flot2	1367798_at	Ahcy
1367695_at	Qdpr	1367747_at	Arl3	1367799_at	Stnl
1367696_at	Ifitm2	1367748_at	Arf5	1367800_at	Plat
1367697_at	Mapk14	1367749_at	Lum	1367801_at	Ece1
1367699_at	RGD:708456	1367750_at	Prpsap1	1367802_at	Sgk
1367700_at	Fmod	1367751_at	Dpm2	1367803_at	Nup54
1367701_at	Ramp2	1367752_at	Bcar1	1367804_at	Sap
1367702_at	Acadm	1367753_at	Sec31l1	1367805_at	Gls
1367703_at	Crygd	1367754_s_at	Asl /// Hnrpab	1367806_at	Gls
1367704_at	Ap2b1	1367755_at	Cdo1	1367807_at	Plod1
1367705_at	Glrx1	1367756_at	Gfm	1367808_at	Timm8b
1367706_at	Vdac1	1367757_at	Cox6c	1367809_at	Prlpa
1367707_at	Fasn	1367758_at	Afp	1367810_at	Slc6a8
1367708_a_at	Fasn	1367759_at	H1f0	1367811_at	Phgdh
1367709_at	Cd63	1367760_at	Map2k1	1367812_at	Spnb3
1367710_at	Psme2	1367761_at	Ndel1	1367813_at	Ppp1r14a
1367711_at	Psmc2	1367762_at	Sst	1367814_at	Atp1b1
1367816_at	Hod	1367763_at	Acat1	1367815_at	Slc5a6
1367817_at	Hdgf	1367870_at	Txnl2	1367924_at	Pacs1
1367818_at	Coq3	1367871_at	Cyp2e1	1367925_at	Mvp
1367819_at	Got2	1367872_at	Ap1b1	1367926_at	Phb
1367820_at	Banf1	1367873_at	Atp6ap1	1367927_at	Phb
1367821_a_at	Cacna1a	1367874_at	Rhoq	1367928_at	Myh7
1367822_at	Cacna1a	1367875_at	Gak	1367929_at	Cd59
1367823_at	Timp2	1367876_at	Ipo13	1367930_at	Gap43
1367824_at	Fnta	1367877_at	Slc11a2	1367931_a_at	Ptbp1
1367825_at	Ralgds	1367878_at	Stx5a	1367932_at	Hmgcs1
1367826_at	Nfe2l2	1367879_at	Cdk5rap3	1367933_at	Amd1
1367827_at	Ppp2cb	1367880_at	Lamb2	1367934_at	Rpl39
1367828_at	Acads	1367881_at	Ptpns1	1367935_at	Smu1
1367829_at	Echs1	1367882_at	Mtap1a	1367936_at	Stk10
1367830_a_at	Tp53	1367883_at	SMN1	1367937_at	Aldrl6
1367831_at	Tp53	1367884_at	Rab14	1367938_at	Ugdh
1367832_at	Lypla1	1367885_at	Pxmp2	1367939_at	Rbp1
1367833_at	RGD:708376	1367886_at	Pcsk7	1367940_at	Cmkor1
1367834_at	Srm	1367887_at	Lcat	1367941_at	Tfam

1367835_at	Pcsk1n	1367888_at	Pcdh21	1367942_at	Acp5
1367836_at	Cpt1a	1367889_at	Camk1	1367943_at	Nfkbib
1367837_at	Psma4	1367890_at	Casp2	1367944_at	Chst10
1367838_at	Cth	1367891_a_at	Casp2	1367945_at	Atox1
1367839_at	Fdft1	1367892_at	Pdk2	1367946_at	Pdlim1
1367841_a_at	Prlpc2	1367893_a_at	RGD:708359	1367948_a_at	Kdr
1367842_at	Apbb1	1367895_at	Hnrpk	1367949_at	Penk-rs
1367843_at	RGD:620311	1367896_at	Ca3	1367950_at	Slc22a5
1367844_at	Gnai2	1367897_at	Acadvl	1367951_at	Pgam2
1367845_at	Nef3	1367898_at	Bnip3l	1367952_at	Lrp2
1367846_at	S100a4	1367899_at	F2r	1367953_at	Tyro3
1367847_at	Nupr1	1367900_at	Gyg1	1367954_at	Gfra1
1367848_at	Dctn1	1367901_at	Gusb	1367955_at	Rab4b
1367849_at	Sdc1	1367902_at	Gng11	1367956_at	Ncdn
1367850_at	Fcgr3	1367903_at	Hmox2	1367957_at	Rgs3
1367851_at	Ptgds	1367904_at	Resp18	1367958_at	Abi1
1367853_at	Slc12a2	1367905_at	Enpp3	1367959_a_at	Scn1b
1367854_at	Acly	1367906_at	Acp2	1367960_at	Arl4
1367855_at	Scarb1	1367907_a_at	Cltb	1367961_at	Ngfg
1367856_at	G6pdx	1367908_at	Gcsh	1367962_at	Actn3
1367857_at	Fads1	1367909_at	Dcxr	1367963_at	Gbl
1367858_at	Mmp11	1367910_at	Madh4	1367964_at	Tnni2
1367859_at	Tgfb3	1367912_at	Ltbp1	1367965_at	Slc9a1
1367860_a_at	Mmp14	1367913_at	Cygb	1367966_at	Dpp3
1367861_at	Evl	1367914_at	Emp3	1367967_at	Lepre1
1367862_at	Rrad	1367915_at	Dgat1	1367968_at	RGD:708577
1367863_at	Bnip1	1367916_at	Plcd1	1367969_at	Prdx6
1367864_at	Pfkm	1367917_at	Cyp2d26	1367970_at	Pfn2
1367865_at	Lkap	1367918_at	Fez1	1367971_at	Ptp4a2
1367866_at	Fbln5	1367919_at	Pom210	1367972_at	RGD:620479
1367867_at	Gfer	1367920_at	Edg5	1367973_at	Ccl2
1367868_at	Adrm1	1367921_at	Ilkap	1367974_at	Anxa3
1367869_at	Oxr1	1367922_at	Adam17	1367975_at	Anxa3
1367977_at	Snca	1367923_at	RGD:708557	1367976_at	Tpp2
1367978_at	Adcy2	1368029_at	Gnai3	1368082_at	Slc4a2
1367979_s_at	Cyp51	1368030_at	Gnai3	1368083_at	Ccnh
1367980_at	Rabep1	1368031_at	Nolc1	1368084_at	Dnase1
1367981_at	Rabep1	1368032_at	Nolc1	1368085_at	Gchfr
1367982_at	Alas1	1368033_at	Nolc1	1368086_a_at	Lss
1367983_at	Fen1	1368034_at	Chgb	1368087_a_at	Ptpn21
1367984_at	RGD:708405	1368035_a_at	Ptprf	1368088_at	Cdk5
1367985_at	Alas2	1368036_at	Ptprf	1368089_at	Pde2a
1367986_at	Ptgfrn	1368037_at	Cbr1	1368090_at	Prx
1367987_at	Rnpep	1368038_at	Synj2bp	1368091_at	Oplah
1367988_at	Cyp2c23	1368039_at	Synj2bp	1368092_at	Fah
1367989_at	Slc2a4	1368040_at	Synj2bp	1368093_at	Myh6
1367990_at	Crybb3	1368041_at	Synj2bp	1368094_at	Secisbp2
1367991_at	Gcs1	1368042_a_at	Hmgb1	1368096_at	Rab7l1

1367992_at	Sgne1	1368043_at	Snx1	1368097_a_at	Rtn1
1367993_at	Rsn	1368044_at	Scg2	1368098_a_at	Snrpn
1367994_at	Dpyd	1368045_at	RGD:620059	1368099_at	Clasp2
1367995_at	Cat	1368046_at	RGD:620059	1368100_at	Pcyt2
1367996_a_at	Lphn1	1368047_at	Slc13a3	1368101_at	Calm3
1367997_at	Skd3	1368048_at	Spin2b	1368103_at	Abcg1
1367998_at	Slpi /// LOC296356	1368049_at	Tcp1	1368104_at	Tspan2
1367999_at	Aldh2	1368050_at	Ccnl1	1368105_at	Tspan2
1368000_at	C3	1368051_at	Hsd17b12	1368106_at	Plk2
1368001_at	Apeg1	1368052_at	Tm4sf3	1368107_at	Prlpi
1368002_at	Msh2	1368053_at	Pard3	1368108_at	Atp2a1
1368003_at	Aldh1a2	1368054_at	Lmna	1368109_at	Siat9
1368004_at	Mrpl23	1368055_a_at	Lmna	1368110_a_at	Syngap1
1368005_at	Itpr3	1368056_at	Tsc2	1368111_at	Abtb2
1368006_at	Laptm5	1368057_at	Abcd3	1368112_at	Sag
1368007_at	Dmbt1	1368058_at	Safb	1368113_at	Tff2
1368008_at	Prom1	1368059_at	Crym	1368114_at	Fgf13
1368009_at	Uae1	1368060_at	Hrsp12	1368115_at	Cldn3
1368010_at	Ptpn6	1368061_at	Kcnh1	1368116_a_at	Rps6kb1
1368011_at	Fdxr	1368062_at	Ap3m1	1368117_at	Gphn
1368012_at	Tep1	1368063_a_at	RGD:621706	1368118_at	Bcl10
1368013_at	Ddit4l	1368064_a_at	Ddc	1368119_at	Pib5pa
1368014_at	Ptges	1368065_at	Rgs19ip1	1368120_at	Nell1
1368015_at	Ptges	1368066_at	Bak1	1368121_at	Akr7a3
1368016_at	Pecr	1368067_at	Znf148	1368122_at	Rnf103
1368017_at	Lgals7	1368068_a_at	Pacsin2	1368123_at	Igf1r
1368018_at	Mkln1	1368069_at	RGD:631353	1368124_at	Dusp5
1368019_at	Frap1	1368070_at	Stx8	1368125_at	Slc12a4
1368020_at	Mvd	1368071_at	Mg87	1368126_at	Aacs
1368021_at	Adh1	1368072_at	Btg3	1368127_at	Neu2
1368022_at	Inppl1	1368073_at	Irf1	1368128_at	Pla2g2a
1368023_at	Qscn6	1368074_at	Gale	1368129_at	Sfmbt1
1368024_at	Qscn6	1368075_at	Lipa	1368130_at	Aldh3a1
1368025_at	Ddit4	1368076_at	Vhl	1368131_at	Capn6
1368026_at	Hdgfrp2	1368077_at	Fbp1	1368132_at	RGD:621126
1368027_at	Tbxas1	1368078_at	Esm1	1368133_at	Mpdz
1368028_at	Prph1	1368079_at	Pdk1	1368134_a_at	Il4r
1368136_at	Tmpo	1368081_at	Abca2	1368135_at	Ninj2
1368137_at	Mapt	1368191_a_at	Slc22a1	1368243_at	Amhr2
1368138_at	Mapt	1368192_at	Cxcr3	1368244_at	As3mt
1368139_s_at	Alpl	1368193_at	Slc26a4	1368245_at	RGD:620091
1368140_at	Prkwnk1	1368194_at	Agpat4	1368246_at	Ap3m2
1368141_at	Cnbp1	1368195_at	Hspbap1	1368247_at	Hspa1a /// Hspa1b
1368142_at	Anxa7	1368196_at	Clps	1368248_at	Cds1
1368143_at	Anxa7	1368197_at	Oprk1	1368249_at	Klf15
1368144_at	Rgs2	1368198_at	Oprk1	1368250_at	Tekt1
1368145_at	Pcp4	1368199_at	Nup88	1368251_at	Jak3
1368146_at	Dusp1	1368200_at	Cx3cl1	1368252_at	Kbtbd10

1368147_at	Dusp1	1368201_at	Npr1	1368253_at	Gamt
1368148_at	Ngfr	1368202_a_at	Dab2	1368254_a_at	Sphk1
1368149_at	Hif1a	1368203_at	Scnn1a	1368255_at	Hnt
1368150_at	Slc27a2	1368204_at	Lig1	1368256_at	Serpini1
1368152_at	Zdhhc7	1368205_at	Cfi	1368257_at	Cgm3
1368153_a_at	Nelf	1368206_at	Pte1	1368258_at	Apln
1368154_at	Gucy1a3	1368207_at	Fxyd5	1368259_at	Ptgs1
1368155_at	Cyp2c40	1368208_at	Cml1	1368260_at	Aurkb
1368156_at	Camkk1	1368209_at	Map17	1368261_at	Nrxn3
1368157_at	Stmn3	1368210_at	Il24	1368262_at	Plekhe1
1368158_at	Scfd1	1368211_at	Rps14 /// RGD1306596_predicted	1368263_a_at	Mobp
1368159_at	Abcb6	1368212_at	Csnk2b	1368264_at	Pex6
1368160_at	Igfbp1	1368213_at	Por	1368265_at	RGD:620086
1368161_a_at	Ahsg	1368214_at	Madh2	1368266_at	Arg1
1368162_at	Cst6	1368215_at	Cln2	1368267_at	Pomt1
1368163_at	Dpp4	1368216_at	Rab28	1368268_at	RGD:620959
1368164_at	Blvra	1368217_at	Ralbp1	1368269_at	Lgals4
1368165_at	Prps1	1368218_at	Ralbp1	1368270_at	Apobec1
1368166_at	Arl2	1368219_at	Clcn2	1368271_a_at	Fabp4
1368167_at	Ctse	1368220_at	Gtf2b	1368272_at	Got1
1368168_at	Slc34a2	1368221_at	Nr3c1	1368273_at	Mapk6
1368169_at	Prkcabp	1368222_at	Nr3c1	1368274_at	Dbnl
1368170_at	Slc6a1	1368223_at	Adamts1	1368275_at	Sc4mol
1368171_at	Lox	1368224_at	Spin2c	1368276_at	Syp
1368172_a_at	Lox	1368225_at	Sec5l1	1368277_at	Ppp3ca
1368173_at	Nol5	1368226_at	C6orf108	1368278_at	Lgals2
1368175_at	Zhx1	1368227_at	Slc28a2	1368279_at	RGD:620940
1368176_at	Rara	1368228_at	Zfp265	1368280_at	Ctsc
1368177_at	Acsl3	1368229_at	Sip1	1368281_at	Dpep1
1368178_at	Pdzk1	1368230_a_at	RGD:708545	1368282_at	Dpep1
1368179_at	Tslpr	1368231_at	Stat5a	1368283_at	Ehhadh
1368180_s_at	Gsta2	1368232_at	Mvk	1368284_at	Plvap
1368181_at	Mthfd1	1368233_at	Gtf2f2	1368285_at	Shbg
1368182_at	Acsl6	1368234_at	Prep	1368286_at	Slc2a8
1368183_at	Plcg1	1368235_at	Clk3	1368287_at	Chn1
1368184_at	Psmd9	1368236_at	Mep1a	1368288_at	Gc
1368185_at	Gnaz	1368237_at	Tnmd	1368289_at	Gc
1368186_a_at	Syk	1368238_at	Pap	1368290_at	Cyr61
1368187_at	Gpnmb	1368239_at	Lrp3	1368291_at	Birc2
1368188_at	Hpd	1368240_a_at	Prkcb1	1368292_at	Dnm1
1368189_at	Dhcr7	1368241_a_at	Flot1	1368293_at	Cpz
1368295_at	Slco2b1	1368242_at	Kcnb1	1368294_at	Dnase1l3
1368296_at	Slco2b1	1368348_at	Slc6a4	1368401_at	Gria2

1368297_at	Gata2	1368349_at	Fgfbp1	1368402_at	Dncli2
1368298_at	Adcy5	1368350_at	Ptprz1	1368403_at	Rbl2
1368299_at	Gpr83	1368351_at	Scn10a	1368404_at	Dbn1
1368300_at	Adora2a	1368352_at	Stx1b2	1368405_at	Rala
1368301_at	Adora2a	1368353_at	Gfap	1368406_at	Star
1368302_at	Msx1	1368354_at	Gstt1	1368407_at	Hpse
1368303_at	Per2	1368355_at	Myo5b	1368408_at	Gprk5
1368305_at	Casp6	1368356_a_at	Arts1	1368409_at	Gstt2
1368306_at	Grin2c	1368357_at	Kcnh4	1368410_at	Mpg
1368307_at	Ggtl3	1368358_a_at	Ptprr	1368411_a_at	Mtap2
1368308_at	Myc	1368359_a_at	Vgf	1368412_a_at	Ptpro
1368309_at	Txnrd2	1368361_a_at	Ptpn2	1368413_at	Abp1
1368310_at	Myog	1368362_a_at	Asgr2	1368414_at	Slc5a2
1368311_at	Mgmt	1368363_at	Klf5	1368415_at	Myh3
1368312_at	Oxt	1368364_at	Mcsp	1368416_at	Ibsp
1368313_a_at	Trpv1	1368365_at	Aldh3a2	1368417_at	Syt5
1368314_at	Ggcx	1368366_at	Cml2	1368418_a_at	Cp
1368315_at	Entpd6	1368367_at	Cuzd1	1368419_at	Cp
1368316_at	Aqp8	1368368_a_at	Lisch7	1368420_at	Cp
1368317_at	Aqp7	1368369_at	Pnoc	1368421_at	Ptpn5
1368318_at	Homer1	1368370_at	Adcy4	1368422_at	Meox2
1368319_a_at	Homer1	1368371_at	Kcnq1	1368423_at	Retnla
1368320_at	Ncam1	1368372_at	Sts	1368424_at	Ikbkb
1368321_at	Egr1	1368373_at	Rgs7	1368425_at	Caskin1
1368322_at	Sod3	1368374_a_at	Ggt1	1368426_at	Crot
1368323_at	Tfpi	1368375_a_at	Il15	1368427_at	Akap11
1368324_at	Brca2	1368376_at	Nr0b2	1368428_at	Xpnpep2
1368325_at	Egf	1368377_at	Gzmc	1368429_at	Taf9l
1368326_at	Eif2ak3	1368378_at	Fthfd	1368430_at	Lgmn
1368327_at	Slc12a9	1368379_at	Scarb2	1368431_at	Hpn
1368328_at	Gys2	1368380_at	Vtn	1368432_a_at	Ros1
1368329_at	Slc22a6	1368381_at	Crtac1	1368433_at	Sacm1l
1368330_at	Aatf	1368382_at	S100a3	1368434_at	Nat1
1368331_at	Ctbs	1368383_at	Npff	1368435_at	Cyp8b1
1368332_at	Gbp2	1368384_at	Klk6	1368436_at	Nudc
1368333_at	Umod	1368385_a_at	Grb2	1368437_at	Ca4
1368334_at	Grb7	1368386_at	Grb2	1368438_at	Pde10a
1368335_at	Apoa1	1368387_at	Bdh	1368439_at	Sox10
1368336_at	Fdx1	1368388_at	Maf	1368440_at	Slc3a1
1368337_at	Glycam1	1368389_at	Apba3	1368441_at	Msln
1368338_at	Cd52	1368390_at	Araf1	1368442_at	F2
1368339_at	Calb3	1368391_at	Slc7a1	1368443_at	Efcbp2
1368340_at	Impk	1368392_at	Slc7a1	1368444_at	Sgta
1368341_at	Polb	1368393_at	C1qr1	1368445_at	Shank1
1368342_at	Ampd3	1368394_at	Sfrp4	1368446_at	Spink1
1368343_at	Kcnh2	1368395_at	Gpc3	1368447_x_at	Spink1
1368344_at	Gad1	1368396_at	Cel	1368448_at	Ltbp2
1368345_at	Mtap6	1368397_at	Ugt2b5 /// Ugt2b4 /// MGC93327	1368449_at	Centa1

1368346_at	B3galt4	1368398_at	Cacna1h	1368450_at	Myo5a
1368347_at	Col5a3	1368399_a_at	Pgcp	1368451_at	Hrh3
1368453_at	Fads2	1368400_at	Timm8a	1368452_at	Abcc6
1368454_at	Plfr	1368505_at	Rgs4	1368557_s_at	RGD:619872 /// RGD:620384
1368455_at	Nkg7	1368506_at	Rgs4	1368558_s_at	Aif1
1368456_at	Gabrr1	1368507_at	Psma3	1368559_at	Pcsk1
1368457_at	Gabrr1	1368508_at	Psma3	1368560_at	Kcnj5
1368458_at	Cyp7a1	1368509_at	Bbs2	1368561_at	Abcd2
1368459_at	Gdf10	1368510_at	Gata1	1368562_at	Sult4a1
1368460_at	Slc2a5	1368511_at	Bhlhb3	1368563_at	Aspa
1368461_at	Slc22a8	1368512_a_at	Enpep	1368564_at	Slc17a6
1368462_at	Itpka	1368513_at	Enpep	1368565_at	Slc1a3
1368463_at	Vegfc	1368514_at	Maob	1368566_a_at	RGD:621020
1368464_at	Mgl1	1368515_at	Epb4.1l3	1368567_at	RGD:621020
1368465_at	Accn1	1368516_at	Ptpra	1368568_at	Aqp2
1368466_at	Odf2	1368517_at	Ssdp3	1368569_at	Akr1b7
1368467_at	Cyp4f2	1368518_at	Cd53	1368570_at	Lrat
1368468_at	Cyp11a1	1368519_at	Serpine1	1368571_at	Cyln2
1368469_at	Aqp5	1368520_at	Apoa4	1368572_a_at	Grin1
1368470_at	Ggh	1368521_at	Napsa	1368573_at	Kpnb1
1368471_at	Guca2a	1368522_at	Timeless	1368574_at	Adra1b
1368472_at	Celsr3	1368523_at	Cadps	1368575_at	Slc6a18
1368473_at	Gja5	1368524_at	Kcnc1	1368576_at	Cart1
1368474_at	Vcam1	1368525_at	Mrs2l	1368577_at	Gjb6
1368475_at	Colq	1368526_at	Pex3	1368578_at	Hsd3b1_predicted
1368476_at	Nr3c2	1368527_at	Ptgs2	1368579_at	Prlpm
1368477_at	Atp2a3	1368528_at	RGD:620896	1368580_at	Sdc3
1368478_at	Drd1a	1368529_at	RGD:620896	1368581_at	Sdc3
1368479_at	Drd1a	1368530_at	Mmp12	1368582_at	Slc7a3
1368480_at	Cdw92	1368531_at	Prlpc1	1368583_a_at	Hrg
1368481_at	Gipr	1368532_at	Pnliprp1	1368584_a_at	Cplx2
1368482_at	Bcl2a1	1368533_at	Heph	1368585_at	Cart
1368483_at	Slit1	1368534_at	Adra1d	1368586_at	Zg16
1368484_at	Abcb9	1368535_at	Bid3	1368587_at	Apoc1
1368485_at	Avil	1368536_at	Enpp2	1368588_at	Ddx52
1368486_at	Irs3	1368537_at	Dctn4	1368589_at	Ptprj
1368487_at	Serpinb2	1368538_at	Exoc7	1368590_at	Mmp16
1368488_at	Nfil3	1368539_at	Scn9a	1368591_at	Usf2
1368489_at	Fosl1	1368540_at	Tpbg	1368592_at	Il1a
1368490_at	Cd14	1368541_at	Emb	1368593_at	Cd1d1
1368491_at	Dlad	1368542_at	RGD:621664	1368594_at	Pla2g2c
1368492_at	Ptgds2	1368543_at	Nox4	1368595_at	Mmp24
1368493_at	Lim2	1368544_a_at	Nol3	1368596_at	Snf1lk
1368494_at	S100a8	1368545_at	Cflar	1368597_at	Snf1lk
1368495_at	Rln1	1368546_at	Hivep2	1368598_at	Sstr3

1368496_at	Odf1	1368547_at	Ocil	1368599_at	Slc9a2
1368497_at	Abcc2	1368548_at	Slc12a1	1368600_at	Slc26a1
1368498_a_at	RGD:621387	1368549_at	Hbp1	1368601_at	Slc6a3
1368499_at	Sycp2	1368550_at	Foxq1	1368602_at	Slc6a3
1368500_a_at	Rgs9	1368551_at	Prps2	1368603_at	Add2
1368501_s_at	Mcpt8 /// Mcpt10 /// Mcpt9	1368552_at	Grpel1	1368604_at	Mefv
1368502_at	Gast	1368553_at	Acvrl1	1368605_at	Aps
1368503_at	Gch	1368554_at	Pnlip	1368606_at	Slco1a2
1368504_at	Lamp1	1368555_at	Cd37	1368607_at	RGD:628846
1368609_at	Slc10a1	1368556_at	RGD:620384	1368608_at	Cyp2f2
1368610_at	Mca32	1368662_at	Rnf39	1368714_at	Dtprp
1368611_at	Grp	1368663_at	RGD:708544	1368715_s_at	Dtprp
1368612_at	Itgb4	1368664_at	RGD:708544	1368716_at	Ppp1r14c
1368613_at	Stag3	1368665_at	Ufd1l	1368717_at	Faah
1368614_at	RGD:620400	1368666_a_at	Lphn3	1368718_at	Aldh1a4
1368615_a_at	Slc18a3	1368667_at	P2rx3	1368719_at	Pfkfb4
1368616_at	Fancc	1368668_at	Plaa	1368720_at	Tdo2
1368617_at	Serpina5	1368669_at	Ucp2	1368721_at	Ascl2
1368618_at	Grb14	1368670_a_at	Pde4a	1368722_at	Lta
1368619_at	Ddx25	1368671_at	Srpx	1368723_at	Lat
1368620_at	Spag4	1368672_at	Arg2	1368724_a_at	Tpm1
1368621_at	Aqp9	1368673_at	Ddr2 /// Ddr2_predicted	1368725_at	Jag1
1368622_at	Fbp2	1368674_at	Pygl	1368726_a_at	RGD:620185
1368623_at	Ceacam9	1368675_at	Chn2	1368727_at	Slc7a9
1368625_at	Prap1	1368676_at	Dnch2	1368728_at	P2y12
1368626_at	Kcnn3	1368677_at	Bdnf	1368729_a_at	Adcyap1r1
1368627_at	Rgn	1368678_at	Bdnf	1368730_a_at	Adcyap1r1
1368628_at	Ton	1368679_a_at	Lyn	1368731_at	Orm1
1368629_at	Reg1	1368680_a_at	Slc34a1	1368732_at	Tap2
1368630_at	Fabp9	1368681_at	Pthlh	1368733_at	Ste
1368631_at	Dbil5	1368682_at	Sv2a	1368734_at	Chrnd
1368632_at	Foxg1	1368683_at	Oldlr1	1368735_a_at	Trpv2
1368633_at	Crisp1	1368684_at	Fath2	1368736_at	Tsx
1368634_at	Kcnh3	1368685_at	Cspg4	1368737_at	RGD:619853
1368635_at	Tnfrsf8	1368686_at	Ambp	1368738_at	Cyp11b1
1368636_at	Cyp27b1	1368687_at	Tesk1	1368739_s_at	Cyp11b1 /// Cyp11b2 /// RGD:727886
1368637_at	RGD:708370	1368688_at	Ntsr2	1368740_at	P2rxl1

1368638_at	Gpr147	1368689_at	Gjb5	1368741_at	C9
1368639_at	Kcnip2	1368690_a_at	Grm4	1368742_at	C5r1
1368640_at	Spas1	1368691_at	Gria3	1368743_a_at	Dspp
1368641_at	Wnt4	1368692_a_at	Chka	1368744_a_at	Dspp
1368642_at	Cdh2	1368693_at	Fgr	1368745_at	Slc10a2
1368643_at	Spata6	1368694_at	RGD:727932	1368746_a_at	Atp12a
1368644_at	Spata6	1368695_at	C4bpb	1368747_at	Nup98
1368645_at	Ptpn1	1368696_at	Fxyd7	1368748_at	Tesk2
1368646_at	Mapk9	1368697_at	Fabp6	1368749_at	Kcns1
1368647_at	Gprk6	1368698_at	Atp2b2	1368750_a_at	Pde4d
1368648_at	Cox4i2	1368699_at	Dscam	1368751_at	Kcns3
1368649_at	Dkc1	1368700_at	RGD:708420	1368752_at	Tacr3
1368650_at	Tieg	1368701_at	Atp1a3	1368753_at	Camkk2
1368651_at	Pklr	1368702_at	Pawr	1368754_at	P2ry6
1368652_at	Casp9	1368703_at	Enh	1368755_at	Clecsf13
1368653_a_at	Park7	1368704_a_at	Cspg5	1368756_at	Thedc1
1368654_at	Npap60	1368705_at	Edg8	1368757_at	RGD:620606
1368655_at	RGD:619969	1368706_at	Tm4sf4	1368758_a_at	Galr2
1368656_at	Scg3	1368707_at	Itih4	1368759_at	Cacng2
1368657_at	Mmp3	1368708_a_at	Drd2	1368760_at	Cxcl2
1368658_at	Cntf	1368709_at	Fut1	1368761_at	Ppp3r2
1368659_at	Agxt2	1368710_at	Mark2	1368762_at	Ubd
1368660_at	Rapgef3	1368711_at	Foxa2	1368763_at	Il3
1368661_at	Slc13a2	1368712_at	Znf386	1368764_at	Hist1h2ba
1368766_at	Mmp7	1368713_at	Mmp10	1368765_at	Clcnk1
1368767_at	Cst8	1368821_at	Fstl1	1368874_a_at	Mafg
1368768_at	Scn11a	1368822_at	Fstl1	1368875_a_at	Nrxn2
1368769_at	Abcb11	1368823_at	Cald1	1368876_a_at	Nrxn2
1368770_at	Gcnt1	1368824_at	Cald1	1368877_at	Znf354a
1368771_at	Sulf1	1368825_at	Shox2	1368878_at	Idi1
1368772_at	Slc4a3	1368826_at	Comt	1368879_a_at	Gnao
1368773_at	Fshprh1	1368827_at	Gata6	1368880_at	Ntn1
1368774_a_at	Espn	1368828_at	Gata6	1368881_at	Bet1
1368775_at	Giot1	1368829_at	Fbn1	1368882_at	Siat7c
1368776_at	Alox5	1368830_at	Src	1368883_at	Nov
1368777_at	Bard1	1368831_at	Mark3	1368884_at	Entpd1
1368778_at	Slc6a6	1368832_at	Akt2	1368885_at	Entpd1
1368779_a_at	Gucy1b2	1368833_at	Camk2d	1368886_at	Map3k12
1368780_at	Adrb3	1368834_at	Camk2d	1368887_at	Cdh22
1368781_at	Rasgrp4	1368835_at	Stat1	1368888_a_at	Rtn4
1368782_at	Sstr2	1368836_a_at	Agc1	1368889_at	Vti1a
1368783_at	Icos	1368837_at	Arid4b	1368890_at	Gnpat
1368784_at	Acf	1368838_at	Tpm4	1368891_at	Gnpat
1368785_a_at	Pitx2	1368839_at	Wfs1	1368892_at	Adcyap1
1368786_a_at	Gpcr12	1368840_at	RGD:708403	1368893_at	Cap2
1368787_at	Mutyh	1368841_at	Tcf4	1368894_at	Cap2
1368788_at	Chad	1368842_at	Tcf4	1368895_at	Nlgn2

1368789_at	Acpp	1368843_at	Yme1l1	1368896_at	Madh7
1368790_at	Serpina10	1368844_at	Stch	1368897_at	Madh7
1368791_at	Oprd1	1368845_at	RGD:621488	1368898_at	Madh7
1368792_at	Psen1	1368846_at	RGD:621488	1368899_at	Bmpr1a
1368793_at	Kcnj2	1368847_at	Rab10	1368900_at	Thbd
1368794_at	Haao	1368848_at	Lman1	1368901_at	Thbd
1368795_at	Gpr66	1368849_at	Csnk1g3	1368902_at	Pak3
1368796_at	Gpr54	1368850_at	Csnk1g3	1368903_at	Strbp
1368797_at	Nr1i3	1368851_at	Ets1	1368904_at	Capn10
1368798_at	LOC499761	1368853_at	Vsnl1	1368905_at	Ces2
1368799_at	Birc5	1368854_at	Vsnl1	1368906_at	Pgk1
1368800_at	Tnfsf5	1368855_at	Ighmbp2	1368907_at	Scamp5
1368801_at	Cxxc4	1368856_at	Jak2	1368908_at	Anxa4
1368802_at	Pmch	1368857_at	Ugt8	1368909_a_at	Gripap1
1368803_at	Insl6	1368858_at	Ugt8	1368910_at	Ppm2c
1368804_at	Lif	1368859_at	Ppm1a	1368911_at	Kcnj8
1368805_at	Uts2	1368860_at	Phlda1	1368912_at	Trh
1368806_at	Sepp1	1368861_a_at	Mag	1368913_at	Csn2
1368807_at	Rtn3	1368862_at	Akt1	1368914_at	Runx1
1368808_at	Cap1	1368863_at	Nme3	1368915_at	Kmo
1368809_at	Cap1	1368864_at	Synpr	1368916_at	Asl
1368810_a_at	Mbp	1368865_at	Synpr	1368917_at	Nudt1
1368811_at	Lmnb1	1368866_at	Eif2c2	1368918_at	Pgf
1368812_at	Lmnb1	1368867_at	Eif2c2	1368919_at	Pgf
1368813_at	Cebpd	1368868_at	Akap12	1368920_at	Slit3
1368814_at	Aldh6a1	1368869_at	Akap12	1368921_a_at	Cd44
1368815_at	Mpz	1368870_at	Id2	1368922_at	Ecel1
1368819_at	Itgb1	1368871_at	Map3k1	1368923_at	Ecel1
1368820_at	Nfyc	1368872_a_at	Homer2	1368924_at	Ghr
1368926_at	Sema4f	1368873_at	Hoxa2	1368925_a_at	Arhgef7
1368927_at	Mbc2	1368978_at	Scrg1	1369033_at	Lhcgr
1368928_at	Trim3	1368979_at	Kalrn	1369034_at	Kcnj6
1368929_at	Npl4	1368980_at	Plce1	1369035_a_at	Kcnj6
1368930_at	Kcnn4	1368981_at	Aqp4	1369036_at	Grik2
1368931_at	Sh3gl3	1368982_at	Pkia	1369037_at	Slk
1368932_at	Rock1	1368983_at	Dtr	1369038_at	Itgax
1368933_at	Adarb1	1368985_at	Grin2a	1369039_at	Pik4cb
1368934_at	Cyp4a10 /// Cyp4a22	1368986_at	Slc17a7	1369040_at	Cdc42bpa
1368935_at	Camk2a	1368989_at	Timp3	1369041_at	Nlgn1
1368936_at	Txnl1	1368990_at	Cyp1b1	1369042_at	Pigm
1368937_at	Ncoa2	1368991_at	Smpd3	1369043_at	Kcna4
1368938_at	Dll1	1368992_a_at	Sfrs5	1369044_a_at	Pde4b
1368939_a_at	Ntrk3	1368993_at	RGD:727907	1369045_at	Rgs14
1368940_at	P2ry2	1368994_a_at	Garnl1	1369046_at	Syt6
1368941_at	Ptger4	1368995_at	Garnl1	1369047_at	Sult1d1
1368942_at	Hes5	1368996_at	Ceacam3	1369048_at	Gabrd
1368943_at	Rnase4	1368997_at	Tceb3	1369049_at	Rere
1368944_at	Dlgh1	1368998_at	Nkx6-1	1369050_at	Pik3c2g
1368945_at	Bmp2	1368999_a_at	Begain	1369051_at	Insr

1368946_at	Arf2	1369000_at	Ntrk1	1369052_at	Zfp111
1368947_at	Gadd45a	1369001_at	Chrna3	1369053_at	Syt2
1368948_at	Msn	1369002_at	Soat1	1369054_at	Rph3a
1368949_at	Ebf1	1369003_at	Dedd	1369055_at	RGD:620565
1368950_a_at	Grin2d	1369004_at	Rab26	1369056_at	Rpe65
1368951_at	Grin2d	1369005_at	Kcnq3	1369057_at	Stxbp2
1368952_at	Gpr51	1369006_at	Hk2	1369058_at	Syt3
1368953_at	Ugcgl1	1369007_at	Nr4a2	1369059_at	Trpm7
1368954_at	Pld2	1369008_a_at	Olfm1	1369060_a_at	Hdac3
1368955_at	Cask	1369009_at	Serpinh1	1369061_at	Gsr
1368956_at	Pcdh8	1369010_at	Chek2	1369062_at	Madcam1
1368957_at	Gng7	1369011_at	Apoa5	1369063_at	Anp32a
1368958_at	Pacsin1	1369012_at	Inhba	1369064_a_at	Scn8a
1368959_at	Pacsin1	1369013_a_at	Mrpl17	1369065_a_at	Atp2a2
1368960_at	Lgals8	1369014_at	Nf1	1369066_at	Madd
1368961_at	Mmp23	1369015_at	Nos1	1369067_at	Nr4a3
1368962_at	Nxph3	1369016_at	Cdon	1369068_at	Cul5
1368963_at	Mxi1	1369017_at	Kcnh6	1369069_at	Akap1
1368964_at	Lrrn3	1369018_at	Foxm1	1369070_at	Pex12
1368965_at	Slc16a3	1369019_at	Chrna5	1369071_at	Edg1
1368966_at	Mybph	1369020_at	Slc5a5	1369072_at	Adh7
1368967_at	Eif2b3	1369021_at	Hcrtr1	1369073_at	Nr1h4
1368968_at	Arrb1	1369022_at	RGD:620277	1369074_at	Slc38a4
1368969_at	Sost	1369023_at	Mipep	1369075_a_at	Gmeb2
1368970_at	Cdh23	1369024_at	Rabep2	1369076_at	RGD:708371
1368971_a_at	Synj2	1369025_at	Cd5	1369077_at	Asah1
1368972_at	Ntrk2	1369026_at	RGD:708401	1369078_at	Mapk1
1368973_at	Adar	1369027_at	A4galt	1369079_at	Nxph1
1368974_at	Gucy1a2	1369028_at	Six3	1369080_at	Prph2
1368975_at	Cd38	1369029_at	Plscr1	1369081_at	Neu1
1368976_at	Cd38	1369030_at	Prss1	1369082_at	Dffa
1368977_a_at	Fxc1	1369031_at	Il18bp	1369083_at	Cirbp
1369085_s_at	Snrpn /// Snurf	1369032_at	Blcap	1369084_a_at	Bok
1369086_a_at	Cacna1d	1369138_a_at	Park2	1369190_at	Cd2
1369087_at	Flt1	1369139_at	Pdc	1369191_at	Il6
1369088_at	Erbb3	1369140_at	Rcvrn	1369192_at	Cdkn1b
1369089_at	Prkcc	1369141_at	Csh1	1369193_at	Cdkn2b
1369090_at	Prkg2	1369142_at	Bglap2	1369194_a_at	RGD:2323
1369091_at	Chrnb1	1369143_at	Chrnb3	1369195_at	Fabp2
1369092_at	Sec22l2	1369144_a_at	Kcnd3	1369196_at	Ppy
1369093_at	Reln	1369145_a_at	Kcnd3	1369197_at	Apaf1
1369094_a_at	Ptprd	1369146_a_at	Ahr	1369198_at	Apaf1
1369095_at	Ppp1r9a	1369147_at	Ahr	1369199_at	Tacr1
1369096_at	Epha7	1369148_at	Tcf1	1369200_at	Nt5
1369097_s_	Gucy1b3	1369149_at	Limk1	1369201_at	Mgat3

at					
1369098_at	Vldlr	1369150_at	Pdk4	1369202_at	Mx2
1369099_at	Slc30a1	1369151_at	Dlk1	1369203_at	Wif1
1369100_at	Nalp6	1369152_at	Ppp3r1	1369204_at	Hck
1369101_at	Rxra	1369153_at	Nphs1	1369205_at	Neurod3
1369102_at	Mapk10	1369154_at	Nphs1	1369206_at	Cpb2
1369103_at	Fyn	1369155_at	Cntn4	1369207_at	Il7
1369104_at	Prkaa1	1369156_at	Frk	1369208_at	Il7
1369105_a_at	Pkib	1369157_at	Pde3b	1369209_at	RGD:621601
1369106_at	Tcea2	1369158_at	Casr	1369210_at	Scn1a
1369107_at	Sftpa1	1369159_at	Ar	1369211_at	Cacna1i
1369108_at	Trp63	1369160_a_at	Slc4a7	1369212_s_at	Epb4.1l1
1369109_at	Oprm1	1369161_at	Abcb4	1369213_at	RGD:619777
1369110_x_at	RT1-Aw2	1369162_at	Gucy2c	1369214_a_at	Mhc2ta
1369111_at	Fabp1	1369163_at	Grik4	1369215_a_at	Cpd
1369112_at	Chrm3	1369164_a_at	Trpc4	1369216_a_at	Flt4
1369113_at	Cktsf1b1	1369165_at	Trpc3	1369217_at	Nr4a3
1369114_at	Vcsa1	1369166_at	Mmp9	1369218_at	Met
1369115_at	Adrb2	1369167_at	Gfra2	1369219_at	Tgfbr3
1369116_a_at	Calca	1369168_a_at	Clock	1369220_at	Dnm1l
1369117_at	Calca	1369169_at	Slc23a1	1369221_at	Ppp2r2a
1369118_a_at	Gnrhr	1369170_at	Khsrp	1369222_at	RGD:621106
1369119_a_at	Htr7	1369171_at	Mst1	1369223_at	Gucy2d
1369120_a_at	Lhb	1369172_at	Pde1a	1369224_at	Cdh17
1369121_at	Gdf9	1369173_at	C3ar1	1369225_at	Kng1
1369122_at	Bax	1369174_at	Smad1	1369226_at	Kng1 /// MGC108747
1369123_a_at	Atp7b	1369175_a_at	Ambn	1369227_at	Chm
1369124_at	Htr2a	1369176_at	Slc36a1	1369228_at	Lifr
1369126_at	Ptgfr	1369177_at	Pi4k2a	1369229_at	Pde5a
1369127_a_at	Ptgfr	1369178_a_at	P2rx1	1369230_at	Gabrr2
1369128_at	Grik5	1369179_a_at	Pparg	1369231_at	RGD:708369
1369129_at	Rasgrp1	1369180_at	Bcl2l1	1369232_at	Kcnk10
1369130_at	Rasgrp1	1369181_at	Cybb	1369233_at	Kcnk10
1369131_at	Slc18a2	1369182_at	F3	1369234_at	Slc20a2
1369132_at	Slc18a2	1369183_at	Mapk13	1369235_at	Unc5b
1369133_a_at	Kcnc3	1369184_at	Cldn16	1369236_at	Prdm4
1369134_x_at	Kcnc3	1369185_a_at	Syt7	1369237_at	Slc6a7
1369135_at	Syt11	1369186_at	Casp1	1369238_at	Inhbe
1369136_at	Cyp2a3a	1369187_a_at	Ptger3	1369239_at	Clcn5
1369137_at	Chrne	1369188_at	Fbxo32	1369240_a_at	Avpr1b

1369243_at	RGD:621082	1369189_at	Ppyr1	1369242_at	Pax6
1369244_at	Arnt	1369296_at	Sult1a2	1369348_at	Trpm8
1369245_at	Chrm2	1369297_at	RGD:620920	1369349_a_at	Pde11a
1369246_a_at	Npy5r	1369298_at	Aqp6	1369350_at	Kcnq2
1369247_at	Sp1	1369299_at	Ptafr	1369351_at	Cntn3
1369248_a_at	Birc4	1369300_at	Ncr1	1369352_at	Hipk3
1369249_at	Ank	1369301_at	Agtrl1	1369353_at	Erbb4
1369250_at	Slc28a1	1369302_at	Gpr30	1369354_at	Csf1
1369251_a_at	Syn1	1369303_at	Crh	1369355_at	Grm5
1369252_a_at	Chrna4	1369304_at	Pts	1369356_at	Gucy2f
1369253_at	Kremen	1369305_at	Rab3il1	1369357_at	Phka1
1369254_a_at	Ptger1	1369306_at	Klrd1	1369358_a_at	Hap1
1369255_at	Il1r1	1369307_at	Ep300	1369359_at	Il9r
1369256_at	Bace	1369308_at	Stx3	1369360_at	Gucy2e
1369257_at	Grk1	1369309_a_at	Tac1	1369361_at	Kl
1369258_at	Fut9	1369310_at	Basp1	1369362_at	Tsc1
1369260_a_at	Mpp4	1369311_at	Scn2b	1369363_at	Sp4
1369261_at	Kcnj13	1369312_a_at	Csnk1a1	1369364_at	Atp1a4
1369262_at	Casp8	1369313_at	Fhl2	1369365_at	Pde3a
1369263_at	Wnt5a	1369314_at	Fgf5	1369366_at	Cntn5
1369264_at	Cyp21a1	1369315_at	Il12a	1369367_at	Trpc2
1369265_at	Senp2	1369316_s_at	Snap29	1369368_at	RGD:619787
1369266_at	Il13ra2	1369317_at	Erabp	1369369_at	Kcnb2
1369267_at	Gabrg3	1369318_at	Fhit	1369370_s_at	Trpv4 /// Trpv1
1369268_at	Atf3	1369319_at	Arl6ip5	1369371_a_at	Gabbr1
1369269_at	Galnt1	1369320_at	Mia	1369372_at	Gabbr1
1369270_at	Nr1i2	1369321_s_at	Cyct /// Pde11a	1369373_at	Fgfr3
1369271_at	Prkab2	1369322_at	Kcne2	1369374_at	Selp
1369272_at	Adora3	1369323_at	Leprot	1369375_a_at	Capn3
1369273_a_at	Npr3	1369324_at	Sval2	1369376_a_at	Lnpep
1369274_a_at	Cdkl3	1369325_at	Lyst	1369377_at	Hcrtr2
1369275_s_at	Cyp2a1 /// Cyp2a2	1369326_at	Akap6	1369378_at	Slc23a2
1369276_at	Smad5	1369327_at	Pdzk3	1369379_at	Epha3
1369277_at	Mecp2	1369328_at	Acacb	1369380_at	Kif2c
1369278_at	Gna12	1369329_at	Notch3	1369381_a_at	Slc15a1
1369279_at	Dhrs9	1369330_at	Unc13a	1369382_at	Mertk
1369280_at	Kcnk9	1369331_a_at	Unc13b	1369383_a_at	Gabre
1369281_at	Tnfsf11	1369332_a_at	RIMS1	1369384_at	Gria4
1369282_at	Tnfsf11	1369333_a_at	Rims2	1369385_at	Afap
1369283_at	Tub	1369334_at	Kcnma1	1369386_at	Slc26a2
1369284_at	RGD:620726	1369335_at	RGD:620450	1369387_at	Vav1
1369285_at	Pggt1b	1369336_at	Hr	1369388_at	Musk

1369286_at	Proc	1369337_at	RGD:708450	1369389_at	RGD:727958
1369287_at	Syt9	1369338_at	Robo1	1369390_a_at	Dpp6
1369288_at	Pitx1	1369339_at	Dcc	1369391_at	Grm8
1369289_at	Hnf4a	1369340_at	RGD:708439	1369392_at	Akap4
1369290_at	Ccr5	1369341_a_at	Acvrinp1	1369393_at	Map3k8
1369291_at	Agtr1a	1369342_at	Atp7a	1369394_at	Unc5a
1369292_at	Hsd17b1	1369343_at	Grip1	1369395_at	Tpc1808
1369293_at	Rtn4r	1369344_at	Wdr7	1369396_at	Mgat5
1369294_at	Bst1	1369345_at	Inpp4b	1369397_at	Tas1r3
1369295_at	Pgc	1369346_at	Slit2	1369398_at	Naaladl1
1369400_a_at	Pfkfb2	1369347_s_at	Prom2	1369399_at	Ms4a2
1369401_at	Slc21a13	1369453_at	Epn1	1369505_at	Cds2
1369402_at	Adnp	1369454_at	Vdr	1369506_at	Gcm1
1369403_at	Adrbk2	1369455_at	Abcg5	1369507_at	V1rb6
1369404_a_at	Nrxn1	1369456_at	Htr2b	1369508_at	Kcnj15
1369405_a_at	Chrnb4	1369457_a_at	RGD:620204	1369509_a_at	A1bg
1369406_at	Asah2	1369458_at	Gab2	1369510_at	Gapds
1369407_at	Tnfrsf11b	1369459_at	Pip5k2b	1369511_at	Ednra
1369408_at	RGD:708519	1369460_at	Slc7a2	1369512_at	Chst3
1369409_at	Nab1	1369461_at	Pthr2	1369513_at	Ccl28
1369411_at	Gfi1	1369462_at	Gad2	1369514_at	Insrr
1369412_a_at	Slc19a1	1369463_at	Htr5a	1369515_s_at	Insrr
1369413_at	Uncx4.1	1369464_at	Zp1	1369516_at	Pdx1
1369414_at	Stxbp3	1369465_at	Hsd3b	1369517_at	Pscd1
1369415_at	Bhlhb2	1369466_at	Chrna9	1369518_at	Pik3r3
1369416_at	Hcn3	1369467_a_at	Pfkfb1	1369519_at	Edn1
1369417_a_at	Opcml	1369468_at	Fzd4	1369520_a_at	Bcat1
1369418_at	Kcnj9	1369469_s_at	Spdy1	1369521_at	Ube2d2
1369419_at	Efha1	1369470_at	RGD:708510	1369522_a_at	Cd244
1369420_at	Neu3	1369471_at	Fnbp1	1369523_at	Ccbp2
1369421_at	Top1	1369472_a_at	Atf2	1369524_at	Zic1
1369422_at	Fap	1369473_at	Pgm1	1369525_at	Gata3
1369423_at	Syn3	1369474_a_at	P2rx2	1369526_at	Acadsb
1369424_at	Cyp2a2	1369475_x_at	P2rx2	1369527_at	Cx3cr1
1369425_at	Cdh13	1369476_at	Efnb1	1369528_at	Madh3
1369426_at	RGD:620696	1369477_at	Pnma1	1369529_at	Csf3
1369427_at	Mpeg1	1369478_at	Nr0b1	1369530_at	Isl2
1369428_a_at	Htr3a	1369479_at	Doc2b	1369531_at	RGD:621064
1369429_at	Pdha2	1369480_at	Slc16a8	1369532_at	Gpr73l1
1369430_at	Bcdo	1369481_at	Tnfsf4	1369533_a_at	Htr4
1369431_at	Galnt7	1369482_a_at	Syn2	1369534_at	Il11
1369432_at	Chrnb2	1369483_at	Cd4	1369535_at	Tpra40
1369433_at	RGD:620464	1369484_at	Wisp2	1369536_at	Edn2
1369434_at	Dnttip1	1369485_at	Cach	1369537_at	Gpr24
1369435_at	Ttpa	1369486_at	RGD:621579	1369538_at	Cdk5r
1369436_at	Chrna10	1369487_a_at	Kcnj4	1369539_at	Siat6

1369437_at	Slco4a1	1369488_at	Fut4	1369540_at	Efcbp1
1369438_at	N5	1369489_at	Aif1	1369541_at	Tmod2
1369439_at	Agtr1	1369490_at	Glp2r	1369542_at	Gpr73
1369440_at	Abcg8	1369491_at	Dao1	1369543_s_at	RGD:621729
1369441_at	Capn5	1369492_at	Aadac	1369544_a_at	Hoxa1
1369442_at	RGD:708564	1369493_at	Prlr	1369545_at	Egr3
1369443_at	Angptl2	1369494_a_at	Ghrhr	1369546_at	Bbox1
1369444_at	Cyp19a1	1369495_at	Crhr2	1369547_at	Serpinb7
1369445_at	Mre11a	1369496_at	Ptpn12	1369548_at	Gtf2a1
1369446_at	Cry2	1369497_at	LOC24906	1369549_at	Nkrp2
1369447_at	Slc28a3	1369498_at	Mc5r	1369550_at	Gdf8
1369448_at	B3gat1	1369499_at	Tyms	1369551_at	Sreb3
1369449_at	Plin	1369500_at	Kcnk1	1369552_at	Samsn1
1369450_at	RGD:620985	1369501_at	Zfp260	1369553_at	Hsd17b3
1369451_a_at	Kcnj1	1369502_a_at	Amy1 /// Amy2	1369554_at	Syngr2
1369452_a_at	Picalm	1369503_at	Amy2	1369555_at	Ccr4
1369557_at	Casp7	1369504_at	Tgfbr1	1369556_at	Ltb4r2
1369558_at	Inhbc	1369609_at	Cldn11	1369666_at	Gpd2
1369559_a_at	Cd47	1369610_at	Lin7c	1369667_at	Vps52
1369560_at	Gpd1	1369611_at	Bcl2l2	1369668_x_at	Vps52
1369561_at	Cysltr1	1369612_at	RGD:708570	1369669_at	Nln
1369562_at	Hpcal1	1369613_at	RGD:620425	1369670_at	Mox2
1369563_at	Vax1	1369614_at	Rap2b	1369671_at	Otc
1369564_at	Rem2	1369615_at	Rap2a	1369672_at	Alox5ap
1369565_at	Il12b	1369616_at	Fgf22	1369673_at	P2rx5
1369566_at	Tas2r1	1369617_at	RGD:621096	1369674_at	P2rx5
1369567_at	Taar1	1369618_at	Il13	1369675_at	Itpr2
1369568_at	Stx6	1369619_at	Ucn2	1369676_at	Itpr2
1369569_at	Olr226	1369620_at	Hint1	1369678_a_at	Nfia
1369570_at	Sult2a1	1369621_s_at	Fkbp1a /// Fkbp2	1369679_a_at	Nfia
1369571_at	Golph3	1369622_at	Prok2	1369680_at	Slc2a13
1369572_at	Mcpt1	1369623_at	Morp1	1369681_at	Isl1
1369573_at	Mcpt4	1369624_at	Prlh	1369682_at	Tcf2
1369574_at	Tas2r13	1369625_at	Aqp1	1369683_at	Bid
1369575_at	Tas2r5	1369626_at	Ide	1369684_at	RGD:620914
1369576_at	Tas2r105	1369627_at	Sv2b	1369685_at	Twist2
1369577_at	Socs2	1369628_at	Sv2b	1369686_at	Dcamkl1
1369578_at	Tas2r7	1369629_at	Adk	1369687_at	Kcnab3
1369579_at	Stc2	1369630_at	Adk	1369688_s_at	Ptk2b
1369580_at	Tas2r16	1369632_a_at	Abcc8	1369689_at	Nsf
1369581_at	Pemt	1369633_at	Cxcl12	1369690_at	Nsf
1369582_at	Vax2	1369635_at	Sord	1369691_at	Scn3a
1369583_at	RGD:621611	1369636_at	Sord	1369692_at	Tnr
1369584_at	Socs3	1369637_at	Kif3c	1369693_a_at	Slc1a2
1369585_at	Tore	1369638_at	Eef2k	1369694_at	Slc1a2
1369586_at	Mcpt8	1369639_at	Gja1	1369695_at	Wt1
1369587_at	Ereg	1369640_at	Gja1	1369696_at	RragB

1369588_a_at	Atpi /// LOC497807	1369641_at	Pafah1b2	1369697_at	Il8rb
1369589_x_at	Amelx	1369642_at	Pafah1b2	1369698_at	Abcc3
1369590_a_at	Ddit3	1369643_a_at	Lphn2	1369699_at	Glp1r
1369591_at	Csn10	1369644_at	Lphn2	1369700_at	Clcn7
1369592_at	Wbp2	1369645_at	Oprl	1369701_at	Lipc
1369593_at	Cgi94	1369646_at	Oprl	1369702_at	Ensa
1369594_at	Efna5	1369647_at	Calcrl	1369703_at	Epas1
1369595_at	Fgf23	1369649_at	Cacna2d1	1369704_at	RGD:621651
1369596_at	Il2	1369650_at	Pak2	1369705_at	RGD:621651
1369597_at	Vapb	1369651_at	Thy1	1369706_at	Cacng1
1369598_at	Gdnf	1369653_at	Tgfbr2	1369707_at	Myo9a
1369599_at	Galp	1369654_at	Prkaa2	1369708_a_at	Creb1
1369600_at	Fgf11	1369655_at	Pik3c3	1369709_at	Sca1
1369601_at	Nyw1	1369656_at	Pcyt1a	1369710_a_at	Snap91
1369602_at	Fgf17	1369657_at	Cpa1	1369711_at	Agtr2
1369603_at	Kcnip1	1369658_at	Cebpa	1369712_at	Stk3
1369604_at	Fgf10	1369659_at	Cga	1369713_at	Cckbr
1369605_at	Hes2	1369661_at	Dnm2	1369714_at	Dnajc14
1369606_at	Fgf20	1369662_at	RGD:3632	1369715_at	Slc6a11
1369607_at	Fgf6	1369663_at	Ephx2	1369716_s_at	Lgals5 /// Lgals9
1369608_at	Fgf16	1369664_at	Avpr1a	1369717_at	Nmu
1369719_at	Phex	1369665_a_at	Il18	1369718_at	Ssr3
1369720_at	Myo1b	1369771_at	Irs1	1369823_at	Adam7
1369721_at	Strn	1369772_at	Slc6a9	1369824_at	Nrp2
1369722_a_at	Xylt2	1369773_at	Bmp3	1369825_at	Mmp2
1369723_at	Xylt2	1369774_at	Cnga4	1369826_at	Atxn3
1369724_at	F13a	1369775_at	Nucks	1369827_at	Clstn3
1369725_at	Centa2	1369776_a_at	Shank2	1369828_at	Csf2rb1
1369726_at	Tapbp	1369777_a_at	Shank2	1369829_at	RGD:621829
1369727_at	Apoa2	1369778_at	Dio2	1369830_at	Prkch
1369728_at	Hist1h4m_predicted	1369779_at	Myo1c	1369831_at	Bcan
1369729_at	Arl5	1369780_at	Rasgrf2	1369832_at	Adam3
1369730_a_at	Gfra4	1369781_at	Grm7	1369833_at	Adam2
1369731_at	Cnksr2	1369782_a_at	Kcnj11	1369834_at	Foxa1
1369732_a_at	Siat4b	1369783_a_at	Nrg1	1369835_at	Omp
1369733_at	Catnb	1369784_at	Tpo	1369836_at	Ifit1
1369734_at	Acox3	1369785_at	Ppat	1369837_at	Gulo
1369735_at	Gas6	1369786_at	Chrm5	1369838_at	Hif3a
1369736_at	Emp1	1369787_at	Cckar	1369839_at	Amph1
1369737_at	Crem	1369788_s_at	Jun	1369840_at	RGD:620976
1369738_s_at	Crem	1369789_at	Glra3	1369841_at	Hspa2

1369739_at	Lepr	1369790_at	Tat	1369842_at	Accn5
1369740_at	Kcnj3	1369791_at	RGD:708381	1369843_at	Chrna1
1369741_at	Kcnj3	1369792_at	Gpr6	1369844_at	Gabra3
1369742_at	Kcnj3	1369793_a_at	Mcam	1369845_at	Chrna6
1369743_a_at	P2rx4	1369794_a_at	Pfkfb3	1369846_at	Ivl
1369744_at	Tg	1369795_at	Kcnj12	1369847_at	Kcnab1
1369745_at	Grin2b	1369796_at	Gja9	1369848_at	Kcns2
1369746_a_at	Slc21a10	1369797_at	Adra1a	1369849_at	Cnr2
1369747_at	Nat2	1369798_at	Atp1b2	1369850_at	Ugt2a1
1369748_at	Serpini2	1369799_at	Abat	1369851_at	Mef2d
1369749_a_at	Svs2	1369800_at	F2rl3	1369852_at	F10
1369750_at	Tshb	1369801_at	Sell	1369853_at	Neurog3
1369751_at	Trhr	1369802_at	Kcna3	1369854_a_at	Ceacam1
1369752_a_at	Camk4	1369803_at	Ptf1a	1369855_at	Hrh1
1369753_at	Camk4	1369804_a_at	Csnk1e	1369856_at	Drd5
1369754_a_at	Cast	1369805_at	Sc65	1369857_a_at	Slc14a1
1369755_at	B3gat2	1369806_at	Adrb1	1369858_at	Grpr
1369756_a_at	Slc4a4	1369807_at	Bdkrb1	1369860_a_at	Htr2c
1369757_at	Itpkb	1369808_at	Ccr3	1369861_at	Gabra6
1369758_at	Gpam	1369809_at	Htr1a	1369862_at	Pim1
1369759_at	Slc5a1	1369810_at	Dmd	1369863_at	Adh4
1369760_a_at	Esr2	1369811_at	Cplx1	1369864_a_at	Sds
1369761_at	Pou1f1	1369812_at	P2ry4	1369865_at	Cd28
1369762_at	Pou1f1	1369813_at	Dnajc5	1369866_at	RGD:708486
1369763_at	Gprk2l	1369814_at	Ccl20	1369867_at	Siat8a
1369764_at	C4bpa	1369815_at	Ccl3	1369868_at	Iag2
1369765_at	Ascl1	1369816_at	Rab3a	1369869_at	Capza3
1369766_at	Ptger2	1369817_at	Hand2	1369870_at	Admr
1369767_a_at	Kcnmb1	1369818_at	Gabrb2	1369871_at	Areg
1369768_at	H1f4	1369819_at	Bsn	1369872_a_at	Fcer2a
1369769_at	Kcne1	1369820_at	Mcf2l	1369873_at	Avpr2
1369770_at	Sstr1	1369821_a_at	Cngb1	1369874_at	Gpr1
1369876_at	RGD:708344	1369822_at	Kit	1369875_at	Il8ra
1369877_at	Cd8a	1369932_a_at	Raf1	1369996_at	RGD:708567
1369878_at	Olr1654_predicted	1369933_at	Vdac2	1369997_at	Dvl1
1369879_a_at	Tegt	1369934_at	Ppib	1369998_at	Arf6
1369880_at	Msx2	1369935_at	Ccnd3	1369999_a_at	Nnat
1369881_at	Gja6	1369936_at	Calm1	1370000_at	Nucb2
1369882_at	Pdyn	1369937_at	Calm1	1370001_at	Rab8a
1369883_at	Pth	1369939_at	Cycs	1370002_at	Arhgef1
1369884_at	Fgf7	1369940_at	Taldo1	1370003_at	Eef2
1369885_at	Porf1	1369941_at	Dap	1370004_at	H2afy

1369886_a_at	Cabp1	1369943_at	Tgm2	1370005_at	Cyb5m
1369888_at	Gcg	1369944_at	Mlp	1370007_at	Erp70
1369889_at	Ifnb1	1369945_at	Grid1	1370009_at	Apoc3
1369891_at	Jdp1	1369946_at	RGD:708553	1370010_at	Lamp2
1369892_at	RGD:621437	1369947_at	Ctsk	1370011_at	Ak1
1369893_at	Hist1h2aa	1369948_at	Ngfrap1	1370012_at	Ptgis
1369895_s_at	Podxl	1369949_at	Lu	1370013_at	Cnga1
1369896_s_at	Rbm16	1369950_at	Cdk4	1370014_at	Stx4a
1369897_s_at	Gnas /// RGD:621483	1369951_at	Ctrb	1370015_at	Git1
1369898_a_at	Gip	1369952_at	Pabpc1	1370016_at	Nell2
1369899_s_at	Rabggta	1369953_a_at	Cd24	1370017_at	Emd
1369900_at	RGD:619831	1369954_at	Idh1	1370018_at	Hspb2
1369901_at	Tubb3	1369955_at	Col5a1	1370019_at	Sult1a1
1369902_at	Bmf	1369956_at	Ifngr	1370020_at	RGD:621430
1369903_at	Gabrb3	1369957_at	Rgs5	1370021_at	Rho
1369904_at	Gabrb1	1369958_at	Rhob	1370022_at	Tnp2
1369905_at	Gabra4	1369959_at	Zfp36l1	1370023_at	Gja4
1369906_s_at	Mcfd2	1369962_at	Atic	1370024_at	Fabp7
1369907_at	Alpi	1369963_at	RGD:620333	1370025_at	Pip5k2c
1369908_at	Crhbp	1369964_at	Coro1a	1370026_at	Cryab
1369909_s_at	RGD:619998	1369966_a_at	Rps24	1370027_a_at	Mug1 /// LOC297568
1369910_at	Gpr10	1369967_at	Cs	1370028_at	Ace
1369911_at	Blr1	1369968_at	Ptn	1370029_at	Ctbp1
1369912_at	Crk	1369969_at	Adprt	1370030_at	Gclm
1369913_at	Opn1mw	1369971_a_at	Hnrpd	1370031_at	Gosr2
1369914_at	Hrh2	1369972_at	Serpinb5	1370032_at	Slc9a3r1
1369915_at	Mki67ip	1369974_at	Vamp2	1370034_at	Cdc25b
1369916_at	LOC308586	1369975_at	Secp43	1370035_at	Kras2
1369917_at	RGD:708524	1369976_at	Dnclc1	1370036_at	Suox
1369918_at	Klrh1	1369977_at	Uchl1	1370037_at	Fbn2
1369919_at	Tef	1369978_at	Prpsap2	1370038_at	Rfrp
1369920_at	Hist1h1t	1369979_at	Scap2	1370040_at	Ogg1
1369921_at	Gstm4	1369981_at	Igbp1	1370041_at	Stmn2
1369922_at	RGD:708461	1369982_at	Ap2a2	1370042_at	Stmn2
1369923_at	Og9x	1369985_at	Crybb1	1370043_at	Alcam
1369924_at	Sncb	1369987_at	Nkx2-5	1370044_at	Faim
1369925_at	Cst11	1369988_at	Epor	1370045_at	Polg
1369926_at	Gpx3	1369989_at	Pnpo	1370046_at	Polg
1369927_at	Mor1	1369990_at	RGD:735045	1370047_at	Enpp1
1369928_at	Acta1	1369992_at	Psmd1	1370048_at	Edg2
1369930_at	Psma6	1369993_at	Camk2g	1370049_at	Smpd2
1369931_at	Pkm2	1369994_at	Crcp	1370050_at	Atp2b1
1370052_at	Pdpk1	1369995_at	Faf1	1370051_at	Tgm1

1370053_at	Dlgap1	1370117_at	Fgf8	1370173_at	Sod2
1370054_at	Cdkn2c	1370118_at	Ccl17	1370174_at	Myd116
1370055_at	Rab3d	1370119_at	Lst1	1370175_a_at	Znf384
1370057_at	Csrp1	1370120_at	Fstl3	1370176_at	Als2cr3
1370058_at	RGD:621458	1370121_at	Add1	1370177_at	PVR
1370059_at	RGD:621458	1370122_at	LOC363410	1370178_at	Cacnb2
1370060_at	RGD:708476	1370123_a_at	Cttn	1370179_at	Dncl2a
1370062_at	RGD:620215	1370124_at	Mt3	1370180_at	Nudt4
1370063_at	Nr2f2	1370126_at	Prss2	1370182_at	Ptprn2
1370064_at	Psen2	1370127_at	Pold1	1370183_at	Dyrk1a
1370065_at	Hpx	1370128_at	Hand1	1370184_at	Cfl1
1370067_at	Me1	1370129_at	Mgea5	1370185_at	Cntnap1
1370068_at	Pla2g5	1370130_at	Rhoa	1370186_at	Psmb9
1370069_at	RGD:620811	1370131_at	Cav	1370187_at	Pccb
1370070_at	Synj1	1370132_at	Fkbp1b	1370188_at	Sfrs10
1370071_at	Ada	1370133_at	Rgs19	1370189_at	Sfrs10
1370072_at	Mme	1370134_at	Slc33a1	1370190_at	RGD:621095
1370073_at	Dnajc3	1370135_at	RGD:620348	1370191_at	Oazin
1370074_at	Baiap2	1370136_at	Lbr	1370192_at	Stx12
1370075_at	Dhfr	1370137_at	Agps	1370193_at	Ptp4a1
1370076_at	Kcnj16	1370138_at	Lef1	1370196_at	Pias3
1370077_at	Ins2	1370139_a_at	Trpc6	1370197_a_at	Prkcz
1370079_at	Rhced	1370140_a_at	Pax4	1370198_at	Trdn
1370081_a_at	Vegfa	1370141_at	Mcl1	1370199_at	Nucb1
1370082_at	Tgfb1	1370142_at	Pem	1370200_at	Glud1
1370083_at	Ccr1	1370144_at	Gtpbp4 /// LOC364763	1370201_at	Calb1
1370087_at	Rab2	1370145_at	Znf354c	1370202_at	Hrasls3
1370088_at	Spa17	1370146_at	Glrb	1370203_at	Frag1
1370089_at	Ppargc1a	1370148_at	Hp	1370204_at	Frag1
1370091_at	Gnaq	1370149_at	Asgr1	1370205_at	Slco1c1
1370092_at	Mas1	1370150_a_at	Thrsp	1370208_at	Nr1h2
1370093_at	Htr1f	1370151_at	Cps1	1370209_at	Bteb1
1370094_at	Acrv1	1370152_at	Gp5	1370210_at	RGD:708473
1370095_at	Ltb4r	1370153_at	Gdf15	1370211_at	Nrgn
1370096_at	Prf1	1370154_at	Lyz	1370212_at	Homer3
1370097_a_at	Cxcr4	1370155_at	Col1a2	1370213_at	Nsep1
1370099_at	Fbxl20	1370156_at	Prnp	1370214_at	Pvalb
1370100_at	Pik3r2	1370158_at	Myh10	1370215_at	C1qb
1370101_at	Crx	1370159_at	Smarcd2	1370216_at	Ddr1
1370102_at	Kcnn1	1370160_at	Xpnpep1	1370218_at	Ldhb
1370103_at	Hcn1	1370161_at	Ssg1	1370219_at	Cyba
1370105_at	Lfng	1370162_at	Ppp4r1	1370220_at	Scpep1
1370106_at	Fgf18	1370163_at	Odc1	1370221_at	Wisp1
1370107_at	Ctrl	1370164_at	Hadha	1370222_at	Pitx3
1370108_a_at	Lin7a	1370165_at	Smpx	1370223_at	Arfrp1
1370109_s_at	Eef1a1	1370166_at	Sdc2	1370224_at	Stat3

1370110_at	Kcnk4	1370167_at	Sdc2	1370225_at	Cited4
1370111_at	Kcnn2	1370168_at	Ywhaq	1370226_at	Cstb
1370113_at	Birc3	1370169_at	RGD:619726	1370227_at	RGD:620115
1370114_a_at	Pik3r1	1370170_at	Hnrpu	1370228_at	Srprb_predicted
1370115_at	Slc7a10	1370171_at	Hnrpu	1370229_at	Ndr4
1370231_at	Gtf3c1	1370172_at	Sod2	1370230_at	Atp5j
1370232_at	Ivd	1370288_a_at	Klks3	1370345_at	Ccnb1
1370234_at	Fn1	1370290_at	Pdlim3	1370346_at	Pdlim7
1370235_at	Dbi	1370291_at	Crygc	1370347_at	Ninj1
1370236_at	Ppt	1370292_a_at	Gata4	1370348_at	Atpi
1370237_at	Hadhsc	1370293_at	Cdc20	1370349_a_at	Atpi
1370238_at	Hba-a1	1370294_a_at	Nme1	1370350_x_at	Tdrd7
1370239_at	Hba-a1	1370295_at	Scp2	1370351_at	RGD:621508
1370240_x_at	Cyp2c7	1370296_at	Plk1	1370352_at	Timm22
1370241_at	Rps23	1370297_at	RGD:628654	1370353_at	Parg
1370242_at	Ptma	1370299_at	Preb	1370354_at	Scd1
1370243_a_at	Ctsl	1370300_at	Mmp2	1370355_at	Rbm10
1370244_at	Ctsl	1370301_at	RGD:620882	1370357_at	Tpcn1
1370245_at	Calm2	1370302_at	Slc35a4	1370358_at	Amy1
1370246_at	Pmp22	1370305_at	Pex14	1370359_at	RGD:621352
1370247_a_at	Fxyd6	1370306_at	Agrn	1370360_at	Cgref1
1370248_at	Bzrp	1370307_at	Rs21c6	1370361_at	Ptprn
1370250_at	Avpi1	1370308_at	Hnrpab	1370362_at	Ces3
1370252_at	Rpl22	1370309_a_at	Hmgcs2	1370363_at	Arfgap1
1370253_at	Clic5	1370310_at	Eif2b1	1370364_at	Gss
1370254_at	Sftpc	1370311_at	Spon1	1370365_at	Timm10
1370255_at	Fzd1	1370312_at	Bach	1370366_at	Slc1a1
1370256_at	Pla2g1b	1370313_at	Slc20a1	1370367_at	Cabin1
1370257_at	Bzw2	1370314_at	Stmn4	1370368_at	Gzmm
1370258_at	Pthr1	1370315_a_at	Hspbp1	1370369_at	Hyal2
1370259_a_at	Add3	1370316_at	RGD:708500	1370370_at	Ceacam1 /// Ceacam10
1370260_at	Rps6ka1	1370317_at	Pik4ca	1370371_a_at	Rasd2
1370261_at	Mtdh	1370318_at	Ppif	1370372_at	Rasd2
1370262_at	Dll3	1370319_at	Mawbp	1370373_at	RGD:708552
1370263_at	RGD:620546	1370320_at	Pdcd8	1370374_at	Gls2
1370264_at	Arrb2	1370321_at	Stk16	1370375_at	Csda
1370266_at	Gsk3b	1370322_at	Thop1	1370376_a_at	Cyp2d9 /// Cyp2d10
1370267_at	Kcna5	1370323_at	Atp7b	1370377_at	Atp5a1
1370268_at	Cyp1a1	1370324_at	MGC93180	1370378_at	Prss8
1370269_at	Tcam1	1370325_at	Pctk1	1370379_at	Nr2f6
1370270_at	Grpca /// RGD:735181	1370326_at	Commd5	1370380_s_at	Pnrc1

1370271_a_at	Grpca	1370327_at	Dkk3	1370381_at	RT1-Db1
1370273_at	Ubb	1370328_at	Cyp2d22	1370382_at	RT1-Db1
1370274_at	Atp5b	1370329_at	Sipa1l1	1370383_s_at	Prlr
1370275_at	Atp5o	1370330_at	Il11ra1	1370384_a_at	Pla2g6
1370276_at	Slc25a3	1370331_at	Unc13h4	1370385_at	Ruvbl1
1370277_at	Atp5d	1370332_at	Igf1	1370386_at	Cyp3a13
1370278_at	Cryaa	1370333_a_at	Plekhb1	1370387_at	Slc9a5
1370279_at	Hprt	1370334_at	Dab2ip	1370388_at	Gpm6b
1370280_at	Fabp5	1370335_at	Okl38	1370389_at	RGD:708560
1370281_at	Csrp2	1370336_at	Ctcf	1370390_at	Crabp2
1370282_at	Hspa5	1370337_at	Hrh1	1370391_at	Trpm4
1370283_at	Atp5e	1370339_at	RGD:708368	1370392_at	Ccdc5
1370284_at	RGD:619812	1370340_x_at	Eno2	1370393_at	IgG-2a
1370285_at	Slc38a2	1370341_at	Kcnk2	1370394_at	Hdh
1370286_at	Tpm1	1370342_at	Xab2	1370395_at	Atpi
1370287_a_at	Tpm1	1370343_at	Hspa4	1370396_x_at	Cyp4a14
1370398_at	Cyp4b1	1370344_at	Ccnb1	1370397_at	RGD:621010
1370400_at	Ly6b	1370452_at	Tex101	1370506_at	Dlgap4
1370401_at	Egfl7	1370453_at	Homer1	1370507_at	Cacna1g
1370402_at	Prlpk	1370454_at	Olfm3	1370508_a_at	Pdp2
1370403_at	RGD:708514	1370455_a_at	Fat3	1370509_at	Arntl
1370404_at	Mcpt1	1370456_at	RGD:708447	1370510_a_at	Fgb
1370405_at	Daf1	1370457_at	Hdgfrp3	1370511_at	Cbl27
1370406_a_at	Pcyox1	1370458_at	RGD:631378	1370512_at	Tpm1
1370407_at	Nid67	1370459_at	Usp15	1370513_at	Syt7
1370408_at	Slc38a1	1370460_at	Hmmr	1370514_a_at	Syt7
1370409_at	Igsf1	1370461_at	Hmmr	1370515_x_at	Slc15a3
1370410_at	Trpc1	1370462_at	RT1-CE12	1370516_at	Nptx1
1370411_at	Tnnt1	1370463_x_at	Abcb1a	1370517_at	Stxbp1
1370412_at	RGD:628790	1370464_at	Abcb1a	1370518_a_at	Stxbp1
1370413_at	Rab38	1370465_at	Lhx5	1370519_at	RGD:727791
1370414_at	Rassf5	1370466_at	Slc13a1	1370520_at	Vps33b
1370415_at	Mxd3	1370467_at	Slc13a1	1370521_at	Gcgr
1370416_at	Gnrh1	1370468_at	RGD:708516	1370522_at	Ube2d2
1370417_at	RGD:708576	1370469_at	RGD:727857	1370523_a_at	
1370418_s_at	Sh3kbp1	1370470_at	Prlpb	1370524_at	Ube2d2
1370419_a_at	Srd5a1	1370471_at	Kcnma1	1370525_at	Itgae
1370420_at	RGD:620480	1370472_a_at	Ptpn23	1370526_at	Csnk1d
1370421_a_at	Ripk3	1370473_a_at	Thrb	1370527_a_at	Csnk1d
1370423_at	Prpg2	1370474_at	RGD:628627	1370528_at	Pld1
1370424_at	RGD:708501	1370475_at	Stambp	1370529_a_at	Pld1
1370425_at	Atp2a2	1370476_at	Ocm	1370530_a_at	Pld1
1370426_a_at	Pdgfa	1370477_at	Myr8	1370531_a_at	Pld1

1370427_at	RT1-Aw2 /// RT1-A2 /// RT1-A3	1370478_at	RGD:708508	1370532_at	Dlgap3
1370428_x_at	RT1-Aw2	1370479_x_at	Prlpl	1370533_at	Acvr1c
1370429_at	Lmo3	1370480_at	Scnn1g	1370534_at	Myt1l
1370430_at	Syn2	1370481_at	Scnn1b	1370535_at	Hrmt1l3
1370431_at	Pou3f1	1370482_at	Cd244	1370536_at	G22p1
1370432_at	Hsd3b7	1370483_at	Olr1466_predicted /// Olr1467_predicted /// Olr1482_predicted /// Olr1481 /// Olr1470 /// Olr1469 /// Olr1468	1370537_at	Lama3
1370433_at	Mobp	1370484_at	Bcl2l1	1370538_at	Rab8b
1370434_a_at	Nudt6	1370485_a_at	RGD:708532	1370539_at	Nr1d2
1370435_a_at	RGD:708383	1370486_a_at	Kalrn	1370540_at	Nr1d2
1370436_at	Nupl1	1370487_a_at	Ptprd	1370541_at	Elf1
1370437_at	Capon	1370488_a_at	Plcb4	1370542_a_at	Ogt
1370438_at	Kcnc2	1370489_a_at	Pcdh3	1370543_at	Eml2
1370439_a_at	Slc15a4	1370490_at	Hdc	1370544_at	Kcna1
1370440_at	RGD:731250	1370491_a_at	Flt1	1370545_at	Unc13c
1370441_at	RGD:708373	1370492_a_at	Lilrb3_predicted	1370546_at	Pzp
1370442_at	Dnase2	1370493_a_at	Slc14a2	1370547_at	Slc16a10
1370443_at	Cacna1b	1370494_at	Cyp2c13	1370548_at	Vps45
1370444_at	RGD:621261	1370495_s_at	Cyp2d13	1370549_at	Lsamp
1370445_at	Nme7	1370496_at	RGD:727886	1370550_at	Sema6c
1370446_at	Phlpb	1370497_at	Abo	1370551_a_at	Ppm1f
1370447_at	Gpc2	1370498_at	Klrb1a	1370552_at	Epim
1370448_at	Gpr105	1370499_at	Mobp /// LOC360443	1370553_at	LOC498560
1370449_at	RGD:621546	1370500_a_at	Ube2g1	1370554_at	RGD:628710
1370450_at	Cacna1c	1370502_at	Epb4.1l3	1370555_at	Vamp1
1370451_a_at	Cacna1c	1370503_s_at	Pmp22	1370556_at	Kcnc2
1370558_a_at		1370504_a_at	Adprh	1370557_a_at	Kcnc2
1370559_at	Hit39	1370612_at	Ugt1a1 /// Ugt1a6 /// RGD:620950 /// Ugt1a8 /// Ugt1a2 /// Ugt1a4 /// Ugt1a11	1370666_at	Slc9a4
1370560_at	RGD:727913	1370613_s_at	Stk39	1370667_at	Cnksr2
1370561_at	Calcb	1370614_s_at	RGD:708417	1370668_a_at	Pde10a

1370562_at	RGD:708361	1370615_at	Nrg1	1370669_a_at	Zfp37
1370563_at	Dbh	1370616_at	Grb2	1370670_at	Gucy2g
1370564_at	RGD:727834	1370617_at	Optn	1370671_at	RGD:727949
1370565_at	RGD:735050	1370618_at	Ccl22	1370672_a_at	RGD:708385
1370566_at	Adra2b	1370619_at	Ccl22	1370673_at	RGD:727942
1370567_at	Adra2c	1370620_at	Cd3z	1370674_at	Trpv1
1370568_at	Pde4d	1370621_at	Mc4r	1370675_at	Cfh
1370569_at	Nrp1	1370622_at	Fgl2	1370676_at	Rin1
1370570_at	Slco3a1	1370623_at	F2rl2	1370677_at	Maoa
1370571_at	Gpr149	1370624_at	Faim2	1370678_s_at	Pld1
1370572_at	Sardh	1370625_at	Tspy	1370679_at	RGD:621479
1370573_at	Ptpns1	1370626_at	Rhov	1370680_at	Pacs1
1370574_a_at	Oazin	1370627_at	Gzmb	1370682_at	Kcnk15
1370575_a_at	Dncli1	1370628_at	Art2b	1370684_s_at	Trpv1
1370576_at	Zfp455	1370629_at	Fgfr2	1370685_at	Sec6l1
1370577_at	Lin10	1370630_a_at	Reg3g	1370686_at	Ntrk2
1370578_at	RGD:708505	1370631_at	Obp2b	1370687_a_at	Gclc
1370579_at	RGD:620377 /// RGD:619934 /// LOC293989	1370632_at	Gm1960	1370688_at	Pam
1370580_a_at	Fgf14	1370633_at	Gm1960	1370689_at	Hspa9a_predicted
1370581_at	Amelx	1370634_x_at	RGD:708352	1370690_at	Thra
1370582_a_at	Abcb1 /// Abcb1a	1370635_at	Ppbp	1370691_a_at	Il1rl1
1370583_s_at	Adora1	1370636_at	Cacna1d	1370692_at	Cnp1
1370584_a_at	Prkcb1	1370637_at	Ank3	1370693_a_at	Trib3
1370585_a_at	RGD:2246	1370638_at	LOC313678	1370694_at	Trib3
1370587_at	Slc8a1	1370639_at	Cacna1d	1370695_s_at	RGD:727794
1370588_a_at	Znf14	1370640_a_at	Cacna1i	1370696_at	Nexn
1370589_at	Gpsm1	1370641_s_at	Pdgfrb	1370697_a_at	RGD:708541
1370590_at	Recc1	1370642_s_at	Kalrn	1370698_at	Egfr /// Pepd
1370591_at	Keg1	1370643_a_at	Trpv5	1370699_a_at	Pcyt1b
1370592_at	Cyp3a11	1370644_at	RGD:708409	1370700_at	Gabrq
1370593_at	Igsf1	1370645_at	Rmt1	1370701_at	Gabrr3
1370594_at	Kcnip4	1370646_at	RGD:708358	1370702_at	Mrgprf
1370595_a_at	RGD:708559	1370647_at	RGD:708559	1370703_at	Kcnj6
1370596_a_at	RGD:708499	1370648_a_at	Bdkrb2	1370704_at	RGD:628674
1370597_at	Kcnj6	1370649_at	Bdkrb2	1370705_at	Cyp2j9

1370598_a_at	Ptprd	1370650_s_at	Inppl1	1370706_a_at	Fev
1370599_a_at	Fgd4	1370651_a_at	Ntrk2	1370707_at	RGD:708361
1370600_at	Grin3a	1370652_at	RGD:708412	1370708_a_at	Lrrc15
1370601_a_at	Atp2b4	1370654_at	RGD:708439	1370709_at	Asmt
1370602_at	Ptprc	1370655_a_at	Homer1	1370710_at	Nupl1
1370603_a_at	Lepr	1370656_a_at	Cdh6	1370711_a_at	Vnr2
1370604_at	Lepr	1370657_at	St18	1370712_at	Cdc2l1
1370605_s_at	P2ry1	1370658_a_at	RGD:708398	1370713_at	Siat1
1370606_at	Nrg1	1370659_at	RGD:708406	1370715_at	Madh9
1370608_at	Slc16a7	1370660_at	Gucy2g	1370716_at	Ap1gbp1
1370609_a_at	Slc34a1	1370661_a_at	Ap2b1	1370717_at	Syt10
1370610_at	Arnt2	1370663_at	RGD:708397 /// RGD:708414	1370718_at	RGD:708359
1370611_at	Kcna2	1370664_a_at	Hyou1	1370719_a_at	RGD:708509
1370721_a_at	Cngb1	1370665_at	RGD:727949	1370720_at	Cngb1
1370722_at	Grasp	1370777_at	Mup5	1370840_at	Gnrhr
1370723_at	Nfia	1370778_at	Mup5	1370841_a_at	Bckdk
1370724_a_at	G6pc	1370779_x_at	Rab31	1370842_at	Gng8
1370725_a_at	Vnr1	1370780_at	Kcnip1	1370843_at	Hnrpf
1370726_at	Pdgfd	1370781_a_at	Prpg1	1370844_at	Entpd2
1370727_at	Il13ra1	1370782_a_at	Ms4a2	1370845_at	RGD:727814
1370728_at	Ss18l1	1370783_a_at	Cacng6	1370846_at	RGD:708584
1370729_at	Ghrhr	1370784_a_at	Tomm20	1370847_at	Slc2a1
1370730_a_at	RGD:620386	1370785_s_at	RGD:708555	1370848_at	Hapln2
1370731_at	Vnr3	1370786_at	Bcl2l11	1370849_at	Scn3b
1370732_at	RGD:628724	1370787_at	Fgf4	1370850_at	Kalrn
1370733_at	Dspp	1370788_at	Prlr	1370851_a_at	RGD:727919
1370734_a_at	Olr1278	1370789_a_at	Ifng	1370852_at	RGD:708430
1370735_at	Trhr	1370790_at	LOC498659	1370853_at	Nexn
1370736_s_at	Casp9	1370791_at	Mapre1	1370854_at	Cst3
1370737_at	Trdn	1370793_at	Spag11	1370855_at	Actc1
1370738_a_at	Trdn	1370794_at	Foxc2	1370856_at	RGD:621676
1370739_x_at	Klra5	1370795_at	Foxi2	1370857_at	Scgb1d2
1370740_at	Olr1696	1370796_at	Foxe3	1370858_at	Txndc7
1370741_at	RGD:620592	1370797_at	Ngb	1370859_at	Svs1
1370742_at	Lnpep	1370798_a_at	Slc9a1	1370860_at	Cox6a1

1370743_a_at	Gpr26	1370799_at	Slc9a1	1370861_at	Apoe
1370745_at	LOC293508	1370800_at	Itgb5	1370862_at	Krt2-5
1370746_at	Fgf9	1370802_at	Zwint	1370863_at	Col1a1
1370748_at	V1rb7	1370803_at	Gabarap	1370864_at	Idh3g
1370749_at	Il1r1	1370804_at	Cited1 /// LOC309188	1370865_at	Rpl41
1370750_a_at	RGD:727924	1370806_at	RGD:70367	1370866_at	Gnb2
1370751_at	Tp53	1370807_at	Dia1	1370867_at	Kb1
1370752_a_at	Olr1078	1370808_at	Tubg1	1370868_at	Bcat1
1370753_at	Tas2r14	1370809_at	Ccnd2	1370869_at	Me1
1370754_at	Cacng4	1370810_at	Mpst	1370870_at	LOC288146
1370755_at	Olr1082	1370811_at	Bcl2l1 /// LOC293190	1370871_at	LOC288146 /// RGD:727807 /// LOC363971
1370756_at	Cacng3	1370812_at	Gstm5	1370872_at	Calm3
1370757_at	Rab15	1370815_at	Nr1d1	1370873_at	Csh2
1370759_at	Gad1	1370816_at	RGD:628665	1370874_at	Vil2
1370760_a_at	Olr1361	1370817_at	Decr2	1370875_at	Nfasc
1370761_at	Olr287	1370821_at	RT1-Ba	1370876_at	Nfasc
1370762_at	Olr1496	1370822_at	Bambi	1370877_at	Urod
1370763_at	Tg	1370823_at	Slc38a3	1370878_at	Dlst
1370764_a_at	RGD:628603	1370824_at	Cdc42	1370879_at	Rnh1
1370765_at	Snap29	1370825_a_at	Nap1l1	1370880_at	Tst
1370766_at	RGD:735056	1370826_at	Ncb5or	1370881_at	RGD:735096
1370767_at	RGD:727899	1370827_at	Zdhhc2	1370882_at	RT1-Da
1370768_at	Icos	1370828_at	Fntb	1370883_at	Spr
1370769_a_at	Kitl	1370829_at	Egfr	1370884_at	RGD:708479
1370770_s_at	Cacng7	1370832_at	Pex2	1370885_at	Kns2
1370771_at	Hfe	1370833_at	Hs3st1	1370886_a_at	Tgfb1i1
1370772_a_at	Kcnip2	1370834_at	RGD:708449	1370887_at	Cox5a
1370774_at	Calca	1370835_at	Serpina4	1370888_at	RGD:708530
1370775_a_at	Kcnk6	1370836_at	Sycn	1370889_at	Actr3
1370776_a_at	Ear11	1370837_at	Spna2	1370890_at	Cd48
1370892_at	Acaca	1370838_s_at	Accn3	1370891_at	C4a /// C4-2
1370893_at	Cldn7	1370949_at	Ppap2b	1371010_at	RGD:708515 /// LOC365807

1370894_at	Col5a2	1370950_at	Ppap2b	1371011_at	Hpcl2
1370895_at	Myh11	1370951_at	Gstm2	1371012_at	Gria1
1370896_a_at	Bckdha	1370952_at	LOC288065	1371013_at	Plcb1
1370897_at	Snn	1370953_at	P4ha1	1371014_at	Mx1
1370898_at	Sfpq	1370954_at	Adam10	1371015_at	LOC364379
1370899_at	RGD:620703	1370955_at	Dcn	1371016_at	Tcrg
1370901_at	Akr1b8	1370957_at	Kcnc3	1371017_at	Celsr2
1370902_at	Ephb1 /// LOC296318	1370958_at	Col3a1	1371018_at	Trib1
1370903_a_at	RGD:735053	1370959_at	Igfbp5	1371019_at	RGD:708533
1370904_at	Dock9	1370960_at	Dci	1371020_at	Arsb
1370905_at	Bckdhb	1370961_at	RGD:708342	1371021_at	Tgm4
1370906_at	Siat1	1370962_at	Gas7	1371022_a_at	Egfl4
1370907_at	RGD:619976	1370963_at	Ass	1371023_at	Cutl1
1370909_at	Rfc2	1370964_at	Tcf8	1371024_at	Masp2
1370910_at	Akap8	1370965_at	Hcn2	1371025_at	Ppfia4
1370911_at	Hspa1a	1370967_at	Nfkb1	1371026_at	Cblb
1370912_at	RGD:620495	1370968_at	Hoxa5	1371027_at	Tgoln2
1370913_at	Dnttip1	1370969_at	Kcnj14	1371028_at	Pkd1
1370914_at	Dnttip1	1370970_at	Myh1	1371029_at	Spp2
1370915_s_at	RGD:620973	1370971_at	RT1-Aw2 /// RT1-A1 /// RT1-A2 /// RT1-CE12 /// RT1-CE1 /// RT1-CE5 /// RT1-A3 /// RT1-CE7 /// RT1-CE2 /// RT1-149 /// RT1-CE15	1371030_at	Mat1a
1370916_at	Hsf1	1370972_x_at	RGD:61922	1371031_at	Nid
1370917_at	Atp5c1	1370973_at	Vps54	1371032_at	RT1-Bb
1370918_a_at	Hnrpm	1370974_at	Jmjd1a	1371033_at	Onecut1
1370919_at	Srpk2_predicted	1370975_at	G3bp	1371034_at	Gtf3a
1370920_at	Scamp3	1370976_at	Neud4	1371035_at	Nrcam
1370921_at	Ctxn	1370977_at	Scamp1	1371036_at	Pros1
1370922_at	Nme6	1370978_at	RGD:621744	1371037_at	Cebpg
1370924_at	LOC291411	1370979_at	Sftpb	1371038_at	Cacnb4
1370925_at	Muc4 /// LOC303887	1370982_at	Pou6f1	1371039_at	Slc1a5
1370926_at	Col12a1	1370984_at	Mapk7	1371040_at	Ndufv2
1370927_at	RGD:69294	1370986_s_at	Spn	1371041_at	Map4k3
1370928_at	Lrpap1	1370989_at	RGD:621517	1371042_at	Pou3f3
1370930_at	Xrcc5	1370990_at	Cml3	1371043_a_at	Pde7a
1370931_at	Lrp4	1370991_at	Fga	1371044_at	Accn2
1370932_at	Myo1e	1370992_a_at	Lamc1	1371046_at	Slc6a5
1370933_at	Nup153	1370993_at	Hip1r	1371047_at	Foxe1
1370934_at	Cdw92	1370994_at	Pou2f1	1371048_at	Dpysl4

1370935_at	Dmgdh	1370995_at	Rasgrf1	1371049_at	Pon1
1370936_at	Itga7	1370996_at	Homer1	1371050_at	Grinl1a
1370937_a_at	Rbp1	1370997_at	Grm2	1371051_at	Nog
1370938_at	Acsl1	1370998_at	Spag5	1371052_at	Myh8
1370939_at	Tjp2	1370999_at	Cacna1s	1371053_at	Pnmt
1370940_at	Pdgfra	1371001_at	Pdcd2	1371054_at	Rab12
1370942_at	RGD:621064 /// Sult1c1_predicted /// LOC367201	1371002_at	Map1b	1371055_at	Neo1
1370943_at	Col10a1	1371003_at	Sort1	1371056_at	Gabra5
1370944_at	Inpp5e	1371004_at	Abcc1	1371058_at	Prkar2a
1370945_at	Nfix	1371005_at	Jag2	1371059_at	Trim23
1370946_at	RGD:619899	1371006_at	Epha5	1371060_at	Pou3f2
1370947_at	LOC294446	1371007_at	Pmpca	1371061_at	LOC291133
1370948_a_at	LOC294446	1371008_at	Muc5ac	1371062_at	Sh3gl2
1371064_at	RT1-Bb	1371009_at	Titf1	1371063_at	Pcm1
1371065_at	Snrk	1371121_at	RGD:628859	1371174_s_at	Cacna1b
1371066_at	Adam6	1371122_at	RT1-S3	1371175_a_at	Nfic
1371067_at	Pcdha13	1371123_x_at	Kng1	1371176_at	Cask
1371068_at	Nritp	1371125_at	Gzmb	1371177_a_at	Il5
1371069_at	Zbp1	1371126_x_at	RGD:620739	1371178_at	Fgfr2
1371070_at	Gnb4	1371127_at	Il4	1371179_a_at	Grm1
1371071_at	Ncoa6	1371128_at	Cpg1	1371180_a_at	Grm1
1371072_at	B4galt1	1371129_at	Slc1a3	1371181_x_at	Tpo
1371073_at	Mcmd6	1371130_at	Txnip	1371182_at	Dlgh4
1371074_a_at	Myh13	1371131_a_at	Ank3	1371183_a_at	Tpm3
1371075_at	LOC361523	1371132_a_at	Prkar2b	1371184_x_at	Itga6
1371076_at	Htr3b	1371133_a_at	Atp2c1	1371185_at	Itga6
1371077_at	RT1-Aw2	1371134_at	Xylt1	1371186_at	Ubtf
1371078_at	Fcgr2b	1371135_at	Ppm1b	1371187_a_at	Ubtf
1371079_at	RGD:735228	1371136_at	Acox2	1371188_a_at	Lamr1
1371080_at	Rapgef4	1371137_at	Trdn	1371189_x_at	
1371081_at	Arr3	1371138_at	Pls3	1371190_at	Nf2
1371082_at	Spin2a	1371139_at	Accn1	1371191_at	Nf2
1371083_at	RGD:735032	1371140_a_at	Slc25a27	1371192_at	Tnfaip6
1371084_at	Ascl3	1371141_at	Cyp2g1	1371193_at	Tnfaip6
1371085_at	Ptprf	1371142_at	Serpina7	1371198_at	Rapgef1
1371086_at	Mtap6	1371143_at	Treh	1371199_at	Kcnc2
1371087_a_at	Capn9	1371144_at	Lrpap1	1371200_at	Sstr1
1371089_at	Scamp2	1371145_at	Tfec	1371201_at	Nfib
1371090_at	RGD:708546	1371146_at	Serpina3m	1371202_a_at	RGD:620961
1371091_at	RGD:708585	1371147_at	Inexa	1371203_at	Slc14a2
1371092_at	Znf291	1371148_s_at	Adam18	1371204_at	Slc14a2
1371093_at	Lhx2	1371149_at	Ccnd1	1371205_at	Igf2
1371094_at	Kif6	1371150_at	Cpa3	1371206_a_at	Nupl1

1371097_at	Masp2	1371151_at	Oas1	1371207_at	Nupl1
1371099_at	Es2	1371152_a_at	Glra2	1371208_at	RT1-CE5
1371100_at	Ryk	1371153_a_at	Pou2f3	1371209_at	RT1-Aw2 /// RT1-CE5
1371101_at	Hbb	1371154_a_at	Klrc1	1371210_s_at	Nrg1
1371102_x_at	Rab6	1371155_at	Glra1	1371211_a_at	Nrg1
1371103_at	Srebf1	1371156_a_at	Apob	1371212_at	RT1-A3
1371105_at	Itgb7	1371157_at	RGD:708543	1371213_at	Itga7
1371106_at	Trp63	1371158_at	Cckbr	1371214_at	Fut2
1371107_a_at	Atp1a1	1371159_a_at	Vamp2	1371215_at	Fut2
1371108_a_at	C8b	1371160_at	Ppp1r3b	1371216_s_at	Apex1
1371109_at	RGD:727910	1371161_at	RGD:632282 /// RGD:738050	1371217_at	Nrg1
1371110_at	RT1-Aw2	1371162_at	RGD:621336	1371218_a_at	Pde1c
1371111_at	Ret	1371163_at	Mcpt10	1371219_a_at	RGD:621858
1371112_at	Tfrc	1371164_at	Atp2a3	1371220_at	RGD:621858
1371113_a_at	Kcnj4	1371165_a_at	Nos3	1371221_at	Lepr
1371114_at	Ptpre	1371166_at	Dusp3	1371222_at	Lepr
1371115_at	Masp1	1371167_at	Mpp2	1371223_a_at	RGD:621750
1371116_at	Adam32	1371168_at	Vcsa2	1371224_a_at	RGD:621750
1371117_at	IgE FE-3	1371169_at	Il1a	1371225_at	Col2a1
1371118_a_at	RGD:727839	1371170_a_at	RT1-Aw2	1371226_at	Csf2
1371119_at	Bdkrb2	1371171_at	Atp2b3	1371227_at	Csf2
1371120_s_at	RGD:620279	1371172_at	Cast	1371230_x_at	Spnb1
1371232_a_at	Cspg2	1371173_a_at	Sstr2	1371231_at	Cspg2
1371233_at	Fgb	1371308_at	Tegt	1371378_at	LOC289182
1371234_at	Grm6	1371309_at	Serpinh1	1371379_at	Pdha1
1371235_at	Grm6	1371310_s_at	Sdhc	1371382_at	Drap1_predicted
1371236_at	Mt1a	1371311_at	LOC288622	1371383_at	Btf3_predicted
1371237_a_at	Grm1	1371312_at	Rpl23a_predicted	1371384_at	Dscr2_predicted
1371238_at	RGD:621546 /// RGD:708368	1371313_at	Nedd4a	1371385_at	RGD1306643_predicted
1371239_s_at	Tpm1	1371314_at	Myl7_predicted	1371386_at	RGD:727789
1371240_at	Tpm1	1371316_at	Ldb1_predicted	1371387_at	Pdhb
1371241_x_	Grm8	1371317_at	Rps16	1371388_at	LOC3067

at					66
1371242_at	Grm8	1371318_at	Itm2b	1371389_at	RGD:735101
1371245_a_at	NTF2	1371319_at	Itm2b	1371390_at	Txndc5_predicted
1371248_at	RGD:1303073	1371321_at	Lamc1	1371391_at	Gpi
1371251_at	Socs1	1371324_at	Ppgb_predicted	1371392_at	Clstn1_predicted
1371252_at	Etfa	1371325_at	Csnk2a2_predicted	1371394_x_at	Cbx3
1371253_at	RGD:628838	1371328_at	Eif5a_predicted	1371395_at	Tpm3
1371254_at	Hras	1371329_at	Rpl11_predicted	1371396_at	Nosip_predicted
1371256_at	Rorb_predicted	1371330_at	Fstl1	1371399_at	Thrsp
1371257_at	Fga	1371332_at	Hnrpdl_predicted	1371401_at	Atp6v1b2
1371258_at	Ngfb	1371333_at	Itm2c_predicted	1371402_at	RGD:735038
1371260_at	Ptpn2	1371334_at	RGD:1303259	1371403_at	Eif4b_predicted
1371261_at	LOC314492 /// LOC314501 /// LOC362796 /// LOC366746 /// IgG-2a	1371336_at	Cox7a2l_predicted	1371406_at	Nckap1
1371262_at	Camk2d	1371339_at	Rplp2	1371407_at	Cryba1
1371264_at	Avpr2	1371340_at	Snrpd2_predicted	1371409_at	LOC288925
1371265_at	Afm	1371341_at	Cyc1_predicted	1371410_at	Plxnb2_predicted
1371266_at	RT1-Aw2 /// RT1-Cl /// RT1-A3 /// RT1-CE11	1371342_at	Srpr_predicted	1371412_a_at	Crygb
1371267_at	Olr1641_predicted	1371343_at	Rpl27a_predicted	1371413_x_at	RGD:1303089
1371268_at	Olr857_predicted	1371345_at	Ndufb6_predicted	1371414_at	Uqcrh_predicted
1371269_at	Olr442_predicted	1371347_at	Psmb5	1371415_at	Ndufv1
1371270_at	Olr416_predicted	1371348_at	LOC294337	1371417_at	Cct2
1371271_at	Klra5 /// Ly49s7	1371351_at	RGD:620649	1371418_at	Spnb2
1371273_at	RGD:735160	1371352_at	Sqstm1	1371419_at	LOC494529
1371276_at	Cdx1_predicted	1371353_at	Tncc_predicted	1371421_at	Morf4l2
1371278_at	RGD:621437 /// LOC306962 /// Hist1h2an_predicted /// Hist1h4a_predi	1371354_at	Ndufa8_predicted	1371423_at	RGD1304823_predicted

	cted /// Hist1h2ao_predicted				
1371280_at	Hoxc8	1371356_at	Igfbp7_predicted	1371424_at	Srrm1_predicted
1371281_at	Prm3	1371357_at	Gpsn2	1371426_at	RGD1309125_predicted
1371284_at	Hoxc4	1371358_at	Mlf2_predicted	1371428_at	Dag1
1371286_at	Gap43	1371359_at	Ndrg1_predicted	1371429_at	Dag1
1371289_at	Htr7	1371361_at	Ddx17_predicted	1371430_at	Pex5
1371291_at	Msx2	1371362_at	Gpd1	1371434_at	Naca_predicted
1371294_at	Rps20	1371363_at	Andpro	1371435_at	RGD:1302955
1371295_at	Sdhd	1371364_a_at	LOC292588	1371436_at	Sec13l1
1371296_at	Rpl7a_predicted	1371365_at	Arhgdia	1371439_at	B2m
1371297_at	H19	1371366_at	Tardbp_predicted	1371440_at	Pea15_predicted
1371298_at	Rps3	1371367_at	Sec61a1	1371441_at	Hyou1
1371299_at	Rpl3	1371368_at	Col6a2_predicted	1371442_at	RGD1304567_predicted
1371300_at	Rpl9	1371369_at	Svs6_predicted	1371444_at	RGD1305092_predicted
1371302_at	Tdh_predicted	1371370_a_at	Ndufb4_predicted	1371445_at	Mapkapk2
1371303_at	Myl6_predicted	1371371_at	LOC362809	1371446_at	Plac8_predicted
1371304_a_at	Rpl8	1371372_at	MGC94464	1371448_at	Pin1_predicted
1371306_at	Rplp1	1371373_at	Maf1	1371449_at	Sox11
1371307_at	Rps4x	1371376_at	LOC499100	1371450_at	Rnaseh2a_predicted
1371452_at	RGD:1303210	1371377_at	Sui1-rs1_predicted	1371451_at	RGD:1303055
1371453_at	RGD1309231_predicted	1371545_at	LOC361128	1371683_at	Pelo
1371454_at	Pmm1_predicted	1371546_at	RGD1309695_predicted	1371685_at	Canx
1371455_at	Abcf3_predicted	1371547_at	Mrps25_predicted	1371686_at	Canx
1371460_at	RGD1305453_predicted	1371548_at	Wdr23_predicted	1371687_at	Tram1
1371462_at	Phf5a	1371555_at	Pias4_predicted	1371688_at	Eef1a1
1371463_at	zgc:101121	1371556_at	Thap4	1371689_at	Arl1
1371466_at	LOC293103	1371557_at	Nisch_predicted	1371691_at	RGD1305525_predicted

1371468_at	Chp	1371559_at	Irf3	1371693_at	Dpysl2
1371469_at	Adh4	1371560_at	G6pc3	1371695_at	Gpr56
1371470_at	RGD:1303085	1371561_at	Epn2	1371696_at	RGD1309044_predicted
1371472_at	Clptm1_predicted	1371562_at	RGD1309986_predicted	1371697_at	LOC287739
1371473_at	Mtch1_predicted	1371563_at	RGD:735157	1371699_at	Mfap4_predicted
1371474_at	Rnase4	1371565_at	RGD1311830_predicted	1371700_at	Ndufb9_predicted
1371475_at	RGD:1302952	1371566_at	Aldh7a1_predicted	1371701_at	Tm4sf2
1371477_at	RGD1307752_predicted	1371570_at	App	1371703_at	Ddx23_predicted
1371481_at	Ndufs2_predicted	1371572_at	Rpl36a_predicted	1371704_at	MGC94168
1371485_at	Snrp1c_predicted	1371573_at	Ghitm	1371705_at	Sdccag3_predicted
1371486_at	Sh3bgrl3_predicted	1371574_at	Msn	1371707_at	Car6_predicted
1371487_at	LOC308494	1371575_at	Mrps36_predicted	1371708_at	Mrpl3_predicted
1371488_at	Rnf4	1371576_at	Ndufs1	1371711_at	LOC292030
1371489_at	Hsbp1	1371581_at	LOC310612	1371712_at	Abl1
1371490_at	Notch1	1371582_at	Rbm3	1371721_at	RGD1311547_predicted
1371491_at	Apobec2_predicted	1371583_at	Trpc4ap_predicted	1371722_at	Rragc_predicted
1371492_at	Ap2a2	1371584_at	Gspt1	1371723_at	Smfn_predicted
1371494_at	M6pr	1371585_at	Mrpl48_predicted	1371724_at	Myh9
1371496_at	Asb6_predicted	1371586_at	Map2k1ip1_predicted	1371728_at	Ypel5_predicted
1371498_at	Cd9	1371640_at	Cct7_predicted	1371729_at	RGD1305466_predicted
1371499_at	Ltbp4_predicted	1371641_at	Eif4a2_predicted	1371730_at	Pfkl
1371501_at	RGD1306184_predicted	1371642_at	Ccnd1	1371731_at	Dpt
1371502_at	Nubp1_predicted	1371643_at	Ptk9_predicted	1371751_at	LOC287419
1371505_at	Scarb2	1371644_at	Sdf2_predicted	1371752_at	LOC296235
1371507_at	Myh13	1371645_at	Pgd	1371753_at	Slc25a25
1371508_at	Tbrg1_predicted	1371646_at	LOC309475	1371757_s_at	RGD:1303313
1371509_at	RGD:727975	1371647_at	Ddb1	1371760_at	Rpl34_predicted
1371510_at	Arpc2_predicted	1371648_at	Mrps24_predicted	1371761_at	Rbp4

1371515_at	Xpo7_predicted	1371649_at	Senp3_predicted	1371762_at	RGD1309534_predicted
1371517_at	Nid	1371654_at	Mpdu1_predicted	1371763_at	MGC94113
1371518_at	RGD:735052	1371655_at	Cct4	1371767_at	RGD1307854_predicted
1371520_at	Pdha2	1371656_at	Uble1b_predicted	1371768_at	Scamp2
1371524_at	Kcc4	1371657_at	Noc4_predicted	1371769_at	RGD:1303006
1371525_at	Rnf10_predicted	1371671_at	Cbx7	1371771_at	LOC362169
1371526_at	Emp1	1371672_at	Tcfl1_predicted	1371773_at	Sat
1371527_at	Fkbp8_predicted	1371673_at	Klhdc3_predicted	1371774_at	Acadsb
1371529_at	Krt2-8	1371674_at		1371775_at	Pik3r1
1371531_at	Hif1a	1371675_at		1371776_at	Pabpc4_predicted
1371532_at	Dctn6_predicted	1371676_at	RGD1307150_predicted	1371777_at	Rnf146_predicted
1371533_at	RGD1307826_predicted	1371677_at		1371779_at	Kdelr2_predicted
1371535_at	Carhsp1	1371678_at		1371780_at	Stat3
1371538_at	Nola2_predicted	1371679_at		1371781_at	MGC105691
1371539_at	Krtcap2_predicted	1371680_at	RGD:708449	1371782_at	RGD:1303129
1371541_at	MGC94628	1371681_at	Map1lc3a	1371784_at	Tnfrsf12a
1371788_at	LOC301117	1371682_at	Lsm4_predicted	1371786_at	Tceb3
1371789_at	Mrpl45_predicted	1371886_at	LOC305373		Gpx7_predicted
1371790_at	Surf1	1371887_at	mrpl24		Ubap2_predicted
1371797_at	Gna12	1371888_at	Slc22a17		Mrps12_predicted
1371798_at	RGD:735227	1371889_at	Rere		RGD1310147_predicted
1371802_at	Gm2a	1371890_at	RGD1308430_predicted		Cndp2_predicted
1371803_at	Cdadc1_predicted	1371918_at	RGD:1302935		Chchd6_predicted
1371804_at	RGD1309382_predicted	1371919_at	Poldip2_predicted		Ptk9l_predicted
1371805_at	Dgcr8_predicted	1371920_at	Catna1		Igfbp6
1371806_at	RGD1311605_predicted	1371929_at	Qars		Acy1
1371807_at	Blmh_predicted	1371930_at	RGD:727961		Phc1_predicted
1371808_at	RGD:1302998	1371931_at	RGD1309341_predicted		Nphp1_predicted

1371810_at	Bscl2_predicted	1371934_at	Tmem9_predicted	RGD1309198_predicted
1371811_at	RGD:1303261	1371935_at	RGD:735141	Peflin
1371812_at	Hirip3_predicted	1371938_at	Gpiap1_predicted	Prkca
1371814_at	Mfap2_predicted	1371940_at	RGD1310230_predicted	Mocs2
1371816_at	LOC290651	1371942_at	RGD:727884	Hpcal1
1371818_at	Hdac5	1371944_at	Ube2l3_predicted	Sdc3
1371819_at	Mesdc2_predicted	1371945_at	RGD:1303130	Rpa1_predicted
1371821_at	Polr3d_predicted	1371946_at	Ndn_predicted	Pfkp
1371823_at	Ak3l2	1371947_at	Dscr5_predicted	Kpna1
1371824_at	Snapc2_predicted	1371948_at	Bzw1	RGD:62048
1371835_at	LOC287708 /// Rab5c_predicted	1371949_at	LOC302422	Aqp4
1371836_at	RGD:619906	1371952_at	Ccng2	Impact
1371837_at	Sfrs2	1371954_at	Mrpl35_predicted	Tnnc2_predicted
1371838_at	Sfrs2	1371956_at	RGD1308463_predicted	LOC304361
1371839_at	Edg1	1371958_at	Hist2h2aa_predicted	Pink1_predicted
1371840_at	Mtpn	1371960_at	Pld3_predicted	RGD:1303014
1371842_at	LOC361315	1371961_at	Tufm_predicted	RGD:1302978
1371843_at	Ahcyl1_predicted	1371962_at	Pcca	RGD1310553_predicted
1371844_at	Pop4_predicted	1371964_at	RGD:1303272	Snx27
1371848_at	RGD1305524_predicted	1371965_at	Pcmt1	RGD1307475_predicted
1371849_at	Papss1_predicted	1371966_at	Mrpl16	Brd8_predicted
1371850_at	RGD:735127	1371967_at	RGD:735173	Ppp1r1b
1371852_at	Mrpl42_predicted	1371968_at	Cald1	Cops5_predicted
1371856_at	Kctd10	1372085_at	RGD1311955_predicted	Mospd3_predicted
1371857_at	Ap1s1_predicted	1372086_at	RGD:727866	Mafk
1371859_at	RGD1305031_predicted	1372087_at	Rnf25_predicted	Paox_predicted
1371861_at	Rrm1	1372088_at	Casc3	Asmtl_predicted
1371863_at	Bteb1	1372090_at	RGD:1303258	Pdk3
1371864_at	RGD1311566_predicted	1372091_at	Als2cr3	RGD1304706_predi

					cted
1371867_at	Bcas2_predicted	1372092_at	Mxi1		Wbp1_predicted
1371868_at	Psma7	1372096_at	Icsbp1		Sdbcag84_predicted
1371869_at	RGD1309054_predicted	1372098_at	RGD:735230		Sgca_predicted
1371871_at	Nap1l1	1372099_at	RGD1305638_predicted		Oaz1
1371873_at	RGD:1303276	1372100_at	Ppap2b		Ddx3x
1371875_at	Tnfsf5ip1_predicted	1372101_at	Ncor1		Cab39_predicted
1371880_at	RGD1307918_predicted	1372104_at	Smhs2		Cab39_predicted
1371881_at	Sh2bpsm1	1372118_at	Ube1dc1_predicted		Ciao1_predicted
1371882_a_at	Maf	1372119_at	Ube1dc1_predicted		Ddost_predicted
1371884_at	Ckap1_predicted	1372121_at	Tsg101		Sesn1_predicted
1371885_at	RGD:1303031	1372122_at	Sdhb_predicted		Rbm5_predicted
1372252_at	Cnot8_predicted	1372123_at	Eif4b_predicted		Trappc1_predicted
1372253_at	RGD:735225	1372648_at	Hspb7	1372806_at	Clcn2
1372254_at	Rars_predicted	1372650_at	Cdw92	1372807_at	LOC313410
1372258_at	RGD:1303246	1372652_at	Fkbp11_predicted	1372808_at	LOC290595
1372259_at	LOC287061	1372653_at	Eps8l2_predicted	1372809_at	Hnrpdl_predicted
1372263_at	Pck1	1372655_at	Snx15_predicted	1372811_at	LOC296115
1372264_at	RGD1304719_predicted	1372656_at	RGD1311532_predicted	1372812_at	RGD1306682_predicted
1372265_at	Rev3l_predicted	1372657_at	Dmn	1372831_at	Epim
1372266_at	Psmd5_predicted	1372659_at	Tubgcp3_predicted	1372832_at	Wdr7
1372413_at	Map1lc3b	1372660_at	Tbl3_predicted	1372833_at	Vps4b_predicted
1372415_at	RGD:628790	1372661_at	Fbxo34_predicted	1372834_at	Rhoj_predicted
1372416_at	Sertad1	1372663_at	Traf2_predicted	1372851_at	Rps6kb2
1372418_at	Vrk3	1372666_at	MGC94797	1372852_at	RGD:727889
1372419_at	RGD1308064_predicted	1372669_at	RGD1307682_predicted	1372855_at	Hdgfrp2
1372420_at	Aga_predicted	1372670_at	LOC317214	1372856_at	Pacsin2
1372422_at	Perp_predicted	1372671_at	Qprt_predicted	1372859_at	MGC95092
1372426_at	LOC298705	1372674_at	RGD1306954_predicted	1372860_at	Pip5k1c
1372427_at	Dnajc4_predict	1372675_at	RGD1304560	1372861_at	Rab22a_p

	ed		_predicted		redicted
1372429_at	RGD1311739_predicted	1372676_at	RGD1304783_predicted	1372862_at	Phr1_predicted
1372430_at	LOC303746	1372689_at	Rtn4rl1	1372863_at	Adcy5
1372431_at	Prpf3_predicted	1372690_at	Upp1_predicted	1372864_at	Zfp364_predicted
1372432_at	RGD1310211_predicted	1372691_at	Tnk2_predicted	1372865_at	RGD1311914_predicted
1372433_at	Cip98	1372693_at	Cdk105	1372866_at	Rnmt_predicted
1372435_at	Tpd52l2	1372694_at	Fndc5	1372867_at	Tor3a_predicted
1372436_at	Skp1a	1372696_at	Mrps15	1372869_at	Kdelr3_predicted
1372437_at	RGD1310494_predicted	1372699_at	Trp53inp1	1372870_at	RGD:735175
1372438_at	Col4a1_predicted	1372700_at	Hspca	1372872_at	Fbxo38_predicted
1372439_at	Serpine2	1372701_at	PRP-2	1372873_at	Sdccag8
1372495_at	LOC313786	1372702_at	Ube2r2_predicted	1372875_at	Sephs2_predicted
1372496_at	Ca125	1372703_at	LOC362040	1372876_at	Plod3
1372497_at	MGC94686	1372704_at	Cherp_predicted	1372878_at	Akt1s1_predicted
1372498_at	Ankrd24_predicted	1372705_at	Hexb_predicted	1372879_at	Zfp100_predicted
1372499_at	Tmod3_predicted	1372708_at	Bcap29	1372881_at	RGD1308635_predicted
1372500_at	Sf3b3_predicted	1372709_at	Bet1	1372882_at	Cenpb_predicted
1372504_at	Ykt6	1372710_at	LOC498750	1372884_at	Cebpg
1372505_at	Psme3_predicted	1372711_at	Ttc1	1372885_at	RGD:1302948
1372506_at	LOC306587	1372712_at	RGD1309550_predicted	1372886_at	Scarf2_predicted
1372510_at	Dazap2_predicted	1372713_at	RGD1307778_predicted	1372887_at	RGD:1303173
1372511_at	Stx18_predicted	1372756_at	Stat1	1372888_at	Slco2a1
1372512_at	Rac1	1372758_at	Cdk9	1372889_at	Spgl1
1372513_at	Dnalc4_predicted	1372768_at	LOC498225	1372890_at	RGD1305631_predicted
1372515_at	Kif22_predicted	1372769_at	Calm1	1372892_at	RGD:735206
1372516_at	Ppil1_predicted	1372783_at	RGD1311221_predicted	1372893_at	RGD1310540_predicted
1372517_at	Fbln1_predicted	1372789_at	Mdh1	1372894_at	RGD1309676_predicted
1372518_at	Nup93_predicted	1372790_at	Prkwnk1	1372896_at	Plod2

1372519_at	Mcl1	1372791_at	LOC292780	1372958_at	Decr2
1372520_at	Rohn_predicted	1372792_at	Ssbp1	1372959_at	Xylt2
1372522_at	Gclc	1372796_at	LOC302557	1372960_a_at	RGD:735120
1372524_at	Fkbp14_predicted	1372797_at	Kua	1372961_at	Tarbp2_predicted
1372525_at	RGD:735088	1372798_at	Dguok_predicted	1372965_at	RGD1310174_predicted
1372526_at	RGD:1303245	1372799_at	Mrg2_predicted	1372966_at	RGD:735210
1372527_at	Nsf	1372800_at	RGD:1303015	1372968_at	Fbxl3a_predicted
1372972_at	Lss	1372805_at	Vps35	1372969_at	RGD1309281_predicted
1372973_at	LOC298528	1373234_at	Syap1	1373462_at	Col5a2
1372975_at	RGD1309721_predicted	1373239_at	Dhrs3_predicted	1373464_at	Pqlc1_predicted
1372980_at	RGD1311257_predicted	1373240_at	Mrpl49_predicted	1373467_at	Ccnf
1372981_at	Ppp3r1	1373241_at	Tbpl1_predicted	1373470_at	RGD:1302950
1372982_at	Rala	1373242_at	Pmvk_predicted	1373471_at	Actr6_predicted
1372984_at	Znf444_predicted	1373243_at	RGD1304758_predicted	1373472_at	Nap1l1
1372987_at	MGC94752	1373244_at	Col4a1_predicted	1373474_at	LOC288065
1372989_at	Creb3_predicted	1373255_at	Chd3	1373475_at	LOC297428
1373079_at	Papola_predicted	1373256_at	RGD:1307215	1373476_at	LOC297372
1373080_at	Baiap2	1373343_at	LOC363471	1373477_at	Mybph
1373081_at	Pkia	1373344_at	RGD:727911	1373478_at	Ppp3ca
1373088_at	Cdh3	1373345_at	RGD1306508_predicted	1373509_at	Vamp1
1373092_at	RGD1307599_predicted	1373346_at	Acbd3	1373511_at	Ilvbl_predicted
1373095_at	Actr8_predicted	1373349_at	Psip1	1373512_at	Gch
1373097_at	Bcas1	1373357_at	Usp8_predicted	1373513_at	RGD1308168_predicted
1373098_at	Pigs	1373359_at	Eif2ak3	1373522_at	Fcgr3a
1373100_at	Pigk_predicted	1373361_at	Uqcrc2	1373525_at	LOC365601
1373101_at	Cdh13	1373362_at	Map1b	1373530_at	Cpsf1_predicted
1373102_at	Mta2_predicted	1373364_at	RGD1310116_predicted	1373531_at	Plekhf1_predicted
1373103_at	RGD1309570_predicted	1373365_at	G2an_predicted	1373533_at	RGD1307395_predicted

1373107_at	Ppp1r3c_predicted	1373372_at	MGC95214	1373534_at	Enah_predicted
1373109_at	Gng10	1373373_at	Lmo4_predicted	1373543_at	Cxcl9
1373127_at	Rcn3	1373374_at	Rab6ip1_predicted	1373546_at	RGD1308147_predicted
1373129_at	Myom2	1373375_at	Unc84a	1373548_at	Ddx10_predicted
1373133_at	LOC296131	1373376_at	Scnm1_predicted	1373551_at	LOC296865
1373135_at	RGD1307672_predicted	1373377_at	Agtpbp1_predicted	1373552_at	Top3b_predicted
1373137_at	Nudt5	1373378_at		1373554_at	Dctn4
1373139_at	Il6st	1373379_at	LOC362154	1373555_at	LOC298861
1373141_at	Ghitm	1373380_at	Herc4_predicted	1373556_at	
1373142_at	RGD1309621_predicted	1373381_at	RGD1306324_predicted	1373557_at	
1373144_at	LOC306991	1373382_at	RGD:735158	1373558_at	
1373145_at	Ssx2ip	1373398_at	Wdr6_predicted	1373559_at	LOC303100
1373148_at	LOC293491	1373399_at	Prkar2a	1373560_at	D1bwg1363e
1373149_at	Comtd1_predicted	1373400_at	Tnc	1373561_at	RGD1309370_predicted
1373151_at	Prss23	1373410_at	RGD1309241_predicted	1373562_at	RGD1310925_predicted
1373152_at	Mog	1373411_at	Nt5c3_predicted	1373563_at	Hibch_predicted
1373154_at	Mrpl46_predicted	1373412_at	RGD1310481_predicted	1373564_at	Smarca4
1373155_at	LOC367903	1373413_at	RGD1305557_predicted	1373570_at	Rtn3
1373186_at	Kif5a	1373423_at	Dgcr6_predicted	1373571_at	LOC296462
1373187_at	Scn4b	1373424_at	LOC365842	1373572_at	RGD:708389
1373188_at	Rutbc3	1373426_at	Rragd_predicted	1373587_at	RGD1310323_predicted
1373199_at	Eef1e1_predicted	1373427_at	Brms1_predicted	1373588_at	Mtmr3_predicted
1373200_at	Dbt	1373428_at	RGD:1303317	1373589_at	Stom_predicted
1373201_at	Gng3	1373430_at	Lrrc5_predicted	1373590_at	RGD:1303204
1373203_at	RGD1310725_predicted	1373431_at	LOC294446	1373591_at	MGC94010
1373211_at	Atp5s	1373432_at	Nsbp1_predicted	1373659_at	Afg3l1_predicted
1373213_at	Kdelc1_predicted	1373434_at	Fxr2h_predicted	1373660_at	Cxcr4

1373214_at	Abr_predicted	1373441_at	Os-9	1373661_a_at	Tor2a
1373218_at	Snai1	1373442_at	Th	1373662_at	LOC361548
1373223_at	RGD:1303068	1373443_a_at	Ppfia1_predicted	1373663_at	Pigc_predicted
1373224_at	Mcl1	1373460_at	RGD:1303303	1373667_at	Polr2i_predicted
1373673_at	Mfap5_predicted	1373461_at	Eed_predicted	1373668_at	Gnpda2_predicted
1373674_at	Glrx2	1373946_at	Dpt_predicted	1374339_at	Glrx2
1373677_at	Clic4	1373950_at	Prkar1a	1374340_at	Thap7_predicted
1373680_at	Mpi	1373951_at	RGD:727782	1374341_at	RGD:1302999
1373681_at	Ddx51_predicted	1373952_at		1374342_at	
1373682_at	Fyn	1373954_at	Kpnb3_predicted	1374343_at	RGD:727823
1373684_at	LOC361149	1373956_at	Reln	1374351_at	Actc1
1373685_at	Serpina6	1373957_at	LOC367902	1374352_at	Actc1
1373686_at	Rutbc3	1373958_at	Ppp2r1b_predicted	1374353_x_at	
1373687_at	LOC498145	1373959_at	RGD1311474_predicted	1374354_at	LOC315283
1373714_at	LOC304396	1373960_at	MGC95208	1374355_at	LOC302999
1373715_at	Armc5_predicted	1373963_at	RGD1305487_predicted	1374356_at	RGD:727825
1373716_at	Opcml	1373964_at	RGD1310931_predicted	1374357_at	RGD1307648_predicted
1373718_at	Map4k3	1373965_at	Rai1_predicted	1374359_at	Faf1
1373720_at	RGD1308426_predicted	1373968_at	Sh3d4	1374402_at	Efnb1
1373722_at	LOC300027	1373969_at	RGD1311155_predicted	1374403_at	Jun
1373723_at	Kb4	1373970_at	RGD1311177_predicted	1374404_at	RGD:727807
1373727_at	MGC93972	1373971_at	Nav1_predicted	1374405_at	Klhdc2_predicted
1373731_at	Acp6_predicted	1373972_at	LOC360662	1374407_at	RGD1309199_predicted
1373732_at	Bok	1374177_at	Arl5	1374408_at	Taf6l_predicted
1373733_at	Slco3a1	1374178_at	RT1-A3	1374410_at	Mrpl52_predicted
1373734_at	Klc3	1374179_at	LOC317163	1374413_at	RGD1306844_predicted
1373736_at	ORF19_predicted	1374182_at	RGD1309624_predicted	1374414_at	RGD1308086_predicted
1373740_at	Pus1_predicted	1374184_at	RGD1307538_predicted	1374417_at	RGD1308816_predi

					cted
1373741_at	Grcc9_predicted	1374187_at	Tloc1_predicted	1374419_at	RGD1308874_predicted
1373802_at	Ghr	1374188_at	Znf219	1374441_at	Sfrs9_predicted
1373803_a_at	Foxp1_predicted	1374189_at	Clybl_predicted	1374442_at	Ict1_predicted
1373804_at	Ctsr	1374192_at	Galnt7	1374443_at	LOC316009
1373805_at	RGD1311732_predicted	1374195_at	Lancl1	1374444_at	Grca_predicted
1373806_at	Vegf	1374197_at	RGD:727815	1374451_at	Pde9a
1373808_at	Ddx21b_predicted	1374199_at	Slc29a3	1374459_at	Cops7a_predicted
1373809_at	Pla2g12a_predicted	1374203_at	Wsb1_predicted	1374460_at	Zdhhc4_predicted
1373811_at	Cdkn1b	1374204_at	pur-beta	1374461_at	Kifap3_predicted
1373812_at	Dnajc10_predicted	1374205_at	RGD1307357_predicted	1374462_at	Qki
1373813_at	RGD1310066_predicted	1374207_at	Zc3hdc7_predicted	1374463_at	Tfg_predicted
1373814_at	Lman2_predicted	1374208_at	RGD1309010_predicted	1374464_at	MGC105797
1373816_at	Ing4_predicted	1374220_at	Slc29a3	1374465_at	Prkce
1373857_at	Kpnb1	1374221_at	RGD:1303323	1374466_at	Trap1
1373859_at	Sox4_predicted	1374225_at	Col7a1_predicted	1374467_at	RGD:735043
1373860_at	Ndfip2_predicted	1374226_at	RGD1305264_predicted	1374469_at	Dhx57_predicted
1373861_at	LOC252889	1374227_at	Trim47_predicted	1374470_at	Cpne2_predicted
1373862_at	Map4k4_predicted	1374228_at	RGD1308556_predicted	1374471_at	LOC290775
1373863_at	Map4k4_predicted	1374234_at	Dscr1l1	1374619_at	Ceacam1
1373864_at	Snap91	1374244_at	LOC363251	1374620_at	LOC361420
1373865_at	MGC109115	1374246_at	Stab1_predicted	1374623_at	Galnt11
1373867_at	Bclaf1_predicted	1374248_at	RGD1304580_predicted	1374624_at	Hes6_predicted
1373868_at	Soat1	1374253_at	LOC300441	1374625_at	MGC95065
1373869_at	RGD1305486_predicted	1374255_at	Wwp2_predicted	1374627_at	Cryz_predicted
1373870_at	LOC313905	1374256_at	Tiam1_predicted	1374628_at	Med8_predicted
1373873_at	Sgpp1	1374263_at	LOC362304	1374629_at	Clic3_predicted
1373874_at	RGD1308261_predicted	1374332_at	RGD1306058_predicted	1374630_at	RGD1308158_predicted
1373876_at	Picalm	1374333_at	Igha	1374631_at	Ptdsr_predicted

1374636_at	RGD1309263_predicted	1374334_at	Gata6	1374633_at	RGD1310503_predicted
1374637_at	Pex13_predicted	1374846_at	Lztr1_predicted	1374995_at	Npl4
1374645_at	Csnk1a1	1374848_at	Adamts7_predicted	1374996_at	Map3k11
1374653_at	Btrc	1374850_at	RGD1311009_predicted	1375002_at	RGD:735108
1374655_at	Sec6l1	1374851_at	LOC362592	1375007_at	Aurkc_predicted
1374658_at	LOC363153	1374852_at	RGD1305622_predicted	1375008_at	Nudt14_predicted
1374659_at	RGD1309025_predicted	1374853_at	LOC305963	1375009_at	Cd68_predicted
1374660_at	LOC361571	1374854_at	Per1	1375012_at	MGC94018
1374662_at	Dnajc5	1374855_at	RGD1306433_predicted	1375017_at	LOC311592
1374688_at	Pik4cb	1374866_at	Ptgis	1375018_at	Hnrph3_predicted
1374690_at	Sult5a1_predicted	1374869_at	Col27a1	1375019_at	Rin3
1374692_at	RGD1306243_predicted	1374870_at	Asrgl1	1375020_at	Bat3
1374696_at	RGD:1303132	1374881_at	RGD1306063_predicted	1375021_at	Afg3l2_predicted
1374707_at	LOC306618	1374882_at	Mtmr7_predicted	1375025_at	Cln6_predicted
1374710_at	Cpsf3_predicted	1374883_at	Ppm1d_predicted	1375030_at	Ttn
1374711_at	Psmd11_predicted	1374885_at	Bcs1l	1375032_at	Cpt1c_predicted
1374714_at	RGD1309487_predicted	1374886_at	Tubgcp6_predicted	1375033_at	LOC361401
1374715_at	RGD1306106_predicted	1374888_at	LOC296468	1375034_at	Mfn1
1374720_at	Eif2s2	1374890_at	Brf2_predicted	1375069_at	Hsp60
1374721_at	C1qtnf1	1374891_at	Sat2_predicted	1375070_at	Nup133_predicted
1374723_at	Mapk4	1374894_at	Myom1	1375103_at	Ppp1r14b
1374724_at	LOC310756	1374898_at	LOC290877	1375105_at	Amn_predicted
1374725_at	Fndc1_predicted	1374899_at	Gosr2	1375111_at	Nr2f6
1374726_at	LOC294513	1374901_at	Iqgap3_predicted	1375116_at	Akt1s1_predicted
1374731_at	RGD1311635_predicted	1374902_at	Gcnt2	1375118_at	Nedd4a
1374732_at	Sympk_predicted	1374905_at	LOC313450	1375119_at	Idb4
1374734_at	Arhgap4	1374909_at	Celsr2	1375120_at	Smad6_predicted
1374735_at	Prdm4	1374910_at	RGD:1303142	1375123_at	LOC360760

1374737_at	Sdccag10_predicted	1374912_at	RGD1309550_predicted	1375124_at	Nudt4
1374740_at	Esrra	1374913_at	Ppard	1375127_at	Lyric
1374778_at	F13a	1374918_at	Recc1	1375130_at	Mtch2_predicted
1374779_at	Znf22	1374920_at	RGD1306721_predicted	1375131_at	RGD1307892_predicted
1374780_at	Rabep1	1374921_at	RGD1311749_predicted	1375134_at	Gcn1l1_predicted
1374783_at	Prtfdc1_predicted	1374922_at	Nyw1	1375137_at	Syn3
1374784_at	LOC296985	1374924_at	Nab2	1375138_at	Dlgh2
1374786_at	Kcnf1	1374927_at	LOC360954	1375139_at	Mbnl2_predicted
1374787_at	Trp53bp1_predicted	1374932_at	Mcam	1375141_at	Sv2b
1374789_at	Gnptag_predicted	1374941_at	RGD1310955_predicted	1375142_at	Basp1
1374790_at	Pte1	1374943_at	RGD1308150_predicted	1375143_at	Timp2
1374792_at	Wdr3_predicted	1374944_at	MGC94251	1375148_at	Lrrc4b_predicted
1374811_at	Ptpn13	1374950_at	Obscn	1375153_at	Htatip
1374814_at	Stard3nl_predicted	1374965_at	Dcx	1375157_at	Lisch7
1374815_at	LOC363091	1374972_at	RGD1305137_predicted	1375160_at	Mrpl55_predicted
1374820_at	RABIN3	1374975_at	Soat1	1375162_at	Rab11b
1374826_at	Ndst2_predicted	1374978_at	LOC301122	1375163_at	Atp2a2
1374827_at	Pdia5	1374980_at	RGD1311135_predicted	1375168_at	Myo9b
1374834_at	Klhl12	1374981_at	Ppp1r16a_predicted	1375169_at	RGD:1303295
1374835_at	Rnu3ip2_predicted	1374982_at	Klhdc4_predicted	1375177_at	Akt1
1374836_at	Bcl7c_predicted	1374983_at	Epb4.1l5_predicted	1375180_at	Rpl12_predicted
1374837_at	Sp140_predicted	1374989_at	Rpl22	1375181_at	Slc3a1
1374838_at	RGD:727940	1374990_at	LOC287938	1375182_at	Idb4
1374842_at	Cbx3	1374992_at	RGD1304934_predicted	1375213_at	Galnt2_predicted
1375215_x_at	Pvrl2_predicted	1374994_at	Elmo3_predicted	1375214_at	Pgpep1
1375216_at	Mgea5	1375367_at	RGD1307773_predicted	1375502_at	RGD1308257_predicted
1375228_at	Klc1	1375370_at	LOC294429	1375503_at	Polg2_predicted
1375230_at	Cxxc5	1375373_at	Sqstm1	1375505_at	Adck5_predicted
1375244_at	Ppp2r1a	1375374_at	Rpl14	1375507_at	Kif2
1375247_at	Klf2	1375377_at	Qki	1375510_x_at	Neo1

1375249_at	B4galt1	1375378_at	Tap1	1375511_at	Par3
1375252_at	Nfe2l1_predicted	1375379_at	Gcl	1375546_at	Thap11_predicted
1375253_at	Slc35a1_predicted	1375380_at	SCIRP10	1375547_at	RGD1310351_predicted
1375257_at	Ascl1	1375381_at	Mdc1	1375548_at	Usp2
1375261_at	Egln1	1375383_at	Sp3	1375550_at	MGC94720
1375262_at	Alcam	1375387_at	Grp58	1375552_at	RGD1311742_predicted
1375270_at	Nek9_predicted	1375388_at	Shox2	1375556_at	Otp
1375271_at	Pi4KII	1375392_at	Bace	1375557_at	Rab34_predicted
1375272_at	Trim47_predicted	1375394_at	Znf324_predicted	1375565_at	Agtrap
1375273_at	Hipk3	1375395_at	Pum1_predicted	1375566_at	RGD1308684_predicted
1375275_at	LOC317374	1375400_at	Mvk	1375567_at	Socs1
1375277_at	Trim2_predicted	1375402_at	Rap2a	1375568_at	Glul
1375279_at	PNAS-4	1375403_at	Strbp	1375569_at	Notch4
1375280_at	Tbx2_predicted	1375404_at	Brinp3	1375574_at	Camk2b
1375283_at	Catnb	1375405_at	Fnbp1	1375575_at	Ddx28_predicted
1375285_at	Faf1	1375408_at	Grin2a	1375589_at	RGD1308290_predicted
1375287_at	Gcn1l1_predicted	1375410_at	Ndufa7_predicted	1375590_at	Cugbp2
1375296_at	LOC363474	1375411_at	Arsb	1375593_at	Gprk2l
1375298_at	Dullard_predicted	1375412_at	Sirt2	1375597_at	Camk4
1375299_at	Prkwnk1	1375413_at	RGD:727861	1375601_at	Rin2_predicted
1375300_at	Cgm3	1375414_at	LOC366468	1375606_at	Foxc2
1375304_at	LOC362256	1375423_at	Actr2_predicted	1375609_at	Pepp2
1375305_at	RGD1308120_predicted	1375424_at	RGD1309400_predicted	1375610_at	Hcn2
1375306_at	Cbx6_predicted	1375425_at	Khsrp	1375611_at	Hnrpa1
1375308_at	Hdlbp	1375437_at	Gosr2	1375612_at	Gata6
1375321_at	Sema6c	1375438_at	Wdr18_predicted	1375615_at	Apba2
1375322_at	Bat3	1375439_at	Ppil2_predicted	1375616_at	Camk2d
1375323_a_at	Cltb	1375440_at	Sars1	1375619_at	Prkar2a
1375327_at	RGD:727870	1375441_at	Mphosph10_predicted	1375621_at	Zfyve20_predicted

1375329_at	Hdh	1375454_at	Guca1a_predicted	1375624_at	RGD1311710_predicted
1375332_at	Akap6	1375457_at	Asrgl1	1375625_at	OSP94
1375334_at	RGD:1303075	1375458_at	Srpk2_predicted	1375626_at	RGD1307791_predicted
1375335_at	RGD:1303075	1375459_at	RGD1309441_predicted	1375629_at	RGD:1303103
1375337_at	Rab10	1375460_at	MGC109149	1375632_at	RGD:1303043
1375340_at	Kua_predicted	1375461_at	Ddr1	1375633_at	LOC299707
1375341_at	Nfic	1375468_at	Smarca4	1375635_at	Csnk2a1
1375350_at	LOC364534	1375472_at	Flt1	1375637_at	Sdpr
1375351_at	B4galt2_predicted	1375473_at		1375639_at	Fkbp9
1375355_at	RGD1310262_predicted	1375474_at	Dusp5	1375640_at	Arpc5l_predicted
1375356_at	Dyt1	1375475_at	Pygm	1375641_at	RGD:708345
1375358_at	Gfra2	1375476_at		1375645_at	RGD1308593_predicted
1375359_at	Rheb	1375477_at	RGD1306498_predicted	1375647_at	RGD1307966_predicted
1375360_at	Snag1_predicted	1375478_at	Slipr	1375649_at	Brd4_predicted
1375363_at	Stk11	1375480_at	Tead1	1375651_at	Ssr3
1375365_at	Zfp503	1375481_at	LOC362398	1375653_at	Ckap4_predicted
1375366_at	Pdlim2	1375482_at	RGD1305680_predicted	1375655_at	RGD1306873_predicted
1375660_at	Sox11	1375493_at	Nlgn3	1375658_at	Sec61a2_predicted
1375662_at	RGD1307608_predicted	1375801_at	Prss15	1376261_at	Uxs1
1375665_at	Dmtf1	1375802_at	Ptger1	1376262_at	RGD1306222_predicted
1375668_at	LOC293702	1375805_at	LOC299339	1376266_at	Slc16a6
1375672_at	Map3k1	1375806_at	Kcnk3	1376267_at	Arf6
1375673_at	RGD1310686_predicted	1375808_at	Yy1	1376268_at	Osbp2_predicted
1375676_at	Tob2	1375810_at	Pald_predicted	1376380_at	LOC497083
1375677_at	Mib1_predicted	1375812_at	LOC299569	1376382_at	Camk2g
1375680_at	RGD1304881_predicted	1375817_at	Lactb_predicted	1376383_at	Dusp19_predicted
1375681_at	Pura	1375818_at	RGD1307254_predicted	1376386_at	Alk
1375682_at	Cdc25a	1375822_at	Slc4a4	1376411_at	Gria4

1375683_at	Neu1	1375874_at	Kif5a	1376412_at	Apba1
1375684_at	Clasp1_predicted	1375875_at	RGD1308049_predicted	1376413_at	RGD1309414_predicted
1375685_at	Ppil3	1375876_at	Syt4	1376414_x_at	Mrrf_predicted
1375686_at	Rab14	1375877_at	RGD1307479_predicted	1376430_at	RGD:735103
1375687_at	Foxo1a	1375878_at	Gpr48	1376431_at	Tex27_predicted
1375690_at	RGD1310052_predicted	1375901_at	Gnao	1376435_at	RGD1308805_predicted
1375691_at	Mapk1	1375902_at	Yaf2_predicted	1376439_at	Rnf139_predicted
1375693_at	Rasip1_predicted	1375904_at	Leng8_predicted	1376440_at	RGD1305147_predicted
1375694_at	Ythdf2_predicted	1375906_at	Ascc1	1376443_at	Yy1
1375695_at	Ifnar1_predicted	1375909_at	Cdc42ep3_predicted	1376444_at	Il17b
1375696_at	RGD1307736_predicted	1375910_at	RGD:735140	1376445_at	MGC93707
1375712_at	Hes5	1375913_at	RGD1306967_predicted	1376446_at	LOC308341
1375713_at	LOC365661	1375914_at	Irak1bp1_predicted	1376447_at	Wdfy1
1375714_at	sarip	1375916_at	Gp49b	1376448_at	LOC304971
1375715_at	Ifngr2_predicted	1376159_at	LOC365510	1376449_at	Tmem5_predicted
1375716_at	Aes	1376160_at	RGD1306319_predicted	1376480_at	Adamts9_predicted
1375717_at	LOC498525	1376161_at	Col6a2_predicted	1376481_at	Mip1
1375718_at	Cdh13	1376162_at	RGD1305043_predicted	1376484_at	Traip_predicted
1375719_s_at	Gabbr1	1376163_at	Sf4_predicted	1376485_at	Sh3glb2_predicted
1375735_at	Etohi2	1376182_at	Dpp6	1376486_at	RGD:727859
1375736_at	Vamp5	1376183_at	Lynx1_predicted	1376487_at	LOC367171
1375737_at	Sprn	1376184_at	Kifc1	1376489_at	Sgtb
1375738_at	Ehd4	1376185_at	Waspip	1376490_at	Cdk9
1375739_at	Slc7a8	1376188_at	Zmym1_predicted	1376511_at	Ftsj2_predicted
1375740_at	Rps6ka4_predicted	1376189_at	Pik3r2	1376513_a_at	Arl3
1375742_at	LOC315776	1376190_at	Hpgd	1376515_at	RGD1309385_predicted
1375743_at	Foxd1	1376191_at	RGD1307096_predicted	1376518_at	Brp16
1375744_at	Gnaq	1376208_at	RGD1311310	1376521_at	Fabp3

			_predicted		
1375748_at	Sec3l1_predicted	1376209_at	Foxo3_predicted	1376522_at	Arid4a_predicted
1375752_at	RGD1308283_predicted	1376238_at	LOC362802	1376524_at	Khsrp
1375753_at	Impact	1376242_at	LOC304692	1376700_at	MGC94282
1375754_at	B4galt1	1376243_at	Slc6a11	1376711_at	Txndc4
1375756_at	Cdk6	1376246_at	Pck2_predicted	1376713_at	RGD1308119_predicted
1375759_at	Tob2	1376247_at	Sult2b1_predicted	1376714_at	RGD:735033
1375761_at	Dnajb5_predicted	1376248_at	RGD:1303053	1376717_at	RGD1306932_predicted
1375781_at	Fads1	1376249_at	Nufip1	1376718_at	RGD1305703_predicted
1375782_at	Grik5	1376250_at	Kif1b	1376719_at	Adck2_predicted
1375783_at	Egr4	1376253_at	RGD1308908_predicted	1376726_at	RGD1310157_predicted
1375788_at	Pthr1	1376254_at	Map4k1_predicted	1376728_at	RGD1309388_predicted
1375791_at	Znf532_predicted	1376255_at	Wdfy1_predicted	1376732_at	Igsf11_predicted
1375795_at	Igtp_predicted	1376256_at	Znf629_predicted	1376733_at	Nov
1376738_at	Ddx24	1376260_at	Bag5_predicted	1376737_at	RGD1310409_predicted
1376740_at	Hook3	1377048_at	RGD:708466	1377454_at	Slc6a11
1376744_at	Mss4	1377050_at	Mpv17l_predicted	1377485_at	Rbm16
1376745_at	Ldhd_predicted	1377051_at	Trim26	1377488_at	SREBP-2
1376750_at	Stk19	1377058_at	Mapk10	1377498_at	Hrc
1376753_at	Cars_predicted	1377059_at	Mccc2_predicted	1377502_at	Riok2_predicted
1376754_at	Rarb	1377060_at	RICS_predicted	1377505_at	Gdf1_predicted
1376760_at	Hdac4_predicted	1377061_at	LOC311573	1377513_at	Gnao
1376764_at	LOC361348	1377063_at	Dusp6	1377517_at	Camk1g
1376765_at	Fmnl1_predicted	1377076_at	Plxna3	1377523_at	RGD1307155_predicted
1376766_at	Gpr116	1377077_at	Ppp3cc	1377525_at	Snx27
1376768_at	LOC363135	1377078_at	Ppox_predicted	1377526_at	Msra
1376774_at	RGD1309969_predicted	1377079_a_at	RGD:708524	1377527_at	Cd47

1376775_at	LOC313519	1377080_at	Eif4a1	1379242_at	Ndufa6_predicted
1376776_at	Rbp3	1377086_at	Sec31l1	1379243_at	LOC299199
1376778_at	Foxo1a	1377090_at	Ng5	1379247_at	Galm
1376780_at	Glb1	1377133_at	LOC304809	1379272_at	Sostdc1
1376784_at	Sycp3	1377135_at	Mapk14	1379359_at	Pex11a
1376789_at	Galc	1377137_at	Sca10	1379371_at	Pdgfa
1376795_at	Rab14	1377138_at	Tbx5	1379458_at	Kif4
1376796_at	Csrp2bp_predicted	1377142_at	RGD:727783	1379740_at	Prss35
1376799_a_at	Chn2	1377144_at	LOC294614	1379884_at	Ddx42_predicted
1376800_at	LOC294291	1377145_at	RGD:621647	1379896_at	Tpm1
1376802_at	Rgs3	1377159_at	Ak3	1379936_at	Usp14
1376808_at	LOC304572	1377170_at	Lzts1	1379993_at	Sybl1
1376809_at	Adprtl1_predicted	1377178_at	Pqlc2_predicted	1380142_at	Immt_predicted
1376812_at	Grcc3f_predicted	1377181_at	Itgb3bp_predicted	1380158_at	Txnl1
1376815_at	Brca1	1377188_at	RGD1307390_predicted	1380192_at	Tcf8
1376834_at	Slc35b2	1377190_at	Atp5i	1380200_at	Gch
1376842_at	Bmpr2	1377194_a_at	Atp1b3	1380479_at	RGD1309034_predicted
1376843_at	Ap3b2_predicted	1377361_at	Kcnab1	1380513_at	LOC317260
1376844_at	isg12(b)	1377362_at	Rab25_predicted	1380517_at	LOC298250
1376845_at	Hlals	1377363_at	RGD1308908_predicted	1380546_at	Clcn3
1376848_at	Usp48	1377364_at	RGD1311019_predicted	1380547_at	Ddb2_predicted
1376849_at	Ccl27_predicted	1377366_at	Kazald1_predicted	1380933_at	RGD1309414_predicted
1376971_at	Slc40a1	1377367_at	Ncam1	1380979_a_at	RGD1309414_predicted
1376975_at	Sectm1	1377368_at	Cybrd1_predicted	1380980_at	Serpinf1
1376976_at	Ptger3	1377382_at	Efs_predicted	1381012_at	Spats1
1376985_at	Mettl3_predicted	1377384_at	Arhgap15	1381043_at	Usp14
1376986_at	RGD1309466_predicted	1377385_at	Atp2c1	1381084_at	LOC288717
1376987_at	Grip1	1377427_at	Lama5	1381499_at	LOC306805
1376997_at	RGD1308093_predicted	1377428_at	Lpo_predicted	1381505_at	Glmn
1376999_at	LOC293057	1377430_at	RGD1307648_predicted	1381636_at	Dcc
1377000_at	Nrcam	1377432_at	Zfp580_predicted	1381961_at	Rnpc2_predicted

1377002_at	Ugp2	1377433_at	Mfrp_predicted	1381980_at	Brunol4_predicted
1377003_at	Usp15	1377434_at	Camk4	1381995_at	Rod1
1377012_at	Wbscr14	1377435_at	Gpatc1_predicted	1382012_at	Arpc5l_predicted
1377013_at	RGD1308116_predicted	1377436_at	RGD1308217_predicted	1382016_at	Itgb3
1377024_at	Kif3a	1377437_at	Diras1_predicted	1382027_at	LOC289233
1377025_at	LOC314323	1377438_at	RGD1310081_predicted	1382028_at	Tbp
1377026_a_at	LOC314323	1377451_at	Tna_predicted	1382035_at	Atp6v1a1_predicted
1377040_a_at	Mfng	1377452_at	RGD1309108_predicted	1382048_at	RGD1304607_predicted
1382059_at	Ldhd_predicted	1377453_at	RGD:1303050	1382049_at	Fbxo30
1382061_at	Slc37a1_predicted	1385360_at	Gkn1	1386896_at	Hrmt1l2
1382087_at	MGC94168	1385372_at	Rpn2	1386897_at	Hspe1
1382099_at	Gnb5	1386592_at	Spdy1	1386898_at	Ctsh
1382105_at	LOC291844	1386596_at	Spdy1	1386899_at	RAMP4
1382117_at	RGD1307882_predicted	1386597_s_at	Art1_predicted	1386900_at	Cd36
1382262_at	Naga_predicted	1386598_at	Dusp3	1386901_at	Vdac3
1382285_at	LOC361366	1386604_at	Mrpl37	1386902_at	S100b
1382292_at	Ppp1r12a	1386606_at	Fbxo23_predicted	1386903_at	Cyb5
1382318_at	RGD1307315_predicted	1386614_at	RGD1309385_predicted	1386904_a_at	Prkar1a
1382345_at	Dhodh	1386831_at	Znf574_predicted	1386907_at	Glrx1
1382348_at	Stat6_predicted	1386836_at	Znf574_predicted	1386908_at	Vdac1
1382406_at	Nup155	1386837_x_at	RGD1311251_predicted	1386909_a_at	Apex1
1382413_at	Atp5s	1386838_at	Ppt2	1386910_a_at	Atp1a2
1383058_at	Gkap1_predicted	1386851_a_at	Ubb	1386911_at	Pcolce
1383059_a_at	Gkap1_predicted	1386856_a_at	Stmn1	1386912_at	Gp38
1383072_at	Ccnd1	1386857_at	Rpl13	1386913_at	Gmpr
1383075_at	Lamp2	1386858_at	Tkt	1386914_at	Anp32b
1383080_at	Aplp2	1386859_at	Mfge8	1386915_at	Aco1
1383102_at	Cul2_predicted	1386860_at	H2afz	1386916_at	Pc
1383106_at	Akt1	1386861_at	Anxa5	1386917_at	Oprs1
1383126_at	RGD1311612_predicted	1386862_at	Ppp1ca	1386918_a_at	RGD:620116
1383134_at	Ssh3_predicted	1386863_at	Pgam1	1386919_at	RGD:620116
1383138_at	Spock2_predicted	1386864_at	Sparcl1	1386920_x_at	Cpe
1383140_at	RGD1305441_	1386865_at	Ywhag	1386921_at	Ca2

	predicted				
1383141_a_at	Mrpl44_predicted	1386866_at	Brp44l	1386922_at	RGD:708345
1383338_at	Rev1l_predicted	1386867_at	Rps10	1386923_at	RGD:708345
1383406_at	Pstpip1_predicted	1386868_at	Actg2	1386924_at	Arpc1b
1383438_at	RGD1309314_predicted	1386869_at	Glul	1386925_at	Acsl5
1383460_at	LOC289233 /// Pex19_predicted /// Gm672_predicted	1386870_at	Gpx4	1386926_at	Cpt2
1383468_at	Mdm2_predicted	1386871_at	Igf2r	1386927_at	Bcat2
1383499_at	Rrbp1_predicted	1386872_at	Tnni1	1386928_at	Hk1
1383500_at	Hk2	1386873_at	Rps15	1386929_at	Psmd4
1384746_at	Ctrc_predicted	1386874_at	Clta	1386930_at	Tnni3
1384778_at	Cd3g_predicted	1386875_a_at	Adcy6	1386931_at	Gls
1384802_at	Hlf	1386876_at	Ap2s1	1386932_at	Gp2
1384811_at	Shc3	1386878_at	Lgals3	1386933_at	Slc6a8
1384833_at	MGC94788	1386879_at	Acaa2	1386934_at	Nr4a1
1384883_at	Col11a1	1386880_at	Igfbp3	1386936_at	Atp1b1
1384967_at	LOC361340	1386881_at	Tctex1	1386937_at	Anpep
1384970_at	Serpinb3	1386883_at	Prss11	1386938_at	Cacna1a
1384987_at	RGD1311019_predicted	1386884_at	Ech1	1386939_a_at	Timp2
1385003_at	Smarca4	1386885_at	Cd164	1386940_at	Plec1
1385047_x_at	Znf292	1386886_at	Cox5b	1386941_at	Golga2
1385065_at	Galm	1386887_at	Eif4ebp1	1386942_at	Tm4sf11
1385206_at	Pik4cb	1386888_at	Scd2	1386943_at	G6pc
1385241_at	Maf	1386889_at	S100a10	1386944_a_at	Prkab1
1385243_at	LOC305103	1386890_at	Pbp	1386945_a_at	Cpt1a
1385247_at	Ogn_predicted	1386891_at	Ptms	1386946_at	Cdh1
1385267_at	Npap60	1386892_at	Grn	1386947_at	Nes
1385312_at	Rab14	1386893_at	Hspd1	1386948_at	Mta1
1385337_at	Itga8	1386894_at	Maged1	1386949_a_at	Ppp1cb
1386951_at	Dncic2	1386895_at	Khdrbs1	1386950_at	Ndufa5
1386952_a_at	Hsd11b1	1387006_at	Gfra1	1387059_at	Copeb
1386953_at	Ak2	1387007_at	Sfxn3	1387060_at	Jup
1386955_at	Scarb1	1387008_at	Capn1	1387061_at	Chek1
1386956_at	Pom121	1387009_at	Scn1b	1387062_a_at	Ihpk2
1386957_at	Txnrd1	1387010_s_at	Lcn2	1387063_at	Pxmp3
1386958_at	Map2k5	1387011_at	Sart1	1387064_at	Plcd4
1386959_a_at	Slc37a4	1387012_at	Tmem27	1387065_at	Rgs12
1386960_at	Pfkm	1387013_at	Muc10	1387066_a_at	Lenep
1386961_at	Plcb4	1387014_at	Pfn2	1387067_at	Arc
1386962_at	Trip10	1387015_at	Sdfr1	1387068_at	Tbxa2r

1386963_at	Smgb	1387016_a_at	Sqle	1387069_a_at	Tmpo
1386964_at	Lpl	1387017_at	Argbp2	1387070_at	Mapt
1386965_at	Pkcbpb15	1387018_at	Atp5i	1387071_a_at	Prkwnk1
1386966_a_at	Rhoq	1387019_at	Cyp51	1387072_at	Snap25
1386967_at	Ppp1r1a	1387020_at	Wig1	1387073_at	Rgs2
1386968_at	Nrn1	1387021_at	Aldh1a1	1387074_at	Th
1386969_at	Eif2b4	1387022_at	Gstm3	1387075_at	Hif1a
1386970_at	Ppp1r10	1387023_at	Dusp6	1387076_at	Arpp19
1386971_at	Drpla	1387024_at	Dncic1	1387077_at	Inpp4a
1386972_at	Mapk8ip	1387025_at	Smc1l1	1387078_at	Gucy1a3
1386973_a_at	Phldb1	1387026_at	Lgals9	1387079_at	Cspg6
1386974_at	Pdk2	1387027_a_at	Id1	1387080_at	Rcn2
1386975_at	Kai1	1387028_a_at	Cfh	1387081_at	Fetub
1386976_at	Ca3	1387029_at	Abcc5	1387082_at	Ctf1
1386977_at	Bnip3l	1387030_at	Erp29	1387083_at	Dpp4
1386978_at	RGD:621571	1387031_at	Cck	1387084_at	Prps1
1386979_at	Apom	1387032_at	Ucp1	1387085_at	Camlg
1386980_at	Slc16a1	1387033_at	Pah	1387086_at	Cebpb
1386981_at	Mgat2	1387034_at	Arhgap17	1387087_at	Gal
1386982_at	Hmbs	1387035_a_at	Hes1	1387088_at	Prei3
1386983_at	Madh4	1387036_at	Cubn	1387089_at	Limk2
1386984_at	Gstm1	1387037_at	Ccs	1387090_a_at	Padi2
1386985_at	Ogfr	1387038_at	Gpc1	1387091_at	Fxyd4
1386986_at	Il6r	1387039_at	Mal	1387092_at	Slco1a4
1386987_at	Deaf1	1387040_at	Ubqln1	1387093_at	Slco1a4
1386988_at	Edg5	1387041_at	Cacnb3	1387094_at	Gnaz
1386989_at	Ebp	1387042_at	C4.4a	1387095_at	Hps1
1386990_at	Bad	1387043_at	Gpha2	1387096_at	Fut2
1386991_a_at	Pkn1	1387044_at	Atp6v0a1	1387097_at	Rpo1-4
1386992_at	Myh7	1387045_at	RGD:620744	1387098_at	Npr2
1386993_at	Btg2	1387046_at	Hspb3	1387099_at	Aqp3
1386994_at	Btg2	1387047_at	RGD:619920	1387100_at	Acsl4
1386995_at	Mrlcb	1387049_at	Kng1 /// MGC108747	1387101_at	Oprk1
1386996_at	Eif4e	1387050_s_at	Stau1	1387102_at	Dio2 /// Slc25a14
1386997_at	Aldoc	1387051_at	Gpt1	1387103_s_at	Scnn1a
1386998_at	Ywhab	1387052_at	Fmo1	1387104_at	RGD:620229
1387000_at	Ralb	1387053_at	Abcg1	1387105_at	Sh3bp4
1387002_at	Luzp1	1387054_at	Appbp1	1387106_at	Zbtb7
1387003_at	Nbl1	1387055_at	Axin1	1387107_at	Csnk2b
1387004_at	Ctss	1387056_at	Slc7a8 /// Syngap1	1387108_at	Por
1387005_at	Smp2a	1387057_at	Pctp	1387109_at	Nrd1
1387111_at	Plp	1387058_at	Stk39	1387110_at	Ddah1
1387112_at	Ctbp2	1387163_at	Lect1	1387215_at	Ldhc
1387113_at	Prkcd	1387164_at	Maf	1387216_at	Ghrh
1387114_at	Ikbkap	1387165_at	Aipl1	1387217_a_at	Tff3
1387115_at	Dnajb9	1387166_at	Slc7a1	1387218_at	Adm

1387116_at	Zfp265	1387167_at	C1qr1	1387219_at	Mcpt9
1387117_at	RGD:628626	1387168_at	Tle3	1387220_at	Gch
1387118_at	Mvk	1387169_at	Csnk2a1	1387221_at	Cript
1387119_at	Psmc3	1387170_at	Gria2	1387222_at	Aadat
1387120_at	Ndrg2	1387171_at	Tgfb2	1387223_at	Dgkb
1387121_a_at	Plagl1	1387172_a_at	Cma1	1387224_at	RGD:708423
1387122_at	Cyp17a1	1387173_at	Star	1387225_at	Inexa
1387123_at	Inha	1387174_a_at	Bat3	1387226_at	Waspip
1387124_at	S100a9	1387175_a_at	Rph3al	1387227_at	Slc2a2
1387125_at	Atp2c1	1387176_at	Vipr2	1387228_at	Ppig
1387126_at	Atrn	1387177_at	Cbs	1387229_at	Slc12a3
1387127_at	Adcy3	1387178_a_at	Adcy8	1387230_at	Mrs2l
1387128_at	Xrcc1	1387179_at	Il1r2	1387231_at	Bmp4
1387129_at	Slc40a1	1387180_at	Myf6	1387232_at	Hsd17b7
1387130_at	Serpini1	1387181_at	Gpr37	1387233_at	Azgp1
1387131_at	Lipe	1387182_at	Crot	1387234_at	Chga
1387132_at	Calb2	1387183_at	Axin2	1387235_at	Dctn4
1387133_at	Slfn3	1387184_at	Apbb3	1387236_at	Exoc7
1387134_at	Adam15	1387185_at	Rab9	1387237_at	Phox2a
1387135_at	Ptprv	1387186_at	Nat1	1387238_at	Padi4
1387136_at	Comp	1387187_a_at	Slc17a1	1387239_a_at	Rdh3
1387137_at	Tac2	1387188_at	Slc22a3	1387240_at	Gpr88
1387138_at	Hao2	1387189_at	Dgka	1387241_at	Prkr
1387139_at	Taok2	1387190_at	Pbsn	1387242_at	Cyp1a2
1387140_at	Dpysl5	1387191_at	Shank1	1387243_at	Cgrrf1
1387141_at	Polb	1387192_at	Spink1	1387244_at	Lipf
1387142_at	Ppp1r9b	1387193_a_at		1387245_at	RGD:619872
1387143_at	Itga1	1387194_at	St14	1387246_at	Pcsk1
1387144_at	Gjb1	1387195_at	Khdrbs3	1387247_at	Kcnj5
1387145_at	Ednrb	1387196_at	Omd	1387248_at	Biklk
1387146_a_at	Rab3c	1387197_at	Inpp5d	1387249_at	Pla2g10
1387147_at	Gprasp1	1387198_at	Arhgef9	1387250_at	Msmb
1387148_at	Arts1	1387199_a_at	Olig1	1387251_at	Sec14l2
1387149_at	Padi1	1387200_at	Rnf138	1387252_at	Guca2b
1387150_at	Nup107	1387201_at	Icam1	1387253_at	Ghrl
1387151_at	Nrbf2	1387202_at	Gckr	1387254_at	Aanat
1387152_at	Ril	1387203_at	Negr1	1387255_at	Adam1a
1387153_at	Npy	1387204_at	RT1-M3	1387256_at	Sct
1387154_at	Pcsk2	1387205_at	B4galt6	1387257_at	Pcmt1
1387155_at	Hsd17b2	1387206_at	Gja5	1387258_a_at	Cdh2
1387156_at	Pmfbp1	1387207_at	Ngb	1387259_at	Klf4
1387157_at	Mep1b	1387208_at	Rgpr	1387260_at	Ppp3cb
1387158_at	Ager	1387209_at	Dlgh4	1387261_at	Ssb
1387159_at	Kcne3	1387210_at	Barhl1	1387262_at	Pklr
1387160_at	Slc1a6	1387211_at	Mist1	1387263_at	Kcnk6
1387161_at	TPSB1	1387212_at	Pcsk4	1387264_at	Dgkg
1387162_at	HcRt	1387213_at	RGD:621508	1387265_at	RGD:620449
1387267_at	Rpo1-2	1387214_at	Agxt	1387266_at	Ntf3
1387268_at	Plaur	1387319_at	RGD:708527	1387374_at	Khk

1387269_s_at	Hhex	1387320_a_at	Atp1b4	1387375_at	Aox1
1387270_at	Phyh	1387321_at	Sema6b	1387376_at	Pak1
1387271_at	Eif2ak1	1387322_at	Klkb1	1387377_a_at	Fcnb
1387272_at	Il1rl1	1387323_at	Mak	1387378_at	Rock2
1387273_at	Dlx5	1387324_at	Slc27a5	1387379_at	Viaat
1387274_at	Sox11	1387325_at	Spam	1387380_at	Cit
1387275_at	RGD:621187	1387326_at	Khdrbs2	1387381_at	Hnmt
1387276_at	Lyn	1387327_at	Cyp2c	1387382_at	Gpr51
1387277_at	Ppara	1387328_at	Rnf38	1387383_at	Pld2
1387278_at	F11r	1387329_at	Mepe	1387384_at	Cntn1
1387279_at	Slc7a5	1387330_at	Atp4b	1387385_at	Foxj1
1387280_a_at	Pnck	1387331_at	Nmur2	1387386_at	Hpca
1387281_a_at	Cryac	1387332_at	Il5ra	1387387_at	Chp
1387282_at	Mx2	1387333_at	Mcpt6	1387388_at	Ramp3
1387283_at	Dpys	1387334_at	Abo /// LOC499761	1387389_at	Gzmk
1387284_at	Atp2b2	1387335_s_at	Nat8	1387390_at	Cdkn1a
1387285_at	Grm1	1387336_at	Cort	1387391_at	RGD:708561
1387286_at	Abcc9	1387337_at	Bcl2l11	1387392_at	Dlgh3
1387287_a_at	Neurod1	1387338_s_at	Sepp1	1387393_at	Il2rb
1387288_at	Apba2	1387339_at	Rtn3	1387394_at	Adora2b
1387289_at	Galnt10	1387340_at	Mbp	1387395_at	Hamp
1387290_at	Itih3	1387341_a_at	Gng5	1387396_at	Aqp4
1387291_at	Capn8	1387342_at	Cebpd	1387397_at	Pkia
1387292_s_at	Zp2	1387343_at	Aldh6a1	1387398_at	Pclo
1387293_at	Sh3bp5	1387345_at	Itgb1	1387399_at	Grin2a
1387294_at	Slc6a12	1387346_at	Igfbp5	1387400_at	Casq2
1387295_at	Cyp2j4	1387347_at	Igfbp5	1387401_at	Myh9
1387296_at	Klrg1	1387348_at	Shox2	1387402_at	Rgs8
1387297_at	Pga5	1387349_at	RGD:620551	1387403_at	Slc8a3
1387298_at	Miz1	1387350_at	Fbn1	1387404_at	Garnl1
1387299_at	Crnkl1	1387352_at	Akt2	1387405_at	Kist
1387300_at	Fgf1	1387353_at	Stat1	1387406_at	Nap1l3
1387301_at	Adcyap1r1	1387355_at	Wfs1	1387407_at	RGD:620778
1387302_at	Slc22a2	1387356_at	Tmlhe	1387408_at	Nlgn3
1387303_at	Uts2r	1387357_at	Arl1	1387409_x_at	Nr4a2
1387304_at	Cyp11b1 /// Cyp11b2	1387358_at	Stx1a	1387410_at	Ptprk
1387305_s_at	Egr2	1387359_at	Stx1a	1387411_at	Pip5k2a
1387306_a_at	Hal	1387360_at	Pgk1	1387412_at	Ncf1
1387307_at	Epo	1387361_s_at	Scn4a	1387413_at	Duox2
1387308_at	Grik1	1387362_at	Folh1	1387414_at	RGD:708517
1387309_a_at	RGD:620647	1387363_at	Folh1	1387415_a_at	Rest

1387310_at	Nox1	1387364_at	Nr1h3	1387416_at	Sh2bpsm 1
1387311_at	Gck	1387365_at	Ilf3	1387417_a_at	Slc6a2
1387312_a_ at	Myoc	1387366_at	Glg1	1387418_a_at	Chrna7
1387313_at	Sult1b1	1387367_at	Mras	1387419_at	Clic4
1387314_at	Sftpd	1387368_at	Sec15l1	1387420_at	Csen
1387315_at	Cxcl1	1387369_at	Tmod1	1387421_at	Pglyrp1
1387316_at	Avp	1387370_at	Cdc25a	1387422_at	Lhcgr
1387317_at	Kcnmb4	1387371_at	Slc6a13	1387423_at	Cntn2
1387318_at	Scya11	1387372_at	RGD:708410	1387424_at	Apba1
1387426_at	Rad50	1387373_at	Tcf12	1387425_at	Slc25a21
1387427_at	Cacnb1	1387479_at	Notch2	1387531_at	Fgf3
1387428_at	Adrbk1	1387480_at	Nptxr	1387532_at	Pspn
1387429_at	Hsf2	1387481_at	Grid2	1387533_at	Cyct
1387430_at	Kab	1387482_at	Plcg2	1387534_at	Gnrh1
1387431_at	Rod1	1387483_at	Tgfbr3	1387535_at	Scn5a
1387432_at	Slc25a27	1387484_at	Ppp2r2a	1387536_at	Ptprq
1387433_a_ at	Slc22a4	1387485_a_at	Trim9	1387537_at	Acaca
1387434_at	Siat8c	1387486_at	Calcr	1387538_at	Si
1387436_at	Fbxo2	1387487_a_at	Calcr	1387539_at	Brca1
1387437_at	Ltc4s	1387488_a_at	Extl3	1387540_at	Cspg3
1387438_at	Egfl3	1387489_at	Tgm4	1387541_at	Slc9a3
1387439_at	Ireb2	1387490_at	Gyk	1387542_at	Slc5a7
1387440_at	Kcnk3	1387491_at	Slco2a1	1387543_at	RGD:6211 65
1387441_at	Egr4	1387492_at	Akap5	1387544_at	Mtr
1387442_at	Btbd14b	1387493_at	RGD:620278	1387545_at	Crk7
1387443_at	Ptprh	1387494_at	Tle4	1387546_at	Eltd1
1387444_at	Phkg1	1387495_at	Cnga3	1387547_a_at	Has2
1387445_at	C1galt1	1387496_a_at	Npy5r	1387548_at	Ndst1
1387446_at	Arf3	1387497_at	Fgfr1	1387549_at	Slc14a2
1387447_at	Bet1l	1387498_a_at	Pdcl	1387550_a_at	Kcnh7
1387448_at	Tshr	1387499_a_at	Mid1	1387551_at	Dlgap2
1387449_at	Tgfa	1387500_at	Synpo	1387552_at	Sycp1
1387450_at	Dcbld2	1387501_at	Stk17b	1387553_at	Galnt5
1387451_at	Nfyb	1387502_at	Cpn1	1387554_at	Accn2
1387452_a_ at	RGD:708377	1387503_at	Il1rl2	1387555_at	Cntn6
1387453_at	Niban	1387504_at	Gnai1	1387556_at	Vps33a
1387454_at	Vldlr	1387505_at	Foxa3	1387557_s_at	Trpv4
1387455_a_ at	RGD:621479	1387506_at	Il1rap	1387558_at	Grin3b
1387456_at	Dusp12	1387507_at	Baat	1387559_at	RGD:6217 50
1387457_at	Rnf4	1387508_at	Dio3	1387560_a_at	Vipr1
1387458_at	Pkib	1387509_at	Snx16	1387561_at	Padi3
1387459_at	Sftpa1	1387510_at	Cyp2a1	1387562_at	Pgr
1387460_at	Oprm1	1387511_at	Zfp238	1387563_at	Slc8a2
1387461_at	Chrm3	1387512_at	Pscd3	1387564_at	Trpv6
1387462_at	Vcsa1	1387513_at	RGD:708495	1387565_at	Pla2g4a
1387463_at	Glra1	1387514_at	Nmbr	1387566_at	Slc21a1

1387464_at	Gnrhr	1387515_at	Pnliprp2	1387567_at	Pirb
1387465_a_at	Htr7	1387516_at	Syt13	1387568_at	Sv2c
1387466_a_at	Kcnj10	1387517_at	Crisp2	1387569_at	Manea
1387467_at	Sstr5	1387518_at	Vamp1	1387570_at	Nr2f1
1387468_at	Galr3	1387519_at	Drd4	1387571_at	Psd
1387469_at	Cldn1	1387520_at	Pdcd4	1387572_at	Nr5a2
1387470_at	Ela2	1387521_at	Rhag	1387573_a_at	Chrna2
1387471_at	Cd3d	1387522_at	Ptgdr	1387574_at	Rbbp9
1387472_at	Tnp1	1387523_at	Cysltr2	1387575_at	Trim17
1387473_at	Tacr1	1387524_at	Nxph4	1387576_at	Neurod2
1387474_at	Adarb2	1387525_at	Gpr27	1387577_at	P2rx2
1387475_at	Kcnd2	1387526_at	Syngr1	1387579_at	Srd5a2
1387476_at	Kcnk12	1387527_at	Mbl2	1387580_at	Pamci
1387477_at	Otx1	1387528_at	Tagln3	1387581_at	Pde7b
1387478_at	Runx3	1387529_a_at	Fosl2	1387582_a_at	Cyp26a1
1387584_at	Slc29a2	1387530_a_at	Msra	1387583_at	Shh
1387585_at	Csnk1g1	1387636_a_at	Fgf14	1387689_at	Casp3
1387586_at	Tnfsf6	1387637_a_at	Ctla4	1387690_at	Tnf
1387587_at	Ehd3	1387638_a_at	RGD:708491	1387691_at	Sstr1
1387588_at	Rims3	1387639_at	Fgf15	1387692_a_at	Slc6a9
1387589_at	Hrh4	1387640_at	Rab5a	1387693_a_at	Cnga4
1387590_at	Il2ra	1387641_at	Il23a	1387694_at	Cdc42bpb
1387591_at	Akt3	1387642_at	Fgf21	1387695_at	Glra2
1387592_at	Pwwp1	1387643_at	Btc	1387696_a_at	Kcnh5
1387593_at	Qtrt1	1387644_at	Ucn	1387697_at	Kcnj11
1387594_at	Gif	1387645_at	Max	1387698_at	Cnga2
1387595_at	F2rl1	1387646_a_at	RGD:620707	1387699_at	Cckar
1387596_at	Dmrt1	1387647_at	RGD:708540	1387700_at	Hgf
1387597_at	Thpo	1387648_at	RGD:708411	1387702_at	Usp2
1387598_at	Nqo1	1387649_at	Prok1	1387703_a_at	Esr1
1387599_a_at	Gabrp	1387650_at	Aqp1	1387704_at	Sstr4
1387600_at	Dcx	1387651_at	Ide	1387705_at	Gabrg1
1387601_at	Htr3b	1387652_at	Tsnax	1387706_at	Slc2a3
1387602_a_at	Klrc2	1387653_at	RGD:620443	1387707_at	Adra2a
1387603_at	Dffb	1387654_at	Cxcl12	1387708_at	Figf
1387604_at	Casp12	1387655_at	Slc4a1	1387709_at	Oxtr
1387605_at	Fgf2	1387656_at	Kif3c	1387710_at	Il10
1387606_at	Gpr74	1387657_at	Eef2k	1387711_at	Hes3
1387607_at	Indo	1387658_at	Gda	1387712_at	Fcer1a
1387608_at	Ca5a	1387659_at	Iapp	1387713_a_at	Crem
1387609_at	Mcp	1387660_at	Oprl	1387714_at	Expi
1387610_at	Bcl2	1387661_a_at	Syt4	1387715_at	Utrn
1387611_at	Hoxa1	1387662_at	Gmfb	1387716_at	Plcb2
1387612_at	Npy2r	1387663_at	Atp6v1b2	1387717_at	P2rx7
1387613_at	Sycp3	1387664_at	Bhmt	1387718_at	Clcn1
1387614_at	Siat8b	1387665_at	Gpr85	1387719_at	Clstn2
1387615_at	Pdgfc	1387666_at	Nos2	1387720_at	Adora1
1387616_at	RGD:621546	1387667_at	Ptpn11	1387721_at	Cyp2b15
1387617_at	Bcl2l10	1387668_at	Ephx1	1387722_at	Sema3a

1387618_at	Crebbp	1387669_a_at	Gpd2	1387723_at	Omp
1387619_at	RGD:620654	1387670_at	Sctr	1387724_at	Gulo
1387620_a_at	Tnfrsf4	1387671_at	Gnmt	1387725_at	Cdx2
1387621_at	Rfng	1387672_at	Anxa6	1387726_at	Chrng
1387622_at	Stc1	1387673_a_at	Cnr1	1387727_at	Il10ra
1387623_at	Usf1	1387675_at	Mark1	1387728_at	Ggtla1
1387624_at	Igfbp6	1387676_at	Pou3f4	1387729_at	Pax8
1387625_at	Dck	1387677_at	Nras	1387730_at	Gja3
1387626_at	Cd86	1387678_at	Slc21a10	1387731_at	Mterf
1387627_at	Tas2r10	1387679_at	Pde1b	1387732_at	Drd3
1387628_at	Bspry	1387680_at	Ucp3	1387733_at	Bmp15
1387629_at	Elovl5	1387681_at	Trhr	1387734_at	RGD:631408
1387630_at	Hpgd	1387682_at	Crhr1	1387735_at	Chrm1
1387631_at	RGD:708453	1387683_at	Ppard	1387736_at	Mat2a
1387632_at	Prg2	1387684_at	Freq	1387737_at	Mycs
1387633_at	Amelx	1387685_at	Mos	1387738_at	Cd8b
1387634_a_at	Hmga2	1387686_at	Igsf6	1387739_at	Pex11a
1387635_at	RGD:621692	1387687_at	Htr6	1387740_at	Htr1b
1387742_at	Gpr20	1387688_at	Kcnab2	1387741_at	Ccr2
1387743_at	Nppc	1387801_at	Dlgap1	1387865_at	Myo9b
1387744_at	Mox2r	1387802_at	Ppp2r2b	1387867_at	Lbp
1387745_at	Olr414_predicted	1387803_at	Trim63	1387868_at	Rabggta
1387746_at	Gjb3	1387804_at	Bnip3	1387869_s_at	Zfp36
1387747_at	Lep	1387805_at	Rap1b	1387870_at	Cfl1 /// LOC315997
1387748_at	Cd79b	1387806_at	Pafah1b1	1387871_at	Hnrpa1
1387749_at	Twist1	1387807_at	Slc7a7	1387872_at	Wfdc1
1387750_at	RGD:621851	1387808_at	Map2k6	1387873_at	Dbp
1387751_at	Htr2a	1387809_at	Keap1	1387874_at	Ptk2
1387752_s_at	Magi3	1387810_at	Agt	1387875_at	Stat5b
1387753_s_at	Tacr2	1387811_at	Pace4	1387876_at	Ftcd
1387754_at	Tgoln2	1387813_at	Cav3	1387877_at	Glud1
1387755_s_at	Hemgn	1387816_at	Nsg1	1387878_at	Cugbp2
1387756_s_at	RGD:708471	1387817_at	Casp11	1387879_a_at	Cugbp2
1387757_at	RGD:621650	1387818_at	Ela1	1387880_at	Kcnv1
1387758_at	Ugt1a1 /// Ugt1a6 /// RGD:620950 /// Ugt1a8 /// Ugt1a2 /// Ugt1a4 /// Ugt1a11	1387819_at	Klk7	1387881_at	Bteb1
1387759_s_at	Onecut1	1387820_at	Rab3ip	1387882_at	Tmsb4x
1387760_a_	Prp15	1387821_at	Gna11	1387883_a_at	Psma5

at					
1387761_at	Jund	1387822_at	Plrg1	1387884_at	Fcgrt
1387762_s_at	Rab27a	1387824_at	Ugt2b	1387885_at	Prelp
1387763_at	Cebpe	1387825_at	Pdxk /// LOC361819	1387886_at	Rpl14
1387764_at	Mlb1	1387826_at	Hist3h2ba_predicted	1387887_at	Rps9
1387765_at	Rbp2	1387827_x_at	Centg1	1387888_at	Folr1
1387766_a_at	Col2a1	1387828_at	Slc24a1	1387889_at	Rps29
1387767_a_at	Mb	1387831_at	Bche	1387890_at	Prdx4
1387768_at	Id3	1387832_at	Tmprss2	1387891_at	Tubb5
1387769_a_at	RGD:1303168	1387833_at	Matk	1387892_at	C1s
1387770_at	Mapk3	1387834_at	Il1rn	1387893_at	Gata4
1387771_a_at	Calm1	1387836_at	Apc	1387894_at	Cdc20
1387772_at	Cycs	1387837_at	Lalba	1387895_s_at	Scp2
1387773_at	Ywhaz	1387839_at	Acp1	1387896_at	Cnp1
1387775_at	Tgm2	1387840_at	RGD:708408	1387897_at	Hspb6
1387776_at	Ilk	1387842_at	Fst	1387898_at	Crmp1
1387779_at	Dnaja2	1387843_at	Lasp1	1387899_at	Cdipt
1387780_at	Pmpcb	1387845_at	Cacna1f	1387900_at	Ptprd
1387781_at	Dlc2	1387847_at	Hmgcr	1387902_a_at	Pja2
1387782_at	Acaa1	1387848_at	Epn2	1387903_at	Ihpk1
1387784_at	Mtpn	1387849_at	Tmeff1	1387904_at	Jdp1
1387785_at	Mtpn	1387850_at	Pter	1387905_at	Gnas
1387786_at	Myl2	1387851_at	Thrsp	1387906_a_at	Itpr1
1387787_at	Junb	1387852_at	Acr	1387907_at	Rasd1
1387788_at	Erg	1387853_at	Col1a2	1387908_at	Abi2
1387789_at	Paics	1387854_at	Gdi1	1387909_at	Epb4.1l1
1387790_at	Ace	1387855_at	Cnn3	1387910_at	Rabggtb
1387793_at	Fcna	1387856_at	Stx7	1387911_at	Ddx46
1387795_at	Alox15	1387857_at	Ppp4r1	1387912_at	Cyp2d22
1387796_at	Rab7	1387859_at	Capn2	1387913_at	Cyp27a1
1387797_at	Crry	1387860_at	Aes	1387914_at	RGD:628897
1387798_a_at	Fxyd2	1387861_at	Ywhaq	1387915_at	RGD:708365
1387799_at	Daxx	1387862_at	RGD:619726	1387916_at	Lap1b
1387800_at	Ppp6c	1387863_at	Kidins220	1387917_at	RGD:708368
1387919_at	Man2c1	1387864_at	Dutp	1387918_at	Mfn2
1387920_at	Npuk68	1387974_a_at	Ugcg	1388029_at	Gabbr1
1387921_at	Lgl1	1387975_at	Slc9a3r2	1388030_a_at	RGD:708503 /// Mup5
1387922_at	Znf179	1387976_at	Nbn	1388031_x_at	Gm1960
1387923_at	RGD:628687	1387977_at	RGD:708360	1388032_a_at	Gm1960
1387924_at	Asns	1387978_at	RGD:708429	1388033_at	Kif1b
1387925_at	Sc5d	1387979_at	Ctsq	1388034_at	Scn5a
1387926_at	Olfm1	1387980_at	Olr59	1388035_a_at	RGD:7085

					61
1387927_a_at	Rap2ip	1387981_at	Tlr4	1388036_a_at	Atp2b3
1387928_at	RGD:620149	1387982_at	Thrb	1388037_at	Atrn
1387929_at	Reg3a	1387983_at	Cklf1	1388038_at	Gabbr1
1387930_at	Cryge	1387984_at	RGD:708508	1388039_a_at	Myr8
1387931_at	Slc1a1	1387985_a_at	Scnn1g	1388040_a_at	Nfasc
1387932_at	Podxl	1387986_at	Slc22a19	1388041_s_at	Kcnh8
1387933_s_at	Bcan	1387987_at	Hsd3b1	1388042_at	Atp4a
1387934_at	Il3ra	1387988_at	Grm6	1388043_at	Pfkfb2
1387935_at	LOC361510	1387990_at	Capn8	1388044_at	Cdh22
1387936_at	Tpbpa	1387992_at	RGD:735174	1388045_a_at	Itgam
1387937_at	Baalc	1387993_at	Hsd17b9	1388046_at	RGD:708402
1387938_at	Pnrc1	1387994_at	Ifitm3	1388047_at	Inpp4b
1387939_at	Eif2b5	1387995_a_at	Hps1	1388048_a_at	Gabre
1387940_at	Pla2g6	1387996_a_at	Hcn4	1388049_a_at	RGD:708442
1387941_s_at	RGD:708484	1387997_at	Exoc8	1388050_at	Slc26a3
1387942_at	Defa	1387998_at	Slc18a1	1388051_at	Kcnq3
1387943_at	Ccdc5	1387999_at	Slc24a2	1388052_a_at	Cdk5rap1
1387945_at	Lgals3bp	1388000_at	Lrrc21	1388053_at	Cspg2
1387946_at	Mafb	1388001_at	RGD:708455	1388054_a_at	RGD:708364
1387947_at	Ick	1388002_at	Nfya	1388055_at	RGD:708393
1387948_at	Cyp2c70	1388003_at	Gpr37l1	1388056_at	Dlgap1
1387949_at	RGD:620069	1388004_at	Pprf18	1388057_a_at	Taf6_predicted
1387950_at	Daf1	1388005_at	RGD:708547	1388058_at	Slc11a2
1387951_at	Cd44	1388006_at	Amelx	1388059_a_at	Syt12
1387952_a_at	Coil	1388007_x_at	RGD:621262	1388060_at	Epha7
1387953_at	Grip2	1388008_at	RGD:621262	1388061_a_at	RGD:628675
1387954_a_at	RGD:628623	1388010_at	Tgfb2	1388062_at	Pfkfb2
1387955_at	Cklf1	1388011_a_at	Prrxl1	1388063_a_at	Slc1a3
1387956_s_at	Sh3kbp1	1388012_at	Cd80	1388064_a_at	Insrr
1387957_a_at	RGD:708428	1388013_at	Obp1f	1388065_at	Gprk6
1387958_at	RGD:708388	1388014_at	Ptprz1	1388066_a_at	Gmeb2
1387960_at	Opcml	1388015_at	Grip2	1388067_a_at	Klc3
1387961_at	RGD:631380	1388016_a_at	RGD:708583	1388068_at	Klrb1b
1387962_at	Uox	1388017_at	Sele	1388069_at	Akap1
1387963_a_at	Ero1l	1388018_at	Odf2	1388070_a_at	RT1-Aw2
1387964_a_at	Havcr1	1388019_at	Pde1c	1388071_x_at	Sbk
1387965_at	Asrgl1	1388020_a_at	Sfrp4	1388072_at	Nupl1
1387967_at	Slc6a15	1388021_at	Dnm1l	1388073_a_at	Krt20

1387968_at	Cxcl10	1388022_a_at	Cacnb2	1388074_at	Bach
1387969_at	Slc38a5	1388023_a_at	Lap1b	1388075_at	Pairbp1
1387970_at	Mapk8ip	1388024_s_at	Opn1sw	1388076_at	P2rx3
1387971_a_at	Mucdhl	1388025_at	Cd3z	1388077_a_at	Accn2
1387972_at	RGD:708363	1388026_at	Rtn4	1388078_a_at	Cacng8
1387973_at	RGD:621387	1388027_a_at	Ttl	1388079_at	Hrh3
1388082_at	Casp9	1388028_at	Anubl1	1388081_at	Dusp4
1388083_a_at	Klra22	1388138_at	Myh4	1388197_at	Nupl1
1388084_at	Gpx6	1388139_at	Rab13	1388198_at	Tacstd1
1388085_at	Rest	1388140_at	Cetn3	1388200_at	Bmp6
1388086_a_at	V1rb9	1388141_at	Cspg2	1388201_at	RT1-Aw2
1388087_at	Usf2	1388142_at	Col18a1	1388202_at	RT1-Aw2 /// RT1-T24-1 /// RT1-CE14 /// RT1-CE2 /// RT1-CE15 /// RT1-CE10
1388088_a_at	Rnf4	1388143_at	Bfsp1	1388203_x_at	Mmp13
1388089_a_at	Epor	1388144_at	Tnxa	1388205_at	Eif5
1388090_a_at	Olr1500	1388146_at	Muc3	1388206_a_at	RGD:735046
1388091_at	Olr1493	1388147_at	Lrpap1	1388207_at	Ret
1388092_at	Tas2r41	1388148_a_at	Tap1	1388208_a_at	RGD:621142
1388094_at	RGD:727822	1388149_at	Xpo1	1388209_at	Mte1
1388095_at	Kitl	1388150_at	Coro7	1388210_at	Cte1 /// Mte1
1388096_at	Cacng5	1388151_at	Mtap2	1388211_s_at	RT1-S3
1388097_at	RGD:727877	1388152_at	Acsl1	1388212_a_at	RT1-S3
1388098_at	Tfpt	1388153_at	Sap2	1388213_a_at	Pcsk5
1388099_a_at	Cdk5rap2	1388155_at	Plcb3	1388214_at	Pvrl1
1388100_at	Dpysl3	1388156_at	LOC294446	1388215_at	RGD:621664
1388101_at	Ltb4dh	1388157_at	Bat1a	1388216_at	Calu
1388102_at	Pr1	1388159_at	Idh3B	1388217_a_at	Ldlr
1388103_at	Gpr48	1388160_a_at	Adam10	1388218_at	Htr5b
1388104_at	RGD:619766	1388161_at	Kcnc3	1388219_at	Pou2f3
1388105_at	RGD:727814	1388162_a_at	Slc25a5	1388220_at	Slc24a3
1388106_x_at	Ppp2r2d	1388163_at	RT1-S3	1388221_at	Tert
1388107_at	Elovl6	1388164_at	RGD:735095	1388222_at	Gnat3
1388108_at	Gpr116	1388167_at	Fgfr2	1388223_at	Sec14l3
1388109_at	Eef1a1	1388168_a_at	RGD:708458	1388224_at	Kcnc2
1388110_at	Eln	1388169_at	RGD:621566	1388225_at	Olr1271
1388111_at	Slc25a4	1388170_at	Cdk7	1388226_at	Hlals

1388112_at	Cox8a	1388171_at	RGD:621104	1388227_at	Mthfr
1388113_at	LOC501203	1388172_at	Kcnd1	1388228_at	Mug1
1388114_at	Svs3	1388173_at	Wnt2b	1388229_a_at	Jub
1388115_at	Col1a1	1388174_at	Clcnkb	1388230_at	RGD:735036
1388116_at	Snrpb	1388175_at	Cml5	1388231_at	Lepr
1388117_at	Hibadh	1388176_at	Ddn	1388232_a_at	Cish
1388118_at	LOC288146 /// RGD:727807	1388177_at	Ncoa3	1388234_at	VCS-beta1
1388119_at	Pdcd6ip	1388178_at	Acvr2b	1388235_at	RT1-CE12
1388120_at	Aplp2	1388179_at	RGD:708448	1388236_x_at	Atp2b3
1388121_at	Gstp1 /// Gstp2	1388181_at	RGD:621380	1388238_at	Per3
1388123_at	Ctsj	1388182_at	CSN1S1	1388239_at	Itga7
1388124_at	Kns2	1388183_at	Icmt	1388240_a_at	Insl3
1388125_a_at	Minpp1	1388184_at	Rb1	1388241_at	Gm1012
1388126_at	RGD:708530	1388185_at	RGD:708437	1388242_at	Gm1012
1388127_at	Actr3	1388186_at	Camk2a	1388243_at	Lamr1
1388128_at	Ssrp1	1388187_at	Cyp7b1	1388244_s_at	Nrg1
1388131_at	Sfpq	1388188_at	Grm3	1388245_a_at	Clu
1388132_at	Pippin	1388189_at	Apob	1388248_at	Rapgef1
1388133_at	Eef1d	1388190_at	Chrm4	1388249_at	Nfib
1388134_at	Rpa2	1388191_at	Rwdd3	1388250_at	RGD:620961
1388135_at	RGD:621656	1388193_at	Dlat	1388252_at	Scd2
1388136_at	RGD:628711	1388194_at	Cugbp2	1388254_a_at	RT1-CE5
1388137_a_at	Thbs4	1388195_at	Nckap1	1388255_x_at	
1388257_at	Nrg1	1388196_at	Hoxa4	1388256_at	RGD:708527
1388258_at	Snrpn	1388326_at	LOC294362_predicted	1388424_at	RGD1305890_predicted
1388259_at	Lepr	1388327_at	Eif3s2	1388425_at	Srebf1
1388260_a_at	RGD:621750	1388329_at	RGD:1303107	1388426_at	1200013a08rik
1388261_at	Kcna6	1388330_at	Tra1_predicted	1388429_at	Ptov1_predicted
1388262_at	Kcna6	1388332_at	Rbx1_predicted	1388430_at	Ss18_predicted
1388263_at	Spnb1	1388334_at	Tagln2_predicted	1388431_at	Optn
1388264_at	Cspg2	1388336_at	Np	1388432_at	Krt1-19
1388265_x_at	Fgb	1388338_at	Pea15_predicted	1388433_at	C12orf10
1388266_at	Mt1a	1388350_at	RGD1305831_predicted	1388437_at	Nap1l4_predicted
1388267_a_at	RGD:621546	1388351_at	Nat5_predicted	1388438_at	LOC360627
1388268_at	Hbg1	1388352_at	RGD:1302994	1388439_at	LOC300802
1388269_at	Hbe1_predicted	1388353_at	LOC296126	1388441_at	Canx
1388271_at	Igh-	1388354_at	Rbm17_predi	1388442_at	Cdk2ap1_

	1a_predicted		cted		predicted
1388272_at	Ly6c /// LOC300024 /// Ly6a_predicted	1388355_at	S100a16_predicted	1388443_at	Ubxd2_predicted
1388273_at	Bmyc	1388357_at	RGD:1303312	1388444_at	Anxa11_predicted
1388275_at	Hist1h4a_predicted	1388358_at	Eif4g2	1388452_at	RGD:727835
1388276_at	LOC363828	1388359_at	Npepps	1388454_at	Gng10
1388277_at	Hspa1l	1388361_at	LOC290671	1388455_at	S100a1
1388278_at	Sry	1388362_at	Raly_predicted	1388456_at	RGD:735220
1388279_at	Dlgh3	1388363_at	Ndufs3_predicted	1388457_at	Rfc4_predicted
1388280_a_at	LOC309584	1388364_at	Atp6v0d1_predicted	1388458_at	Col18a1
1388281_at	Klra5 /// Ly49s7	1388365_at	Mrpl4_predicted	1388459_at	Capg_predicted
1388286_a_at	LOC497985	1388366_at	Pole4_predicted	1388460_at	LOC316507
1388287_at	Slco2b1	1388367_at	RGD1305875_predicted	1388462_at	MGC94635
1388288_at	Fshb	1388368_at	RGD1307627_predicted	1388465_at	Psmd3_predicted
1388291_at	Kcnj3	1388371_at	RGD:1303007	1388466_at	Sgta
1388293_at	Sdhd	1388372_at	RGD:1303151	1388509_at	LOC287873
1388295_s_at	Rps18	1388374_at	Prkar1a	1388510_at	Centd2_predicted
1388296_at	RGD:1302939	1388377_at	Eif3s8_predicted	1388511_at	Pde6d_predicted
1388299_at	Mgst3_predicted	1388378_at	Ptpn11	1388543_at	Bpgm
1388300_at	RGD:1303314	1388379_at	RGD:1303219	1388544_at	Smoc1
1388301_at	Andpro	1388380_at	Eif3s4_predicted	1388546_at	Cldn4_predicted
1388302_x_at	Rpl26_predicted	1388381_at	LOC361985	1388547_at	RGD1309752_predicted
1388303_at	Ndufb5_predicted	1388383_at	Dnclc1	1388548_at	Msmb
1388304_at	Araf1	1388384_at	Cryba2	1388549_at	LOC298012
1388305_at	RGD1305593_predicted	1388386_at	Ubadc1	1388550_at	Pcdhga10_predicted
1388306_at	Tde2	1388389_at	RGD:735178	1388551_at	Smpd1
1388308_at	Hmga1	1388390_at	LOC363441	1388553_at	Bzw1
1388309_at	Sui1-rs1_predicted	1388391_at	Tax1bp3_predicted	1388554_at	Txnl5_predicted
1388310_at	RGD:628631	1388392_at	Plp2	1388555_at	Stx6
1388311_at	Timp2	1388393_at	Aars_predicted	1388557_at	Ak3
1388312_at	Rps25	1388394_at	G0s2_predicted	1388558_at	Ube2m_predicted

1388313_at	Hmgn1_predicted	1388395_at	RGD:727809	1388559_at	LOC310769
1388314_at	LOC299310	1388396_at	Ebna1bp2_predicted	1388561_at	Stard7_predicted
1388315_at	LOC296207	1388407_at	RGD1307129_predicted	1388562_at	RGD1305492_predicted
1388317_at	Pgk1	1388409_at	Ugp2_predicted	1388563_at	RGD:1303127
1388319_at	RGD:735123	1388410_at	RGD1304593_predicted	1388564_at	Spg21
1388320_at	RGD1306825_predicted	1388412_at	Rrbp1_predicted	1388565_at	Lasp1
1388323_at	Nit1	1388413_at	Ndufs5b_predicted	1388566_at	Thumpd1_predicted
1388324_at	RGD:735119	1388421_at	Lims2_predicted	1388567_at	RGD:1303255
1388325_at	Ndufs8_predicted	1388422_at	RGD:1302996	1388568_at	Serpinf1
1388570_at	Syngr2	1388423_at	Eif3s1_predicted	1388569_at	Polr2c_predicted
1388580_at	Hn1	1388756_at	Adrbk1	1388867_at	Zfp216_predicted
1388581_at	Psme3_predicted	1388757_at	Ogt	1388868_at	Tbce_predicted
1388585_at	Synj1	1388758_at	Clic4	1388871_at	Idi1
1388592_at	JSAP1	1388759_at	Slc35b4_predicted	1388872_at	Gtl6_predicted
1388600_at	Abt1_predicted	1388760_at	Hdac1_predicted	1388874_at	Cxxc1_predicted
1388601_at	Adn	1388764_at	Akt2	1388875_at	Pin
1388602_at	Hbld2	1388765_at	Mtx2_predicted	1388876_at	Mrps5_predicted
1388607_at	Hba-a1	1388766_at	Pdcd6_predicted	1388877_at	RGD:735222
1388608_x_at	Plekhm2_predicted	1388774_at	RGD1305356_predicted	1388881_at	Fkbp3_predicted
1388611_at	Ociad1	1388775_at	MGC94600	1388882_at	Pold4_predicted
1388612_at	Hbld2	1388776_at	Ssr3	1388883_at	RGD1310224_predicted
1388614_at	RAP-1A	1388781_at	Tcf21	1388884_at	RGD1311546_predicted
1388615_at	MGC72955	1388782_at	Hmgb1	1388886_at	Ggta1
1388616_at	Bphl_predicted	1388783_at	LOC307403	1388899_at	LOC361797
1388618_at	Rdx	1388784_at	Dnalc4_predicted	1388900_at	Fkbp5_predicted
1388620_at	LOC287456	1388789_at	RGD1310857_predicted	1388901_at	Loxl1_predicted
1388621_at	Nol5a_predicted	1388790_at	RGD1309930_predicted	1388902_at	Tcte1l
1388641_at	Ei24_predicted	1388791_at	Gadd45g_predicted	1388903_at	RGD:735185

1388642_at	RGD:1303096	1388792_at	Pigq	1388904_at	RGD1311136_predicted
1388643_at	Mgll	1388793_at	Rbmxrt_predicted	1388907_at	Peci
1388644_at	RGD1307982_predicted	1388795_at	Gosr1	1388909_at	Mrps24_predicted
1388658_at	Carhsp1	1388796_at	U2af2_predicted	1388910_at	Prim2
1388659_at	LOC302500	1388797_at	Ube2e2_predicted	1388911_at	Xpmc2h_predicted
1388660_at	MGC94604	1388798_at	Klhl7_predicted	1388912_at	Ppap2c
1388663_at	LOC362938	1388799_at	Rab5a	1388916_at	Myo1c
1388664_at	RGD1308134_predicted	1388804_at	Ppp2ca	1388917_at	Hdlbp
1388665_at	RGD:1303152	1388806_at	Csrp2bp_predicted	1388919_at	Bmp6
1388668_at	Sf3a3_predicted	1388807_at	Polr2a	1388921_at	Aip
1388670_at	Doc2b	1388808_at	Smpdl3a	1388923_at	Angptl4
1388678_at	Tbc1d14_predicted	1388809_at	Abce1_predicted	1388924_at	RGD:1303285
1388679_at	RGD1311230_predicted	1388810_at	Syn2	1388925_at	Enpp5
1388680_at	Sara2_predicted	1388812_at	Arf2	1388926_at	Rabl4_predicted
1388681_at	Cnih_predicted	1388813_at	RGD:1303136	1388929_at	RGD1305625_predicted
1388682_at	LOC287429	1388830_at	Slc9a3r2	1388930_at	MGC105961
1388683_at	Fnbp4_predicted	1388831_at	Dhrsx_predicted	1388931_at	Lama5
1388685_at	Dscr1	1388832_at	MGC94182	1388933_at	Vps16
1388686_at	Dhdds_predicted	1388835_at	Prkch	1388940_at	RGD1304846_predicted
1388690_at	RGD1308273_predicted	1388843_at	Zfp523_predicted	1388942_at	Chrac1_predicted
1388692_at	RGD1310875_predicted	1388844_at	Svop	1388943_at	Sox11
1388694_at	Shmt2_predicted	1388846_at	Faf1	1388945_at	RGD1311910_predicted
1388695_at	Ufd1l	1388847_at	RGD1308350_predicted	1388946_at	Eif5b
1388697_at	Ecm1	1388849_at	Hspca	1388951_at	RGD1307935_predicted
1388698_at	Man2b1	1388850_at	Hspa9a_predicted	1388952_at	Gnl3
1388708_at	LOC362703	1388851_at	LOC361578_predicted	1388954_at	MGEPS
1388712_at	Thtpa	1388852_at	Mrpl54_predicted	1388957_at	Slc2a4

1388714_at	Gars_predicted	1388854_at	Cul1_predicted	1388969_at	Rasip1_predicted
1388715_at	RGD:1302972	1388855_at	Kitl	1388970_at	Krtdap
1388717_at	Tmod1	1388857_at	Map2k3_predicted	1388971_s_at	Rtn4r
1388718_at	Ubqln1	1388859_at	Mrpl22_predicted	1388972_at	Col9a1_predicted
1388754_at	Sec23a	1388860_at	RGD1307896_predicted	1388973_at	Srp19_predicted
1388755_at	RGD1311399_predicted	1388861_at	Txnl1	1388975_at	RGD1305975_predicted
1388977_at	MGC94262	1388862_at	LOC298317	1388976_at	MGC95031
1388979_at	RGD:735078	1389100_at	Ccnc	1389228_at	MGC94167
1388980_at	LOC312275	1389102_at	RGD1307397_predicted	1389229_at	Arrdc3
1388982_at	RGD1305045_predicted	1389104_s_at	Dag1	1389231_at	Wdr5b_predicted
1388983_at	LOC362858	1389105_at	Fbxw9_predicted	1389233_at	RGD:621759
1388984_at	LOC310926	1389107_at	LOC363309	1389234_at	Icam2
1388985_at	Copeb	1389108_at	Pip5k2a	1389235_at	RGD1310511_predicted
1388986_at	RGD1305215_predicted	1389113_at	RGD1309144_predicted	1389236_at	LOC296957
1388987_at	MGC93766	1389114_at	Evpl_predicted	1389243_at	Cxcr4
1388988_at	RGD1309517_predicted	1389115_at	Mtmr9	1389257_at	Rnf138
1388989_at	Mki67ip	1389116_at	Osgep_predicted	1389259_at	LOC363332
1388992_at	Rnf34	1389119_at	Kcnc3	1389267_at	LOC361767
1388996_at	Arf3	1389131_at	Hip1	1389268_at	RGD1308470_predicted
1388997_at	Epb4.9_predicted	1389132_at	Slc30a6_predicted	1389273_at	MGC94233
1388998_at	Tcf12	1389135_at	Prkrir_predicted	1389274_at	Rbp1
1388999_at	MGC95293	1389136_at	LOC288698	1389278_at	Ran
1389003_at	RGD1307305_predicted	1389138_at	LOC314013	1389284_at	Dusp3
1389005_at	Mpeg1	1389139_at	RGD1311253_predicted	1389285_at	RGD1308383_predicted
1389006_at	RGD1307524_predicted	1389142_at	Pik3ca	1389288_at	Ewsr1_predicted
1389008_at	RGD1304968_predicted	1389151_at	Zfyve27	1389289_at	Dnajc10_predicted
1389009_at	Lta4h_predicted	1389153_at	Lias_predicted	1389290_at	Chchd3_predicted
1389010_at	RGD1305156_	1389154_at	Dos_predicted	1389291_at	Rab18_pr

	predicted				edicted
1389011_at	Ndufb2_predicted	1389159_at	Eraf_predicted	1389293_at	Cyfip1_predicted
1389012_at	RGD1308469_predicted	1389161_at	Hirip5_predicted	1389294_at	Olfml2b_predicted
1389013_at	Pbef1	1389162_at	Trim32_predicted	1389295_at	RGD1310430_predicted
1389014_at	LOC361288	1389166_at	Mapkap1_predicted	1389296_at	Ero1l
1389015_at	LOC290864	1389167_at	Mkks_predicted	1389298_at	Pcyt1a
1389016_at	LOC305633	1389168_at	Pgrmc2_predicted	1389302_at	RGD1309685_predicted
1389023_at	LOC498353	1389169_at	Casp7	1389304_at	Anxa4
1389024_at	Taf11_predicted	1389174_s_at	Whsc2_predicted	1389323_at	Tie1
1389025_at	RGD1310789_predicted	1389176_at	Perp_predicted	1389324_at	MGC72992
1389027_at	Ncoa6	1389177_at	LOC499191	1389325_at	Rfc3_predicted
1389029_at	Src	1389178_at	Cidea_predicted	1389326_at	Mrpl32_predicted
1389053_at	LOC498368	1389179_at	Phkb	1389328_at	Lgals8
1389054_at	Ppie_predicted	1389180_at	Rapgef6_predicted	1389329_at	Slc5a2
1389055_at	RGD1305992_predicted	1389181_at	RGD1311269_predicted	1389345_at	Adnp
1389056_at	RGD1310264_predicted	1389182_at	Pms2_predicted	1389348_at	Il17re
1389058_at	Lyl1	1389185_at	MGC94207	1389349_s_at	Apoh_predicted
1389060_at	RGD1309268_predicted	1389186_at	MGC93972	1389350_at	LOC367314
1389061_at	Ik	1389187_at	Gpr108	1389351_at	Wbp4
1389064_at	RGD:1310161	1389188_at	Actn1	1389358_at	Smc4l1_predicted
1389065_at	Dscr1l1	1389189_at	LOC365468	1389359_at	Fxyd3
1389067_at	MGC94226	1389190_at	RGD1309754_predicted	1389360_at	LOC363544
1389068_at	Rnf8_predicted	1389191_at	MGC109149	1389362_at	RGD:727828
1389085_at	LOC289335	1389207_at	LOC363495	1389363_at	Ndfip2_predicted
1389086_at	Anapc2_predicted	1389208_at	RGD1306274_predicted	1389365_at	LOC308991
1389087_at	Adnp	1389209_at	Lcp1_predicted	1389366_at	Schip1_predicted
1389088_at	RT1-Ke4	1389211_at	Csnk1e	1389367_at	Magi1_predicted
1389089_at	Wrnip1	1389213_at	LOC309816	1389369_at	RGD:1303205
1389090_at	Usp3_predicted	1389214_at	Sephs1_predicted	1389372_at	Smad1

1389091_at	Il2rg	1389216_at	Rfng	1389376_at	Insig2
1389098_at	LOC361519	1389217_at	Ugcgl1	1389377_at	Cdc42ep5 _predicted
1389379_at	Dek	1389226_at	Rhog_predicted	1389378_at	Snm1l
1389380_at	Sqstm1	1389565_at	Ccnb2_predicted	1389757_at	Tada2l_predicted
1389381_at	Mkrn2_predicted	1389566_at	Scap_predicted	1389759_at	Rnf134_predicted
1389383_at	RGD:735162	1389567_at	Fam26b_predicted	1389764_at	RGD1308301_predicted
1389384_at	Eppb9_predicted	1389568_at	RGD1308508_predicted	1389765_at	RGD1309036_predicted
1389385_at	LOC363169	1389569_at	LOC287533	1389766_at	RGD1304924_predicted
1389402_at	Bmp7	1389570_at	Stat2_predicted	1389767_at	Gpr110_predicted
1389403_at	Fkhl18_predicted	1389571_at	Me3_predicted	1389769_at	LOC311548
1389406_at	MGC94370	1389574_at	RGD1311703_predicted	1389770_at	LOC288485
1389419_at	LOC363334	1389575_at	Snrpb2_predicted	1389776_at	MGC93902
1389420_at	Pole	1389576_at	Cirh1a_predicted	1389777_at	Tceb3
1389425_at	Glul	1389577_at	Isrip	1389778_a_at	Sh2d4a_predicted
1389444_at	RGD1310765_predicted	1389580_at	RGD1311155_predicted	1389779_at	Tfpi
1389445_at	Snrpa1_predicted	1389581_at	Ncam2	1389790_at	Cln8
1389446_at	RGD1311848_predicted	1389584_at	LOC315595	1389791_at	Solh_predicted
1389447_at	Pnutl2_predicted	1389587_at	Entpd8	1389814_at	Ppp1r14b
1389448_at	RGD1306911_predicted	1389592_at	Kif2	1389820_at	LOC117582
1389450_at	LOC362942	1389594_at	RGD1305612_predicted	1389822_at	Prkcm
1389452_at	Rad52b_predicted	1389598_at	Adck1_predicted	1389823_at	Camk2a
1389453_at	Pdcd5_predicted	1389599_at	LOC360998 /// LOC363433	1389826_at	Fdx1
1389454_at	Sec24b_predicted	1389601_at	LOC312159	1389827_at	Cebpd
1389456_at	Mybl2_predicted	1389606_at	Rcor2	1389836_a_at	RGD1308636_predicted
1389474_at	Smo	1389608_at	Tm7sf3_predicted	1389837_at	Marcks
1389477_at	RGD1306288_predicted	1389609_at	Kcnk3	1389842_at	Brd2

1389478_at	Klf3	1389619_at	Suv420h2	1389843_at	Fkbp4
1389489_at	Cd164l1_predicted	1389620_at	Fip1l1_predicted	1389845_at	Tpm3
1389490_at	Sfxn5	1389623_at	Sec6l1	1389846_at	RGD:1303282
1389492_at	Abtb1	1389625_at	Vps33a	1389848_at	RGD1307118_predicted
1389502_at	LOC288748 /// LOC367994	1389626_at	RGD1306209_predicted	1389850_at	Zfp36l2_predicted
1389504_at	Kcnk15	1389627_at	Plcd3_predicted	1389851_at	RGD1307309_predicted
1389505_at	Faf1	1389628_at	RGD1307103_predicted	1389853_at	Nr1h2
1389506_x_at	RGD:735047	1389635_at	LOC362665	1389854_at	Ppp2r2c
1389509_at	Lyar_predicted	1389637_at	MGC94288	1389855_at	Psg16_predicted
1389510_at	Syngr1	1389643_at	LOC299949	1389856_at	LOC294067
1389514_at	Rfxank_predicted	1389644_at	Prodh2_predicted	1389857_at	Sord
1389518_at	Psmd8_predicted	1389650_at	Apln	1389858_at	Csnk1a1
1389519_at	LOC360950	1389654_at	RGD1306819_predicted	1389862_at	Kif1b
1389522_at	Zfp598_predicted	1389655_at	LOC292788	1389864_at	Toe1_predicted
1389524_at	Rnf149_predicted	1389657_at	RGD1311954_predicted	1389866_at	Cugbp2
1389526_at	RGD:727895	1389659_at	Amigo3	1389867_at	Treh
1389527_at	Jun	1389661_at	Prkwnk4	1389870_at	Got2
1389530_at	Zfp330_predicted	1389662_at	RGD1306501_predicted	1389875_at	LOC287005
1389532_at	Fbln2	1389663_at	RGD1305937_predicted	1389877_at	Galnt10
1389533_at	Ube2e3_predicted	1389670_at	Trpc2	1389878_at	Sp3
1389534_at	Dap3_predicted	1389684_at	RGD1309158_predicted	1389894_at	Gna12
1389537_at	Nfkbia	1389686_at	Ahi1	1389901_at	H13_predicted
1389542_at	Masp1	1389704_at	RGD1308478_predicted	1389902_at	Pttg1ip_predicted
1389550_at	Lactb2_predicted	1389707_at	RGD1310006_predicted	1389904_at	Pepd
1389552_at	Dcir3	1389713_at	Gsk3a	1389905_at	Fdft1
1389553_at	Nr2f2	1389718_at	Star	1389906_at	LOC297885
1389554_at	RGD:1302974	1389752_at	Brp16	1389907_at	Nfia
1389555_at	Kifap3_predicted	1389755_at	Melk_predicted	1389910_at	LOC316842
1389917_at	LOC290704	1389756_at	RGD1310159_predicted	1389911_at	Ensa

1389920_at	Evl	1390065_at	Nr2f6	1390295_at	Pkig
1389921_at	Hadhsc	1390066_at	Rhoip3	1390296_at	Npuk68
1389923_at	Cpd	1390071_at	Cspg4	1390303_at	Pepd
1389925_at	LOC363942	1390073_at	RGD1304977_predicted	1390304_at	Prkcbp1_predicted
1389927_at	Itgb5	1390074_at	Olfml2b_predicted	1390309_a_at	Icam2
1389930_at	Crhr2	1390076_at	Tram1	1390310_at	Ttl
1389939_at	Rnp24	1390078_at	Rdh10	1390324_at	Cd38
1389942_at	Crocc_predicted	1390087_at	Nog	1390325_at	Ang1
1389943_at	LOC252889	1390091_at	Mapk4	1390331_at	RGD1306740_predicted
1389944_at	Fga	1390096_at	Tspyl4_predicted	1390332_at	Ppp4c
1389948_at	Siat7c	1390097_at	RGD1306762_predicted	1390351_at	Nspc1
1389963_at	Ndufab1_predicted	1390099_at	Bat1a	1390354_at	Ryr1
1389964_at	Tgoln2	1390100_s_at	LOC313496	1390356_at	Znf574_predicted
1389966_at	Arl6ip1	1390109_at	Urkl1_predicted	1390357_at	Cacna2d3
1389967_at	Eif3s10_predicted	1390111_at	Efemp1_predicted	1390359_at	LOC301126
1389968_at	RGD:1303022	1390113_a_at	Mpzl1	1390364_at	Leng1_predicted
1389969_at	RGD1310606_predicted	1390117_at	RGD1307679_predicted	1390365_at	LOC291002
1389970_at	RGD:1303201	1390118_at	RGD:735163	1390366_at	Camk1
1389971_at	Rgc32	1390119_at	Ring1	1390369_at	Dhrs4
1389972_at	Surf1	1390122_at	RGD1305586_predicted	1390371_at	Map3k12
1389973_a_at	Csnk2a1	1390123_at	LOC363584	1390372_at	Madh5
1389974_at	LOC298359	1390124_at	Tm9sf1_predicted	1390373_at	Fgfrl1
1389978_at	Tnpo3_predicted	1390129_at	Akap6	1390374_at	LOC299569
1389979_at	LOC289324	1390130_at	Srr	1390380_at	Xpc_predicted
1389984_at	LOC317376	1390136_at	RGD:1303240	1390382_at	ADRP
1389988_at	Atrx	1390137_at	MGC72567	1390385_at	Casp3
1389993_at	Sox11	1390138_at	RGD1306073_predicted	1390397_at	Bmpr1a
1389994_at	Srrm1_predicted	1390184_at	Dcps	1390403_at	Lama2_predicted
1389996_at	Cd3e_predicted	1390187_at	Mrpl51_predicted	1390405_at	Arhgap18_predicted
1389997_at	Nr2f2	1390188_at	LOC298977	1390406_at	MGC94479
1389998_at	Eef2k	1390189_at	LOC317316	1390410_at	Cldn19_predicted
1389999_at	Jmjd3_predicte	1390191_at	Slc27a3_predi	1390411_at	Slc40a1

	d		cted		
1390018_at	RGD:621095	1390195_at	Syn1	1390412_at	RGD1310371_predicted
1390020_at	Hist1h2bh_predicted	1390200_at	RAP-1A	1390413_at	RGD1308489_predicted
1390028_at	RGD:735152	1390207_at	Htatip2_predicted	1390414_at	Trip13_predicted
1390030_at	RGD1311873_predicted	1390208_at	Syngr3_predicted	1390415_at	Slc25a30
1390031_at	Rbms2_predicted	1390209_at	Pcyt1b	1390419_a_at	Cpxm1_predicted
1390033_at	LOC304887	1390216_a_at	Tulip1	1390421_at	Pxk
1390034_at	LOC305076	1390228_at	LOC60332	1390422_at	Phr1_predicted
1390035_at	Slc16a6	1390229_at	Mip	1390425_at	Notch1
1390036_at	RGD1305809_predicted	1390231_at	RGD1311946_predicted	1390428_at	Axin2
1390037_at	Adcy5	1390233_at	Sf3b1	1390429_at	Nr1d2
1390038_at	Zdhhc3_predicted	1390236_at	Timm8a	1390431_at	RGD1306586_predicted
1390039_at	RGD:735111	1390237_at	Clca3_predicted	1390433_at	Tradd
1390040_at	Sox17_predicted	1390256_at	Vapb	1390447_at	RGD1308317_predicted
1390041_at	MGC109491	1390266_at	Fars1_predicted	1390451_at	Epb4.1l1
1390048_at	Fhl1	1390267_at	Rab35_predicted	1390506_at	Isg20_predicted
1390049_at	Golph2_predicted	1390268_at	LOC302552	1390509_a_at	Ms4a6b
1390057_at	LOC361990	1390285_at	LOC288559	1390513_at	MGC94223
1390060_at	Tnnt2	1390286_at	Bin2_predicted	1390523_at	LOC317241
1390062_at	Mfap3	1390291_at	Tmem8_predicted	1390530_at	RGD1306056_predicted
1390544_at	Dhx40	1390292_at	Phkb	1390539_at	Snph
1390546_at	Siat7A	1392671_at	Scgf	1398243_at	Gcipip
1390547_at	Cacng4	1392683_at	Dci	1398245_at	Fcgr3
1390557_at	RGD:621479	1392684_at	LOC295337	1398246_s_at	Prss15
1390559_at	LOC360912	1392702_at	Wdfy1	1398247_at	Myh6 /// Myh7
1390568_at	MGC93742	1392713_a_at	RGD1306866_predicted	1398248_s_at	Slc25a20
1390570_at	Gpr4_predicted	1392720_at	Tnfrsf1b	1398249_at	Cte1
1390572_at	Nfatc4_predicted	1392731_at	Kif1b	1398250_at	Camk2b
1390578_at	RGD1305222_predicted	1392746_x_at	RGD:1303100	1398251_a_at	Nrbf1

1390579_at	LOC300238	1392753_at	Pcsk5	1398252_at	Kap
1390581_at	RGD:708524	1392887_at	Pafah1b1	1398253_at	Renbp
1390584_at	Masp1	1392900_at	Sybl1	1398254_at	Slc15a2
1390589_at	Pofut2_predicted	1392919_at	Grp58	1398255_at	Il1b
1390590_at	Slc17a3	1393026_at	Abo	1398256_at	Mog
1390595_at	Mlana_predicted	1393045_at	Prkcl2	1398257_at	Apod
1390599_at	RGD:1303005	1393055_at	MGC95155	1398258_at	Nup155
1390603_at	Itgb3bp_predicted	1393062_at	Tulp1_predicted	1398259_at	Serpind1
1390604_s_at	Cdh11	1393093_at	Tcp11	1398260_a_at	Timm44
1390605_at	LOC291936	1393112_at	Arhgap1_predicted	1398261_at	Prps2
1390606_at	RGD:1303254	1393428_at	LOC309100	1398262_at	RGD:621597
1390614_at	Kpna1	1393436_at	Fmr1	1398263_at	Slc30a2
1390798_at	Ca5b	1393464_at	Pcsk5	1398264_at	Abcc9
1390807_at	LOC366515	1393467_at	Sult2b1_predicted	1398265_at	Egr2
1390811_at	Cdh16_predicted	1393479_at	Ppp1r2	1398266_a_at	Slc22a7
1390822_at	P34	1393480_at	Pdgfa	1398267_at	Nfyc
1390827_at	LOC367171	1393494_at	RGD1311456_predicted	1398268_at	Ntn1
1390831_at	ADRP	1393688_at	Gdf11	1398269_at	Bmp2
1390850_at	Lactb2_predicted	1393962_at	Nthl1_predicted	1398270_at	Pclo
1390932_at	RGD1309051_predicted	1394007_at	RGD:1303100	1398271_at	Galgt1
1390937_at	LOC301709	1394012_at	Phf12_predicted	1398272_at	Efna1
1391004_at	Kcnj11	1394061_at	Smarca2	1398273_at	Spata2
1391012_at	RGD:727858	1394066_at	Klf2	1398274_at	Mmp9
1391074_at	Recc1	1394110_at	Cdc20	1398275_at	Dlgh2
1391078_at	RGD1311654_predicted	1394114_at	Acp2	1398276_at	Acvr1
1391166_at	LOC312310	1394118_at	Fstl1	1398277_at	Prl
1391189_a_at	Tsga2_predicted	1394127_at	Cyp3a3	1398278_at	Trpv5
1391272_at	RGD:631438	1394135_at	Ka25	1398279_at	Impg1
1391273_at	pur-beta	1394153_at	Rbm7_predicted	1398280_at	Tpmt
1391303_at	Prodh	1394247_x_at	Eef2k	1398281_at	Kynu
1391408_a_at	Amn_predicted	1394291_at	Mrpl37	1398282_at	RGD:620394
1391412_at	Nt5c2_predicted	1394330_at	Ptk2	1398283_at	Rax
1391428_at	MGC94339	1394338_x_at	Inpp1_predicted	1398284_at	Ak3l2
1391505_x_at	Tacstd2	1394340_at	Kcne2	1398285_at	Csad
1391509_at	Ebag9_predicted	1394347_at	Nufip1	1398286_at	Plau

1391544_at	LOC287472	1394371_at	LOC305845	1398287_at	Agtr2
1391560_at	Cars_predicted	1394378_at	Drd4	1398288_at	Crhr1
1391589_at	Rab14	1394384_at	Drd4	1398289_a_at	Kcnk13
1391649_a_at	Hprt	1394385_s_at	Vps52	1398290_at	Pres
1391733_at	Txnl1	1394386_s_at	Itsn	1398291_at	Cmklr1
1392549_at	Maf	1397161_a_at	Tpo	1398292_at	Ghsr
1392592_at	Nsdhl	1397162_x_at	Hspa8	1398293_a_at	Actn1
1392652_at	Mtrf1l_predicted	1398240_at	Spt1	1398294_at	Slc29a1
1398296_at	Mapk12	1398241_a_at	Ppp5c	1398295_at	Mir16
1398297_at	Htr1d	1398371_at	LOC361780	1398756_at	Npm1
1398298_at	Arhgef11	1398372_at	B3galt3_predicted	1398757_at	Arf4
1398299_at	Atp1b3	1398373_at	RGD1307128_predicted	1398758_at	Tgfb1i4
1398300_at	Rpl36 /// LOC293291 /// LOC298627	1398374_at	Mta3_predicted	1398759_at	Rpl35a
1398301_at	Prlpf	1398376_at	MGC93893	1398760_at	Rpl5
1398302_at	RGD:708368	1398377_at	RGD:735188	1398761_at	Sdcbp
1398303_s_at	Fzd2	1398379_at	RGD1311476_predicted	1398762_at	Timm23
1398304_at	RGD:708576	1398383_at	Exosc9_predicted	1398763_at	Rpl21
1398305_at	Ampd1	1398386_at	RGD:735075	1398764_at	Ap2m1
1398306_at	RGD:628709	1398388_at	Pafah1b1	1398765_at	Rpn1
1398307_at	Rpa3_predicted	1398389_at	LOC498335	1398766_at	Ubc
1398308_at	Pigl	1398390_at	RGD:1303051	1398767_at	Rbbp7
1398309_at	Akr1d1	1398393_at	Col18a1	1398768_at	Coro1b
1398310_at	Kidins220	1398394_at	Itgb1bp1_predicted	1398769_at	RGD:621156
1398311_a_at	Slc14a2	1398396_at	B130017i01rik	1398770_at	Slc3a2
1398312_s_at	Kcnk3	1398398_at	RGD1304587_predicted	1398771_at	Nsfl1c
1398313_a_at	Hoxd3	1398399_at	RGD:727905	1398772_at	Khdrbs1
1398314_at	Rpl15	1398407_at	Armc3_predicted	1398773_at	Rpl30
1398315_at	RGD:735128	1398408_at	St13	1398774_at	Rps15a
1398316_at	Bpnt1	1398412_at	Znf444_predicted	1398775_at	Rpn2
1398317_at	Muc1	1398415_at	RGD1307626_predicted	1398776_at	Psmb6
1398319_at	Pfkfb2	1398416_at	LOC316131	1398777_at	Psma1
1398320_at	Col12a1	1398422_at	Btn1a1	1398778_at	Arpc1a
1398321_a_at	Igf2	1398423_at	Wsb2	1398779_at	Rabac1
1398323_at	RGD:1302976	1398426_at	Mef2d	1398780_at	Atp6v1f
1398324_at	Tm4sf8	1398428_at	LOC311254	1398782_at	Gps1
1398325_at	MGC105647	1398430_at	Car8_predicted	1398783_at	C1qbp

1398326_at	Plekhc1_predicted	1398435_at	Usp42_predicted	1398784_at	Men1
1398329_at	Stxbp1	1398437_at	Gtpbp3_predicted	1398785_at	Psmb2
1398331_at	Ppm1f	1398438_at	Orc6l_predicted	1398786_at	Rheb
1398332_at	Epas1	1398441_at	RGD1311091_predicted	1398787_at	Grp58
1398333_at	Commd9_predicted	1398445_at	RGD1306107_predicted	1398788_at	Rpl37
1398335_at	Rnf25_predicted	1398448_at	Lcptp	1398789_at	Ppp2ca
1398338_at	RGD:620645	1398452_at	LOC498957	1398790_at	Txnrd1
1398340_at	LOC287661	1398456_a_at	Slc6a7	1398791_at	Psmc1
1398343_at	Crsp6_predicted	1398458_at	Cacna1a	1398792_at	Cdc5l
1398345_at	Mapk1	1398459_at	RGD1311723_predicted	1398793_at	Tceb1
1398346_at	Axl	1398465_at	Eps15	1398794_at	Dars
1398348_at	Ak2	1398466_at	RGD:621616	1398795_at	Tmp21
1398349_at	Basp1	1398562_at	Yy1	1398796_at	Hnrpk
1398351_at	Pias4_predicted	1398572_at	Cdc2l5_predicted	1398797_at	Metap2
1398352_at	Sara1	1398580_at	Krt1-5_predicted	1398798_at	Eif4e
1398353_at	Catnal1_predicted	1398596_at	Akr1c12_predicted	1398799_at	Ywhab
1398354_at	Trpm7	1398646_at	Myod1	1398801_at	Ube2d3
1398356_at	Cplx1	1398675_at	Smfn	1398802_at	Dnch1
1398358_a_at	MGC94464	1398679_at	Rpl4	1398803_at	Mak10
1398361_at	Notch2	1398749_at	Calr	1398804_at	Apg3l
1398363_at	LOC362626	1398750_at	LOC497813	1398805_at	Pitpn
1398364_at	RGD1305061_predicted	1398752_at	Akr1a1	1398806_at	Ppm1b
1398365_at	Pex12	1398753_at	Uba52	1398807_at	Impa1
1398368_at	Akap13	1398754_at	Atp6v0c	1398808_at	Nde1
1398810_at	Jtb	1398755_at	Npm1 /// LOC364556	1398809_at	Pdap1
1398811_at	Psmb1	1398864_at	Unc50	1398931_at	Hint1_predicted
1398812_at	Ube1c	1398865_at	Magi3	1398932_at	RGD1309691_predicted
1398813_at	Rab11a	1398867_at	Timm13	1398933_at	Map3k7ip2_predicted
1398814_at	Apeh	1398868_at	Psmc4	1398936_at	Dhx15_predicted
1398816_at	Arf1	1398869_at	Tomm20	1398937_at	Acp1
1398817_at	Gng5	1398870_at	RGD:1303019	1398938_at	LOC360618
1398818_at	Dnaja1	1398871_at	Rpl13 /// Rps13	1398940_at	Pcbp2_predicted
1398819_at	Mylk2	1398872_at	Hnrpl	1398942_at	LOC2938

1398820_at	Mylk2	1398873_at	Atxn10	1398944_at	Ddx6
1398821_s_at	Gdi2	1398874_at	LOC366277	1398946_at	Pum2
1398822_at	Tsnax	1398876_at	RGD:621599	1398947_at	Tax1bp1
1398823_at	Rnp24	1398877_at	MGC108785	1398948_at	RGD1311072_predicted
1398824_at	Rab11b	1398878_at	RGD:1303011	1398950_at	RGD1308009_predicted
1398825_at	Nr2f6	1398879_at	Rpo2tc1	1398951_at	
1398826_s_at	Cd81	1398880_at	Ddb1	1398952_at	Tsta3_predicted
1398827_at	Fkbp1a	1398881_at	Rps5	1398954_at	Cops8_predicted
1398828_at	Fkbp1a	1398883_at	Pfdn5_predicted	1398958_at	Cebpd
1398829_at	Rpl28	1398884_at	Rpl23	1398959_at	Cct6a_predicted
1398830_at	Psmb4	1398886_at	LOC295234	1398961_at	MGC94549
1398831_at	Ncl	1398887_at	RGD:621095	1398962_at	Taf10_predicted
1398832_at	Mbtps1	1398888_at	Grinl1a	1398967_at	3930401k13rik
1398833_at	Map2k2	1398889_at	RGD:1303214	1398968_at	Mgea5
1398834_at	Actb	1398890_at	Mrpl15_predicted	1398969_at	Tloc1_predicted
1398835_at	Actb	1398891_at	Npc2	1398970_at	RGD1307929_predicted
1398836_s_at	Tceb2	1398892_at	Ndfip1_predicted	1398971_at	RGD:1303002
1398837_at	Rab7	1398893_at	Commd3	1398974_at	Aamp_predicted
1398838_at	RGD:621157	1398894_at	Golga7	1398975_at	Ncor1
1398839_at	Vamp5	1398895_at	Arcn1	1398977_at	Ap1g1
1398840_at	Rab1	1398897_at	Ensa	1398978_at	RGD1305056_predicted
1398841_at	Cltc	1398898_at	Polr2c_predicted	1398981_at	MGC105830
1398843_at	Txn2	1398899_at	Dctn3_predicted	1398982_at	Mrpl30_predicted
1398844_at	Eif5	1398902_at	Esd	1398985_at	Tde1_predicted
1398845_at	Eif5	1398903_at	Nono	1398986_at	Supt4h2_predicted
1398846_at	Nudt4	1398904_at	Atp6v1g1_predicted	1398989_at	Glo1
1398847_at	St13	1398905_at	RGD1306925_predicted	1398992_at	Rnpc2_predicted
1398848_at	RGD:621095	1398906_at	Ormdl2_predicted	1398993_at	Tpst2_predicted

1398849_at	Ppia	1398907_at	Stoml2_predicted	1398994_at	RGD1307009_predicted
1398850_at	Ywhae	1398908_at	LOC301124	1398998_at	LOC363675
1398851_at	Rps21	1398909_at	Stub1_predicted	1399000_at	RGD1305481_predicted
1398852_at	Psmb3	1398911_at	mrpl9	1399001_at	Mrps17_predicted
1398853_at	Rpl24	1398914_at	RGD1309735_predicted	1399002_at	RGD1308813_predicted
1398854_at	Atp5f1	1398915_at	Akip	1399005_at	Usf1
1398855_at	Psma2	1398916_at	Rpl7	1399011_at	RGD1310313_predicted
1398856_at	Surf1	1398917_at	Tex27_predicted	1399012_at	RGD1310905_predicted
1398857_at	Psmd2_predicted	1398918_at	RGD1304704_predicted	1399014_at	Tmp21
1398858_at	Hdlbp	1398920_at	Mrpl37	1399015_at	Myst2
1398859_at	Nedd8	1398922_at	RGD1305687_predicted	1399020_at	Pprf18
1398860_at	Nxf1	1398924_at	RGD1307801_predicted	1399021_at	Clk1_predicted
1398861_at	Atp2a2	1398925_at	Pfdn1_predicted	1399022_at	RGD:727957
1398862_at	Gnb2	1398926_at	RGD1307161_predicted	1399023_at	Scyl1_predicted
1398863_at	Ube2g1	1398927_at	RGD:1303306	1399025_at	LOC361309
1399028_at	Usp48	1398929_at	Atp6v0b_predicted	1399026_at	Rhoa
1399029_at	LOC302559	1399119_at	RGD1306567_predicted		
1399031_at	Ercc1_predicted	1399124_at	Inpp1_predicted		
1399032_at	Cbfb	1399126_at	RGD1309374_predicted		
1399033_at	Pcnx_predicted	1399132_at	Fbxo7_predicted		
1399034_at	Polr3h_predicted	1399134_at	RGD:1303036		
1399037_at	RGD:1303276	1399137_at	RGD1308513_predicted		
1399039_at	Gba2_predicted	1399140_at	Clk4_predicted		
1399042_at	Capza2	1399141_at	Odf2		
1399044_at	Galnt1	1399142_at	RGD:621096		
1399045_at	Top1	1399145_at	Tmem15_predicted		
1399046_at	Mrpl27_predicted	1399146_at	Dncli1		
1399048_at	RGD1308917_predicted	1399147_at	RGD1309002_predicted		
1399054_at	Brd7_predicted	1399148_s_at	RGD1309002_predicted		
1399055_at	LOC365592	1399150_at	RGD1309585_predicted		

1399056_at	Morf4l1_predicted	1399151_at	Eps15_predicted
1399057_at	Mrpl18_predicted	1399157_at	Npm1
1399063_at	Ric8b	1399158_a_at	Vamp3
1399066_at	Hfe	1399159_a_at	Ube2d3
1399067_at	LOC290628	1399160_a_at	Arts1
1399069_at	RGD1310433_predicted	1399161_a_at	Ddb1
1399071_at	Fibp	1399162_a_at	Homer1
1399072_at	Otub1_predicted	1399163_a_at	RGD1305158_predicted
1399073_at	Cdc16_predicted	1399164_a_at	LOC292724_predicted
1399074_at	Map3k7	AFFX_rat_5S_rRNA_at	Actb
1399082_at	Wbscr21_predicted	AFFX_Rat_beta-actin_3_at	Actb
1399083_at	RGD:1302963	AFFX_Rat_beta-actin_5_at	Actb
1399085_at	Zfp105_predicted	AFFX_Rat_beta-actin_M_at	Gapd
1399086_at	RGD1307410_predicted	AFFX_Rat_GAPDH_3_at	Gapd
1399087_at	Tlk2_predicted	AFFX_Rat_GAPDH_5_at	Gapd
1399088_at	Slc38a6_predicted	AFFX_Rat_GAPDH_M_at	Hk1
1399089_at	Dncli1	AFFX_Rat_Hexokinase_3_at	Hk1
1399090_at	Capzb	AFFX_Rat_Hexokinase_5_at	Hk1
1399091_at	LOC362608	AFFX_Rat_Hexokinase_M_at	
1399092_at	LOC293589	AFFX_ratb1/X12957_at	
1399093_at	Churc1_predicted	AFFX_ratb2/X14115_at	bioB
1399094_at	Sumo1_predicted	AFFX-BioB-3_at	bioB
1399095_at	Add3	AFFX-BioB-5_at	bioB
1399097_at	Glo1	AFFX-BioB-M_at	bioC
1399098_at	Hnrpul1_predicted	AFFX-BioC-3_at	bioC
1399100_at	Rnpc2_predicted	AFFX-BioC-5_at	bioD
1399101_at	RGD1306356_predicted	AFFX-BioDn-3_at	bioD
1399104_at	Bin3_predicted		
1399106_at	RGD1305158_predicted		
1399107_at	RGD1308959_predicted		
1399109_at	Znf297		
1399110_at	MGC95239		
1399112_at	LOC299488		
1399113_at	Gtf2e2_predicted		

1399115_at	Luc7l2_predicted
1399116_at	RGD1311745_predicted
1399117_at	LOC303514